NATIONAL TECHNICAL UNIVERSITY OF ATHENS
SCHOOL OF CIVIL ENGINEERING
GRADUATE PROGRAM
´ Analysis & Design of Earthquake Resistant Structures´

Aseismic Design and Reinforcement Recommendations of a Masonry Structure Using Fragility Curves

MASTER THESIS

FOTIS P. GAZEPIDIS
GRAGUATE CIVIL ENGINEER

SUPERVISE PROFESSOR
COSTAS A. SYRMAKEZIS
PROFESSOR N.T.U.A.

JUNE 2011
ATHENS

ABSTRACT

This thesis was part of the Interdepartmental Program of Postgraduate Studies: “Structural Design and Analysis of Structures” of the School of Civil Engineering, National Technical University during the academic year 2010-11. It was carried out under the supervision of Professor N.T.U.A. K.A. Syrmakezis.

The subject of this paper is to investigate the vulnerability and the overall seismic behavior of the Neoclassical Building in Chania. There is developed a methodology for seismic design and evaluation of the response of the masonry construction through the development of fragility curves.

Initially, there was made an elastic analysis of the body through the computer program SAP 2000 14 Nonlinear. The modeling of the masonry was accomplished with shell elements, according to the method of finite elements. The exported tensions, of every masonry, were transferred to be controlled through the computer program FAILURE. This program displays to each examined wall, the areas and the mechanism of failure under biaxial loading (BC, BCT, BTC, BT), using the modified failure criterion Von Mises.

Then follows, the statistical analysis of the failure rates for the whole of the masonry, for different ground accelerations, and observation parameter its tensile strength. Then, having set different levels of damage, the fragility curves were exported.

In addition, three different ways to enhance the existing structure were proposed and the corresponding fragility curves arised.

Moreover, all these results were compared considering the best solution, including the proposed reinforcements as well as the possibility of non-intervention, based on the parameters of cost-effectiveness - intervention.

Finally taking everything into account future recommendations and further studies were proposed.

CREDITS

Before the presentation of this thesis I would like to thank all those interested, involved and participated, each in his own way, resulting in this circumstance.

Initially, I would like to thank the Academic Director and Supervisor, Mr. Costas Syrmakezis. Firstly for the confidence he showed us, the abundant supply of teaching materials and devices, but mainly for the excellent cooperation and support throughout all the way of this study.

Also, sincere thanks to Panagiotis Giannopoulos, for his clear and substantial interest, practical help and especially for his precious time dedicated in our try.

Most importantly, I would like to thank my brilliant parents ‘Polemarchos’ and ‘Dimitra’ as well as my brother ‘Kiriakos’, for their support, encouragement, and understanding all the way through.

It is constantly not possible to individually thank everyone who has made possible the achievement of a project. To those of you who I did not specifically name, I also give my thanks for moving me towards my goals.

TABLE OF CONTENTS

CHAPTER 1

INTRODUCTION (1-11)

1.1	General	1
1.2	Historical Overview	2
1.3	Masonry Categories	3
1.3.1	Stone Masonries	4
1.4	Types of floors and roofs	5
1.4.1	Floors	5
1.4.2	Roofs	7
1.5	Bond Beams – Tie Rods	9
1.5.1	Bond Beams	10
1.5.2	Tie Rods	10

CHAPTER 2

THEORY OF FRAGILITY CURVES (12-31)

2.1	Introduction	12
2.2	Basic theory fragility curves	13
2.3	Applications of empirical fragility curves	19
2.3.1	Application by NCEER-ATC	19
2.3.2	Application by "Hazus"	24
2.4	Applications of analytical fragility curves	26
2.4.1	Comparison of empirical and analytical fragility curves on concrete piers in Japan	26
2.4.2	Fragility curves for reinforced concrete structures in the region of Skopje	28

CHAPTER 3

THE METHOD OF FINITE ELEMENTS (32-61)

3.1	General	32
3.2	Application of the method in construction analysis	34
3.3	Formulation of equilibrium equations of the finite element method with the Principle of Virtual Work	35

3.4	Formulation of equilibrium equations of the finite element method applying the Principle of Change and the method of Weighted Balances	41
3.4.1	The principle of stationary value of potential energy	41
3.4.2	Application of the method Rayleigh – Ritz	43
3.4.3	The method of weighted balance	44
3.5	Rectangular slab elements of four nodes and twelve degrees of freedom	46
3.6	Rectangular membrane finite elements with transverse rotational degrees of freedom	48
3.7	Flat shell elements	52
3.8	Reliability of the finite element method	54
3.8.1	Simulation Stages	54
3.8.2	Simulation of construction and results testing	56
3.8.3	Element behavior control	57
3.8.4	Simulated loads	58
3.8.5	Numerical Errors	59
3.8.6	Convergence of the finite element method	59

CHAPTER4

MASONRY MECHANICS (62-69)

4.1	General	62
4.2.1	Determination of compressive strength of the masonry	64
4.3	Tensile strength of masonry	66
4.4	Determination of the shear strength of the masonry	68

CHAPTER 5

DEVELOPMENT OF FRAGILITY CURVES (70-86)

5.1	Creation of Fragility Curves	70
5.2	Failure Analysis	72
5.2.1	Failure criterion by Von Mises	72
5.2.2	Modified failure criterion by Von Mises	74
5.2.3	Methodology of the Laboratory of Static and Anti-Seismic Research of the National Technical University	76
5.2.4	Failures audit with the PC program "FAILURE"	78
5.3	Statistical Analysis	78
5.3.1	Random Variables and Distributions	79
5.3.2	High Class Means and torques	81
5.3.3	Continuous Distributions	82
5.4	Statistical analysis of failures	84
5.5	Setting of Damage Levels	85

CHAPTER 6
CASE STUDY (87-155)

6.1	Description of the structure	87
6.2	History	89
6.3	Pathology and damage detection	90
6.3.1	Recent Maintenance Procedures	90
6.4	Spatial Model	91
6.4.1	Geometry Simulation	94
6.4.2	Material Simulation	95
6.4.3	Action Simulation	101
6.4.3.1	Seismic response of structures	103
6.4.3.2	Seismic combination of actions	103
6.5	Dynamic Analysis	105
6.6	Assumptions in the simulation	106
6.7	Modal Analysis	108
6.8	Results of the masonry failure – solution with the program Failure	112
6.9	Failure rates & Statistical elaboration of the results	129
6.10	Export of fragility curves	144
6.11	Comparison between the three failure levels of the two distributions	151
6.12	Comparison of the fragility curves of the two distributions	152

CHAPTER 7

REPAIR OF EXISTING MASONRY(REINFORCEMENT A)

(156-187)

7.1	Introduction	156
7.2	Description of ways to reinforce the structure	157
7.3	Pointing (Reinforcement A)	158
7.3.1	*Stages of work and modeling of reinforcement A*	*160*
7.3.2	Walls failure results from software FAILURE	162
7.3.3	Failure rates & Statistical elaboration of the results	171
7.3.4	Export of fragility curves	180
7.3.5	Comparison between the three failure levels of the two distributions	186

CHAPTER 8

REPAIR OF EXISTING MASONRY(REINFORCEMENT B)

(188-219)

8.1	Pointing, reinforced concrete slab at the ground and the first floor level and reinforced concrete bond beam at the roof level (Reinforcement B)	188
8.2	Stages of work and modeling of reinforcement B	189
8.3	Walls failure results from software FAILURE	194
8.4	Failure rates & Statistical elaboration of the results	203
8.5	Export of fragility curves	212
8.6	Comparison between the three failure levels of the two distributions	218

CHAPTER 9

REPAIR OF EXISTING MASONRY(REINFORCEMENT C)

(220-250)

9.1	Pointing and horizontal prestressing (Reinforcement C)	220
9.2	Stages of works and modeling of reinforcement C	220
9.3	Walls failure results from software FAILURE	225
9.4	Failure rates & Statistical elaboration of the results	234
9.5	Export of fragility curves	243
9.6	Comparison between the three failure levels of the two distributions	249

CHAPTER 10

COMPARISONS – CONCLUSIONS (251-266)

10.1	Introduction	251
10.1.1	Pointing (Reinforcement A)	252
10.1.2	Pointing, reinforced concrete slab at the ground and the first floor level and reinforced concrete bond beam at the roof level (Reinforcement B)	252
10.1.3	Pointing and horizontal prestressing (Reinforcement C)	253
10.2	Conclusions from the modal analysis	254
10.3	Comparison between fragility curves	256
10.4	Comparison between failure results of all the reinforcement cases	259
10.5	Reinforcement evaluation criterion	265

BIBLIOGRAPHY (267-268)

APPENDIX 1: MODAL PARTICIPATION MASS RATIOS OF MASONRY WALL

APENDIX 2: ARCHITECTURAL PLANS OF THE BUILDING

APENDIX3:FAILURE RESULTS FOR THE MASONRY WALLS (MW)

CHAPTER 1

INTRODUCTION

1.1 General

The most basic structural material of world history is “masonry”. All of humanity projects, until the means of 19th century, were mainly manufactured by this material, which use was limited to a great degree by modern industrial materials, as steel and concrete.

But despite the fact that the masonry is one of the oldest components, the knowledge for the mechanical behavior of buildings made by bearing masonry is limited. It is worth noting that until the beginning of our century the design of buildings by bearing masonry was empirical. Nevertheless many appreciable research efforts have been developed, in recent decades, on the behavior, use and improvement of masonry, as a result to gradually recover a level of credibility.

The advantages of masonry from a structural point of view is the low cost, better protection against fire, temperature and sound, the ease and speed in the manufacture, the very good aesthetic and resistance in time. Between the disadvantages one could indicate the brittle nature and the lower strength (in relation to concrete).

The basic feature of a masonry structure is the great weight. Especially in high buildings the thickness of the wall on the basis of the structure is very large. This specialty in conjunction with the fact that the floors in stonework are generally made of wood, makes the different response of the masonry construction in relation to a construction of reinforced concrete where the mass is concentrated in the levels of the floors. **Also,** major role in the behavior of a stone building plays the size, the number and the placement of the openings. Large openings or potential openings mismatch in height, is causing great difficulty in the flow of stress from the construction to the footing and finally to the ground, both under vertical, but mostly under seismic, loads. [1][3]

Traditional buildings are composed almost entirely of stone construction with wooden and metal components. In the past, the construction was done by craftsmen with experience and deep knowledge that spreads from generation to generation.

1.2 Historical Overview

It is argued by some, that human history is the history of architecture, which is consistent with the history of masonry. Wall and masonry, are synonymous words, used in construction technology to indicate the vertical components, those resulting from natural or technical construction stone, using mortar or without mortar.

The archetypal form of the masonry consisted of branches and trees to fill both sides with lath mud. The first built walls were made of rough, ashlar or slate stones.

Artistic masonry with mortar, without cement, is found in Egyptian monuments (3000 BC) and in Greek (Mycenae Acropolis 1550-1400 BC). In many areas, however, the stone was scarce, and the processing required a painstaking work. In contrast, clay is easy molding. The plinth is the oldest component, built 10,000 years ago. The excavations of ancient Jericho were bricks in the shape and size of elongated bread. These bricks are dried in the sun and shaped by hand.

The strength, hardness and simplicity of the brick were the qualities that led to its widespread use in residential buildings. In Mesopotamia and Egypt, mud brick manufactured from pieces of dried mud, during the dry season. Around 3000 BC begins the use of ovens for drying bricks. Since that time even, begins the standardization of the scale of the bricks with very simple molds (Khalaf of Iraq, 4000 BC), which were boxes without bottoms, which were placed on a horizontal surface and were filled with clay mixed with straw, manure and twigs. After dried in the sun, they eventually constituted then so called “mud brick”.

The dimensions of the ancient mud brick were (in cm):

• Babylon: 33 × 33 × 6 - 55 × 55 × 9

• Greece: 29.6 × 29.6 × 15.8 - 59.2 × 59.2 × 59.2 - 74 × 74 × 74

• Rome: 60 × 60 × 6 - 45 × 45 × 5 - 20 × 20 × 4

During the Byzantine period, is admirably developed the technique of masonry with clay mortar, with soil or sand and cement from titanium or lime. Common methodology mounting (fastening) of the wall from the Byzantine, was “imantosi”, i.e. the juxtaposition of two or three wooden beams at normal height range (“savakia”), measuring 0.10 × 0.10 m or 0.15 × 0.12 m (“chatilia”), along with longitudinal direction

of the wall, linked together by wooden joints, the blinkers. As interior walls were often used composite brick or sand-brickwork, adding reed or wooden forearms.

In the Roman and Byzantine period, bricks were distinguished for their high level modeling (dimensional stability, strength, physical properties, etc.) and particularly for their strength over time. The course of masonry gradually reaches the Renaissance, at the time of which there is a marked stagnation.

Around 1920, starts in India systematic research on the possibilities of reinforced masonry, leading to new economic systems, illuminating with basic knowledge of the static behavior of the masonry. Europe follows later (1940) serious study of masonry structures, resulting in the application of rational economic calculations for construction of walls.

The development of research around the masonry was important during the last decades, especially in the U.S., resulting in the drafting of Modern regulations and codes. In Europe there is a similar activity, which in 1989 reached the first widely accepted legal framework, namely Eurocode 6 (EC6), which gives the principles for calculating components of masonry as not only filling but also as the bearing structure of buildings.

The bearing masonry buildings show great variety of types. Key elements that define the behavior of buildings as well as constitute factors for discriminating them in categories:

- The type of masonry (vertical bearing structure).
- The type of floor and roof (horizontal main body).
- The presence or absence and type of beams and ties.

[1]

1.3 Masonry Categories

The most prevalent types of masonry that occur in buildings of masonry are:

- Constructed of natural stone (stonemasonry).
- Constructed of artificial stone (brickmasonry)

- masonry infilled timber structures

The mortar connecting the stones in most cases is one of the following:

- Lime-cement mortar
- Lime mortar
- Clay mortar

In this paper we employ the first of the three types of masonry structures that of natural stone (stonemasonry).

1.3.1 Stone Masonries

The structures composed of natural stones are called stone masonries. The stonework has been the prime construction material for centuries and every kind of construction until the appearance of concrete. The stones used in construction of masonry come from further processing of rock. In Greece, the most common stone is limestone.

Depending on the processes, they are divided into the following categories:

- dry stonework
- rubble masonry
- semi-ashlar masonry
- ashlar masonry

Dry Stonework

If in the construction of a wall is not used mortar and the stones used are raw, this is called dry stonework. It is the oldest method of masonry, which tends to be abandoned and used only for temporary structures.

Rubble Masonry

Rubble masonry are called the stone masonries consisted of raw stones and mortar. Typically, the stones come from hard rock and that makes their processing uneconomical. Nevertheless, the size and shape of the stones must be such that there is uniform stress distribution in them. Large stones are difficult in use by craftsmen

while small ones increase the cost of the project since more man hours are required in order to complete it. But the most important reason to avoid small stones in construction is that they increase the ratio of height of mortar joint to height of stone as well as the rate of the mortar, as a result for the construction to be more vulnerable.

Semi-Ashlar Masonry

Semi-ashlar masonry stoneworks are called the stonemasonries built with stones treated in the faces for better contact between the stone and smooth flow of load. To be processed, the origin of these stones is rock, but not hard one. The aesthetic effect of a semi-ashlar masonry construction is satisfactory and for that, such structures are usually not coated.

Ashlar Masonry

Ashlar is called the stonemasonries which construction consists of fully processed stones to all faces. This method was used in the construction of major projects in the ancient period. After the carving, natural stone can acquire perfect contact and the building behaves as a full-length vertical. The horizontal connection is achieved either through appropriate notch where metal connectors are placed, either through an appropriate format given by the technician in the faces, horizontally adjacent to each other.

1.4 Types of floors and roofs

1.4.1 Floors

Floors take place both static function of the building (transfer vertical loads, horizontal stiffness) and functions to create spaces. In its simplest form a wooden floor is composed of the structural elements (beams) and the running surface (floor) consisted of planks.

[2]

Basic mechanical characteristics of a floor that affect the response of a building in a horizontal seismic loading are:

- The level of rigidity
- The diaphragmatic function or not
- The level of mass concentration

These depend on the type of floor as well as its connection to the perimeter walls. The most common types of floor that appear in traditional buildings are:

- Rigid slabs of reinforced concrete.
- Brick arched floors on steel beams. Partial diaphragmatic function to varying degrees in each direction.
- Wooden floors (wooden planking on strong beams): Lightweight and flexible construction with a virtually non-existent diaphragmatic function and strongly anisotropic behavior.
- Heavy, thick arched floors: It is about arched or vaulted players in space that put strong horizontal pressure at perimeter walls.

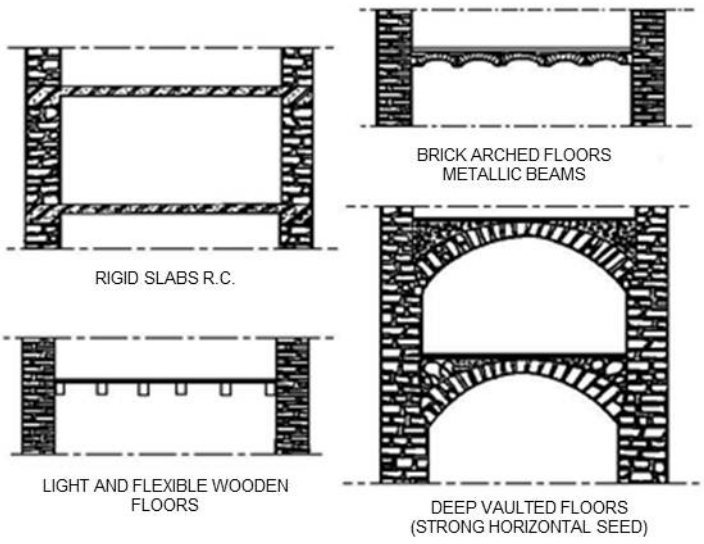

Image 1.1 Types of floors

In most construction cases of bearing masonry, the floor consists of a relatively light and flexible structure, where the diaphragmatic function is considered inadequate and finally ignored. However, in some cases where the wooden floors are suitable can be considered to have a diaphragmatic function in longitudinal direction and if the links are appropriate, in the transverse as well.

Surface of motion can be the floor itself but it is possible to use other materials such as marble, ceramic tiles, boards, etc.

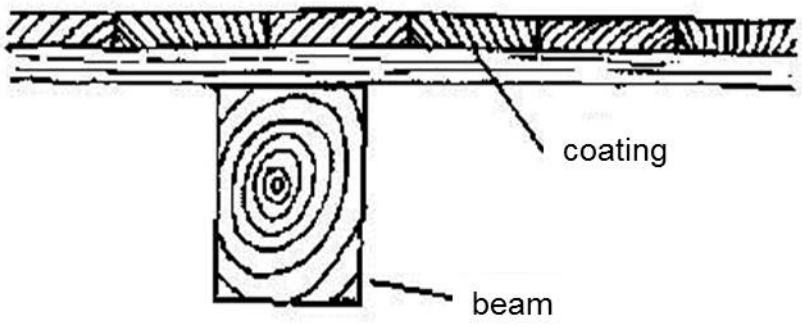

Image 1.2 Floor section

1.4.2 Roofs

The roofs of masonry buildings typically consist of wood trusses with planking and tiling. The trusses rest on the top frieze or on wooden beams (“rivers”) built along the crest of the walls. The wooden roofs are able to develop partial septal function in the direction of couplers, but not in the transverse direction as the transverse link couplers are usually inadequate. Condition of the diaphragmatic function is excellent networking between the couplers and sufficient to anchor the wooden rivers, or in the top tier of the perimeter wall. Many times more often when the roof is based on the internal masonry, the trusses are statically complete elements (no or improper splicing of the wooden beams of the lower pad), thereby exercising a strong pressure from the inclined rafter on the perimeter masonry.
[3]

The main role of the roof is to protect the inside of the building from the weather conditions and only under certain circumstances can act as a diaphragm and assist in the response of the structure, connecting the walls between them and forcing them to cooperate with the result of increasing the stiffness of the structure. Therefore it is understood that a key role in the form of a roof are the weather conditions, the loads to be carried out by the construction and the materials available to the region around the project.

Image 1.3 Wooden Roof of Stone Structure

Structural System

In its simplest form, the main body of a roof consists of parallel beams that rest on two opposite walls, disconnected, on which are placed coated plates, tiles, slate or other material. To cover larger openings is necessary to use couplers. These roofs can work as diaphragm in the direction of the beams and couplers. To make the roof work in both directions it is necessary to connect the couplers between them, or construct truss frame. For the proper diaphragmatic function of a roof, it is important its proper connection with the masonry.

[3]

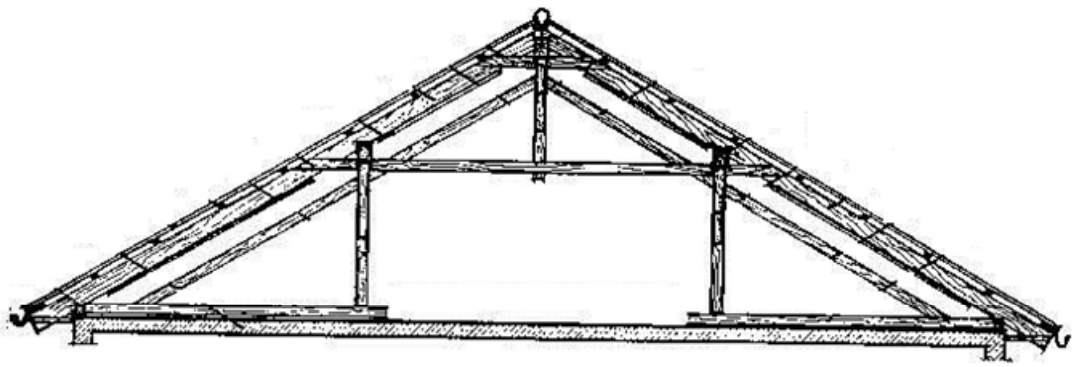

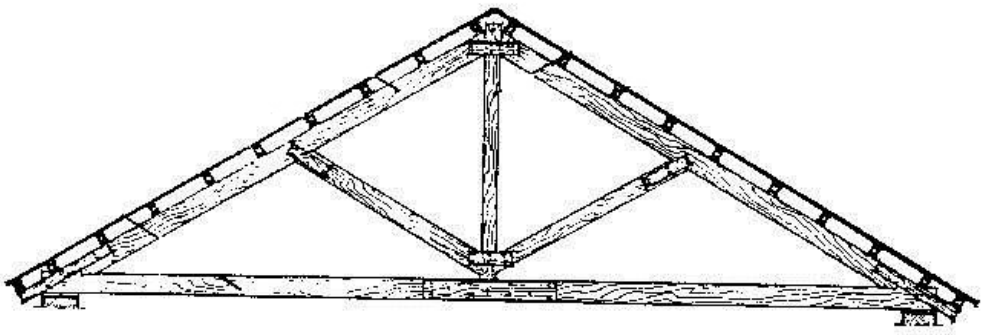

Image 1.4 Wooden roofs: a) With a slight angle collar ties, b) With couplers

Roof Coatings

Roof Coating is called the material which is mounted on the bearing body and has direct contact with the environment. The most common ingredients in traditional stone building structures used as a coating, are tiles, slate and wood.
[3]

1.5 Bond Beams – Tie Rods

The bond beams and the tie rods are components that can dramatically change the response of masonry buildings, especially in horizontal seismic loads. Some of the main mechanical characteristics of bond beam masonry are to provide greater ductility of the structure and to limit the cracks of the walls thus ensuring better continuity of the material. The most prevalent types of beams and tie rods are:

- Wood, metal, or occasionally reinforced concrete headers at the lintels of the openings (no continuous beams)
- Continuous wooden (wooden frames), metal, or occasionally reinforced concrete bond beams on the lintels of the openings or even at the levels of floors and roof.
- Metal tie rods (passive or slightly pre-stressed) at the levels of the floors, roof, or lintels.
- Tie columns made by wood, reinforced concrete and rarely metal.

[3]

1.5.1 Bond Beams

Experimental results have shown that for a reinforced wall with bond beams, collapse is achieved for very large values of lateral load. The bond beams run horizontally and the tie columns vertically in a masonry wall. The main role of the constant horizontal beams is to increase the out-of-plane masonry flexural mode, assuming the horizontal seismic forces perpendicular to the wall and transfer these load to the transverse walls. On the other hand, the tie columns significantly improve the ductility of the construction but have little effect on lateral resistance. To be effective, tie columns should be manufactured in all corners, recesses and connections of bearing walls.
[3][4]

The column ties in cooperation with the bond beams create frames of great stiffness. The wall is boxed in smaller parts, preventing its premature cracking under seismic stress within its plane.
[1]

1.5.2 Tie Rods

The main role of horizontal metal or wooden tie rods is to prevent detachment of cross-walls, vertical edges at the corners Γ or T, either from earthquake forces or arches and roof horizontal pressure. Visible wood or metal tie rods are found in almost all constructions that have vaulted floors, arches, and domes like the Roman, Byzantine and Ottoman monuments.

Image 1.5 Tie rods in Stonemasonry

Tie rods are placed in the genesis of the curved state bodies so as to take the horizontal pressure developed under the vertical loads. These tie rods are usually connected at their ends with the transverse walls.

It is obvious that the role of bond beams and tie rods is to enhance the response of masonry structures against forces outside their plane and ensure the function of masonry as a single set under static and dynamic loads.
[5]

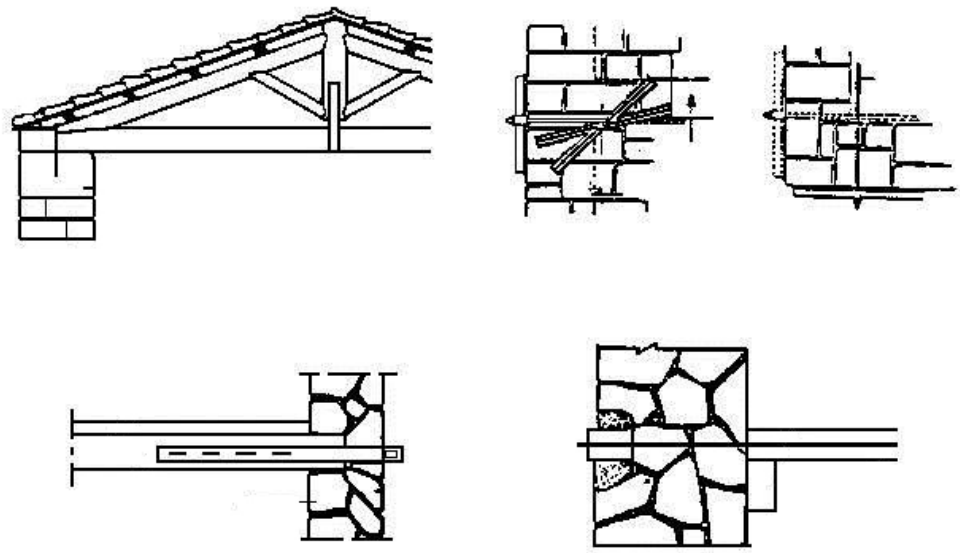

Image 1.6 Types of bond beams, tie rods and connections

CHAPTER 2

THEORY OF FRAGILITY CURVES

2.1. Introduction

For the design of buildings, but also the effective implementation of rehabilitation processes and evaluation is needed to assess the seismic vulnerability. The seismic vulnerability is directly associated with the extent of damage that a structure is expected to undergo while a seismic event.

There are four main groups of methods (UNDP / UNESCO, 1985) to estimate the level of vulnerability of a structure:

- Methods of classification, based on the classification of structures in typological units.
- Methods of inspection and assessment of performance of the numerical values in each structure.
- Analytical methods, based on analysis of the construction to estimate the expected strength during a seismic event.
- Experimental methods, including tests for the detection of structural properties of the whole construction.

  [6]

Economic, social and architectural reasons demonstrate the need for a clear picture about the size of the reliability of construction, with a view to making decisions. At the same time, the random nature of the elements that determine the behavior of the construction of the prescribed loads and the lack of certainty about the size of the expected loads due to the random nature leads to a design based on a probabilistic approach. This introduces the family of fragility curves, which relate in terms of probability of the estimated damage to the building with seismic intensity.

The probabilistic nature of parameters influencing the behavior of a structure of masonry comes from various causes, such as complex geometric changes and complex structural systems (causing difficulties in discretization of the construction during the analysis), the incorrect values of the mechanical properties of materials (due to the large dispersion in the entire construction or the lack of accurate methods

assessment and organs), restrictions on on-site inspections (ban the taking of samples for testing the mechanical properties), etc.
Even the interventions of the past, often change the original static function and cause undesirable behaviors and faults in construction. Also, the actions of the past (e.g. older earthquakes) and the failures they have caused (creep, degradation of building materials etc.) are important factors of uncertainty.

The random nature of the earthquake is directly connected to a large number of parameters, such as the time of the incident, the duration, source, intensity, frequency content, the geological data of the region and other sizes. For this reason, it is of particular importance for the credibility of the identified relationship damage and seismic intensity to select a representative group of different earthquakes to cover as much as possible uncertainties. The ideal solution to this question would be to gather a large number of available recordings of real earthquakes occurring in the considered area, covering all aspects. Because of the scarcity of availability of the required seismic recordings of this file, it is usually selected a representative set of earthquakes, real or artificial, which is used as key input data analysis.

This paper presents the methodology of the analytical fragility curves and their application in construction of walls.

2.2. Basic theory fragility curves

For the development of fragility curves a clear methodology and its applied corresponding stages are followed. The construction of fragility curves includes three sets of information import:

- The ones related to the intensity of the seismic event
- The ones that describe the critical properties for the capacity of the structure
- Those that determine the quantification of the behavior of the structure.

The elements of the seismic response of building can be obtained either analytically (analytical fragility curves) or obtained through empirical data collection and evaluation spotting sizes (empirical fragility curves). Figure 2.1 shows a proposed process flow diagram for deriving the analytical fragility curves. As noted, there are three main stages, leading to fragility diagram curves. In the first stage, the model is

created and the input data is selected, during the second phase, analysis of tensions and failures are made and the process is completed in the third stage with the export of fragility curves through statistical analysis and adaptation of appropriate probability density function on the observations.
[7]

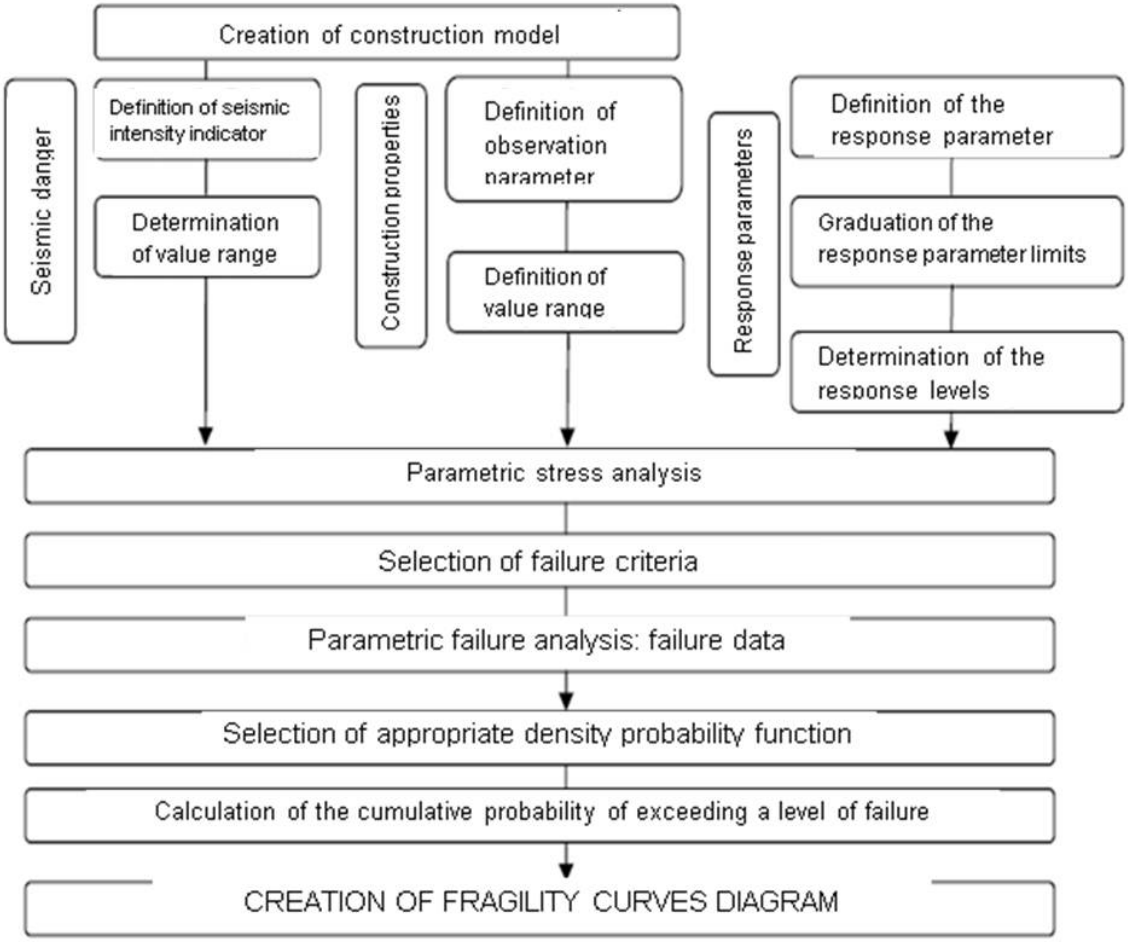

Figure 2.1 Flowchart for creating fragility curves [6]

Seismic Risk

To calculate the response of a structure subjected to a future destructive earthquake, it is imperative to define the characteristics of seismic risk, which are:

- The seismic intensity indicator and
- the extent of change

The seismic intensity ratio is chosen to describe with sufficient precision, the magnitude of seismic activity. The maximum ground acceleration (PGA) in a chronoistoria of accelerations is used mostly as a measure of seismic intensity for growth fragility curves. The maximum spectral acceleration (SA) of a single-degree system subject to territorial stimulation is the main alternative. Other parameters of soil stimulations commonly used to represent the seismic intensity are:

- the maximum territorial speed (PGV)
- the spectral velocity (SV) and
- The maximum speed of the spectral (SI)

[8]

Observation Parameter

In order to determine the profile of the construction which have a random character and influence its behavior, an assessment of the degree of significance of these parameters must be preceded. These parameters can be e.g. the mechanical properties of materials (modulus, compressive strength), the properties of the subsoil bearing construction, etc. The random nature and the uncertainties involved in determining the degree of importance of these properties require a probabilistic approach to the problem.

Examining the change of each parameter that affects the computational model, is a priority the one which is estimated that affects the response of the structure. The one selected, is the one referred as observation parameter. For each observation parameter, it can be developed a family of fragility curves. The development of more than one family of fragility curves, by repeating the methodology, can clearly illustrate the influence of the change of each observation parameter in the vulnerability of the construction.

The determination of the range of values of the observation parameter is a fundamental requirement of the process, since the construction properties have a serious effect on the response of the structure and directly affect the produced fragility curves. The values involved in the computer simulation during the analysis should be consistent with the data of the actual construction and the change must obey the steady incremental rules of growth. The range of values must be specified to cover a full range of statistical parameters of response.

In the case of masonry construction, as observation parameter is usually chosen the tensile strength of masonry, as related to the seismic behavior and is highly dispersed.

[6]

Response Parameter

To determine the effect of a random action in construction is necessary to determine a parameter of response to quantify the effects. The choice of an appropriate response parameter is associated with the assessment of seismic vulnerability of the manufacturing and focuses on economic, practical and functional requirements.

The ratio of conduct (DI), which represents the seismic response of the structure, is equal, under the proposed methodology, to the ratio of the surface of walls that have failed, divided by the total area of the walls of the structure, as shown in the following mathematical fraction (Fraction 2.1).

$$D.I. = \frac{A_{fail}}{A_{tot}} \quad (2.1)$$

Since the vulnerability of the construction depends on the extent of the damages, a reference scale should be used to transform the quantitative values of the index of damage in qualitative descriptions of the extent of the damage. The result of this presentation is the calibration of the markers of the response parameter using price thresholds.

These limits of damage provide a distinction between three levels of damage and can be identified by the designations, "minimal damage", "medium damage, " "great harm" and "collapse. "

The limits and the levels of failure may correspond to safety factors and to the strength of the structure during an earthquake and are usually defined according to the discretion of the engineering major contributor to the final shape of the curves.

Table 2.1 Levels of damage to the structure

Total damage	Light damage	Moderate damage	Great damage
Damage Size Limit	0.3%	0.6%	1.0%
	Minor cracks on the façade. Small coating detachment in corner openings. Insignificant out of plane shifts.	Extensive cracks on the façade. Visible in plane and small out of plane shifts.	Extensive cracks on the façade and coating detachment. Visible in and out of plane shifts.

[6]

The Federal Emergency Management Agency (FEMA) U.S. proposes as "Size Limits Fault" the indicators of failure to determine the response of the structure.

The levels of damage to build non-reinforced masonry are shown in Table 2.1. According to the literature on the database ATC - 38 for the behavior of buildings near the California earthquake of 17 January 1994, the damage levels of construction are:

- No Damage.
- Light Damage.
- Moderate Damage.
- Severe Damage.

The proposed methodology has been a similar case, as shown in Table 2.2 and applied to historic masonry structures.

Στην προτεινόμενη μεθοδολογία έχει γίνει μια παρόμοια υπόθεση, όπως φαίνεται στον πίνακα 2.2 και εφαρμόζεται για ιστορικές κατασκευές από τοιχοποιία.

Table 2.2 Levels of damage to the structure

Total damage	Insignificant damage	Light damage	Moderate damage	Great damage
Damage Level Graduation	0% - α%	α% - 2α%	2α% – 4α%	>4α%
Damage Level Graduation	0% - β%	β% - 2β%	2β% – 4β%	>4β%

[6]

Particularly important is also the education of the models of the structure, usually a larger representative set, and the choice of an appropriate computational tool and analytical method for calculating the response with the desired accuracy. It is necessary to describe the characteristics of materials and components as realistically as possible. Moreover, those also require a probabilistic approach, which often makes them observation variables for the analysis, i.e. for a reasonable price range there are multiple work out of our model in the same ratio of seismic intensity. Variable parameters of the computational model, according to the literature, can be other than construction and geotechnical characteristics (usually through random intrinsic nature of the materials), parameters related to seismic stimulation and as an extreme example, the subjectivity in the assessments of experts surveyed in the empirical growth fragility curves.

Once resolution of the computational model with different sizes of the parameter observation for each of the considered values of the chosen measure of seismic intensity is done, the histogram of density events per damage ratio (normalized discrete values) is created. Then, there is a statistical analysis of these results of the response of the structure and the adjustment, as estimated, of the more appropriate probability density so that now, through the integration of the corresponding region between desirable - in the levels of damage - damage index range, are considered the cumulative chance of exceedance level damage for each indicator of seismic intensity.

It, therefore, derives the desired fragility curves through a new adaptation curve shape function cumulative probability in the points that express in cumulative probability of exceeding each level of damage. Thus, it can be a family of fragility curves which consists of many curves as there are designated distinct levels of damage. Each fragility curve shows the conditional probability of exceeding a certain

level of failure under the seismic loading of certain intensity, and as you might expect, the price curve for some such tension is always greater for lower level harm.

At the moment there was a general overview of concepts and choices inherent in creating fragility curves or tables of potential harm. Below and in order to understand the implementation steps of the method, the utility and its extensions, we will refer to a fully-developed applications, which are selected in such a way as to highlight specific features. So then, we will refer extensively to the development of analytical methodologies, which have varied interest and limit the scope of use of the method.

2.3. Applications of empirical fragility curves

2.3.1. Application by NCEER-ATC

The initials NCEER stand for National Center for Earthquake Engineering Research in the U.S. This research center was established to expand and disseminate knowledge on earthquakes to improve the seismic design and propose relief measures against seismic events in order to minimize loss of life and property. Emphasis is given on construction of the eastern and central United States and in vital networks across the country located in areas of low, moderate and high seismicity. One of the applied research programs of NCEER refers on buildings (Building Project) and focuses on assessing the situation and on proposing any interventions in areas of moderate seismicity.

Under the Plan of Buildings, the research focuses on risk and reliability matters in order to reduce the uncertainty of existing analytical models that provide imported seismic ground motion, the resulting structural damage and the limits of functionality of the system. The aim is to finalize the analytical and empirical procedures to bridge the gap between traditional anti-seismic engineering and socioeconomic considerations towards addressing the destructiveness of the earthquake at a reasonable cost.

In this study, among the many topics examined towards this direction, we are mainly interested in the study of seismic damage and the development of fragility curves for existing structures. So we will deal with the services provided by the promoters of research (ATC, Stanford University) improved relations faults - seismic tension, which

arose under the existing DPM in ATC-13 (Applied Technology Council) and hope to be applied to studies of seismic faults and losses at the local level.

With the publication of ATC-13, "Earthquake Damage Evaluation Data for California" (Seismic Damage Evaluation Data for California), which took place in 1985 there were developed relationships faults - seismic motion on 78 categories of construction (building or otherwise) of California. To overcome the limitations due to the non-sufficient number of available data, questionnaires were submitted to groups of experts who were asked to estimate the probability of failure for each category of construction at different levels of tense of ground motion. The 'Delphi' process followed, in order to gather the different views and so the DPM were developed by collaboration among them. For each of the 78 categories of building, a list of DPM was developed, which linked the tense of seismic excitation, in terms of ranking of the modified scale Mercalli (MMI), with an estimated from the research range of faults.

The scope for improving the DPM in ATC-13 is initially identified. The first area to apply the changes lies in the development of detailed descriptions of 40 planned building construction categories, so as to specify the assumptions made on the freight system and the standard design practices and manufacturing. The 40 categories of ATC-13 can be reduced to 17 if the only considered parameters for classifying them are the type of framing and the structural materials. Detailed descriptions are developed for these 17 categories and include elements of the structural system for building materials, the system cargo weight and resistance to lateral loads.

There is still discrimination in the quality design and construction to Non-Standard, Standard and Special. Finally, a descriptive interpretation of the designated levels of injury (slight, light, moderate, heavy, major, destroyed) is given for each type of construction and matching to a range of values in terms of failure rate: dollar loss / replacement cost, equivalent to the cost ratio repair / replacement costs.

A second intervention relates to the modification of relations damage-seismic tension by facts. After 1985 several destructive earthquakes in California gave data damage that could be incorporated into the statistical analysis. However, many of them have been collected in such a manner as to make them non-useful for the extraction of the probability of failure. The manufacturing category, the location, the size of the seismic excitation or the extent of damage, but even the total number of examined buildings are some of the necessary information but are often not available.

Existing techniques and reconnaissance reports were key sources of data. Other data sources are the inspection reports of damage of FEMA (Federal Emergency Management Agency), municipal and provincial records and databases that were created specifically to identify damaged property and bad press status (red tag) of buildings after an earthquake. After reviewing most of the available data, published and unpublished, it is clear that a more systematic method of collecting data is needed, if we want to actually improve relations predicting vulnerability of seismic events by integrating them. It should also be noted that these data are usually designed for other applications than the association of damage with ground motion. Beyond this, however, no logical basis method is yet recommended for the balance of opinion over the specific facts. A reasonable choice is the interest to opinions of experts according to the number used in the development of relations between seismic tensions - damage. But this solution is not good enough because a very small amount of data is needed to virtually eliminate the contribution of experts.

Bearing in mind that they have come to their conclusions after having examined several buildings, a logical approach would yield a little more per expert. But the application of Bayes techniques does not seem to be possible, giving the deadlock in the analytical combination of seismic data in the existing ATC-13 chance of failure.

The third variation of the relation ground motion - damages is considering the growth of fragility curves based on the statistical analysis of the values of DPM for the 40 construction categories and the 6 levels of damage (lognormal allocation adjustment for easy use and application in local-scale studies assessing damage and casualties). This modified presentation allows the supervisory comparison of the failure probabilities for different types of bearings and can exploit to the maximum extent both experimental and analytical techniques. The resultant of these curves can be compared with empirical fragility curves and may be combined. Also is now quite easy to identify inconsistencies in the opinion of experts, with evidence - for example - to reduce the potential damage to growing MMI.

The curve fragility is likely to approach some level of damage as a function of ground motion. As mentioned above, down 6 levels of damage are delineated by selected ranges in ground fault indicator (cost of repair / replacement costs). The main indicator of failure is defined as the value in the middle of the range of the level of damage. The best estimators of failure indicators are calculated per construction

category, with three grades (low, mean, high) for each index value of seismic tension MMI. For a given MMI there is a 0.9 possibility the damage indicator to be between low (low) and high (high) estimator.

According to these data, the parameters of the probability density function (pdf of) beta are calculated, which will adjust in the points of observations (of expertise) for each construction category and MMI rank. The function can be either symmetric or shifted to the right or left, depending on the values of parameters. Thus, for low levels of ground motion is expected to shift to the left, i.e. to levels of less serious damage, while respectively, most likely the most relevant failure (powerful earthquakes) allocation will lean to the right.

For each construction category, therefore, are developed seven probability density functions beta (MMI = VI, VII, VIII, IX, X, XI, XII). The probability of failure to be within the range df and df + Adf in terms of damage (damage factor - DF) is expressed by the square footage of the area bounded by these limits in the p.d.f.In each case, fragility curves are calculated by integrating the appropriate functions of beta distributions so as to take the chance of damage resulting ratios equal to or greater than a certain level. Then using the least squares methods, curves of lognormal forms are adapted by level of damage resulting in points for the various index values of seismic intensity.

The lognormal probability density function is of the form:

$$f_Y(y) = \frac{1}{y \cdot \sigma_x \sqrt{2\pi}} \exp\left[-\frac{1}{2}\left(\frac{\ln y - m_x}{\sigma_x} \right)^2 \right]$$

where X = lnY and σ_X and m_x are the parameters of the function, the standard deviation of lnY and its mean value, respectively. The Lognormal cumulative probability function is as follows:

$$P[Y \le y] = F_Y(y) = \int_0^y \frac{1}{y \cdot \sigma_x \sqrt{2\pi}} \exp\left[-\frac{1}{2}\left(\frac{\ln y - m_x}{\sigma_x} \right)^2 \right] dy$$

For fragility curves, y corresponds to the MMI and x to ln(MMI). It should be noted however that this function has no physical meaning as the cumulative probability function or the index damage DF or for the ratio of seismic tension MMI. It has only the form of the lognormal cumulative probability and describes the possibility that the construction suffers a given DF or higher, as a function of MMI. The lognormal functions are selected partly because of the computational facilities offered by the combination of many curves and because of the fact that they are well adapted to the discrete points (probability of exceedance level fault MMI) resulting from the processing of data in ATC-13.

This ambitious research program of NCEER leads to fragility curves for the 40 (ATC-13) categories of buildings. After some comparison between them all, relativity is marked per groups to the painted, under the above conditions, response of structures to earthquakes. This leads on one hand to conclusions that require further investigation on related behaviors of different structural systems and construction materials, and on the other means that the total number of curves could be reduced, with the creation of broader categories of construction (pre-existing merger), which also otherwise will facilitate the usability of the method under the varying and often vague input from local scale studies.

Table 2.3 Construction categories with similar fragility curves

Building Classes with similar fragility curves

Bui]ding Class	Similar to Building Class
3 - Low rise RC Shear Wall w/ MRF	84 - Low rise RM Shear Wall w/ MRF
4 - Medium rise RC Shear Wall w/ MRF	85- Medium rise RM Shear Wall w/ MRF
5 - High rise RC Shear Wall w/ MRF	86 - High rise RM Shear Wall w/ MRF
6 - Low rise RC Shear Wall w/o MRF	9 - Low rise RM Shear Wall w/o MRF
7 - Medium rise RC Shear Wall w/o MRF	10 - Medium rise RM Shear Wall w/o MRF
8 - High rise RC Shear Wall w/o MRF	11 - High rise RM Shear Wall w/o MRF
16 -Medium Rise Moment Resisting Steel Perimeter Frame	19 -Medium Rise Moment Resisting Ductile Concrete Distributed Frame
17 -Medium Rise Moment Resisting Steel Perimeter Frame	20 -High Rise Moment Resisting Ductile Concrete Distributed Frame

[9]

2.3.2. Application by "Hazus"

There is a more recent and specific variant of this methodology of development fragility curves, which constitutes a broad and comprehensive sensitivity analysis method of the uncertainty in the estimation of seismic losses realized by using the model of loss (economic and social) by disaster of the federal government of U.S. "HAZUS" (Hazard US), the University of Pennsylvania. As part of this analysis, surveys were carried out to gather information from experts on the vulnerability of the constructions, the benefits of strengthening a structure before the seismic event and its incorporation into Hazus. During the first half of 1998, questionnaires were sent to engineers, structural engineering, California, experienced in assessing the aftershock faults. The aim was to identify the expected benefits, related to strengthening the weak links through walls and rigid support in building construction, in wood (before 1940) urbanites Oakland and Long Beach, California.

The specific application differs from the study by NCEER - ATC, since both refer to a single adequately described building category and secondly examines the influence of structural parameters change through action by aid to the estimated from experts response of the structure. Despite this, however, introduces as proposal the adoption of some measures of reliability of these estimates, as the ranking of their experience in assessing earthquake damage (scale 0-10), by their own experts. Is also asked to be identified, in those estimated, the reliability of their views (scale 0-10) on the expected average damage index (Mean Damage Factor-MDF-) for the given structure before and after the intervention support for MMI levels ranging from VI to XII. As MDF is again the ratio of the repair costs to replacement costs. Obviously, the collected survey results are weighted by weighting factors so as to be appropriate for treatment. For comprehensive studies, there was a use of data by Bayes and adjusted the appropriate distribution points to the number of observations over MDF for a given MMI before and after the intervention scheme.

Then, the probability of failure tables (DPM) are developed for the five levels (none, slight, moderate, extensive, complete) set by the program Hazus, after having chosen the range of values in terms MDF for each one and the enclosing areas of p.d.f.are completed.

Then tables of cumulative probability of failure are developed, which reflect the probability that the failure is equal to or exceed a value which is MDF boundary levels of damage. For various levels of damage is calculated as usual, the probability of

exceeding them at MMI and the resulting points are adjusted below lognormal cumulative distribution. We proceed thus to the development of fragility curves of which are - at least qualitatively - the apparent beneficial effect of intervention measures (Figure 2.2). This study provides the possibility to change the measure of earthquake tense of MMI to PGA (Peak Ground Acceleration), by the following, proposed by Hazus empirical correlation:

MMI	VI	VII	VIII	IX	X	XI	XII
PGA	0.12	0.21	0.36	0.53	0.71	0.86	1.15

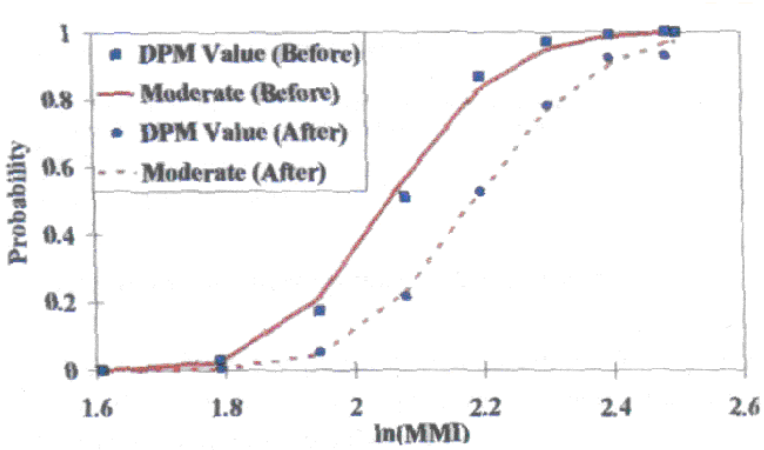

Figure 2.2: Cumulative lognormal distribution

But a new dimension to the use of fragility curves is given, while it refers to the Spectral Method Capacity (Capacity Spectrum Method - CSM) implemented with the conversion of PGA equivalent pair of spectral acceleration (SA) and spectral displacement (SD), through a supposing form spectrum demand response. In other words, a reference spectrum of demand response is developed, which intersects the strength of the structure to the average of the spectral shift for each of the predetermined levels of damage.

[9]

2.4 Applications of analytical fragility curves

The fragility curves, as mentioned, can be developed either empirically for derived values of the variable observation (of actual data or estimates by experts) or for prices, obtained from an analysis model of the construction with the suitable method.

It was extensively presented in the previous subsections the methodology of collecting empirical data and their use to fulfill this goal. Here, we will move smoothly into the development of more complex features and applications of the analytical method through a relatively simple example where there is a comparison of empirical and analytical fragility curves on concrete piers in Japan.

2.4.1 Comparison of empirical and analytical fragility curves on concrete piers in Japan

One of the most destructive earthquakes in Japan, the earthquake Hyogoken - Nanbu (Kobe) in 1995, caused serious damage to structures - motorway sections – in the area of Kobe. A family of empirical fragility curves was developed based on actual data from the earthquake disaster (Yamazaki et al., 1999). These empirical curves give a general idea about the relationship between levels of damage of similar constructions and ground motion indices. So they can be used to assess damage and for other similar bridges in Japan. However, empirical fragility curves do not specify exactly the type of construction, its behavior (static and dynamic) and the volatility of imported ground motion and thus they cannot be used reliably to assess the level of potential damage to the specific bridge. It is therefore an attempt to develop analytical fragility curves with simultaneous inspection of the construction parameters and variability of soil imported stimulation.

As studied construction is chosen a typical construction of Reinforced Concrete Bridge which platforms are examined, designed with the Japanese earthquake regulations of 1964 and simulated as systems of a degree of freedom (SDOF). A non-linear dynamic analysis is performed using 50 different acceleration chronoistoria of strong earthquake records Hyogoken - Nanbu, grouped at certain levels depending on the excitation considered as a measure of intensity (PGA or PGV).

A bilinear lacking model was used and the stiffness after the leak was taken as 10% of the stiffness of the release of radical (power drain / drain shift), at a rate of 5%. For the

assessment of damage to bridge piers we exploit the plasticity index of the top, which is defined as the ratio of maximum displacement (obtained by the nonlinear dynamic analysis) to shift leakage (from the elastic analysis). Practically, we use the ratio of damage (damage index-DI) in Park-Ang (1985), expressed as:

$$D.I. = \frac{(\mu d + \beta \cdot \mu h)}{\mu u} \quad (2.2)$$

where μd is the ductility of travel, the maximum drop mu ductility of the pedestal, b the cyclic loading rate assumed equal to 0.15 and μh the cumulative energy ductility defined as μh = Eh / Ee, Ee and Eh is the aggregate lacking and elastic energy of the radical respectively. For the various platforms of the bridge and the seismic loads which are characterized by the same normalized PGA, is obtained through multiple analysis, the dispersion of price indices of harm, who are categorized by level of damage to the calibration method proposed by Ghobarah et al. (1997):

Table 2.4: Relationship between D.I. and level of damage (Ghobarah et al., 1997)

Damage Index (DI)	Damage Rank(DR)	Definition
0.00 <DI<0.14	D	No damage
0.14<DI<0.40	C	Slight Damage
0.40<DI<0.60	B	Moderate Damage
0.60<DI<1.00	A	Extensive Damage
1.00<DI	As	Complete damage

[9]

Thus, with the possibility of classification of these indicators of failure, the number of observations belonging to each level of damage is taken for each level of arousal, whether expressed through PGA or a compatible price PGV. Macroscopically, it appears that with increasing excitation tense, the small number of incidents of damage is reduced while increasing that of total destruction.

Therefore, for each level of damage we have a set of data pairs: (PGA and damage index) or (PGV and damage index), from which we obtain the fragility curves of bridge piers with a case of lognormal distribution. The cumulative potential PR damage of equal or greater of R level is given as:

$$PR = \Phi\left[\frac{(\ln X - \lambda)}{\zeta}\right] \quad (2.3)$$

where Φ is the standard normal distribution, X is the index of ground motion (PGA or PGV), λ and ζ are the mean and standard deviation of InX.

Comparing empirical and analytical fragility curves is found remarkable agreement between them in terms of PGA, while there is difference in terms of PGV. Of course, we must not forget that the empirical fragility curves cannot include various structural parameters and characteristics of ground motion, as well as they require a large number of facts of a particular category of building damage. However, the analytical method used in this study is applicable to develop fragility curves regardless seismic construction experience.

2.4.2. Fragility curves for reinforced concrete structures in the region of Skopje

Below is a representative application of the general process of development of analytical fragility curves in two types of reinforced concrete structures (buildings higher / lower than 10 floors) in Skopje. The large number of parameters that shape the behavior of reinforced concrete structures under seismic loading and the significant range of possible values of the same characteristics of the earthquake require the probabilistic assessment of the vulnerability of this construction, in the form of relation seismic tension-damage.

It is crucial to choose a seismic tension indicator that describes as completely as possible, as the ultimate goal is to link this with the chance to overcome some level of damage. The peak ground acceleration (PGA) is a widely used measure of seismic tension, but reveals little information on characteristics of the earthquake as the width, frequency content and duration of the largest part of the earthquake. Given the lack of records and data on real earthquakes in the region, in this case-study were rejected the PGA and SA (spectral acceleration) as exponents of seismic tension and instead the levels of MMI were selected with the main disadvantage the subjectivity in assessing the damage. But, is positively work that both the existing data are denominated in this index and also there is already a sufficient number of relations

earthquake tense (MMI) - damage, which would allow for comparisons with the growth curves and tables fragility DPM.

The need for selecting a representative seismic excitations as loads given the limited number of recordings of strong seismic events in the region, led to the creation of synthetic accelerograms as input data in the analysis. So starting with a stationary stochastic process and then measuring the unsteady content of the backs of chronoistoria and integration of data focal mechanism of earthquake wave propagation, the methodology by Trifunac was chosen. According to this theory, the earthquake is defined as overlapping groups of waves with different speeds and frequencies, scattered through the background. The background is simulated by parallel layers of soil, defined by the thickness and the mechanical characteristics of the material, the dispersion of which arose from implementing the program in HASKEL by Trifunac. To determine the genesis parameters of representative values, was used the empirical simulation of expression of the spectrum width by Fourier [FS (ωn)] in terms of MMI, which produces synthetic earthquakes with maximum dispersion characteristics through actual birthplace of random numbers and the validity of influences parameters of the region, as the intensity of stimulation, the characteristics of the background, distance from the epicenter and two orthogonal horizontal components of earthquake.

So there was created a group of 240 synthetic accelerograms with changes in these parameters, which are controlled in terms of acceleration response spectra agreement with some real earthquake, showed that indeed includes features similar to those of existing records in the region. The synthetic earthquakes were categorized into five levels of MMI (VII 4 - XI) to act as compatible with the general methodology of growth curve fragility and DPM, and have been an input of the nonlinear dynamic analysis of representative structures [select 6-storey 16-storey (with core walls) framed building consisting of beams and columns of reinforced concrete]. To clarify here that the random nature of construction, is not taken into account in developing of relations earthquake tense - damage. It also is too extreme the uncertainty associated with earthquakes, which was chosen to analyze thoroughly that the variability of the characteristics of the structure (e.g. material properties) can, in this study, be ignored.

The response of the examined structure obtained by nonlinear analysis (IDARC - 2D program, v.4.0) is calibrated by selecting the amount of DI as a measure of the damage caused, where:

$$D.I. = \frac{\delta_{\mathrm{M}}}{\delta_{\mathrm{u}}} + \frac{\beta}{Q_y \delta_u} \int dE \quad (2.4)$$

The quantities involved are defined by Park-Ang as the maximum deformation under earthquake (δM), the maximum deformation under monotonic loading (δu), the estimated yield strength (Qy) and the increase in absorbed lacking energy (dE). The damage is therefore a linear combination of maximum deformation and lacking energy due to decay, providing an adequate combination of accurate assessment and simplicity. The total damage index (DI) of the construction appears to be the average DI of individual items. The definition of five levels of damage is done in terms of DI with more stringent the one proposed by Park - Ang consideration (which criterion is the economic cost to repair the building under a large number of experimental investigations on data or simple structures) for security.

Before the final stage of development of the fragility curves, is determined analytically, by a slight exception of formal methods, the cumulative probability curve where the considered construction is not more of a specific value DI value for a given MMI and finally, the resulting points ({sum.possibility, DI } / MMI) a normal distribution is adjusted. Then a possible fragility point of a curve is defined by the conditional probability of failure due to earthquake of certain tense Ij to exceed the level of (i):

$$P_{\mathrm{fij}} = Ver, \left(DT \geq DT / \mathrm{MMI} = \mathrm{I}_j \right) \quad (2.5)$$

where DT is the overall DI for earthquake MMI = Ij and DTi the equivalent of (i) level of damage.

[9]

The DPM is another possible form of relation earthquake tense- damage, since each price is likely to approach a certain level of damage.

The described fragility curves development and DPM for two representative buildings of reinforced concrete results in the evaluation of the current provisions of seismic regulation of Skopje, in accordance to which elastic analysis is applied and

equivalent static method for the introduction of seismic loading. Nevertheless, it appears to provide adequate description of the behavior of what are the types of construction purposes, the nonlinear dynamic analysis showed that there is about 50% probability to occur at no or minimal damage in the design earthquake tense. Finally, comparisons of compatibility of the results were similar in both empirical and are similar to the wider application of the general process of development of fragility curves and generally proved successful.

CHAPTER 3

THE METHOD OF FINITE ELEMENTS

3.1 General

The traditional methods for analyzing structures were and still are powerful tools in the hands of engineers. They face successfully a large number of problems related to the static behavior of some players (frames, trusses, linear operators, etc.). All these methods are based on assumptions of classical theory of bending, such as maintaining the flatness of the cross section height. But there are cases of players, who are exempted from these assumptions and their treatment becomes problematic. Examples of such players are the short overhangs, the height beam, the slabs, shells, the flat discs walls, columns and some other types of structures. For the analysis of these cases construction there should be done use of a more accurate method to solve the body, as the one described using the equations of elasticity. Solving a system of equations of elasticity, always gives a more accurate solution. But in cases like in the above players as well as in the majority of the players in practice, the topology data entity, the charge and the conditions of their support, are making it quite difficult to resolve, or in some cases, practically impossible. The need to address such situations, led to the search for new methods of structural analysis.

The finite element method (FEM, Finite Element Method) appeared before about 50 years to fill this gap. Its presentation on a mathematical level is placed at the end of 1943, in a Courant's work on the torsion while in matter of technological application, is located in the two years 1954-56, in the work of Argyris in London and Clough's at Berkeley.

It should be noted that the first application of the logic followed by the finite element method, was in ancient Greece by trying to calculate the length of the circumference of the circle, using the registered polygons.

The basic idea behind the finite element method is the substitution of the actual construction with a simulation, whose individual parts constitute its parts. The main feature of this method is to divide a structure into smaller finite elements, each of which has defined characteristics and boundary conditions. This means that dividing the total system into several finite elements has as result to require the solving of a

very large number of equations. This had as a result until recently that the application of this method is relatively limited. But the rapid development of computers and their dissemination to the public made possible the resolution of vectors with finite data from a large percentage of engineers and has resulted in the current widespread application of the method.

The finite element method even if it also represents an approach (compared with the solution obtained by solving the system of equations of elasticity), gives the 'desired' accuracy in solving the problem of analyzing the behavior of structures. A key drawback of the method, when developed, was the large computational cost. The main feature of this method is to divide a structure into smaller finite elements, each of which has defined characteristics and boundary conditions. This means that dividing the total system into several finite elements is that they require solving a very large number of equations.

For the analysis, according to the method of finite elements, the construction is discretized by using finite element or three-dimensional shell elements, as shown in the diagram for the classical structure of Chania, which was studied. The mass of data collected in the nodes so as to achieve a better distribution of mass throughout the manufacturing and a good simulation of inertial forces during the dynamic analysis. Here is a schematic simulation of the neoclassical building of Chania on the southwest side, which was done according to the method of finite elements.

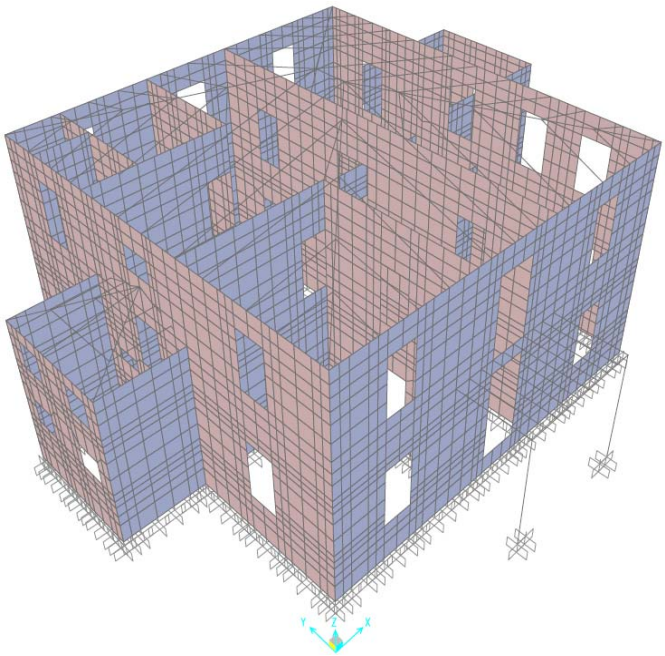

Image 3.1 Simulation of building with the finite element method

Until recently this method was relatively limited. But the rapid development of computers and their dissemination to the public made possible the resolution of vectors with finite data from a large percentage of engineers and has resulted in the current widespread application of the method. Now this method is used by all types of engineers such as the mechanic engineers, shipbuilders, the constructors, architects and civil engineers. Also, the research on this method continues rapidly while continuously new software programs using it are circulating as well as bibliography that presents it to the public.

3.2 Application of the method in construction analysis

To analyze the organization of a structure (e.g. a building) with finite elements, it must be the appropriate modeling of such institution. This is done at first with the mathematical description of the body and then with the numerical analysis of the extracted from this description mathematical model. To make it possible to describe a body in a mathematical way, idealizations in the body and its environment must be done, regarding on the geometry, behavior, etc. Moreover, it is necessary to make certain assumptions such as that the material of the body behaves as linearly elastic. The mathematical of the numerical model is the solution of the system of equations resulting from the idealization of the body. Because these systems are very complex in real applications, large computational power is required in order to solve them.

So to solve a structure with finite elements, first the body must be divided into finite elements. Depending on the precision required, the shape of the body, but also the computing capabilities that exist, the type of finite elements should be chosen as well as the size of each of them. In other words, the number of elements that divide the body. Always accuracy at the expense of computational burden and vice versa. Then follows the formulation of the balance equation: [k] {d} = {r} of each element by calculating the stiffness identification of the element and the loads on nodes. With the help of this equation we can calculate the strain record, {d}, of each point of the item. Once the stiffness of each of the elements on which is divided the body is registered, it is possible to calculate the stiffness of the entire registry operator. Moreover, since the loads and the displacements of all elements of the body are calculated, the body has

been resolved and the intensive sizes and deformations at each point of the body are known.

The wording of the balance equation can be done in two ways, with the **Principle of Virtual Work** and the **Authority of Changes** and the **Method of Weighted Balances**.

3.3 Formulation of equilibrium equations of the finite element method with the Principle of Virtual Work

Suppose we consider a three-dimensional elastic body which is defined in the global Cartesian coordinate system, whose equation of equilibrium must be formulated such as body shape 3.2.

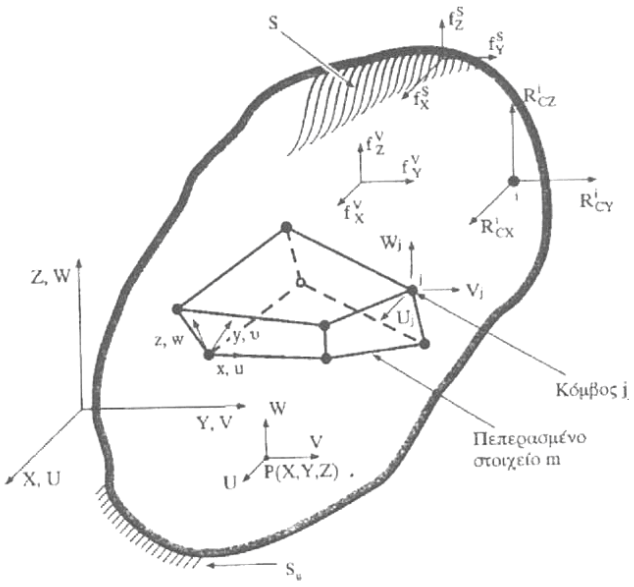

Figure 3.2 Full length three-dimensional six-sided body discretized with eight node finite element

The external actions to which a player is submitted are surface in the area of the surface S, the mass actions and the nodal actions in the node i, which vectors are fs, fv, Ric. Shifts of a random point P (X, Y, Z) of the body, in the universal system are given by the vector:

$\{ U(X,Y,Z) \}=[UVW]^T$ (3.1)

In an elementary parallelepiped body we have the following stresses and strains:

$\{\sigma\}=[\sigma_X \sigma_Y \sigma_Z \tau XY \tau_{YZ} \tau_{ZX}]^T$ (stress vector), (3.2)

$\{\varepsilon\}=[\varepsilon_X \varepsilon_Y \varepsilon_Z \gamma_{XY} \gamma_{YZ} \gamma_{ZX}]^T$ (deformation vector), (3.3)

where γ represents the converted angular deformities:
$\gamma_{XY} =2*\varepsilon_{XY}$, $\gamma_{YZ}=2*\varepsilon_{YZ}$, $\gamma_{ZX}=2*\varepsilon_{ZX}$. It should be noted that it is assumed that the material of the body is linearly elastic.

To express the equation of equilibrium of this body, the principle of virtual work will be applied. In this method, as is well known from engineering, it must be assumed that there exist conditions of small offset so that the equilibrium equations can be formulated based on the geometry of the undeformed body.

According to the Principle of Virtual Work: "When the body is charged with external loads and balances, then for any small deformation of the body possible, compatible with the conditions of support, the possible work of internal forces is equal to the work of external forces" . In this case the equation of the principle of virtual work is written:

$$W_{\text{int}} = W_{ext} \leftrightarrow \int \{\varepsilon\}^T \{\sigma\} dV = \int \{U\}^T \{f^V\} dV + \int \{U^S\}^T \{f^S\} dS + \{D\}^T \{R_C\} \quad (3.4)$$

In the above equation, the tensions { σ } are the tensions that balance the external loads. The possible displacements, {U}, are a continuous field of possible displacements, compatible with the conditions of support.

To find the registry stiffness of each element of the body, the wording of the relations between deformations and displacements of the element is required.

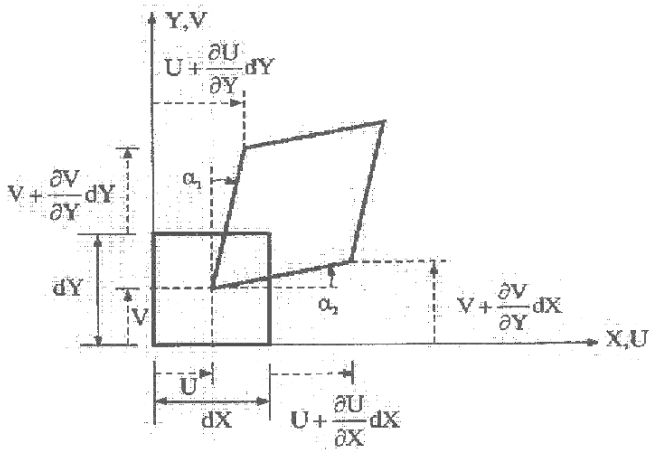

Figure 3.3 Deformation of elementary rectangular dX-Dy

As shown in Figure 3.3, the displacements U and V are functions of the coordinates X, Y: U = U (X, Y), V = (X, Y). Assuming small deformations and after operations, the relationship of reduced distortion - shifts for each element of the vector are defined:

$$\varepsilon_x = \frac{\theta U}{uX}, \varepsilon_y = \frac{\theta V}{\theta Y}, \varepsilon_z = \frac{\theta W}{\theta Z} \tag{3.5}$$

$$\gamma_{XY} = \frac{\theta U}{\theta Y} + \frac{\theta V}{\theta X}, \gamma_{YZ} = \frac{\theta V}{\theta Z} + \frac{\theta W}{\theta Y}, \gamma_{ZX} = \frac{\theta W}{\theta X} + \frac{\theta U}{\theta Z} \tag{3.6}$$

In registral form the above relations can be written:

$$\begin{bmatrix} \varepsilon_X \\ \varepsilon_Y \\ \varepsilon_Z \\ \gamma_{XY} \\ \gamma_{YZ} \\ \gamma_{ZX} \end{bmatrix} = \begin{bmatrix} \theta/\theta X & 0 & 0 \\ 0 & \theta/\theta Y & 0 \\ 0 & 0 & \theta/\theta Z \\ \theta/\theta Y & \theta/\theta X & 0 \\ 0 & \theta/\theta Z & \theta/\theta Y \\ \theta/\theta Z & 0 & \theta/\theta X \end{bmatrix} \cdot \begin{bmatrix} U \\ V \\ W \end{bmatrix} \tag{3.7}$$

or

$$\{\varepsilon\} = [\theta_\varepsilon] \times \{U\}$$

Below is the link between stress and strain of each item. According to the law of Hooke (the tensions are linear functions of the standardized strain) and with the assumption of small deformations the following relations are resulting:

$$\begin{matrix}\{\varepsilon\}=[C]\times\{\sigma\}\\ \{\sigma\}=[\mathrm{E}]\times\{\varepsilon\}\end{matrix} \quad \text{ή} \qquad (3.8)$$

and taking into account the initial stresses and strain, it results:

$$\{\sigma_t\}=[\mathrm{E}]\times(\{\varepsilon\}-\{\varepsilon_0\})+\{\sigma_0\} \qquad (3.9)$$

where $[E] = [C]^{-1}$. Finally, results the relation for the registry [E]:

$$\underset{(6\times6)}{[\mathrm{E}]}=\frac{\mathrm{E}}{(1+\nu)(1-2\nu)}\begin{bmatrix}1-\nu & \nu & \nu & 0 & 0 & 0\\ \nu & 1-\nu & \nu & 0 & 0 & 0\\ \nu & \nu & 1-\nu & 0 & 0 & 0\\ 0 & 0 & 0 & \frac{1-2\nu}{2} & 0 & 0\\ 0 & 0 & 0 & 0 & \frac{1-2\nu}{2} & 0\\ 0 & 0 & 0 & 0 & 0 & \frac{1-2\nu}{2}\end{bmatrix} \qquad (3.10)$$

and for the registry [C]:

$$\underset{(6\times6)}{[C]}=\frac{1}{\mathrm{E}}\begin{bmatrix}1 & -\nu & -\nu & 0 & 0 & 0\\ -\nu & 1 & -\nu & 0 & 0 & 0\\ -\nu & -\nu & 1 & 0 & 0 & 0\\ 0 & 0 & 0 & 2(1+\nu) & 0 & 0\\ 0 & 0 & 0 & 0 & 2(1+\nu) & 0\\ 0 & 0 & 0 & 0 & 0 & 2(1+\nu)\end{bmatrix} \qquad (3.11)$$

In the case where the body before the deformation, due to the external tension, pre-exist initial tensions $\{\sigma_0\}$ with zero deformation, then the final tensions {st} resulting : $\{\sigma_t\}=\{\sigma\}+\{\sigma_0\}$, while in case of initial deformation , $\{\varepsilon_0\}$, which have not caused tensions should be taken into account as follows: $\{\sigma\} = [E]^*(\{\varepsilon\}-\{\varepsilon_0\})$.

Since the wording of the relation between shifts and tensions with reduced deformation of each element is done, then follows the determination of the shape function [N (X, Y, Z)]. This function multiplied with the register of nodal displacements {d} = [U1 V1 W1 U2 V2 W2 ...] ^{T} of every part P (X, Y, Z) of the body, gives the components of the displacement of point U, V , W, in the universal system of the body. This is still one of the assumptions made in applying the finite element method and clearly defines its accuracy. In other words it exists:

$$\begin{bmatrix} U(X,Y,Z) \\ V(X,Y,Z) \\ W(X,Y,Z) \end{bmatrix} = \left[N(X,Y,Z)\right] \begin{bmatrix} U_1 \\ V_1 \\ W_1 \\ \cdot \\ \cdot \\ \cdot \\ U_{n_C} \\ V_{n_C} \\ W_{n_C} \end{bmatrix} \qquad (3.12)$$

The function of the shape to be used in each case depends on the type of finite elements. Also, the converted element deformations are a function of nodal displacements of the body through a compatibility registry [$t^{(m)}$] and deformation registry [$B^{(m)}$]: {ε^{m}} = [$B^{(m)}$][$t^{(m)}$]{D}.

The compatibility registry [$t^{(m)}$], is a Boolean registry, with terms 0 or 1, and connects the local with the catholic degrees of freedom of nodes of the element and reflects the condition of compatibility of displacements of nodes of the element with the nodes of the body which they represent. The deformation registry [$B^{(m)}$] of the element, links the vector of the strain of reduced nodal displacements of the element.

In the case of only nodal load and since the rigidity registries of the elements in the local coordinate system constitute the rigidity registry of the entire body in the catholic system, [K], and based on the possible strong nodal displacements and actions of the body which have been calculated above, results the equation of balance

of the body with nodal load: [K] {D} = { R_C }, where {D} is the vector of possible nodal displacements and { R_C } the vector of nodal activities of the body.

To find the general equation of equilibrium of the body we should take into account the equivalent actions in the nodes of body mass and surface forces and due to initial stresses and initial deformations. The equivalent operations in the nodes of the body mass and surface forces are:

$$\begin{aligned}\{R_V\} &= \sum \left[t^{(m)}\right]^T \int \left[N^{(m)}\right]^T \{f^{V(m)}\} dV_e \\ \{R_S\} &= \sum \left[t^{(m)}\right]^T \int \left[N^{S(m)}\right]^T \{f^{S(m)}\} dS_e\end{aligned} \qquad (3.13)$$

while the equivalent actions in the nodes of the body due to the initial strain $\{\varepsilon_0\}$ are:

$$\{R_{\varepsilon o}\} = \sum [t^{(m)}]^T \int [B^{(m)}]^T [E] \{\varepsilon_0{}^{(m)}\} dV_e \qquad (3.14)$$

and due to the initial tension $\{\sigma_0\}$:

$$\{R_{\varepsilon o}\} = \sum [t^{(m)}]^T \int [B^{(m)}]^T [E] \{\varepsilon_0{}^{(m)}\} dV_e \qquad (3.15)$$

thus, it can now be expressed the general equation of equilibrium of the body:

$$[K]\{D\} = \{R\} \qquad (3.16)$$

The corresponding balance equation of each element is written:

$$[k]\{d\}=\{r\}. \qquad (3.17)$$

[9]

3.4 Formulation of equilibrium equations of the finite element method applying the Principle of Change and the method of Weighted Balances

In the weighted balances method the calculation of the remaining stiffness registry is based on the principle of stationary value of the total potential energy in combination with the method of Rayleigh-Ritz. The Rayleigh-Ritz method is one of the methods of the changes which are alternative methods of applying the Principle of Virtual Work, since they give identical results with each other.

To implement the Rayleigh-Ritz method in one body, there must be a full relationship which contains the differential equations which describe the behavior of the body. In the considered method, the integral equation is the principle of the total potential energy. While with the typical differential equations of the problem, the problem is set to its strong form (that means that is satisfied for every point of service), with the integral formulation of integral equations, the problem is set to its weak form, which means that they met in an area of the body with an average price.

Alternative of the method of change is the method of Galerkin, which gives an approximate solution of differential equations with the endorsement test functions for the characteristic shifts of the problem, avoiding the complete version which is possible with the method of changes. This, although it’s improving the accuracy of the method of Galerkin, makes the wording more difficult.

3.4.1 The principle of stationary value of potential energy

The principle of stationary value of potential energy is: "Among all the kinematically reconcilably positions of a conservative system, those that satisfy the static equilibrium conditions give stationary value to the total potential energy of the system to small and kinematically compatible changes of its displacements".

A system is called conservative if the work produced by external forces and work strain is independent of the path between the initial and final position of the system. A conservative system has dynamic energy which is also called total energy is the sum of elastic strain energy and potential energy of external loads.

The strain energy of a finite element is given by:

$$U_p = \frac{1}{2}\int_V \{\varepsilon\}^T [E]\{\varepsilon\} dV \quad \text{Or, by setting} \quad \{\varepsilon\} = [B]\{d\}:$$

$$U_p = \frac{1}{2}\{d\}^T [k]\{d\}, \qquad (3.18)$$

while the strain energy of the whole body is written respectively:

$$U_p = \frac{1}{2}\{D\}^T [K]\{D\} \qquad (3.19)$$

where {D} is the vector of the nodal displacement of the body and [K] the stiffness registry of the body.

The potential energy of nodal loads $\{R_c\}$, mass actions $\{f^V\}$ and surface actions $\{f^S\}$ is given by:

$$V_p = -\{D\}^T \left\{ R_C - \int_V \{U\}^T [f^V] dV - \int_V \{U^S\}[f^S] dS \right\} \qquad (3.20)$$

The expression of total dynamic energy is the sum of potential energy with the strain energy:

$$\Pi = U_p + V_p \Leftrightarrow$$
$$\Pi = \frac{1}{2}\int_V \{\varepsilon\}^T [E]\{\varepsilon\} dV - \{D\}^T \{R_C\} - \int_V \{U\}^T [f^V] dV - \int_V \{U^S\}[f^S] dS \qquad (3.21)$$

The principle of the stationary value of the total dynamic energy is expressed by:

$$\delta\Pi = \delta U_p + \delta V_p \Leftrightarrow$$
$$\delta\Pi = \frac{1}{2}\int_V \{\delta\varepsilon\}^T \{\sigma\} dV - \{\delta D\}^T \{R_C\} - \int_V \{\delta U\}^T [f^V] dV - \int_V \{\delta U^S\}^T [f^S] dS \qquad (3.22)$$

In the case where pre-exist in the original body tensions and initial deformations, then {σ} in the previous link is replaced with:

$\{\sigma\} = [E]^*(\{\varepsilon\}-\{\varepsilon_0\})$ (3.23)

3.4.2 Application of the method Rayleigh - Ritz

In applying the method of Rayleigh - Ritz to a static problem, is set an approximate displacement field, with the help of which will be made the simulation of the actual deformation caused to the body. This conceptual field is obtained by superposition n kinematically acceptable deformations of the system.

That is the approximate displacements U, V, W of a sign of the body which define the scope of these displacements, resulting from the relationships:

$$U = a_l f_1 + \ldots + a_l f_1$$
$$V = a_{l+1} f_{l+1} + \ldots + a_m f_m \quad (3.24)$$
$$W = a_{m+1} f_{m+1} + \ldots + a_n f_n$$

where the coefficients α_i are called generalized displacements or generalized coordinates and the f_i (X, Y, Z) are kinematically admissible functions that reflect the deformed geometry of the shape.

After replacing the field of the shifts of these relations, the problem has now been simplified and has ***n*** degrees of freedom. After replacing these relations into the equation of the principle of the stationary value of the total dynamic energy, the principle of stationary value of dynamic energy is expressed by:

$$\delta\Pi = \frac{\theta\Pi}{\theta\alpha_1}\delta\alpha_1 + \frac{\theta\Pi}{\theta\alpha_2}\delta\alpha_2 + \ldots + \frac{\theta\Pi}{\theta\alpha_n}\delta\alpha = 0 \quad (3.25)$$

The above relationship is valid for any kinematically admissible deformation of the system. Consequently, it applies to the deformation defined by $\delta\alpha_1 \neq 0$ and zero all other generalized coordinates. Then the relationship becomes: $\theta\Pi/\theta a_1 = 0$. The same

can be done for all other degrees of freedom, with rotation of non-zero $\delta\alpha_i$, which would result n independent equations:

$$\frac{\theta\Pi}{\theta\alpha_i} = 0, i = 1,2,..., \text{n} \qquad (3.26)$$

By solving the system of equations we can find the generalized coordinates α_i, where the scope of shifts will now be known. With known displacements, the registry of the standardized strain {ε}, is easily calculated by their porosity. These tensions can then be found from the relation {σ}=[E]{ε}.

The method of Rayleigh - Ritz, as is clear from the above, gives a rough description of the displacement of the body. Obviously, the higher their number is, and as more suitable selected are the functions $f_i(X,Y,Z)$, the more accurate is the method.

3.4.3 The method of weighted balance

The method Rayleigh - Ritz, requires a suitable functional. But in some cases problems, this functional doesn't exist, so the above method cannot be applied. In these cases it can be applied the method of weighted balances. This method uses totalitarian expressions containing differential equations. If D and B are two differential operators, then the dominant differential equations and the natural boundary conditions of the problem can be formulated as follows:

DU-f = 0 at the field V (i)

BU-g = 0 at the border S of V (ii)

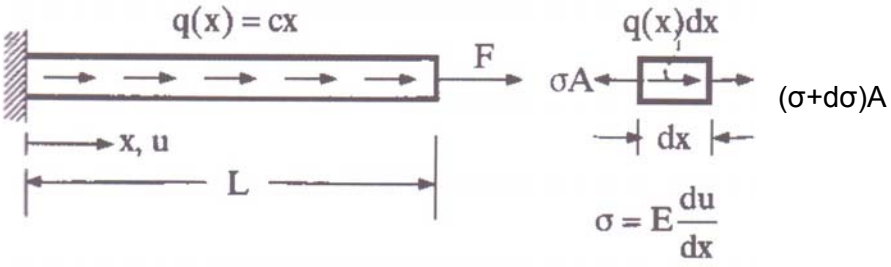

Figure 3.4 Prismatic bar with distributed and concentrated load at its end

So at the bar of Figure 3.4, which is loaded with axial distributed load q (x) and concentrated load F, the equation (i) is written:

$$AEu_{xx} + q = 0, \mu\varepsilon\ D = EA\frac{d^2}{d^2X}, \mu\varepsilon\ f = -q \qquad (3.27)$$

The equation (ii) is written:

$$AEu_x - F = 0, \mu\varepsilon\ B = AE\frac{d}{d\ X}, \mu\varepsilon\ g = F \qquad (3.28)$$

The solution Û is approximated with the help of a polynomial of unknown operators α_i. By replacing Û in (i) and (ii) and symbolizing R_D and R_B the non - zero balances because of the approximated nature of Û, are resulting the following relations:

$R_D(\alpha_i, X) = D\hat{U} - f$

$R_B(\alpha_i, X) = B\hat{U} - g$ (3.29)

The Galerkin method is the most common method of weighted balances. In this method, shape functions are chosen as the weights Wj = Wj (X). The average weighted remaining is zeroed throughout a field V:

$$R_{w_i} = \int_V w_i(X) R_D(a_{i,} X) dV, \text{ όπου } n = 1,2,...., n. \qquad (3.30)$$

In the method of Galerkin, the remainder RB, is used in the completion by members of the above relation, so as the natural boundary conditions to be also used. The weight functions are the coefficients of the generalized coordinates αi :

$$w_i = \frac{\partial \hat{U}}{\partial \alpha_i} \qquad (3.31)$$

3.5 Rectangular slab elements of four nodes and twelve degrees of freedom

We consider as degrees of freedom of each node, the sinking w and the slopes of the average surface of the component in x and y directions

$$\theta_x = \frac{\theta w}{\theta y},\ \theta_y = \frac{\theta w}{\theta x} \quad (3.32)$$

where the vectors of the turns are θ_X and θ_y and are parallel to the axes of x and y, respectively. Positive directions of the turns θ_X and θ_y follow the positive directions of the classical slab theory.

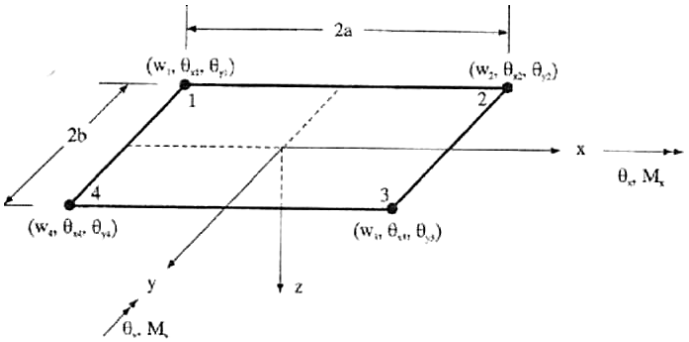

Figure 3.5 Rectangular slab elements of four nodes with the positive direction of turns and torque

In contrast, torques M_X, M_v (Fig. 3.5) follow the convention of the turns θ_X, θ_y, rather than the contract of the classical slab theory. Torques M_{xi} , M_{yi} (i=1,2,3,4) express nodal torques on the node i.

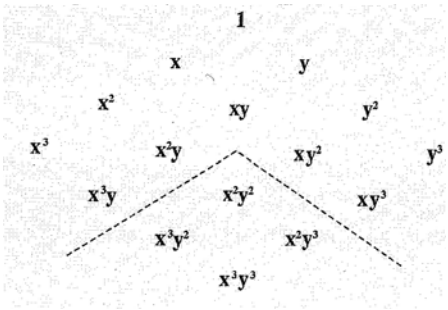

Figure 3.6 Pascal Triangle: The 16 terms of the product of two complete cubic polynomials and the 12 terms selected for the field of displacements of the rectangular slab element 12 degrees of freedom.

The polynomial expression of the displacement field will contain 12 terms arising from the triangle of Pascal. The displacements along each side of the element are defined according to four nodal displacements, two sinking and two turns which shall specify a cubic polynomial in χ and v respectively.

Therefore, the displacements resulting from the product of two cubic polynomials which contains a total of 16 terms of the triangle Pascal (see Figure 3.6). These terms represent a full exploded cubic polynomial in two directions. Of the 16 terms the 12 are selected, after the removal of higher order terms, so as to express the displacement field of the item. So the field of displacements is defined by:

$$w = a_1 + a_2 + a_3 y + a_4 x^2 + a_5 xy + a_6 y^2 + a_7 x^3 + a_8 x^2 y + a_9 xy^2 + a_{10} y^3 + a_{11} x^3 y + a_{12} xy^3$$

$$\text{ή} \quad \mathrm{w} = \begin{bmatrix} 1 & x & y & x^2 & xy & y^2 & x^3 & x^2 y & xy^2 & y^3 & x^3 y & xy^3 \end{bmatrix} \begin{bmatrix} a_1 \\ a_2 \\ \cdot \\ \cdot \\ \cdot \\ a_{12} \end{bmatrix} \quad (3.33)$$

$$\text{ή} \quad \{u\} = [x]\{a\}$$

The vectors of the nodal displacements and actions have the following form:

$$\{d\}=[w_1\ \theta_{x1}\ \theta_{y1}\ w_2\ \theta_{x2}\ \theta_{y2}\ w_3\ \theta_{x3}\ \theta_{y3}\ w_4\ \theta_{x4}\ \theta_{y4}]^T$$

$$\{r\}=[P_1\ M_{x1}\ M_{y1}\ P_2\ M_{x2}\ M_{y2}\ P_3\ M_{x3}\ M_{y3}\ P_4\ M_{x4}\ M_{y4}]^T \quad (3.34)$$

The shape functions derive from the relation:

which is expressed as follows :

$$w = N_1 w_1 \quad N^1_{\theta_x} \theta_{x1} \quad N^1_{\theta_y} \theta_{y1} \quad N_2 w_2 \quad N^2_{\theta_x} \theta_{x2} \quad N^2_{\theta_y} \theta_{y2} \quad N_3 w_3 \quad N^3_{\theta_x} \theta_{x3} \quad N^3_{\theta_y} \theta_{x3} \quad N_4 w_4 \quad N^4_{\theta_\chi} \theta_{x4} \quad N^4_{\theta_y} \theta_{y4}$$

$$\text{ή} \quad \underset{(1\times1)}{\{u\}} = \underset{(1\times12)}{[N]}\ \underset{(12\times1)}{\{d\}} \quad (3.35)$$

where [A] is the registry that links the nodal displacements {d} to the generalized coordinates {α} and

3.6 Rectangular membrane finite elements with transverse rotational degrees of freedom

The complex nature of most buildings and other civil engineering structures requires the co-existence of bar elements with membrane and slab elements in the same simulation model. A typical three-dimensional striatum element has six degrees of freedom per node, three advective and three rotational. A slab element has two rotational, with the torque vector on the plane of the element, and one transposable, perpendicular to this plane.

In contrast, a typical element is an element of flat tension-strain, which as described in the preceding paragraph, has two advective degrees of freedom per node on the plane of the item and no rotational. This implies that such an element cannot handle the bending torques applied perpendicularly to the plane of the element.

However, in many cases, there is requirement for undertaking such bending torques from membrane elements. So it raises the requirement for considerating membrane elements, which have, at each node, other than the two advective degrees of freedom mentioned, and torsion, corresponding to a torque vector perpendicular to the element. These elements are the membrane elements with transverse rotational degrees of freedom.

A rectangular membrane element with transverse rotational degrees of freedom, results from the corresponding rectangular element of flat tension - strain, following the steps below, as shown in Figure 3.7.

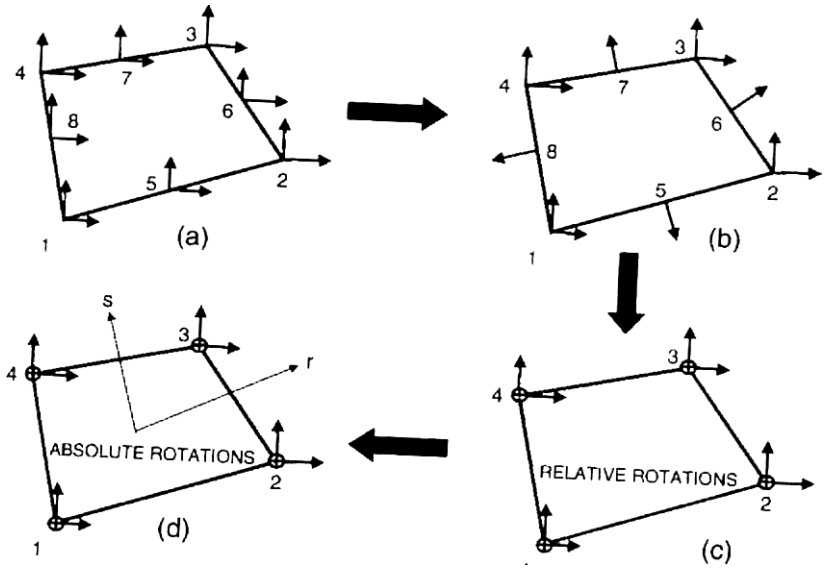

Figure 3.7 Steps followed to move from a rectangular element of flat tension - strain with nine nodes in a rectangular membrane element with transverse rotational degrees of freedom with four nodes

a. At first, a rectangular flat strain-tension element with nine nodes (eight at the perimeter and one at the center) with 16 degrees of freedom is considered (Fig. 3.7a).

b. Then, the relative displacements of intermediate nodes rotate so that they are vertical and tangents on each side and to zero the relative tangential displacement. In this way the degrees of freedom are reduced to 12. (Fig. 3.7b).

c. then, a blocking plate vertical deflection is inserted. This removes the four vertical deformations of the intermediate nodes and introduces four relative vertical rotations to the corner nodes (Fig. 3.7c).

d. The final stage involves the conversion of the relative vertical rotations to absolute vertical rotations and the conversion of the shape functions. Finally, the data generated has 12 degrees of freedom (Fig. 3.7d).

The relocations of the original element of the flat tension - strain are given by the formulas:

$$u_x(r,s) = \sum_{i=1}^{4} N_i(r,s)\,u_{xi} + \sum_{i=5}^{8} N_i(r,s)\,\Delta u_{xi}$$

$$u_y(r,s) = \sum_{i=1}^{4} N_i(r,s)\,u_{yi} + \sum_{i=5}^{8} N_i(r,s)\,\Delta u_{yi} \qquad (3.36)$$

From the relations of the relocations, eight shape functions are extracted:

N1=(1-r)(1-s)/4 N2=(1+r)(1-s)/4

N3=(1+r)(1+s)/4 N4=(1-r)(1+s)/4

N5=(1-r²)(1-s)/2 N6=(1+r)(1-s²)/2

N7=(1-r²)(1+s)/2 N8=(1-r)(1-s²)/2 (3.37)

After inserting rotation in the nodes, the equations of displacement are as follows:

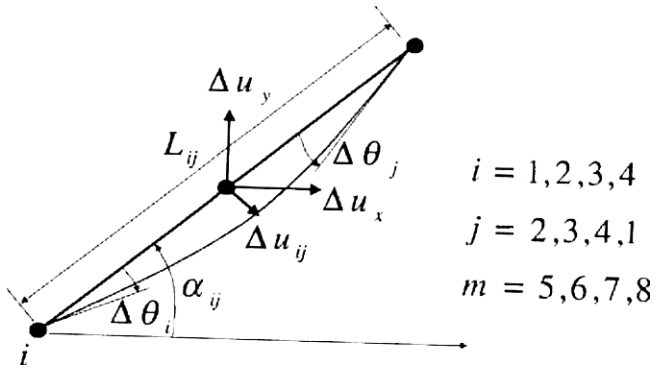

Figure 3.8 Typical side of a rectangular element

It is assumed that the deformation of the sides of the rectangle due to the existence of rotational degrees of freedom θ_1, θ_2, θ_3 and θ_4 is parabolic. Thus, the vertical deformation δ at midpoint of the side i - j of the rectangular element is equal to:

$$\Delta u_{ij} = \frac{L_{ij}}{8}(\Delta\theta_j - \Delta\theta_i) \qquad (3.38)$$

which means that when $\Delta\theta_i = \Delta\theta_j$ is the side which remains straight (Fig. 3.8). When $\Delta\theta_i = -\Delta\theta_j$, then the relocation Δu can be considered equivalent to the sinking of a simply supported beam of length L due to extreme torques that rotations $|\Delta\theta_i = \Delta\theta_j|$ produce to its edges. The components of δ in the x and y directions are equal to δcosα and δsinα respectively. Consequently, the total displacement of a point of the side i - j of the rectangular element is given by the sum of the linear displacement due to u_x, u_y and the parabolic relocation due to $\Delta\theta_i$, $\Delta\theta_j$. As the tangential displacement of

the middle nodes is zero, the total relative displacements of the middle nodes are given by the equations:

$$\Delta u_x = \cos a_{ij} \Delta u_{ij} = \cos a_{ij} \frac{L_{ij}}{8} (\Delta\theta_j - \Delta\theta_i)$$

$$\Delta u_y = -\sin a_{ij} \Delta u_{ij} = -\sin a_{ij} \frac{L_{ij}}{8} (\Delta\theta_j - \Delta\theta_i) \qquad (3.39)$$

The above equations can be applied to all four sides of the element and if they are replaced in the equations that give the displacements of the original element of flat tension – strain, derive the equations that give the displacements of a rectangular membrane element with transverse rotational degrees of freedom:

$$u_x(r,s) = \sum_{i=1}^{4} N_i(r,s) u_{xi} + \sum_{i=5}^{8} M_{xi}(r,s)\Delta\theta_i$$

$$u_y(r,s) = \sum_{i=1}^{4} N_i(r,s) u_{yi} + \sum_{i=5}^{8} M_{yi}(r,s)\Delta\theta_i \qquad (3.40)$$

The equation tension- displacement is as follows:

$$\begin{bmatrix} \varepsilon_x \\ \varepsilon_y \\ \gamma_{xy} \end{bmatrix} = \begin{bmatrix} B_{11} & B_{12} \end{bmatrix} \begin{bmatrix} u \\ \Delta\theta \end{bmatrix} \qquad (3.41)$$

where the element in order to satisfy the control of constant load correction, the registry B12, which is 3x4, should be amended as follows:

$$\overline{B}_{12} = B_{12} - \frac{1}{A\int B_{12} dA} \qquad (3.42)$$

The equation tensions- displacements can be written as follows:

$$\begin{bmatrix} \sigma_x \\ \sigma_y \\ \sigma_z \end{bmatrix} = \begin{bmatrix} D_{11} & D_{12} & D_{13} \\ D_{21} & D_{22} & D_{23} \\ D_{31} & D_{32} & D_{33} \end{bmatrix} \qquad (3.43)$$

The stiffness registry of the rectangular membrane elements with transverse rotational degrees of freedom is 12x12 and is calculated as follows:

$$\overline{K} = \int B^T D B dV \qquad (3.43)$$

3.7 Flat shell elements

As shown in the following schematic (Fig. 3.12), the surface shell elements result from the combination of the slab and membrane elements. The squared elements are 24 degrees of freedom while the triangulated are 18 degrees of freedom.

The stiffness registries for flat shell elements (squared and triangulated, respectively) are:

$$[K]_{24\times24} = \begin{bmatrix} [K_P]_{12\times12} & [0]_{12\times12} \\ [0]_{12\times12} & [K_M]_{12\times12} \end{bmatrix} \qquad (3.45)$$

$$[K]_{18\times18} = \begin{bmatrix} [K_P]_{9\times9} & [0]_{9\times9} \\ [0]_{9\times9} & [K_M]_{9\times9} \end{bmatrix}$$

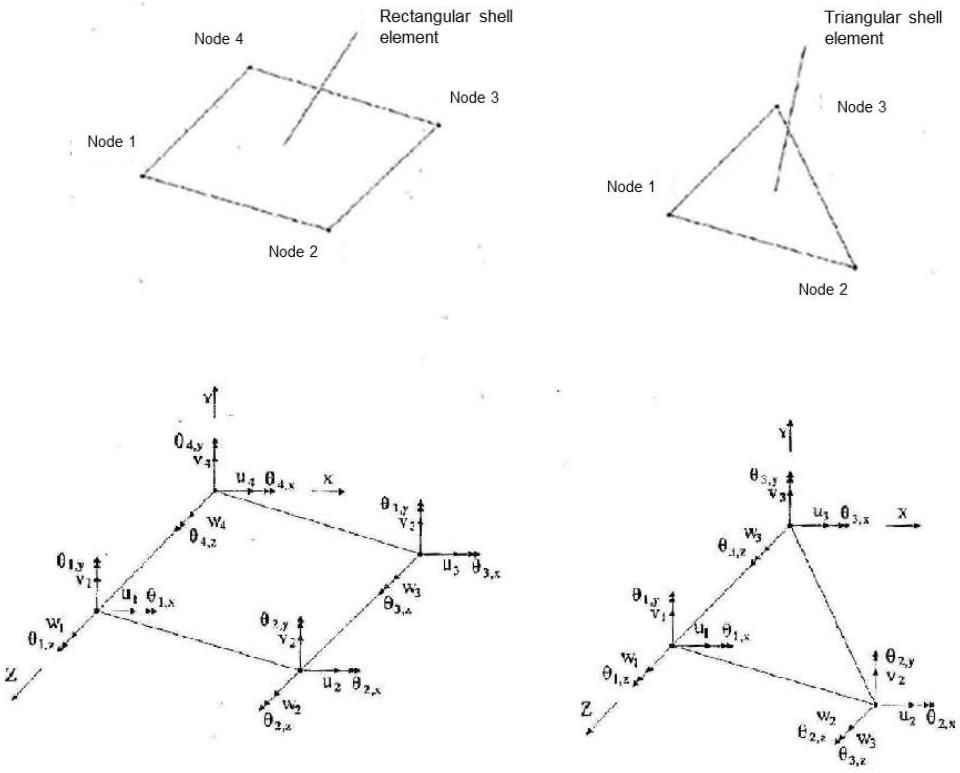

Figure 3.9 Flat shell elements

The slab elements have three degrees of freedom at each node, as shown in Figure 3.9, while the rigidity registries (squared and triangulated, respectively) are:

$$\underset{(12\times12)}{[K]} = \int_{A_e} \underset{12\times3}{[B]}^T \underset{3\times3}{[E]} \underset{3\times12}{[B]}^T dA_e \qquad \underset{(9\times9)}{[K]} = \int_{A_e} \underset{9\times3}{[B]}^T \underset{3\times3}{[E]} \underset{3\times9}{[B]}^T dA_e \qquad (3.46)$$

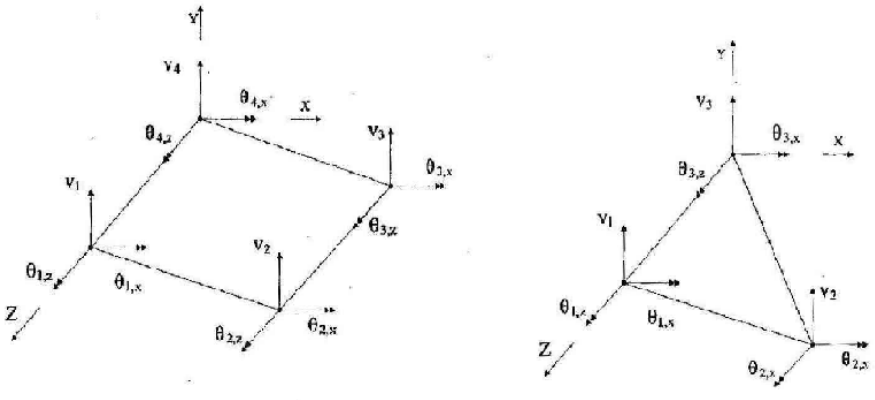

Figure 3.10 Flat slab elements

Finally, the membrane elements have three degrees of freedom at each node, as shown in Figure 3.10, while the rigidity registries (squared and triangulated, respectively) are:

$$\underset{(12\times12)}{[K]} = \int_{A_e} \underset{12\times3}{[B]^T}\ \underset{3\times3}{[E]}\ \underset{3\times12}{[B]^T}\, dA_e \qquad \underset{(9\times9)}{[K]} = \int_{A_e} \underset{9\times3}{[B]^T}\ \underset{3\times3}{[E]}\ \underset{3\times9}{[B]^T}\, dA_e \quad (3.47)$$

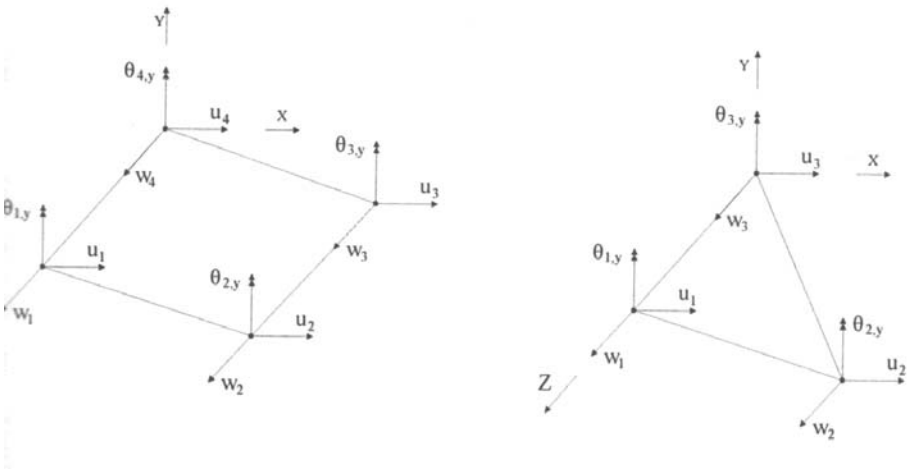

Figure 3.11 Flat membrane elements

3.8 Reliability of the finite element method

3.8.1 Simulation Stages

The finite element method is an approximate method of resolving partial differential equations and therefore requires some criteria for quality control of results as the exact analytical solution is not known.

In the analysis of structures with the finite element method these steps are followed:

1. Transition from the natural problem which is the construction, to the mathematical simulation, which means the body. During this stage there is the idealization of the construction in the form and structural function of its members. The members are classified in bars of the netting or the beam in two-dimensional wall members, discs or plates and shells in three-dimensional members. The material properties of the construction's members are determined, as well as their behavior during the load of

the structure (linear elastic, elastic perfectly plastic, rigid, etc.). The loads that weigh on construction are also determined and boundary conditions (idealization of the foundation, tied shifts, etc.). The mathematical model is governed by the prevailing balance differential equations and boundary conditions that characterize the behavior of the members of the body.

2. Transition from the mathematical model to the finite element simulation. At this stage is done the selection of finite elements for more appropriate modeling of the body. The network of finite elements is created for all members of the body. The records of stiffness and equivalent measures of data are calculated and educates the final registral balance equation of the body is formed.

3. Transition from the finite element simulation to the computational model. This stage includes the numerical treatment of the finite element model from the PC, is estimated the global record and the global stiffness of the equivalent vector operations. It follows the solution of equilibrium equations and the calculation of stress and intensive magnitudes.

Simulation Errors	- Members of the body simulation (beams, slabs, walls, shells, etc.) - Selection of boundary conditions - Loads simulation -
Discretization Errors	- Finite elements selection - Finite element netting form - Numerical completion of rigidity registry, equivalent actions vector - Non-linear kinematic condition assumptions and constituent relations
Numerical Errors	- Detachment errors while formatting the equations - Approximating errors while solving the equations

Figure 3.12 Errors of the finite element method

Stage 1 : Construction → Body

Stage 2 : Body → Simulation of finite elements

Stage 3 : Simulation → Computational simulation of finite elements

Figure 3.13 Simulation Stages

Figure 3.13 shows a schematic representation of the three stages followed in the analysis of structures by finite element method. At each stage there is a risk that a mistake depending on the severity could significantly affect the reliability of the analysis. These errors are divided into: (i) modeling errors which affect the degree of conformity of the body to manufacture, (ii) discretization errors that depend on the type and density of finite elements, (iii) the numerical errors which are due to finite accuracy with which transactions are carried out by the PC and which can significantly alter the final results.

3.8.2 Simulation of construction and results testing

To simulate a structure with finite elements is needed to understand the behavior of the structural design for selecting the appropriate type and number of items. You should avoid elements with poor geometry or big size, which are unable to capture sudden changes in the size of intensive construction, and also should avoid unnecessary densification of the network which requires time for preparation of data and computational work without providing more precision.

The verification of the numerical results is necessary because it is very easy to make mistakes in the simulation of the structure. First we check the shifts and compare the deformed geometry of the body with the expected, due to the specific load and support conditions. If the results obtained, differ significantly from the expected, then there should be an error in the simulation of the structure.

Then we check the stress distribution in the body. If the finite element code that we have is able to normalize the tensions at the nodes, then this possibility should be avoided, at least during the testing, because that is how is lost information as to the adequacy of the network of finite elements. A tension distribution with significant

discontinuity between the data is in a first declarative assessment of the inadequacy of the network.

As mentioned previously, to simulate the construction with the finite element method it requires understanding of the behavior of the construction of the loading that is submitted to, as well as knowledge of the properties and potential weaknesses of finite-elements to be used. It also requires knowledge of the assumptions that have led to the mathematical model and also limits the validity of those assumptions.

A structure with complex behavior or a numerical simulation with many degrees of freedom should be approached carefully and gradually. It is preferable to begin the analysis with special cases of boundary conditions and loading with sparse networks and making sure for the correctness of our decision to proceed to more detailed models for having taken into consideration the stress distribution or intensive quantities to members of the body preliminary analysis.

The choice of appropriate data depends directly on the form and the structurally function of the construction.

3.8.3 Element behavior control

A test way to monitor the effectiveness of finite elements and the correctness of the code we have is the experimental application in simple problems where the solution is known. With these applications is also controlled by the input, the use of coordinate systems, the calculation and graphical presentation of trends or intensive quantities.

The “joining” control is a first investigation of the properties of the element. A second test may be done by calculating the eigenvalue of the stiffness registry of the item. The eigenvalue control is carried out as follows: The singular and the natural frequencies of the item are calculated without frozen degrees of freedom and with a unit mass in each degree of freedom. The frequencies of the element are equal to the eigenvalues of the stiffness registry squared. Each eigenvalue is equal to twice the strain energy of the element produced by the same unique and reflects the strength of the element in a coordinate system in which the registry is a diagonal stiffness registry with zero non-diagonal terms. Consequently there should be as many zero eigenvalues as there are movements of the rigid body component (three levels of

problems and six dimensional). Less zero eigenvalues of the rigid body movements mean that any or some solid body movements cause tension, and more zero eigenvalue means that the element is unstable and shows deformation on the mechanism.

A third audit, which can reveal the strengths and weaknesses of the component is the control of the element - body. The analysis carried out in a body that consists of only one element. By changing the geometry of the element or the completion class of the stiffness registry, it can be revealed the sensitivity of the item on the order of numerical integration of the registry stiffness can reveal the sensitivity of the item on the order of numerical integration and non-normal geometry. In general, the data with regular geometrical shapes (equilateral triangular element - square quadrilateral element) gives greater accuracy.

Monitoring the behavior of the problems with known solutions is a sure way to control the speed of network convergence and the sensitivity of the element in irregular geometric patterns and networks.

3.8.4 Simulated loads

The concentrated loads with the exception of the intermediate concentrated loads on beam elements should be applied to the nodes of finite elements. When the application points of forces is known, then usually is properly configured the network to coincide with nodes of the network. According to classical theories of beams, slabs and flexibility at the point of a concentrated load are caused finite shifts and tensions in the beam, finite shifts and infinite tensions in the slab and endless shifts and tensions in the two-dimensional and three-dimensional whole-body operators. Also a really spotted load will cause leakage of the material in the vicinity area of the point of application.

Unlike to a point-load exerted on a node of a network of finite elements will not cause infinite shifts or tensions. In a two-dimensional or three-dimensional problem of elasticity, shifts and tensions will tend to infinite only with the gradual densification of the network in the area of enforcement charge.

A concentrated torque cannot be applied to a node with transportational degrees of freedom. In that case, it is replaced by the statically equivalent pair of forces to

adjacent nodes. The distributed loads on the volume or the surface of the elements are distributed at the nodes of the elements with the energetically equivalent procedure (procedure of wording of balance equations).

3.8.5 Numerical Errors

Numerical errors are presented during the formation of the stiffness registry and the vector of equivalent operations of the body as well as during the solving of the equilibrium equations and the calculation of intensive magnitudes. These errors, which arise in the numerical simulation, are due to the weakness of the arithmetic processor of the computer to perform operations with mathematical precision. The operations are performed by the computational accuracy of a number t of significant digits which depends on the processor type and on the single or double precision used in numerical calculations. Most computers store, after running an operation, the first t significant digits and cut off the rest. The impact of the limited computational accuracy is evident in cases of numeric non-stable entities to whom the records rigidity is bad.

Non-stable numerical bodies arise when there are large differences in the stiffness of the elements or the material properties of members of the body. They also arise when there are elements of large and small size in a network, and when with little strain energy, significant shifts in the solid body are developed. In all these cases a small change in the stiffness indicators or on the vector of equivalent actions of the body causes large changes in the calculated displacement vector.

3.8.6 Convergence of the finite element method

In case where the influence of other errors is neglected, it can only be appreciated the accuracy of the finite element model. The convergence of results obtained is explored by the gradual densification of the network of the finite elements to the results that would gave the ruling differential equations that describe, together with the boundary conditions, the behavior of the mathematical model.

In the very unlikely case of failure calculation of analytical solution, then control convergence of the finite element method is achieved with the satisfaction of bending, static and statutory conditions that characterize the mathematical model.

So the convergence control of the finite element method refers to the discretization errors and how they affect the convergence to the exact solution of the mathematical model. In linear elastic analysis the solution that exactly meets the prevailing differential equations and mathematical model is an accurate solution to the problem.

In the mathematical model of the structure, are satisfied the condition of compatibility of displacements and equilibrium condition at each elementary solid of the body. Unlike, in the finite element simulation these conditions are not met in each elementary solid of the body.

The compatibility condition of displacements of nodes of the elements with the nodes of the body is given by the expression of equilibrium equations of the problem and their solution to the nodal displacements of the body. The actions developed in the nodes of the elements satisfy the condition of equilibrium because they result from the nodal displacements of nodes on information obtained from the equilibrium {R}-[K]{D}=0 in each node.

The balance tension, however, in the interfaces of the elements shows a peculiarity. Figure 3.14 shows an example of two simple triangular elements of constant tension joined at junctions 2 and 3, where only node 4 is displaced. Because of this shift will only be develop in point b the constant tension σ_X so that the balance of the incremental solid in the interface 2-3 might not be satisfied.

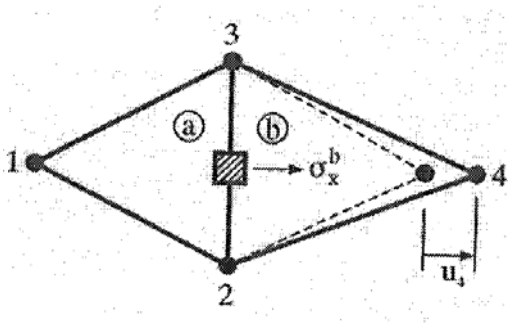

Figure 3.14 Tensions in primary solid surfaces on the interface of two triangular elements of constant tension

Generally there should not be expected to follow the tensions along the interface elements, such as balance and tensions in the common nodes of the elements. The discontinuities, however, are generally small in a well-structured network of finite elements with the appropriate type of data.

The balance of tensions within the data should also not be satisfied because the differential equations of equilibrium are usually not satisfied exactly in the data. To make it possible to approach the exact solution to the gradual densification of the network of finite elements we should aim to satisfy the boundary condition of equilibrium of the tensions within the data.

CHAPTER 4

MASONRY MECHANICS

4.1 General

Although the masonry was the basic structural material of history for whatever type of construction, its design was purely empirical until recently (at the early times of our century). The main reason is that the technology development and engineering led to the creation of strong and ductile construction materials (like steel and concrete) that reduced the cost of the bearing body and the uncertainties of the response of structures, resulting in deterioration of the masonry in the role of body filler.

As for the mechanical properties, the masonry is strongly considered as anisotropic material presented strong in compression, sufficient to shear and weak in strength as a result, the last two characteristics to be the main causes of failures. These weaknesses are not only due to the fragile nature of the bricks and mortar, but mainly on the behavior of interfacial contact in particular along the continuous horizontal joints designated as the "weak levels of masonry".

In recent years, however, there have been done significant research efforts to identify the properties and the response of masonry construction, with a view to strengthening the existing structures and the recovery of the reliability of the material.

4.2 Compressive strength of masonry

The compressive strength of the masonry is determined by many factors and thus the determination of its behavior is very difficult and the need for an experimental approach to the problem urgent. However, it is obvious that the rarely the resistance of an actual wall can be matched with that of specimens, even from the same material, and that because of the improvisation that exists in the construction of actual walls and other features that a real structure can have (e.g. existence of transverse walls). Therefore, the empirical relationship

that will be used to determine the compressive strength of the masonry shall take into account these elements.

Taking the above into account and knowing that the masonry is a composite material, made on site, is understood that its compressive strength depends on factors such as:

- The characteristics of the stone, meaning the resistance, the type and the geometry (solid, perforated, type and rate of holes, height) and their water absorption.
- The characteristics of the mortar, i.e. the strength and composition of the mixture (ratio of water to cement, water retention), the relative thickness of the mortar in relation to natural stone and the related deformation of both materials.
- The conditions on the masonry, that is how the way the stones are involved, the direction of load, the local stress increases, the enforceability of the load, etc.
- The material and thickness of the joint. It is observed that the more the ratio of the thickness of the joint to the amount of walls increases, more both the natural stone tends to fail due to lateral shift due to the deformations of the material of the joint.
- Construction details concerning: Concentrated loads, whose effect depends on many factors such as the ratio of loaded area to the length of the wall, the position of the load along the wall, how the load imposes on the thickness of the wall, the type and material of the masonry, the ratio of height to the length and thickness of the wall and the number of concentrated loads.
- Slots in the body of the wall, which is particularly harmful in thin walls and especially when they have horizontal or diagonal direction, thus affecting a large part of the wall.

- The quality of the construction as the masonry is constructed on-site by technical staff (whose experience ranges), under various climatic conditions, with materials which may not satisfy the requirements of the state (if any). As a result, the strength varies depending on these factors.

  [10]

4.2.1 Determination of compressive strength of the masonry

Calculation of the compressive strength of the masonry according to Tasio (1986):

$$f_{wc} = \frac{2}{3}\sqrt{f_{bc}} - \alpha + \beta f_{mc} \quad \text{(MPa)} \qquad (4.1)$$

where:

f_{bc} : the compressive strength of the wall

f_{mc}: the average compressive strength of the mortar.

α: pejorative factor for natural stone masonry, ranging from 0.5 to cut stones up to 2.5 for gravel (artificial stones for α = 0).

β: factor that takes into account the contribution of the mortar in strength and is β = 0.5 for masonry and β = 0.1 for bricks.

Where the proportion of the mortar is important, then it is calculated a reduced compressive strength by the following formula:

$$f'_{wc} \approx \xi f_{wc} \qquad (4.2)$$

$$\xi \approx \frac{1}{1 + 3.5(k - k_c)} \qquad (4.3)$$

Where:

k: the percentage by volume of mortar in masonry

- ko: the maximum rate of mortar, which is claimed to cause reduction of the strength of the wall and depends on the type of masonry. Is ko = 0.3 to rubble and bricks, and 0.2 for semi-ashlar masonry and 0.1 for ashlar masonry.

Compressive strength of masonry by EC 6 (prEN 1996-1-1:2001)

In the case of absence of experimental data for determining the mechanical properties of the masonry are used the following relations according to EC6.

- Compressive strength of masonry:

$$f_{wc} = K f_{bc}^{0.65} f_{mc}^{0.25} \quad \text{(MPa)} \qquad (4.4.)$$

Where:

K: factor depending on the type of the bricks (material, size and proportion of voids) and the type of masonry construction. It usually takes values from 0.40 to 0.60.

f_{bc}: compressive strength of brick

fmc: compressive strength of mortar

Table 4.1 Indicative values of masonry compressive strength

$f_{wc}(MPa)$	Unreinforced masonry	Brick masonry
Old Structure	1.25	2.50
New Structure	2.50	5.00

- Masonry flexibility measure :

$$E = 1000 * f_{wc} \qquad (4.5)$$

- Ratio Poisson v:

Recommended value from 0,20 to 0,30.

- Shear modulus:

$$G_W = \frac{E_W}{2(1+v)} \qquad (4.6)$$

4.3 Tensile strength of masonry

The tensile strength of the masonry is much lower than the compressive strength. Is highly unreliable because of the large dispersion its values and differentiates itself depending on the angle of the tensile strength in the horizontal joints that are considered weak levels.

The tensile strength of the masonry depends on the cooperation of the mortar with the walls, which in turn is composed of a number of factors, some of which are:

- Strength of mortar, which depends on its composition (content and quality of materials: sand, cement, water, chemical additives).
- The consistency of the mortar with the walls, a level of consistency between the two materials.
- The type of the wall especially the porosity, humidity, type of interface and its visual form (shape, presence and size of holes and slots).

The tensile strength usually refers to the direction of the level of the compressive strength, i.e. whether perpendicular to the joints or parallel to them. The tensile strength perpendicular to the joints will wear out when it comes the detachment of the two walls or because of poor link between natural stone - mortar or due to exhaustion of the tensile strength of the mortar. In the case of tensile strength parallel to the horizontal joints is observed great differentiation of strengths and types of failure as shown in Figure 4.1.

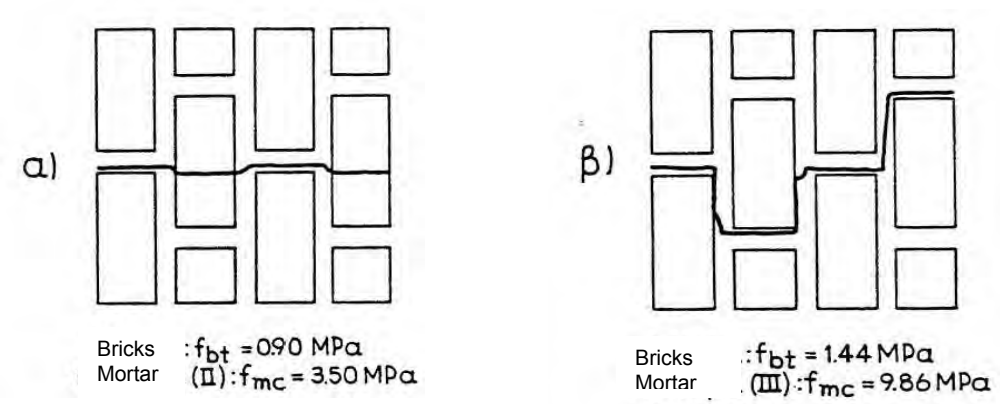

Figure 4.1 Forms of masonry failures under Direct Tension parallel to the horizontal joints (A) Weak Bricks (B) Strong Bricks

The Regulations do not use the tensile strength of masonry in the design. Instead, they specify the flexural tensile strength of the masonry for load perpendicular to its plane (earthquake, wind).

The flexural tensile strength to bending in a plane parallel to the joints has proved more than doubled compared with bending perpendicular to them.

f_{wt} perpendicular to the horizontal joints: f_{wt}= 0.70 f_{mt}

f_{wt} parallel to the horizontal joints: f_{wt}= 1.70 f_{mt}

where:

f_{mt}: the tensile strength of the mortar (indicatively f_{mt} = 0.1MPa)

The ratio of the two strengths depends on the following factors:

- The strength of the walls, because in case of tension parallel to the horizontal joints and for weak bricks, the vertical crack comes through the walls.
- The ratio of the sides of the walls, particularly for solid bricks, when the failure occurs by crack propagation through the walls.

- The existence of vertical compressive stress, which reduces the probability of failure perpendicular to the joints.
- The holes ratio, the strength of the masonry decreases as the percentage of holes increases.
- The interface between natural stone and mortar.

[11]

4.4 Determination of the shear strength of the masonry

In fact pure shear strength does not exist in nature since gravity creates vertical loading and only by the burdens of construction itself, so it is conceivable that shear "T" and right "σ_n" tensions coexist.

The main factors that determine the behavior of a wall are the mechanical characteristics of stone - mortar, the geometry and nature of the charges posed to them. In Figure 4.2 is shown the surrounding failure of the masonry in combination of charges (τ, σn) for all types of fracture of the wall, which are:

- Shear slip through the joints of the mortar, it happens for low values of compressive loads, where failure occurs by slip and separation of the joints (such failure is met on the walls).
- Diagonal tension cracking which penetrates bricks also and usually occurs in piers between openings. In this case, the masonry behaves as a homogeneous material where the mechanical characteristics are determined by natural stone and not by the mortar.
- Compressive failure due to shear that will occur when the right stress exceeds the strength of the wall in compression over the most compressed edge.

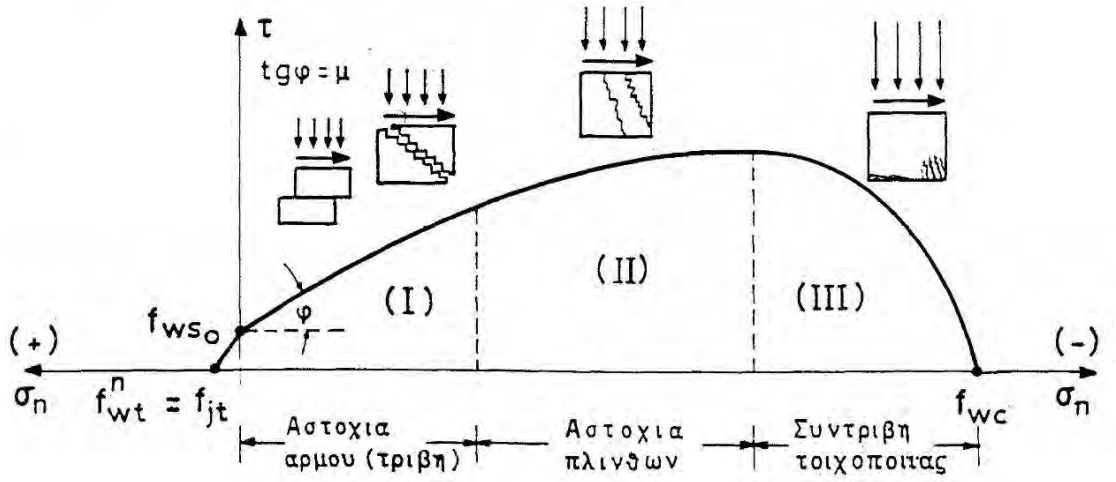

Figure 4.2 Standard form of masonry failure curve (T,Σn)

The masonry is considered as a surface form body which is imposed in random flat stress. This strain equivalent to a pair of main right tensions in whatever angle " θ " in relation to the horizontal joints.

On the masonry the direction of the main tension axis in the direction of joints determines also the form of its failure, unlike with the isotropic brittle materials (e.g. concrete), where is considered as given that the cracking occurs perpendicular to the principal tensile stress. So it is conceivable that for a specific charge to masonry, the surrounding failure is not unique as is the case for an isotropic material, but varies for each value of angle "θ ".

The axial stress, the compressive strength and the connection between natural stone and mortar determine the type of failure and the residual strength after cracking.

In cases where natural stones are quite strong and the axial load is small, the masonry is in danger of failure in the area of the joints. Energy absorption is achieved through friction and the residual carrier after cracking is satisfactory. Instead, to the bricks with small resistance and large axial loads, failure occurs with crossed cracking and breaking of the bricks. Please note that the failure is brittle in nature and the bearing capacity of the structure after cracking is inadequate.

CHAPTER 5

DEVELOPMENT OF FRAGILITY CURVES

5.1. Creation of Fragility Curves

To create the fragility curves three sets of input data are needed:

- Data on the intensity of the seismic event. It is done the determination of the characteristics of seismic risk and is introduced an indicator of seismic intensity. The range of variation of the index should be such that the response of the structure can be calculated when subjected to a future earthquake. The proposed methodology, the seismic intensity indicator is selected to be the maximum ground acceleration PGA = 0.16g, 0.24g, 0.32g and 0.40g [7]
- Data which describe the critical properties for the ability of the construction. To determine the features of the construction which have a random character and influence its behavior, the degree of importance of these parameters must be assessed. These parameters may be the mechanical properties of these materials such as the modulus and compressive strength properties of the subsurface platform construction and more. Another factor may also be the objective assessment of skilled scientists. But in determining the degree of importance of these properties is included the random nature and uncertainties, which necessitates the probabilistic approach to the problem.
- Data setting to determine the behavior of the structure and focus on economic, practical and functional requirements. In order to determine the effect of a random action in the construction, it is necessary to determine a response parameter in the construction so as to quantify the effects. The choice of an adequate response parameter is associated with the evaluation of seismic vulnerability of the construction. So it is chosen, to represent the seismic response of the construction, the behavior index (D.I.), which shall be equal, under the proposed methodology, to the ratio of the surface of the walls that have failed to the total surface of walls, as shown in Equation 5.1.

$$\mathbf{D.I. = A_{\beta\lambda} / A_{o\lambda}} \qquad (5.1)$$

Since the vulnerability of the construction depends on the extent of damage, a reference scale should be used to transform the quantitative values of damage index in qualitative descriptions of the extent of damage. The result of this qualitative presentation is the calibration of the response parameter index, using price thresholds. With the use of these damage boundaries, we have a distinction between three levels of damage. These three levels of damage are characterized with the following names Light Damage, Moderate Damage, Great Damage.

The limits and levels of damage are usually determined according to the engineer's judgment. They can also correspond to safety factors and to the strength of the structure during an earthquake. The determination of levels of damage plays a very important role in the final form of the fragility curves. The characteristics of seismic response of the construction can be obtained analytically (analytical fragility curves) and in some cases empirically through the collection and evaluation of existing sizes.

[7]

Old structures in relation to the modern, present peculiarities in the phase of simulation of the bodies. The mass distribution of the construction in all its height and the relatively small concentrated mass at the floor levels, the diversity, the orthotropic material, the low tensile and flexural strength of the material and the lack of monolithic connections are some characteristics that do not occur in modern construction. It is clear then that in order for the assessment of the response of masonry construction to be realistic, a modification of the mathematical models already used for modern construction of reinforced concrete is needed.

To ensure a reliable distribution of mass across the surface of the construction and a realistic simulation of the inertial forces imposed on it, the method of finite elements needs to be applied. This method also offers the advantage of flexibility during the simulation geometry, the boundary conditions and other important parameters. The results of the analysis with the finite element method can provide with great precision movements of the construction, development trends, the dynamics, the damping capacity of the incoming seismic energy, etc.

5.2. Failure Analysis

Although the masonry is one of the oldest construction materials, its mechanical behavior has not yet been determined satisfactorily. The failure of masonry either under uniaxial or biaxial stress conditions has been tested experimentally in the past, but the tries to express a general criterion of failure were few.

An important indicator of the seismic behavior of masonry structures is to evaluate the areas of construction failures. The analysis of the failure, after the analyzing of trends, shows the areas of damage to walls, under certain loading conditions. For this reason, the modified criterion Von Mises is used.
[6]

5.2.1. Failure criterion by Von Mises

The basic assumption of the criterion is this: The plastic flow at a point on the mass of the material starts when the shear strain energy stored at this point take a firm fixed price. The main tensions are given by the following relations:

$$\sigma_1 = \frac{1}{3}(\sigma_1+\sigma_2+\sigma_3)+\frac{1}{3}(\sigma_1-\sigma_2)+\frac{1}{3}(\sigma_1-\sigma_3)$$

$$\sigma_2 = \frac{1}{3}(\sigma_1+\sigma_2+\sigma_3)+\frac{1}{3}(\sigma_2-\sigma_1)+\frac{1}{3}(\sigma_2-\sigma_3) \qquad (5.2)$$

$$\sigma_3 = \frac{1}{3}(\sigma_1+\sigma_2+\sigma_3)+\frac{1}{3}(\sigma_3-\sigma_1)+\frac{1}{3}(\sigma_3-\sigma_2)$$

The first term of these expressions is the hydrostatic component of stress and deformation and produces only volumetric deformation $\boldsymbol{\varepsilon_v}$:

$$\varepsilon_v = \varepsilon_1+\varepsilon_2+\varepsilon_3 = \frac{\sigma_1+\sigma_2+\sigma_3}{\mathrm{E}}(1-2\nu) \qquad (5.3)$$

And the energy of the volumetric deformation is:

$$U_v = \frac{1}{6E}(\sigma_1+\sigma_2+\sigma_3)(1-2\nu) \qquad (5.4)$$

The next two terms of the expressions of the main trends are responsible for the distortion of the material in the examined position and are related to the energy of drilling distortion Us:

$$U_s = U_{total} - U_v \qquad (5.5)$$

while the total strain energy is:

$$U_{total} = \frac{1}{2E}[\sigma_1^2 + \sigma_2^2 + \sigma_3^2 + 2\nu(\sigma_1\sigma_2 + \sigma_2\sigma_3 + \sigma_3\sigma_1)] \qquad (5.6)$$

From the requirement to apply the yield criterion under conditions of uniaxial tensile and pure shear, is obtained the exact mathematical relationship of the criterion:

$$(\sigma_1 - \sigma_2)^2 + (\sigma_2 - \sigma_3)^2 + (\sigma_3 - \sigma_1)^2 = 2Y^2 = 6k^2 \qquad (5.7)$$

The drilling yield τ_0 in pure shear is:

$$\tau_0 = \frac{\sigma_1 - \sigma_2}{2} = k \qquad (5.8)$$

The drain location of Von Mises criterion is a cylindrical surface with right axis of the system axes (σ_1,σ_2,σ_3) and radius equal to $Y\sqrt{2/3}$. In the case of plane stress condition (σ_1,σ_3), for σ_2=0, the ellipse has the equation:

$$(\sigma_1 - \sigma_2)^2 + \sigma_1^2 + \sigma_2^2 = 2\sigma_0^2 = 6k^2 \qquad (5.9)$$

where:

$$k = \sigma_0 / \sqrt{3} \qquad (5.10)$$

The strain areas for the Von Mises criterion in the system (σ_1,σ_3) are shown in the figure below.

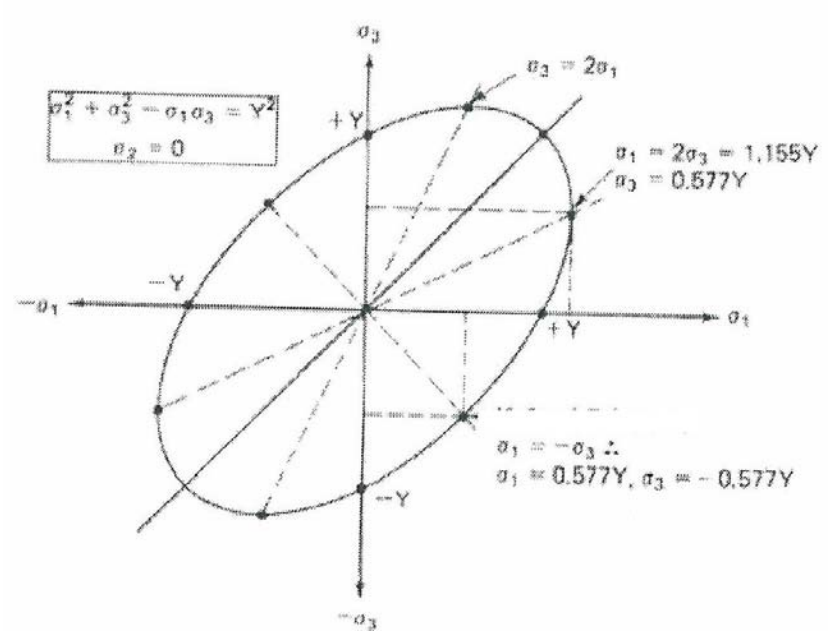

Figure 5.1. Ellipse Von Mises

5.2.2. Modified failure criterion by Von Mises

As developed in the Unit of Structure Analysis of the Static and Anti-Seismic Research Laboratory, in the School of Civil Engineering, with scientific officer the Professor K.A. Syrmakezis, based on the modified criterion, is taken as failure area, a modified area taken by the Von Mises criterion. This area is defined by the union of four areas S1, S2, S3, S4 as shown in section in the plane (σ_{xx}, σ_{yy}) in the figure 5.2.

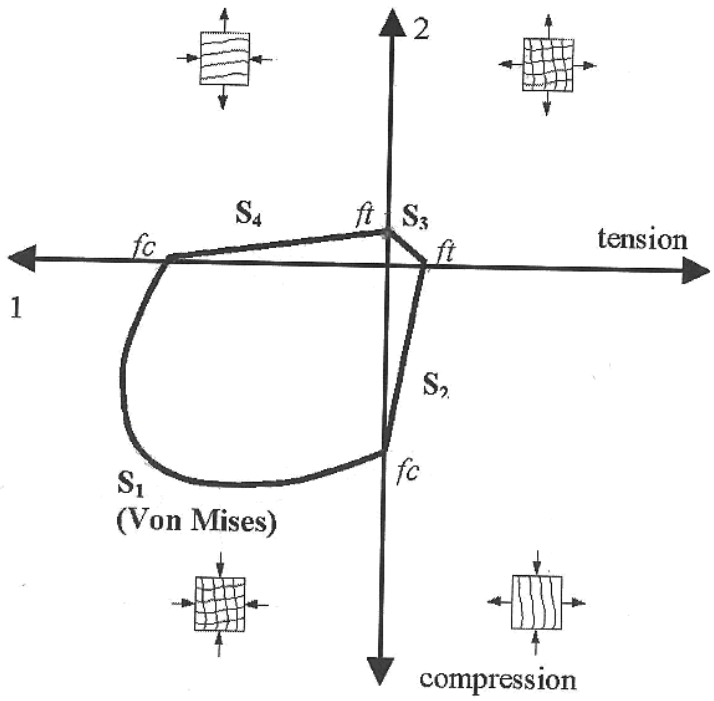

Figure 5.2. Ellipse for the modified criterion Von Mises [6]

The four mentioned areas are expressed by the following equations:

(i) S1 (ellipse Von Mises), σ_{xx} and $\sigma_{yy} \leq 0$:

$$\sigma_{xx}^2 + \sigma_{yy}^2 - \sigma_{xx}\sigma_{yy} + 3\tau^2 - f_{wc}^2 = 0 \qquad (5.11)$$

(ii) S2, $\sigma_{xx} \geq 0$ and $\sigma_{yy} \leq 0$:

$$\sigma_{yy} + (1 - \sigma_{xx}/a)\sqrt{f_{wc}^2 - 3\tau^2} = 0 \qquad (5.12)$$

where :

$$a = \left(f_{wt}/f_{wc}\right)\sqrt{f_{wc}^2 - 3\tau^2} \qquad (5.13)$$

(iv) S4: symmetrical to S2 as to bisect the level of first quarter

where: f_{wc} : the compressive fracture strength

f_{wt} : the tensile fracture strength

5.2.3 Methodology of the Laboratory of Static and Anti-Seismic Research of the National Technical University

Next, will be presented in detail the application of the method of fragility curves in the case of the residence of Prince George in Chania. To extract good results some considerations were made for the use of data obtained by solving the structure with the static software program SAP2000 v10.0.1 Nonlinear (Three Dimensional Static and Dynamic Analysis of Structures).

Apart from the assumptions taken during the simulation of building the finite element method, to draw the fragility curves was necessary to define as variable some of the features that introduce significant uncertainty. Since the factor of interest is the behavior of the masonry and especially of mortar affecting the strength of the wall structure and the response of the building in case of seismic action, as mentioned, were selected as more representative and more uncertain variables, the tensile strength fwt and the peak ground acceleration (PGA). Other parameters that could be considered variables are the modulus, the compressive strength or geometry.

The methodology followed for the analysis of seismic vulnerability of the building is governed by the definition of prevailing mechanical and geometrical characteristics and the response of the building according to the size of the seismic action. An important criterion of the seismic vulnerability of the stone constructions is the failure rate under the influence of a given seismic intensity. The steps followed in the present analytical methodology are:

- Identification of the seismic parameters
- analysis of the construction with the specific earthquake magnitude
- treatment of the results of the analysis that indicate the level of damage to the building
- Correlation between the level of damage to the building with pre-damage levels for the respective structures and with criteria so as to draw final conclusions on its vulnerability.

The criterion used for the control of mechanical failure is the modified failure criterion Von Mises (which we reported extensively in section 6.2.1 and 6.2.2)

and the corresponding program FAILURE made in a Fortran language used (which has been mentioned to paragraph 6.3), both have been developed at the Unit of Structural Analysis of the Laboratory of Static and Anti-Seismic Research, at the School of Civil Engineering, with scientific officer Professor KA Syrmakezis. The program displays the areas and the mechanism of failure under biaxial tension (BC, BCT, BTC, BT) and provides an overview of the likely level and types of damage of the structure. Thus, after identifying the areas of construction that fail under biaxial stress condition (tension and / or compression) it can be calculated also the percentage of lesions on the total surface area. Then the ratio Aβλ/Aoλ (failure surface / total surface) is defined, as an appropriate measure of damage for masonry construction. After a sufficient number of repetitions of the analysis in the same PGA for different values of the one deemed variable parameter, calculation the resulting measure of damage and statistical processing of observations (histogram density), is defined as the corresponding probability density function (p.d.f.), which expresses the probability that the ratio Aβλ/Aoλ can take a specific value for a given PGA.

For the final presentation of statistical results of the response of the structure in the form of fragility curves, it is necessary to calculate the cumulative probability of the potential: "the damage index of the construction takes value equal to or greater than a specified" Thus, for each level of analysis PGA, with integration of the corresponding region (from the lower limit of the alleged damage level to the end of the p.d.f. chart), is taken the value of the demanded cumulative probability.

Therefore, for each PGA result such values "exceedance probability level of damage" as these levels. So it is developed for the structure studied a family of fragility curves with new adaptation - at the level of damage this time-sharing statistics form, to the initially identified in height points (cumulative probability values for each PGA).

5.2.4 Failures audit with the PC program "FAILURE"

To determine the mechanical failure of our examined body, because of the elastic deformation, is adopted the modified Von Mises failure area described above.

More specifically, based on the current stress condition resulting from the elastic analysis of the program PC SAP 2000 14 Nonlinear, the exported tensions of each wall are transferred to be controlled with the computer program FAILURE. This program was created in FORTRAN language and has developed in Structure Analysis Unit, in the Laboratory of Static and Anti- Seismic Research of the National Technical University with scientific responsible KA Syrmakezis, Professor NTUA. This program displays in each wall examined, the areas and the mechanism of failure under biaxial tension (BC, BCT, BTC, BT) using the modified failure criterion Von Mises.

Once identified, therefore, the areas of construction that fail under biaxial stress tension (tension and / or compression) the rate of damage of total area can also be calculated. So, it is defined the ratio $A_{\beta\lambda}/A_{o\lambda}$ (failure surface / total surface) as an appropriate measure of damage for masonry construction.

Therefore, the results obtained from the elastic analysis of the model of the building (for load combinations 1 to 9) were transferred to the program FAILURE to control each wall separately and for different value of tensile masonry strength $f_{wt.}$.

5.3 Statistical Analysis

The concept of probability is very often used in everyday life and is connected with our uncertainty as to the outcome of an experiment. But the term probability is not likely to be interpreted by a unique and only way neither is defined uniquely in each case. There are three different interpretations oftenly used: the subjective interpretation, the classical interpretation and the interpretation of the relative frequency or statistical interpretation of probability.

The foundation of the theory of probability was made by Laplace (1812). Laplace formulated the classic definition of probability of a possibility: "The probability of a possibility is the ratio of favorable cases for the possibility to the total number of cases where nothing makes us believe that some of these cases

take precede over the other.

The empirical law of statistical regularity is the basis of statistical probability. According to it, the possibility of a potential A is defined as the number P (A) which stabilizes the relative frequency of A, n(A)/n, for a large number of π iterations of the experiment with the same or similar conditions. In other words, the relative frequency is just an estimate we assume for a hypothetical value of P (A) and the estimate is considered better as the number of repetitions of the experiment is larger. Such is the statistical interpretation of probability in a single execution of the experiment or observation of the phenomenon.

The statistical definition given by Von Mises in the 1920's, has some weaknesses, such as that the concept of static normality is an empirical law which is difficult to be established mathematically. Another weakness is that it is applicable only in cases where the basic process of observation or experiment can be repeated many times in similar conditions.

It should be noted that the statistical definition and the corresponding interpretation of probability have a narrower scope than the subjective definition. Nevertheless, the statistical probability is that which was created to so as to be used in the spectrum of sciences (physical, biological, economic, social).

According to the definition of subjective probability, each possibility is reflected for example as the degree of personal opinion of a specialist on a phenomenon. The advantage here is that we can always define the probability of a possibility, even if the possibility is referring to a procedure or observation which cannot realistically be repeated under the same conditions.

5.3.1. Random Variables and Distributions

We briefly mention below some basic definitions.

Sample Area (Ω) is all possible results of an experiment and can be determined before performing the experiment. Furthermore, possibility is called every possible subset of Ω and random variable (τ.μ.) is a function X with domain the sampling space Ω and range a whole range of real numbers, i.e. for each value ω of Ω (the result of the experiment) this function corresponds to one and only real number X(ω)=x.

A random variable that takes discrete values is called discrete τ.μ. A τ.μ. which takes values in a continuous space R is called continuous τ.μ. The

probabilistic behavior of each τ.μ. is referred to as a probability distribution or just distribution of τ.μ. A distribution is characterized as discrete or continuous depending on whether it refers to discrete or continuous τ.μ. respectively. In this paper we employ the continuous distributions.

The probability density function (p.d.f.) or simply density function of X (constant τ.μ.) is a normal function with π.ο. the R and π.τ. a subset of R, such that:

f(x)>0, for each x ϵ R and

$$\int_{-\infty}^{\infty} f(x)dx = 1 . \qquad (5.14)$$

For each interval [a, b] of real numbers is:

$$P(a \le x \le b) = \int_{a}^{b} f(x)dx \qquad (5.15)$$

This relation shows that the probability to be observed a value of τ.μ. X which belongs to the interval [a, b] equals to the area under the curve f (x) between a and b. The condition expresses that the probability of finding the value of τ.μ. X between - ∞ and + ∞ is 1. Since f (x) doesn't express possibility, its price is not necessarily less than one.

If we set a = b:

$$P(X = a) = \int_{a}^{a} f(x)dx = 0 \qquad (5.16)$$

So the probability of observing any one specific value a for τ.μ. X is zero. Therefore, in calculating the price of a possibility does not matter whether we include or not the edge of the interval.

The cumulative distribution function (c.d.f.) of X (continuous distribution) is a common function Φ(x) with π.ο. the R and π.τ. a subset of [0.1] such that:

$$F(x) = P(X \le x), \text{ για κάθε } x \in R \qquad (5.17)$$

In other words, for every real number x, the c.d.f. of τ.μ. X takes value equal to the cumulative probability of an observed value of τ.μ. X less than or equal to x. For c.d.f. F(x) of a continuous distribution exist the following:

- It is non-negative and non-decreasing function in R,
- It is a continuous function in R,
- $\lim_{x\to\infty} F(x) = 1$
- $\lim_{x\to-\infty} F(x) = 0$
- $F(x) = \int_{-\infty}^{x} f(u)du,$ for each $x \in R$
- $f(x) = \frac{d}{dx}F(x),$ for each $x \in R$

It should be noted that if F (x) is known then, can be used the relations:

$P(a < X \leq b) = F(b) - F(a)$ και $P(X > x) = 1 - F(x)$ (5.18)

5.3.2. High Class Means and torques

The probability density functions and cumulative distribution fully describe the distribution of a continuous τ.μ. Often, however, we are concerned about some constants that are simpler characterizations of the distribution and are called parameters of the distribution. Knowing the numerical values of these parameters offers a quick and concise knowledge of the probabilistic behavior of τ.μ. X.

One of the main parameters for many probability standards (of distribution) of a τ.μ. X is its average value. Based on this definition, we can obtain the numerical value for the mean when the observed values of random variable (sample) are given. It is also referred that even if X a τ.μ. with p.d.f. fx(x), then the average value of X or the expected value of X is denoted by E (x) or μ_x and is given by:

$$E(X) = \int_{-\infty}^{\infty} x f_x(x)dx \qquad (6.19)$$

Also, the central torque of class r of a τ.μ. X with mean μ is denoted as μ_r and is given by:

$$\mu_r = E\left[(X-\mu)^r\right], \qquad r = 1,2,... \qquad (5.20)$$

The central torques are called torques by the average value. The central of first-class is by identity equal to zero for any τ.μ. with finite mean μ. The central torque of second class, μ_2, is more commonly called dispersion. The dispersion of a τ.μ. X, is denoted as Var(X) or as σ_x^2 and is given by:

$$Var(X) = E\left[(X-\mu)^2\right] \qquad (5.21)$$

The dispersion is a measure of the volatility of τ.μ., i.e. how they can change the possible values of τ.μ. A distribution with high dispersion is "stretched", while a distribution with small dispersion is concentrated around the average.

5.3.3 Continuous Distributions

Normal Distribution

This is one of the most useful continuous distributions in the Probability theory and Statistics as well. The first historical application of the distribution is due to De Moivre (1733) who found that the Binomial Probabilities are well approximated by the Normal function of density probability. A second historically important application of normal distribution is due to Gauss (1777-1855), who found that the random errors in the measurements of a quantity are normally distributed (1809).

Today, in addition to the key role played by the statistics, the normal distribution is used as a probabilistic model for many features that are continuous symmetry around a mean value, such as weight and height of people, the diameters of mechanical components, temperature, humidity, degrees of concentration of chemical solutions, etc. Overall, the distribution range of applications in Statistics and the testing is extensive.

The continuous τ.μ. X follows the normal distribution with parameters μ and σ with (- ∞< μ < +∞), σ > 0) and ⋀ we write X N (μ, σ^2) when it has p.d.f. the following:

$$f(x)=\frac{1}{\sigma\sqrt{2\pi}}\exp\left[-\frac{1}{2\sigma^2}(x-\mu)^2\right], \qquad (5.22)$$

where :

- ∞< x < +∞, xϵR

It is obvious that the p.d.f. has as top point χ=μ and is symmetrical to the axis passing through the μ. Also in the interval (μ-3σ, μ+3σ) are contained almost all the possible values of τ.μ. X. The parameter μ determines the position of the distribution on the axis of x, which is why, is called location parameter while the parameter σ determines how the distribution lies on the axis of x, which is why is called the variation parameter (Figure 6.3).

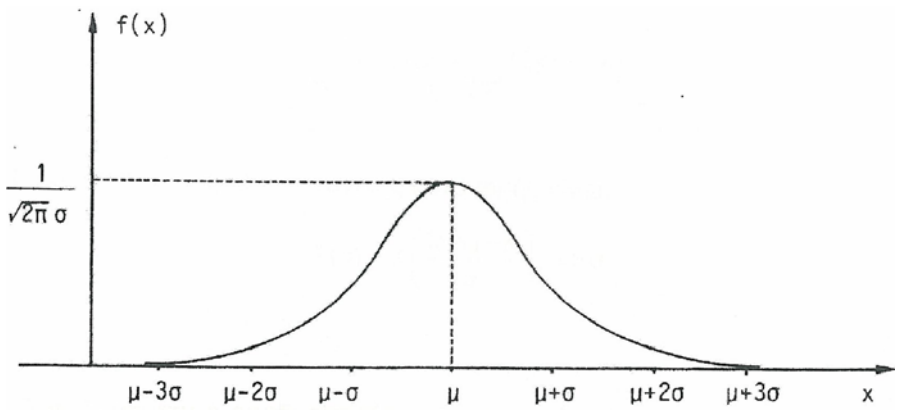

Figure 5.3 Probability density function of normal distribution

Note that generally the c.d.f. of the Normal distribution cannot be found in closed form. But it can be compared with the Standard Normal distribution N (0,1) as follows:

$$F(x)=\Phi\left(\frac{x-\mu}{\sigma}\right), \quad x\in R \qquad (5.23)$$

where Φ the c.d.f. of the Standard Normal Distribution.

Lognormal Distribution

This is a distribution that is widely used in reliability problems. Its applications involve several disciplines. Examples of variables may be cited as examples the following: the size of businesses and other entities, the size of particles, fields, the lifetime of semiconductor etc. We say that the random variable X follows the lognormal distribution with parameters μ (- oo< μ < + oo) and σ (σ > 0), LN(μ, σ), where the natural logarithm of X $Y=\ln X$, follows the Normal distribution with mean μ and standard deviation σ, N(μ,σ). The p.d.f. of a LN(μ,σ) τ.μ. X is:

$$f(x)=\begin{cases}\dfrac{1}{\sigma x\sqrt{2\pi}}\exp\left[-\dfrac{1}{2\sigma^2}\left(\ln(x)-\mu\right)^2\right] & x>0\\ 0 & x\le 0\end{cases} \qquad (5.24)$$

The c.d.f. of the lognormal distribution is:

$$F(x)=\Phi\left(\frac{\ln(x)-\mu}{\sigma}\right),\ x>0 \qquad (6.25)$$

5.4. Statistical analysis of failures

So after exporting the $A_{\beta\lambda}/A_{o\lambda}$ (failure surface / total surface) from the program FAILURE, we can, according to the theoretical background described earlier, to move to their statistical treatment.

More specifically, after a sufficient number of repetitions of the analysis under the current PGA for different values of a considered variable parameter (fwt), a calculation of the resulting measure of damage (for $A_{\beta\lambda}/A_{o\lambda}$) and a statistical processing of the observations (histogram density), is defined the corresponding probability density function (p.d.f.), which expresses the possibility of $A_{\beta\lambda}/A_{o\lambda}$ to take a specific value in given value PGA.

5.5. Setting of Damage Levels

The next important step in the development of the fragility curves is to determine the levels of failure of the construction and also the numerical limits that characterize them. For unreinforced masonry, the directives of FEMA (Federal Emergency Management Agency) suggest specific levels of damage (see Table 5.1).

Table 5.1 Structural Performances Levels [6]

Structural Performance levels			
Total damage	SEVERE DAMAGE	MODERATE DAMAGE	LIGHT DAMAGE
	Extensive crack in the facade and coating detachment. Visible shifts in and out of level	Extensive Cracks in the façade. Visible in level and small out of level shifts .	Minor cracks in the façade. Small coating detachment in corner openings. Not significant out of level shifts.
Limit Level Damage	100%	60%	30%

On the graphic presentation p.d.f. of the distribution chosen as the most appropriate based on its adaptability to the observations, areas of damage index corresponding to discrete levels nominee are delineated.

The probabilities P1, P2 and P3 are the areas between the boundaries of fault and determine the levels of destruction of the construction, and are calculated based on the Probability Density Function (p.d.f.) as follows: for random values (a, b) is expressed the probability that the response of the structure is between those values of the damage index.

In the bibliography is indicated the use of normal, lognormal distribution, of Weibull distribution, the Gamma distribution and others. As part of this work, it makes use of the normal and logarithmic distribution.

Of course, for the final presentation of statistical results of the response of the

structure in the form of fragility curves, it is necessary to calculate the cumulative probability of the potential: "the damage index of the construction takes value equal to or greater than a specified" Thus, for each level of analysis PGA, with integration of the corresponding region (from the lower limit of the alleged damage level to the end of the p.d.f. chart), is taken the value of the demanded cumulative probability.

Therefore, for each PGA result such values "exceedance probability level of damage" as these levels. So it is developed for the structure studied a family of fragility curves with new adaptation - at the level of damage this time-sharing statistics form, to the initially identified in height points (cumulative probability values for each PGA).

CHAPTER 6

CASE STUDY

6.1 Description of the structure

In the present study a landmark building in the area of Chania was examined. This structure is typically a neoclassical building from the late 19th century. This is a representative sample of the architectural heritage of the city of Chania, as it was developed outside the walls of the Old City at the end of Turkish occupation.

Its general form is characterized by symmetry and regularity, and has a uniform and compact size as shown in the picture below. It includes semi-basement and ground floor and first floor (in Annex 2 all floor plans and facades of the building are listed). As it concerns the masonry walls, it is rubble of the local soft limestone and low quality mortar. Noteworthy is the presence of iron tiers who are in the levels of the top floor and roof deck and in the 4 corners of the building. The tiers, until today, and despite the erosion and the subsequent decay, restrained the masonry well. The floors and roof are wooden. The roof is hipped, based on the perimeter bearing walls of the building and is surrounded solid parapet. In the building there are two outbuildings laterally, which operate like one. The two-storey building is older reinforced with concrete elements and its foundation is special non normal. The newest addition is single storey and consists of walls and roof. Below is shown an aerial photograph of the building showing its south side and we can discern both two additions (to the east we see the older two-story addition, while on the west the newest one-storey where are also visible the roof tiles).

Image 6.1 A typical aerial photograph of the building in its present form

The main building has dimensions of 15.2 * 15.85 m². Two outbuildings have dimensions 2.65 * 5.05 m² the two-storey and 5.65 * 7 m² the one-storey. The building has a total height of 10.87 m and the maximum height of the roof is equal to 13.30 m. The ground floor (see Annex 3 project A3) shows almost complete internal symmetry by focusing on the wide main aisle that divides the building into two wings of equal width. At the center of the left is a double staircase. The right wing is still a living room with lounge and dining use. The ground floor is the same as the basement and includes the bedrooms and bathroom, but some of the partitions of the rooms have been removed. Also, the basement also has the same design with the ground floor and the first floor, but is a more simple construction. Abnormalities in the structure of the walls are displayed, there are no floors and coatings, as well as there have not be constructed any plaster ceilings.

As it regards the morphological characteristics it is observed symmetry in the facades, which are characterized by elaborate ornamentation. Most architectural and decorative elements are concentrated on the front facade, but without conflicting with others, which are distinguished by simplicity. This facade is described by the corner pilasters with carved stones. Finally, the whole building was coated outside the quoin at the height of the floor.

6.2 History

In Crete, after the contract of Halepa (1878), was granted limited self-government. At that time, Cretan emigrants from West and East, along with other prominent local people formed the core of the new bourgeoisie. From the first merchants to build their homes in Halepa is Th.Mitsotakis, K.Venizelos, G.Hortatzis and others. In 1882 Th.Mitsotakis begins the construction of the residence mentioned in this study, in the road of Halepa (current Eleftherios Venizelos). The land on which erected the building is estimated to have an area of about 5 acres. The architect is assumed that was probably Nicholaos Magkouzos, whose ancestry was Italian or French. Regarding the cost of construction, it was amounted to 15,000 napoleoan money and for the equipment to 25,000 napoleoan money.

With the arrival of Prince George on the island, as the High Commissioner of the newly Cretan State, he was granted the house, since it was the most suitable building in the region. Having resigned Prince George (1906), the house was occupied by his replacement, Al. Zaimi. But after the removal of the residency status and the union of Crete with Greece the home was used by the respective General Directors.

Subsequently, during the period 1937-1940 the building was used as a military hospital. Then, during the Occupation, it housed the headquarters of the Germans. Eventually the building after liberation came to the heirs of Th. Mitsotakis. At the same time during the period 1968-1982 it housed the offices of I.L.A.E.K. (Historical-Folklore-Archaeological Society of Crete).

The Ministry of Culture, described the building under protection accordingly to the publication in the Official Gazette in 1980, along with other famous buildings of Chania (Italian barracks, Agricultural Bank, Garden Clock, Despotic, Historical Archive, TEE building, Conservatory). In accordance with the relevant extract from the Gazette these buildings are characterized "as works of art that require special state protection as historic buildings, because they are representative samples of the architectural heritage of the city of Chania, as it was developed outside the walls of the old city at the end of Turkish occupation and at the first free steps of the place."

6.3 Pathology and damage detection

In general the condition of the building is good although the structural materials of the bearing walls are not satisfactory. Several problems are listed locally, but not very seriously damages by seismic or geological reasons.

One of the damage that one encounters frequently in this building is of the wood and metal building elements. The damages are due to the presence of moisture, which occurs because of poor construction of the drainage of rainwater through gutters passing through the masonry. Moisture is detected even at the perimeter of the building in the lower section and at a higher altitude. The rising damp is causing serious disruption and damage of masonry mortars and plasters. There is also local damage on the wooden elements of the roof, particularly in the στρωτήρες and at the supports of wooden bodies on the walls of the building and the wooden floors.

Erosion has not only been detected on the wooden items and the iron structural elements. In the iron structural parts are included the tiers of the wall and the blanks of the central balcony. Due to the deterioration of concrete and corrosion of steel reinforcement, there is erosion of the concrete perimeter beam of reinforced concrete.

The latest electrical and sanitation facilities have caused some additional damage to the structural members. Also, the tree growth in the body of the wall has caused the destruction of the external stone staircase. Below we summarize the injuries and damage that have been found in the house:

- Cracks – wall disconnections
- Deterioration of mortar or and stone / brick
- Masonry disruption
- Traces of moisture
- Wear and damage of linear elements on doors and windows
- Deterioration of wooden roof elements and wooden flooring
- Corrosion of embedded iron tiers on the corners of the walls

6.3.1 Recent Maintenance Procedures

In the past, some interventions were made in the building, which were characterized as sloppy and were not fully compatible with the existing construction. Here are some of those as a guide indicatively.

- On the west side there was the addition of a two-storey outbuilding during the German occupation. This addition has an intermediate concrete slab, blanks in the headers of the wooden frames and concrete ποδιές. The damages shown on the masonry are important, especially in the legs of the wooden roof, while the coating is detached from the rubble. The lateral walls of height have been removed because of poor fixation annexes to the building.
- The outbuilding at the northeast was collapsed firstly and then was rebuilt in 1970 with reinforced concrete frame founded at the stone basement. It is covered by a reinforced concrete slab and steel shutters. Previously there was a vaulted cistern, which tangent to the building. Its existence prevented the column construction on the northeast corner so that the beam spread at the top of the basement. Thus, the required column was constructed outside the building by altering thereby the aesthetic result.
- In 1970 the openings were repaired and replaced all the windows of the facades other than the main one. But the intervention was not at all elaborated and there can be seen lots of faults, given the destruction of the frames of the openings. A similar operation was done previously in 1950 in the front façade however with a much more beautiful aesthetic result, since the frames and the openings were found in good condition.
- In the same year (1970) there was one more repair of the roof, by replacing the broken tiles and coating the stormwater gully.Perhaps then were constructed the new gutters. Because of improvisation in the construction of these gutters extensive moisture problems in the body wall were later developed. This resulted in the degradation of coatings and mortar beneath the coronation of the main building and the east side.

6.4 Spatial Model

The program used to simulate the body is the software SAP 2000 14 Nonlinear (Three Dimensional Static and Dynamic Analysis of Structures). With the above program was formed an appropriate FEM model to calculate the various sizes of the response of the structure.

The development of the finite elements networks was such that the ideal concentration of masses at the nodes to help better simulate the real mass

distribution. This ensures faithful simulation of the inertial loads of construction for dynamic analysis.

To fully determine the deformation of the system in space, six degrees of freedom for each node were considered in the rectangular coordinate system O_{xyz}. The six degrees of freedom correspond to three transfers in the axes x, y, z and three rotations of vectors parallel to the same axes. The model of the building is shown schematically in the following images from the three sides.

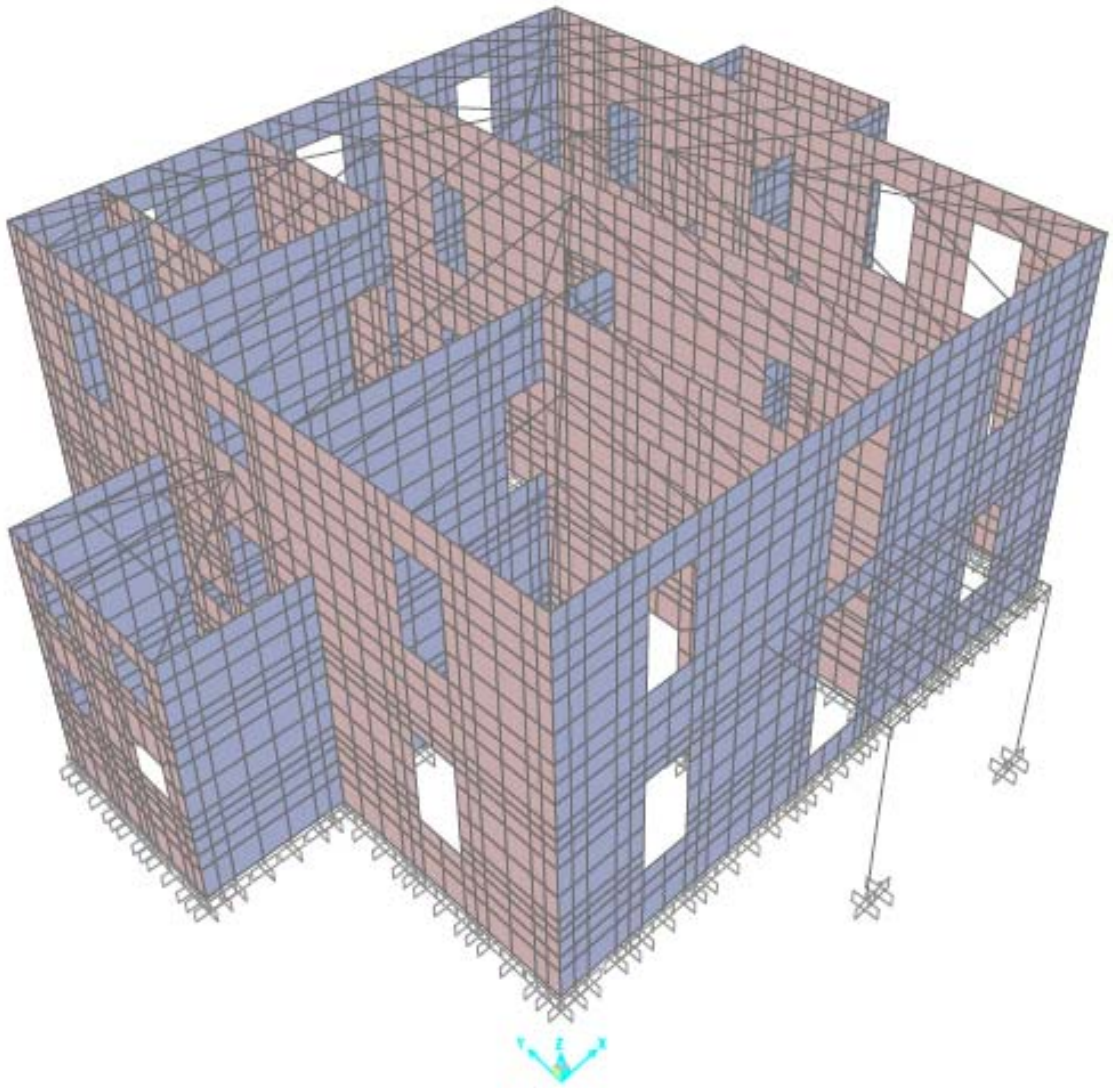

Image 6.2 Simulation of the neoclassical building of Chania on the southwest corner

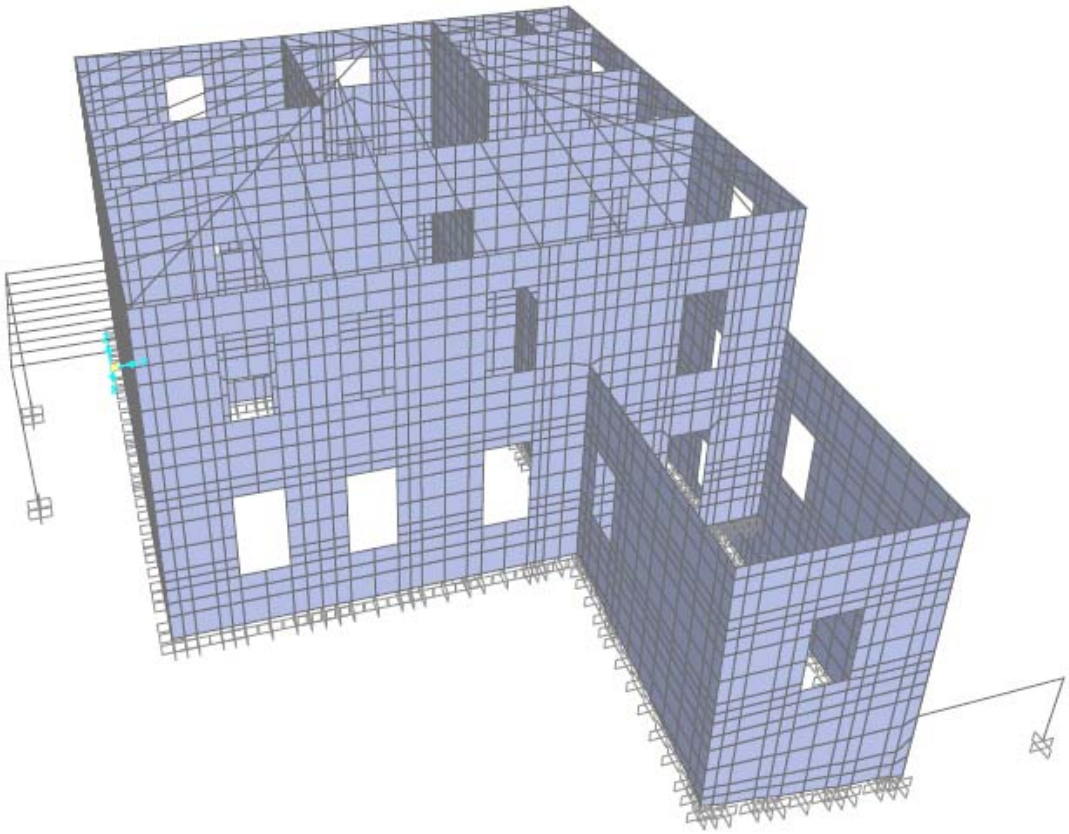

Image6.3 Simulation of the neoclassical building of Chania on the southwest corner

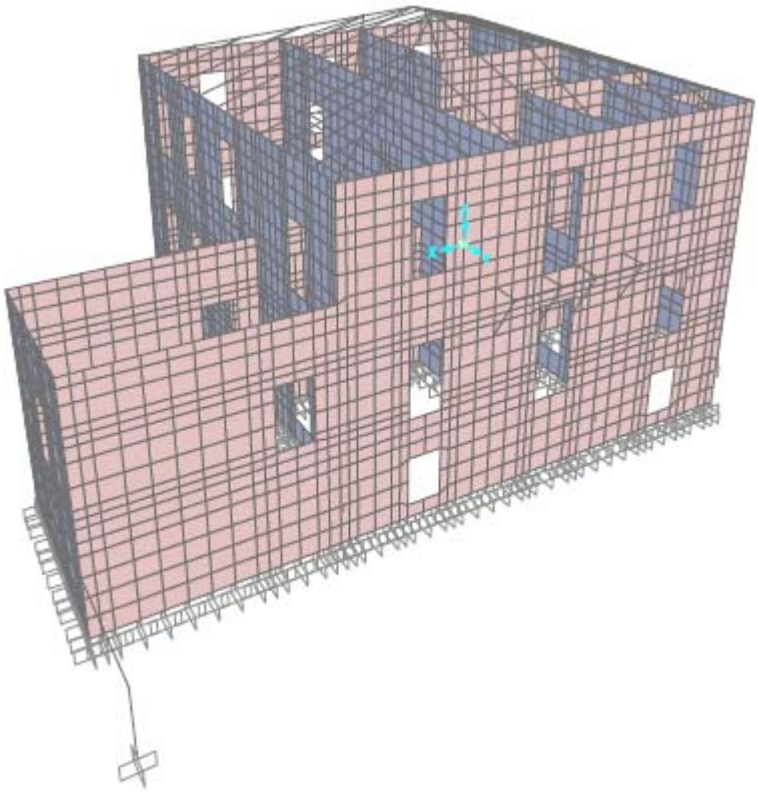

Image 6.4 Simulation of the neoclassical building of Chania on the northeast corner

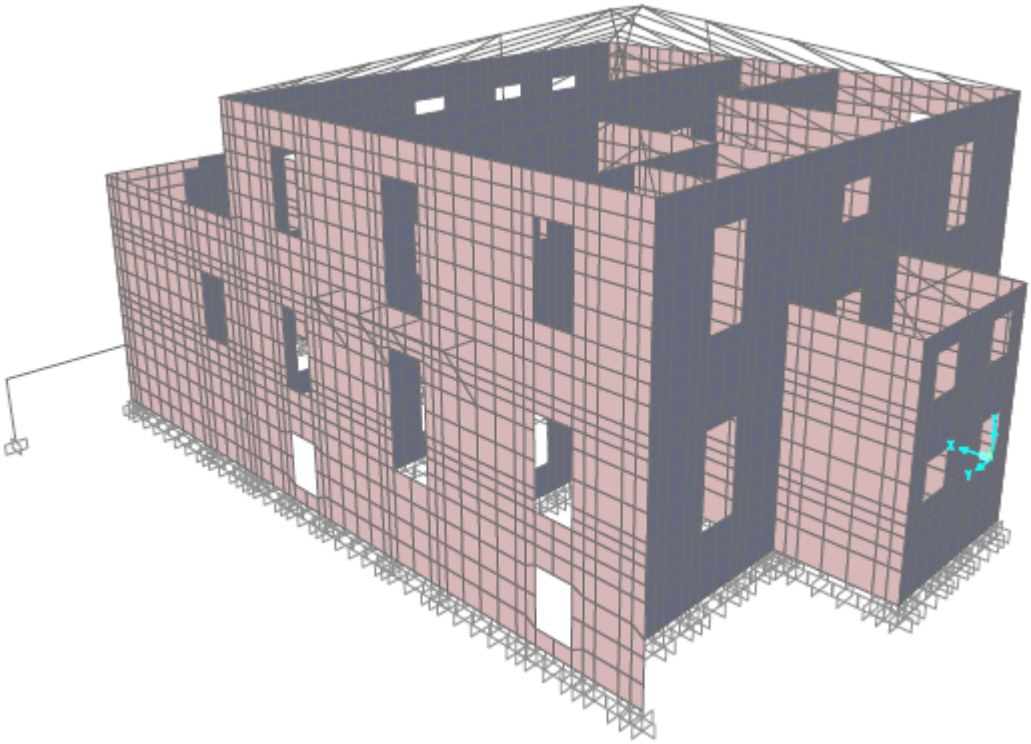

Image 6.5 Simulation of the neoclassical building of Chania on the northwest corner

For a correct simulation of the construction a visit to the site is required in order to determine the characteristics of masonry such as geometry, type and strength of natural stone and mortar as well as soil characteristics. In case where no tests can be done for determining the mechanical characteristics and there is no evidence from previous studies, the experience and knowledge of engineering is conscripted combined with the existing bibliography which allows for significant estimates of the mechanical properties of the material, always in relation to the rocks and the conditions prevailing in the region.

Below are the replication of the vector in the **geometry, the materials** and the **actions.**

6.4.1 Geometry Simulation

The simulation was done by isotropic surface members (shell elements) and isotropic linear members (frame elements), which are considered to represent with sufficient reliability properties of the real body. With surface members the masonry was simulated, while all other structural elements of the design were simulated with linear, so as to be approached with sufficient precision the basic (hard and

deformative) sizes of the response of the body. During the simulation model were used 5197 surface members (Areas), 5745 nodes (Points) and 120 beam elements (Frames).

The model used to analyze the body is spatial. The discretization of the finite element network was through flat quadrilateral and triangular elements. Depending on the geometry and loading conditions prevailing in each region of the model the thickening of the data is chosen. In this way it is accurately simulated the uneven behavior of the masonry structure. Specifically, condensation occurred on the following areas:

- Locations of concentrated loads
- Perimeter openings
- Corner areas (wall compounds)

taking into consideration that the densification of the grid means increasing the computational time and the demands of the computer, there was a try to find the right balance so that the model is realistic and workable together.

6.4.2 Material Simulation

In this paper the data was obtained under the research program under the auspices of Prof. K. Syrmakezis. The materials composing the structure are:

- Natural stone masonry
- Reinforced Concrete
- Wood roof
- Full timber planking
- Metal elements as a basis for developing floor brick

These materials are reflected in the architectural drawings presented in App. 3.

For the simulation of the structure on the software program SAP 2000 14 Nonlinear (Three Dimensional Static and Dynamic Analysis of Structures) had to be provided the material properties and the dimensions of cross sections. Here are the materials introduced in the static software with their respective properties and the names of their importation:

Materials

- MASONRY

In the present construction, masonry is the dominant material and its mechanical characteristics are essentially shaping the response of the building. The properties of the masonry are determined by the materials composing it, i.e. natural stone and mortar. During the simulation of our body there are different thicknesses of the sections of the masonry as they are reflected in the architectural plans. The thicknesses are between 0,15-0,60 m.

In the last years several empirical or semi-empirical methods have been developed for determining the compressive strength of masonry, all taking into account the two materials. For this case, the compressive strength of masonry was used by the EC 6 (prEN 1996-1-1:2001):

$$f_{wk} = K*f_b^{0.7} *f_m^{0.3} \text{ (MPa)} \qquad (6.1)$$

Where:

K: factor depending on the type of brick (material, size and proportion of voids) and the type of masonry construction. It usually takes values from 0.40 to 0.60.

f_b: the reduced compressive strength of walls

fmc: the average compressive strength of mortar

The modulus was taken equal to one thousand times the compressive strength of the masonry

$$E=1000*f_{wk} \qquad (6.2)$$

From the above data results:

f_{wk} = 3.05MPa and E = 1000* 3.05 = 3050MPa

Specific weight: γ = 22 kN/m³

Modulus: E = 3050000 kN/m²

Poisson ratio: v = 0.3

Thermal expansion: $\alpha = 1{,}170*10^{-5}$

- TIMBER

Wooden beam elements were used to simulate the roof the area of which are summarized below:

- Rafters parallel to tiles and gutter of dimensions 0,16-0,14m.
- Rafters 0,08x0,08 m².
- Ridges 0,14x0,14 m².

The properties listed below were given to the structural elements of wood making up the roof. Due to the anisotropic behavior of wood as a material, were given the different properties as per address on the modulus [E], and by extension and shear modulus [G].
Specific weight: γ = 6 kN/m³
Modulus: E1 = 10000000 kN/m² , E2 = E3 = 300000kN/m²
Poisson ratio: v12 = v13 = v23 = 0.3
Thermal expansion: α12 = α13 = α23 = 1,170*10-5
Shear measure: G12 = 115384,62kN/m², G13 = G23 = 76903069kN/m²

- CONCRETE

The name CONCRETE was used for the elements of the beams and columns of reinforced concrete. The features provided in hardware are of the same quality of C16/20 and are shown below. The specific weight was equal to 24 instead of 25kN / m³, due to negligible reinforcement that elements of reinforced concrete brought at the time of the building construction.

Specific Weight: γ = 24 kN/m³
Modulus: E = 27500000 kN/m²
Poisson ratio: v = 0.2
Thermal expansion: α = 1,170*10-5

- Metallic elements / name: STEEL

In the construction are not presented many minerals and their role in the static function of the building is not catalytic. They are presented in the plate of the semi-open space of the main entrance to the south side as basis for developing floor brick (Annex 2 - No.Scheme. A4, Ground floor - construction detail, balcony anopsi α-α) and struts as the projector of the northern facade (Annex 2 - No.Scheme. A8, Section B-B).

The mechanical characteristics given are:

Specific Weight: γ = 78 kN/m³
Modulus: E = 2*10^8 kN/m²
Poisson ratio: v = 0.3
Thermal expansion: α = 1,170*10-5
Minimum yield: F_y = 150000 kN/m²
Minimum tensile stress: F_u = 250000kN/m²
Yield: F_{ye} = 179000 kN/m²
Tensile stress: F_{ue} = 324000kN/m²

Figure 6.6 shows the model of the building to study. Each material with the characteristics presented above is presented in a different color, and precisely:

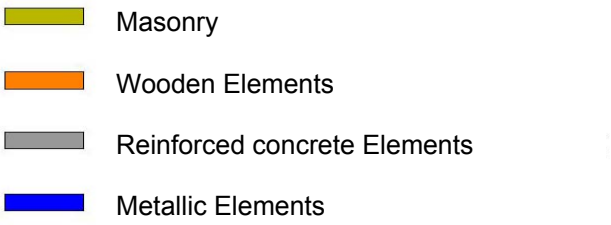

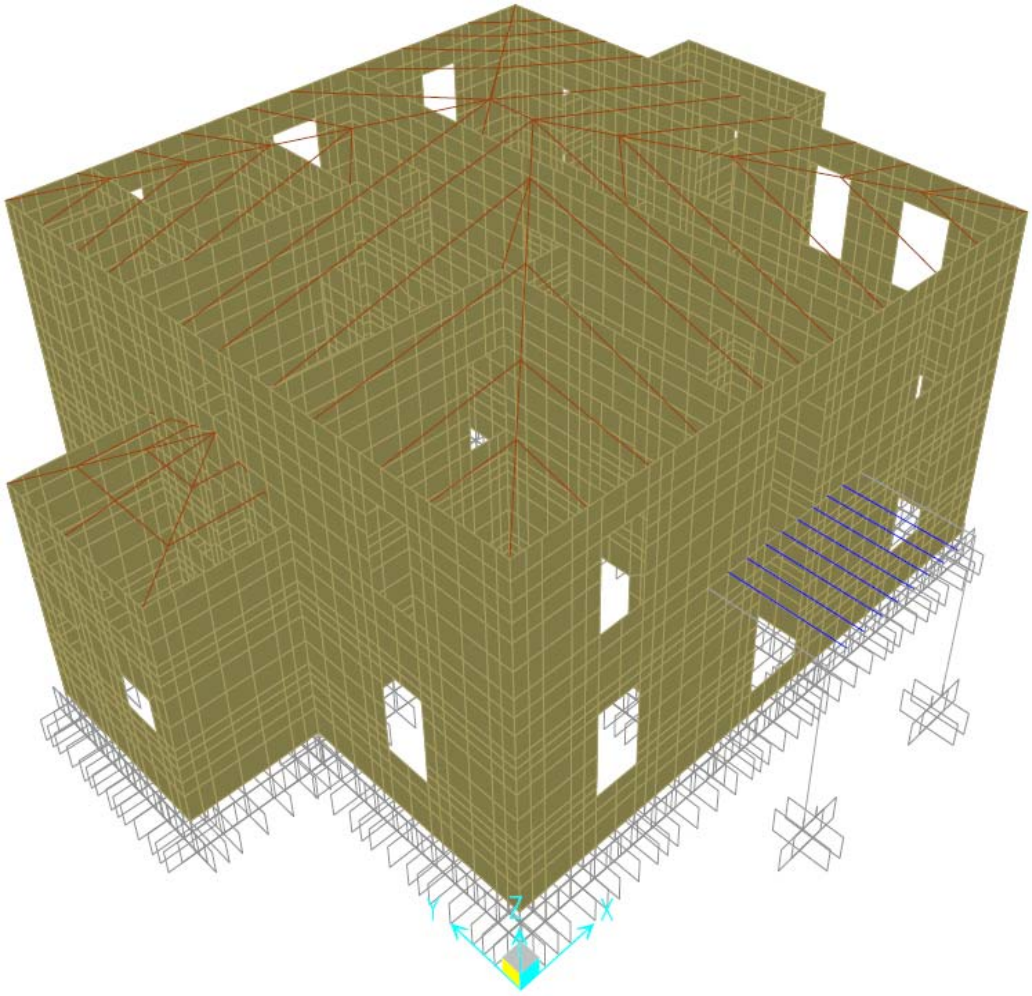

Image 6.6: Southwest Building facade – Colors of the model based on the material

Figure 5.7 shows the simulation with the color at this time to set apart from the material and thickness of the sections. The different structural elements are shown in shades presented in Table 6.1 with the color to deepen as the size of the data is increased. Specifically, are presented below the dimensions of the data:

In reinforced concrete were simulated the columns of the semi outdoor in the south side of the building and the beams around the plate of the semi outdoor.

Table 6.1 : Coloring of bearing elements based on the material

Bearing Elements	Color based on material
walls	earth tones
wood	green
reinforced concrete	gray
steel	blue

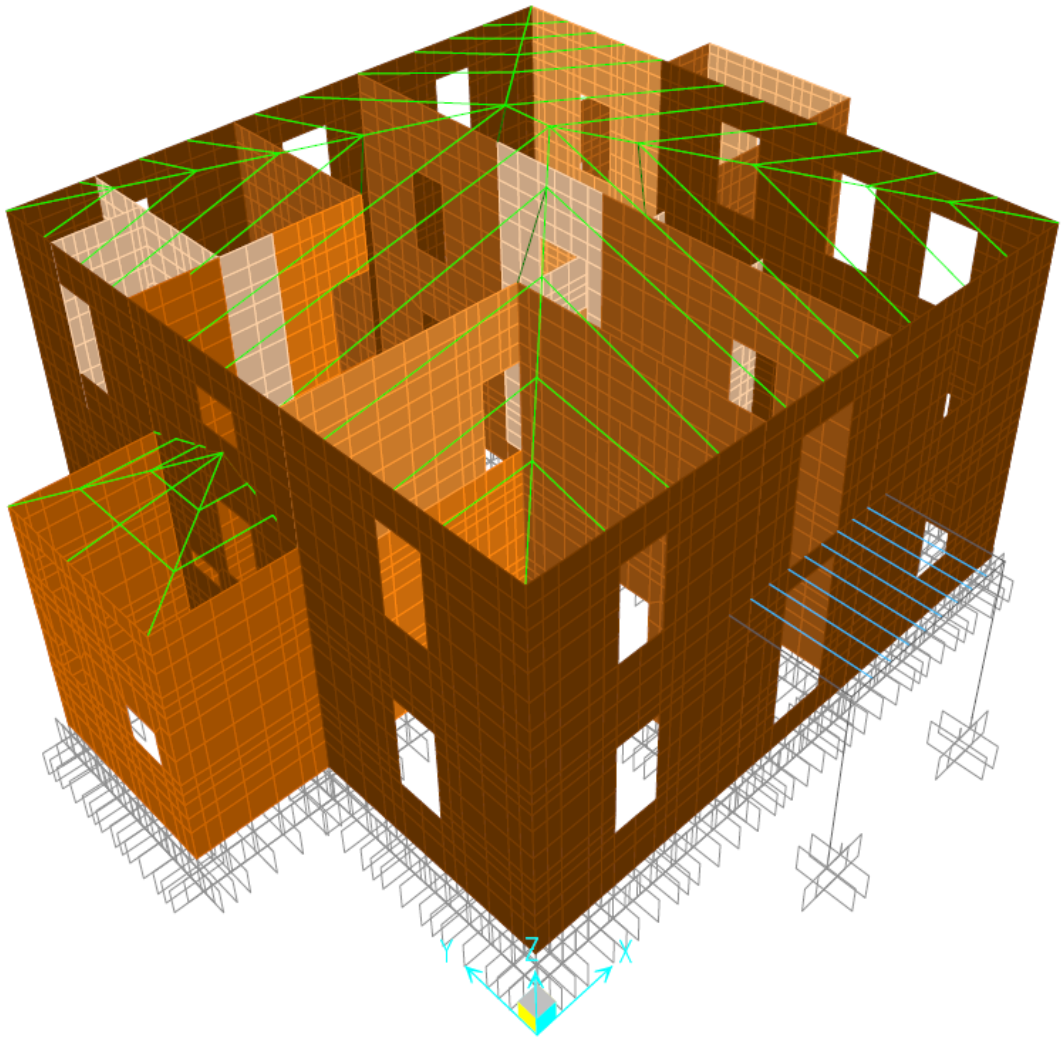

Image 6.7 : Southwest building façade – Colors on the model are based on material and thickness of the profiles

6.4.3 Action Simulation

- **Fixed charges (G) and Mobile or payloads (Q)**

For the simulation of the model there were taken into account both static and dynamic loadings. For static loads other than the same weight of materials, whose prices are presented for each material in paragraph 6.4.2, permanent and moving loads were added where it was considered necessary.

More specifically, fixed charges were included in floors and roofs. Mobile charges were included only in the floors while in the roofs they were considered negligible. Shipments from the wooden floors were transferred to the walls only in the direction of wooden structural elements (beams). On the floors of reinforced concrete the dispatching was based on the theory of plates. For roofs, loads were transferred through the walls of wooden stripe data.

More specifically, where there were moving loads they were considered equal to 2,5 kN / m², while the materials which are not part of the carrier body were not simulated as elements of the model construction, but their cargo was retained. These loads depend on the material. Regarding the permanent loads:

- Unreinforced concrete: 3 kN/m²
- Wooden floor: 0,6 kN/m²
- Roof tiles : 0,5 kN/m²

- **Random loads**

In the random loads seismic design actions are included. With this term are essentially called the oscillatory movements of the ground responsible for the development of significant force-deformation due to inertia of the masses that make up the structure and base of which is necessary to design projects. The seismic movements consist of two horizontal and one vertical component and set the acceleration design spectra, which give the maximum value of spectral acceleration $R_d(T)$ which bears computationally a simple oscillator with period T during the earthquake.

The design spectrums include the shape of the spectrum and the tension of seismic excitations, which is influenced by the seismic hazard zone, the elastic and the damping of the structure.

Horizontal Components

Determined by acceleration design spectrum, whose ordinates R_d (T) for each period of structure T are calculated by:

$$R_d(T)=A \cdot \gamma_I \cdot \frac{\beta_d(T)}{q} \cdot \theta$$

where:

A Seismic ground acceleration,

γ_I Rate of importance of the structure

$\beta_d(T)$ Price of rubber modified spectrum of seismic motion in seismic design normalized ground acceleration A,

q Factor of seismic behavior

θ Rate of foundation

More specifically:

- The value of A depends on the location of the construction.
- The rate of importance γ_I indicates the importance of construction
- The value of θ depends on the depth and stiffness of the foundation and
- The value of q depends on the material of the bearing structure and the structural system. In essence is the ability of the structural system to absorb and dissipate energy with behavior without reducing drastically the resistance.

It is obvious the direct relationship between q and the cost of seismic design. High q defines low seismic actions which in their turn determine seismic low cost.

In the case of masonry construction it cannot be estimated the value of the behavior factor q and therefore we believe that the construction has not elastoplastic behavior, but only flexible, we consider the behavior factor q = 1 and is used the elastic spectrum of EAK2003 § A.1.

Vertical component

During the analysis the vertical seismic component was not taken into account.

6.4.3.1 Seismic response of structures

The Greek Seismic Code provides for the following linear methods for calculating the seismic response (elastic analysis):

a) Method and Spectral Dynamics and

b) Simplified Spectral Method (Equivalent Static Method)

The dynamic spectral method applied in the construction, is applied without restriction in all cases of construction, as it includes a full modal analysis of the system, calculation of the maximum seismic response for each peculiar swing and square superposition of the maximum modal responses.

For the analysis of our body, were taken into account the following regulations and Eurocodes:

- Greek Seismic Code (EAK 2003)
- Greek Regulation of Reinforced Concrete (EKOS 2000)
- Eurocode 6 (Construction Design of Bearing Masonry)

6.4.3.2 Seismic combination of actions

Under the requirements of Greek Earthquake Regulation (EAK 2000), resulted the possible combinations of charges which may incur in the construction. For the case of biaxial bending columns with perpendicular strength, we will have for both horizontal components of earthquake in x and y the relations:

$E= \pm E_x \pm 0.3\ E_y$

$E= \pm 0.3\ E_x \pm E_y$

This creates eight combinations of charges. In each combination is added algebrically and the vector of intensive construction aggregates from the action of the vertical gravity load combination:

$$1.00\ G_k + 0.3\ Q_k$$

It is noted that E_x and E_y of these relations represent extreme non-simultaneous values of intensive sectional sizes of the construction with indeterminate sign, so in fact the possible combinations will be more. Apparently the consideration of these sizes as simultaneous is in favor of safety regarding the response of the structure. Combining the previous relations and from EAK 2000, the simplified combination for ordinary buildings results:

$$S_d = G_k + \psi_2 Q_k \pm E$$

where :

S_d : design tension

G_k : permanent loads

Q_k: moving loads

E : seismic of design

ψ_2: combination rate coefficient for long-term variable actions

Coercive actions, such as caused by change and difference in temperature, drying shrinkage of concrete and retreats mounts do not need to be included in conjunction with the earthquake. Also, the earthquake cannot be combined with other random actions (e.g. vehicle collisions), which is why the price of ψ_2 was taken equal to 0.3.

The combinations considered and finally entered the program in solving the model are listed below.

Seismic action combinations

1. $1.35\ G_k + 1.5\ Q_k$
2. $1.00\ G_k + 0.3\ Q_k + 1\ E_x + 0.3\ E_y$
3. $1.00\ G_k + 0.3\ Q_k + 1\ E_x - 0.3\ E_y$
4. $1.00\ G_k + 0.3\ Q_k - 1\ E_x + 0.3\ E_y$
5. $1.00\ G_k + 0.3\ Q_k - 1\ E_x - 0.3\ E_y$
6. $1.00\ G_k + 0.3\ Q_k + 0.3\ E_x + 1\ E_y$
7. $1.00\ G_k + 0.3\ Q_k + 0.3\ E_x - 1\ E_y$
8. $1.00\ G_k + 0.3\ Q_k - 0.3\ E_x + 1\ E_y$
9. $1.00\ G_k + 0.3\ Q_k - 0.3\ E_x - 1\ E_y$

The method applied, and under the provisions of EAK 2000, is the dynamic spectral method. With this method the potential extremes values of random response size with quadratic superposition of modal values of the considered size are calculated (SRSS rule) [10]. For each component of seismic excitation is taken into account a number of modals, until the sum of modal masses of high-level ΣM_i reaches 90% of the total oscillating mass M of the system. As active modal is defined the percentage of oscillating mass in the considered direction of excitation participating in the modal oscillation. Thus, under the foregoing, result the characteristic features of the construction for the respective periods.

6.5 Dynamic Analysis

Initially, there was a static solution of the model of the construction for the permanent and moving loads and then its modal analysis. After the modal analysis and using its results, followed the dynamic spectral analysis of earthquakes in both horizontal directions using the elastic range of EAK 2003 with the following parameters:

- The model was elastically analyzed for four seismic accelerations: A_1=0.16g, A_2=0.24g, A_3=0.32g, A_4=0.40g
- Factor of importance γ_I=1,15
- Factor of foundation θ=1,00
- Correction factor for decay rate ≠ 5% η=1,00
- Behavior factor q=1,00
- Soil category: B (T_1=0,15 sec, T_2=0,60 sec)
- Factor of spectral support β_0=2,50

For

$$0 \le T \le T_1 \quad \Leftrightarrow \quad \Phi_d(T) = \gamma_I \cdot A \cdot \left[1 + \frac{T}{T_1} \cdot (\eta \cdot \beta_0 - 1)\right]$$

$$T_1 \le T \le T_2 \quad \Leftrightarrow \quad \Phi_d(T) = \gamma_I \cdot A \cdot \eta \cdot \beta_0$$

$$T > T_2 \quad \Leftrightarrow \quad \Phi_d(T) = \gamma_I \cdot A \cdot \eta \cdot \beta_0 \cdot \left(\frac{T_2}{T}\right)$$

To calculate the intense sizes of seismic excitation will be superposition of th calculated modals. The type of superposition chosen is the square root of the sum

of squares (SRSS).

The design spectra used in the solution are given in the chart below:

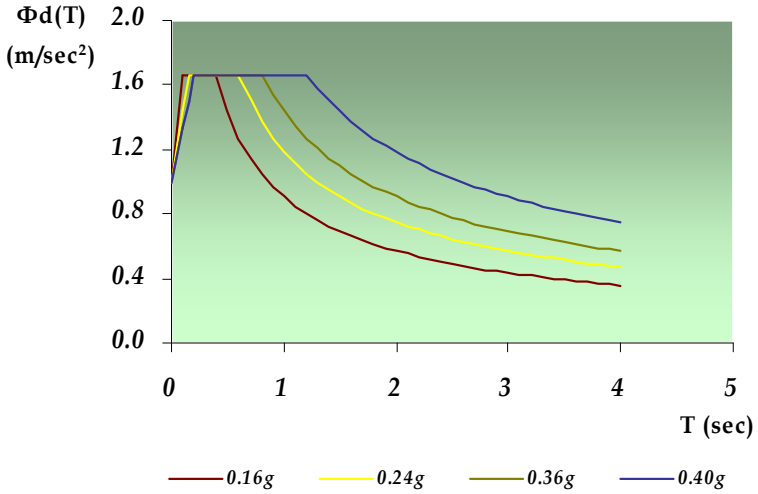

Figure 6.1 Design spectra

6.6 Assumptions in the simulation

- The nodes of finite elements in the state of the foundation have six commitments. The three commitments relate to transfers within the axes Ox, Oy, Oz and the other three at the turnings with vector parallel to the axes Ox, Oy and Oz.
- The mechanical characteristics of masonry were considered the same everywhere.
- During the simulation we assume that the material of the body is linearly elastic.
- The concrete slabs were assumed to operate diaphragmatically, while the wooden floors and the roof are not.
- In the technical description of the building is recorded the presence of some iron tiers, which are at the levels of the top floor and roof deck and also at the 4 corners of the building. However, they are not displayed at the architectural plans, and for this reason they were not simulated. The same exists for the blanks in the headers of the wooden frames of the two-storey outbuilding, whose existence is mentioned in paragraph 5.3.1, but were not simulated because they were not brought out to the architectural plans.
- The floors and the stair were not simulated until only when the loads were

introduced through the resting nodes on the floor of the masonry.

- The roofs have been simulated with beam elements through which is achieved the transfer of cargo from the roof to the walls.
- Some architectural niches that exist in front facade of the building and inside the ground were ignored in the simulated body.
- The east addition has shown apart from the bearing masonry and some elements of reinforced concrete, without being clear their role in the stationary function of the addition. During the simulation was selected the transfer of the loads in the ground through the walls.
- For the metallic elements there was no information from the research team and the mechanical characteristics were approximately evaluated.

6.7 Modal Analysis

The modal analysis is necessary to solve problems of dynamic in a system. In the dynamic phenomena such as earthquake, data is time varying, therefore only the approach to the problem is possible, since there is no single solution. With the modal analysis the response becomes a multi-stage system (i.e.: building) as the sum of responses of single degree oscillators, which combined with the design spectra may be calculated in good approximation movements / deformations and thus the tensions resulting from dynamic phenomena such as earthquake. These results together with the static loads are used for the design of each building. Also is worth noting that in cases of settlement of the body with static program through modal analysis, are identified any errors in the formation of the model, such as: accidentally connected nodes, supports error, error in rigid members, etc.

Annex 1 lists the features of the construction and the proportion of the mass of the building participation in any one of them. Observing the table result the following important conclusions:

1) The first modal is not the fundamental one
2) 300 modals were needed to activate the 90% of the mass at X and Y (transferational modal)
3) 300 modals were needed to activate the 85% of the mass rotationally RX and RY (rotational modal)
4) Main metaphorical modal along the axis x-x is the fifth (T= 0,141835, UX= 0,09383), while in axis y-y is the sixth (T= 0,114667, UY= 0,27315). As clearly seen the active mass in axis y-y is three times that of x-x
5) main rotational modal in axis z-z is the seventh (T= 0,110921, RZ= 0,16127)
6) The first 100 modals were sufficient to assemble the 80% of the mass in both directions and it took another 200 to get to 90%.

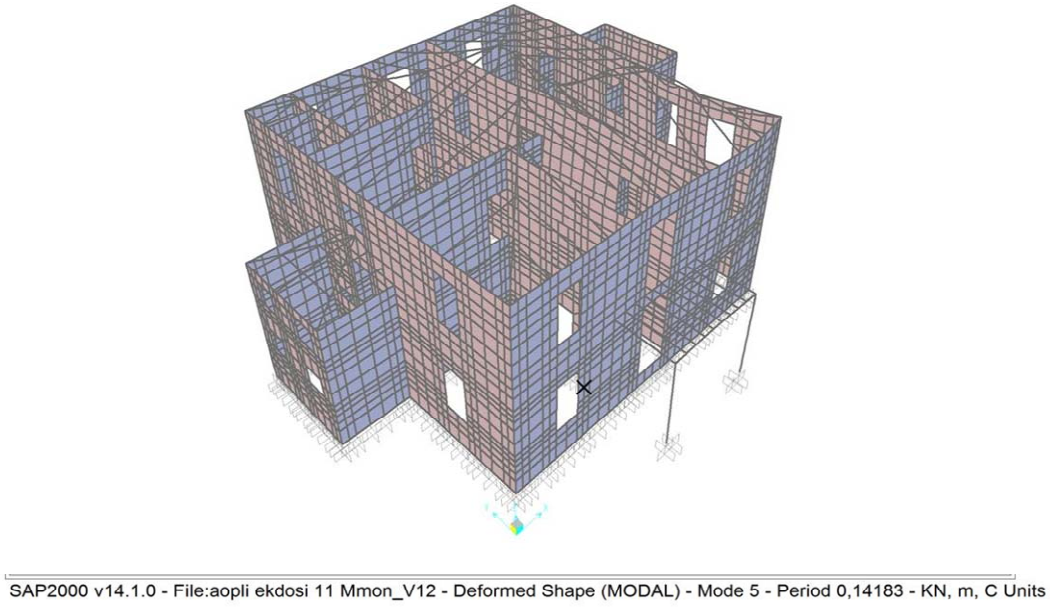

Image 6.8 fifth mode –main transport mode along x-x axis
(T= 0,141835)

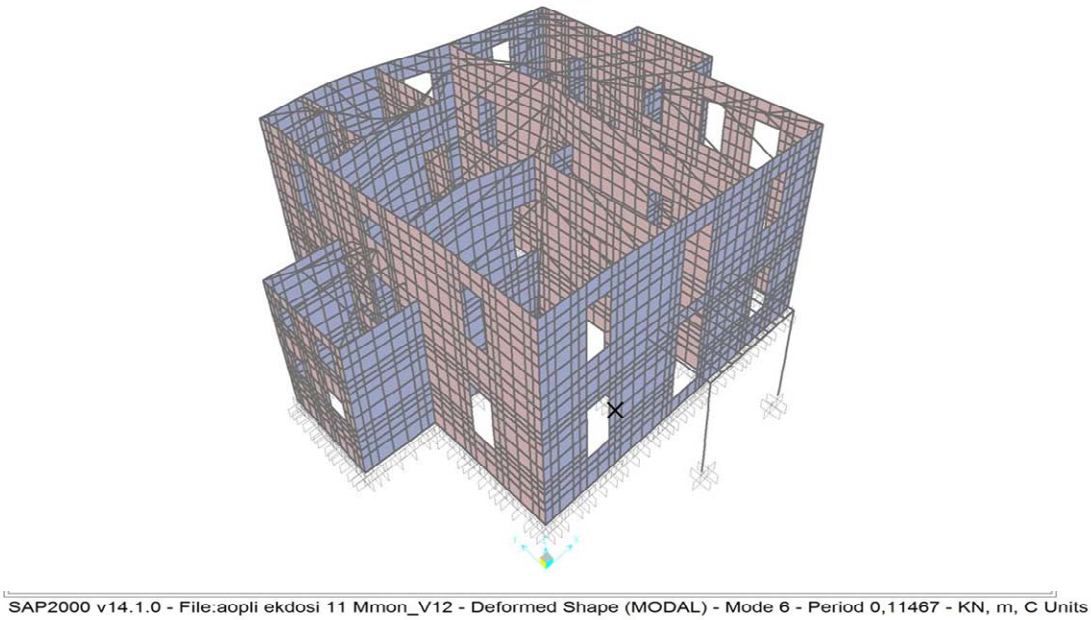

Image 6.9 Sixth mode (fundamental) –main transport mode along y-y axis
(T= 0,114667, UY= 0,27315)

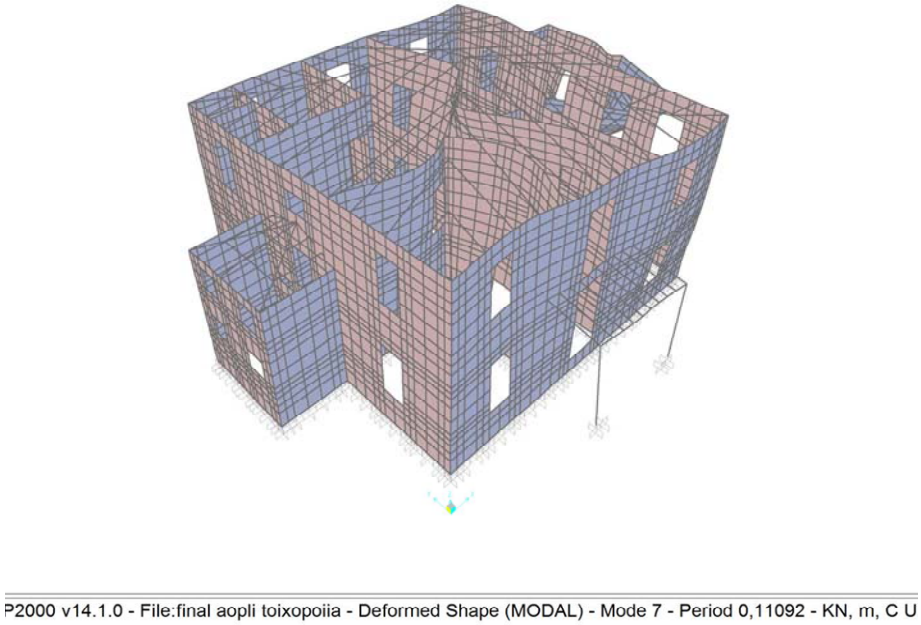

Image 6.10 Seventh mode (fundamental) –main rotational mode around z-z axis (T= 0,110921, RZ= 0,16127)

Below is presented the disfigured body for the combination of the same weight (Combination 1) and the more difficult seismic combination Combination 2 and Combination 3, where:

Combination 1 $1.35\ G_k + 1.5\ Q_k$

Combination 2. $1.00\ G_k + 0.3\ Q_k + 1\ E_x + 0.3\ E_y$

Combination 3. $1.00\ G_k + 0.3\ Q_k + 1\ E_x - 0.3\ E_y$

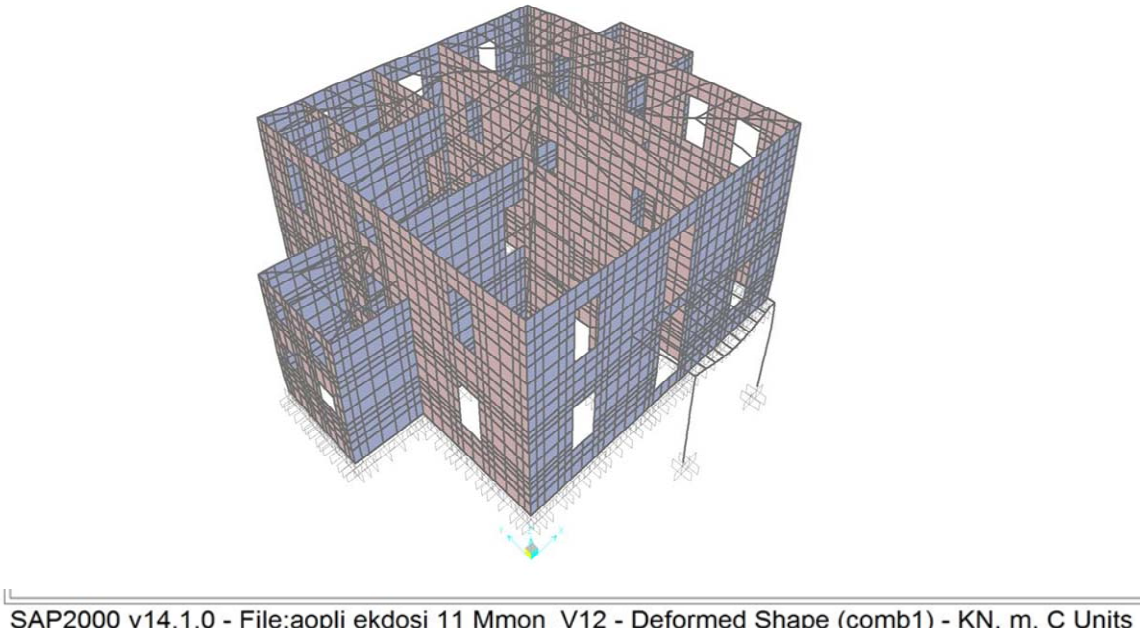

Image 6.11 Deformed shape- static loads combination (Comb 1)

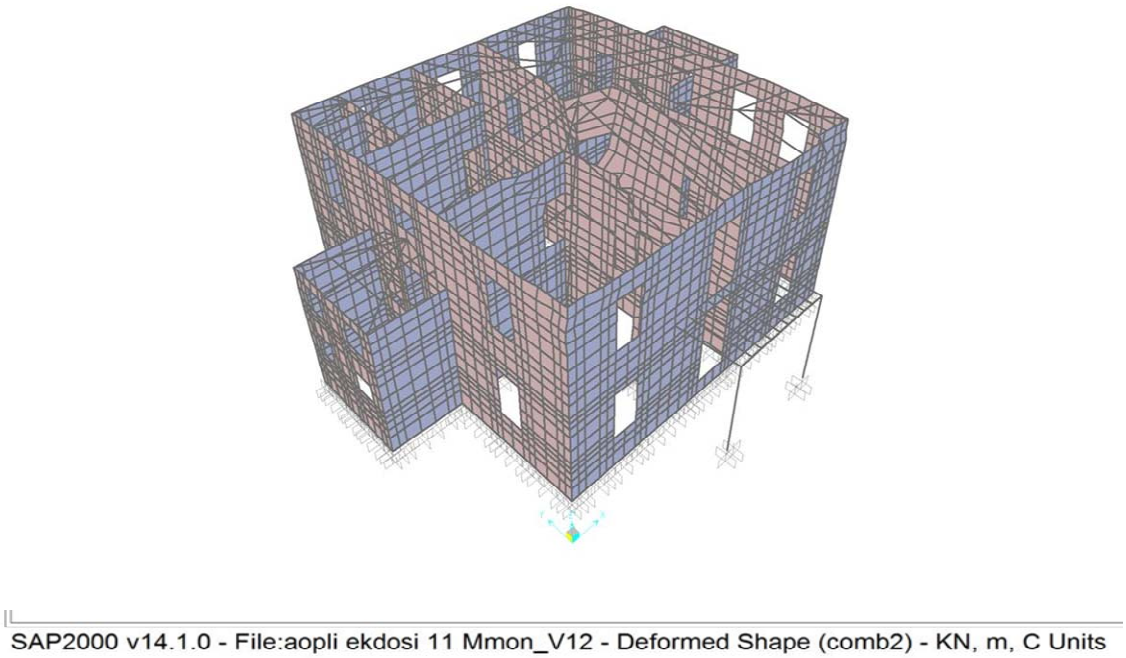

Image 6.12 Deformed shape- seismic combination 2 (Comb 2)

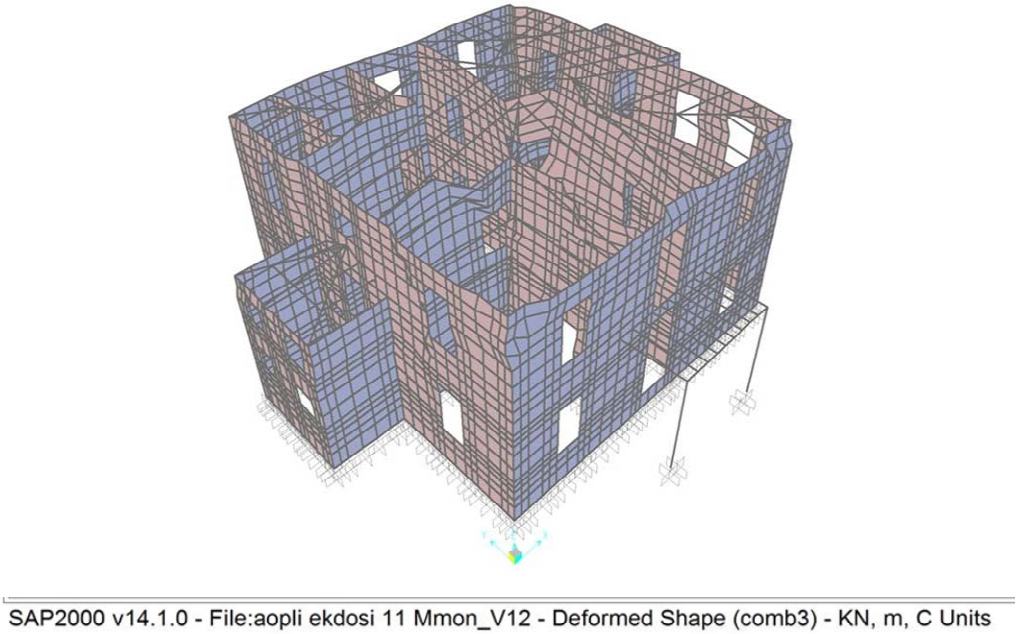

Image 6.13 Deformed shape- seismic combination 3 (Comb 3)

6.8 Results of the masonry failure – solution with the program Failure

The export of fragility curves is affected by applying the methodology described above for different values of ground acceleration and tensile strength. The body was simulated in the static software program SAP2000 v10.0.1 Nonlinear (Three Dimensional Static and Dynamic Analysis of Structures), and then solved for four different values of ground acceleration. As mentioned in section 6.1, the values of seismic tension taken are PGA = 0.16g, 0.24g, 0.36g, 0.40g. Then, the results of the solution were used along with nine pairs of tensile and compressive strength to determine the rate of failure of construction with the assistance of the program FAILURE. The range of values of the variable tensile strength ranges from 50 to 450 kPa, with a scale of 50 kPa. Then result 9 pairs of different strengths - mortars, keeping constant the compressive strength and equal to 1100 kPa and from the program are given the failure rates of finite elements for each wall on both sides of it. The exported from the analysis of the nine loading combinations, with two borders top and bottom of the shell elements at a time, successively are used as input for the program FAILURE, which determines the rate of failure $A_{\beta\lambda}/A_{o\lambda}$ of the construction for nine pairs f_{wt}.

It is recalled that the program FAILURE extracts the finite element failure rate per

wall, for data characteristic of the materials and PGA, while enables an overview of presentation through diverse coloring of the failure regions per mechanism of biaxial tension. The failure rate per wall for each ground acceleration (PGA) and for each variable value of the tensile strength of the masonry is given in Annex 4. Please note that these values have derived from the average rate of failure of both sides (top and bottom) of each wall.

Overall, the walls of the building are 15 and the total number of resolutions from the program FAILURE is amounted to 4860 = 9mortars x 15 walls x 4 earthquakes x 9loading combinations (for the 2 sides of each wall).

Below are indicatively presented, the failures of four wall characteristics (w1, w8, wB, wD) of the building for the maximum load combinations which result from the program FAILURE, for PGA = 0.16g, 0.24g, 0.32g, 0.40g and for tensile strength fwt = 50kPa, 250 kPa and 450 kPa. 0.40g και για εφελκυστική αντοχή fwt = 50kPa, 250 kPa και 450 kPa.

Failure		
wall : **1_2topmax** **Load Cases :** **0.16g**		Failure under biaxial Tension/Tension
		Failure under biaxial Tension/ Compression
		Failure under biaxial Compression /Tension
		Failure under biaxial Compression/ Compression
		NON Failure
fwt = 50 kPa	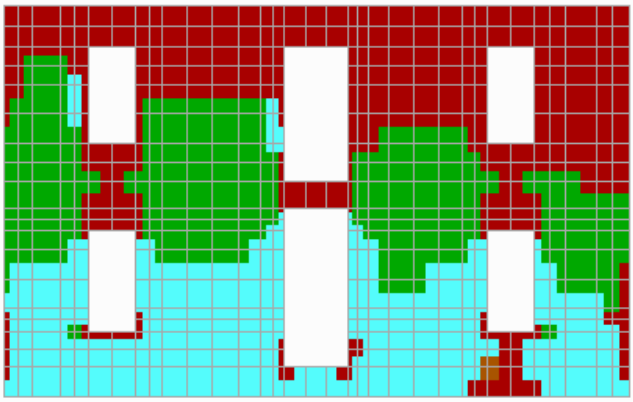	
Joints = 640 Failed = 434 Failure Percentage = 67.81%		
fwt = 250 kPa	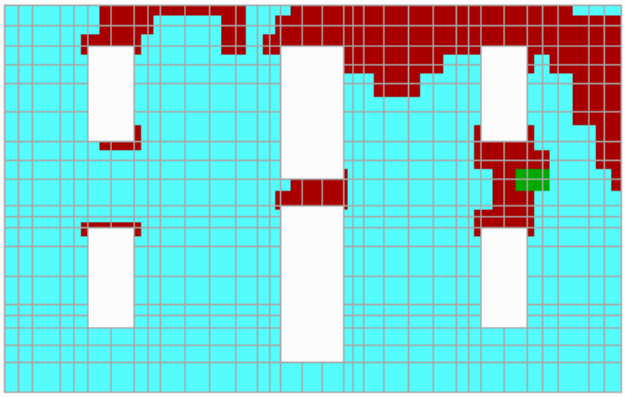	
Joints = 640 Failed = 123 Failure Percentage = 19.22%		
f_{wt} = 450 kPa	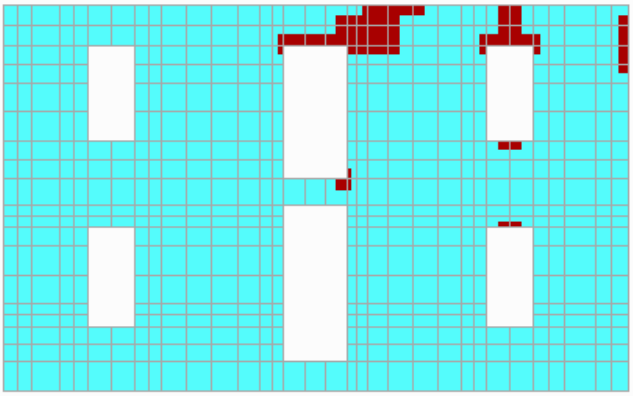	
Joints = 640 Failed = 25 Failure Percentage = 3.91%		

Failure		
wall : **1_2topmax** **Load Cases :** **0.24g**		Failure under biaxial Tension/Tension
		Failure under biaxial Tension/ Compression
		Failure under biaxial Compression /Tension
		Failure under biaxial Compression/ Compression
		NON Failure
fwt = 50 kPa	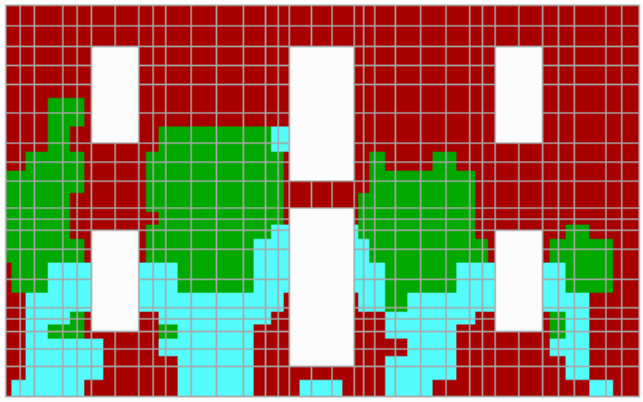	
Joints = 640 Failed = 536 Failure Percentage = 83.75%		
fwt = 250 kPa	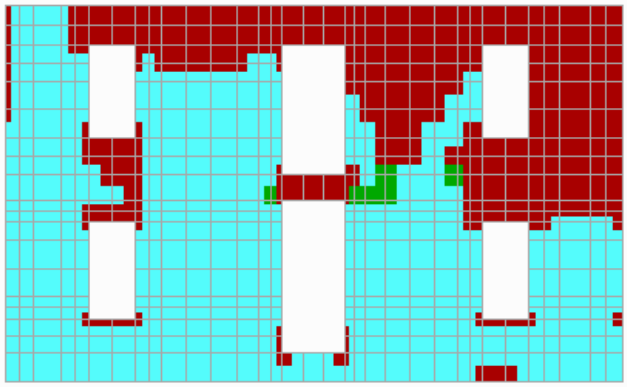	
Joints = 640 Failed = 239 Failure Percentage = 37.34%		
f_{wt} = 450 kPa	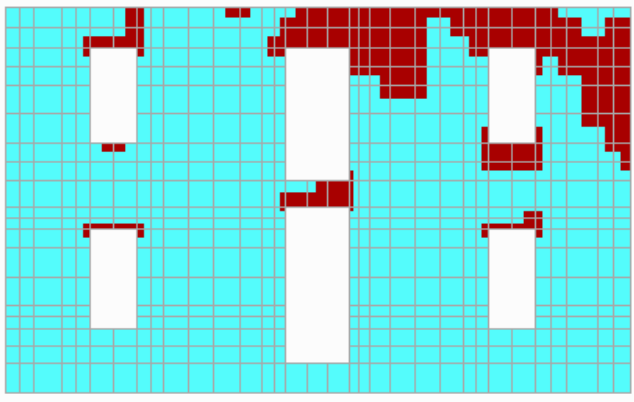	
Joints = 640 Failed = 96 Failure Percentage = 15.00%		

Failure		
wall : **1_2topmax** **Load Cases :** **0.32g**		Failure under biaxial Tension/Tension
		Failure under biaxial Tension/ Compression
		Failure under biaxial Compression /Tension
		Failure under biaxial Compression/ Compression
		NON Failure
fwt = 50 kPa	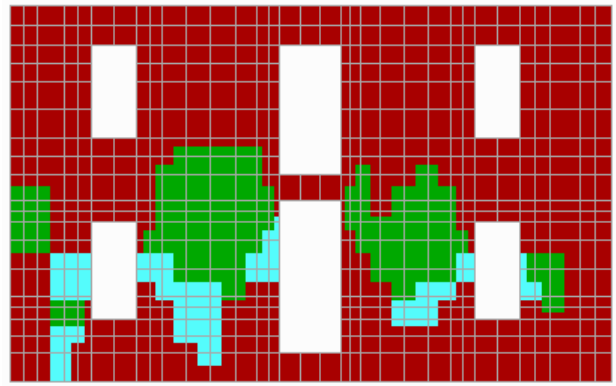	
Joints = 640 Failed = 600 Failure Percentage = 93.75%		
fwt = 250 kPa	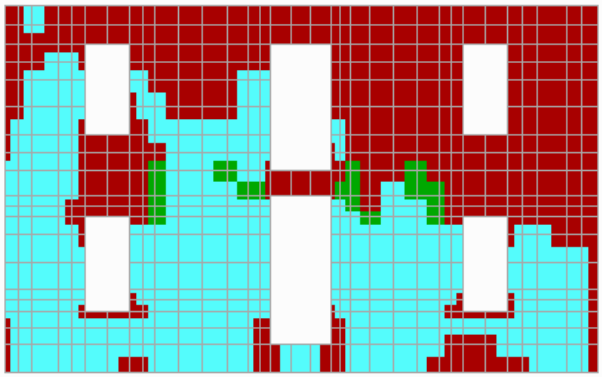	
Joints = 640 Failed = 345 Failure Percentage = 53.91%		
f_{wt} = 450 kPa	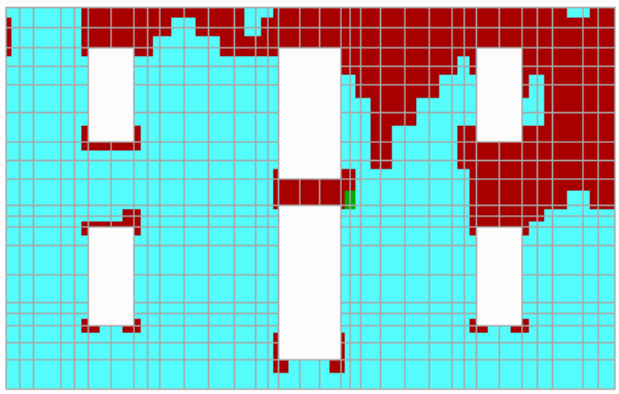	
Joints = 640 Failed = 177 Failure Percentage = 27.66%		

Failure		
wall : **1_2topmax** **Load Cases :** **0.40g**		Failure under biaxial Tension/Tension
		Failure under biaxial Tension/ Compression
		Failure under biaxial Compression /Tension
		Failure under biaxial Compression/ Compression
		NON Failure
fwt = 50 kPa	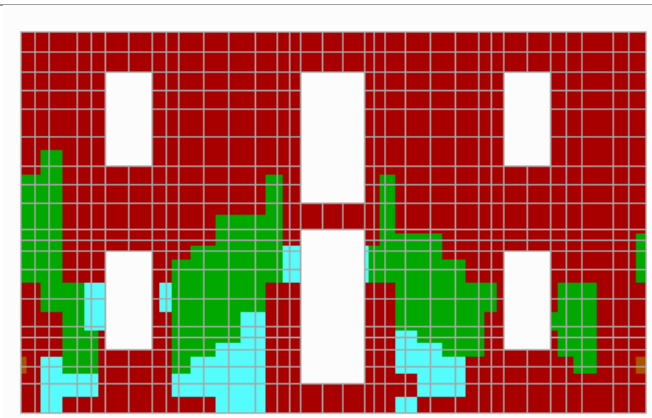	
Joints = 640 Failed = 629 Failure Percentage = 98.27%		
fwt = 250 kPa	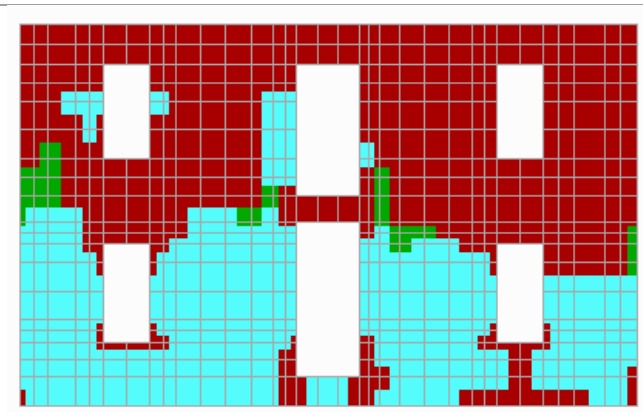	
Joints = 640 Failed = 444 Failure Percentage = 69.38%		
f_{wt} = 450 kPa	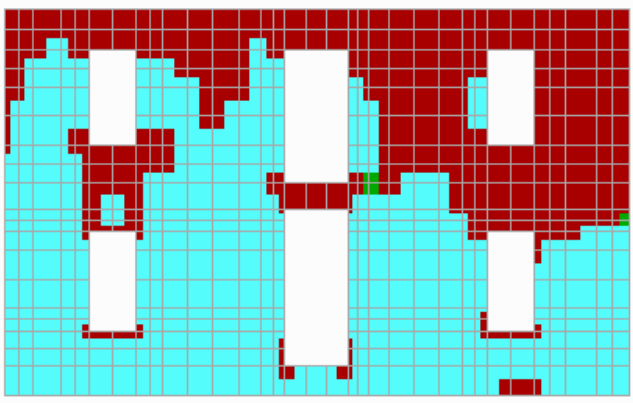	
Joints = 640 Failed = 260 Failure Percentage = 40.63%		

Failure		
wall : **8_2topmax** **Load Cases :** **0.16g**		Failure under biaxial Tension/Tension
		Failure under biaxial Tension/ Compression
		Failure under biaxial Compression /Tension
		Failure under biaxial Compression/ Compression
		NON Failure
fwt = 50 kPa	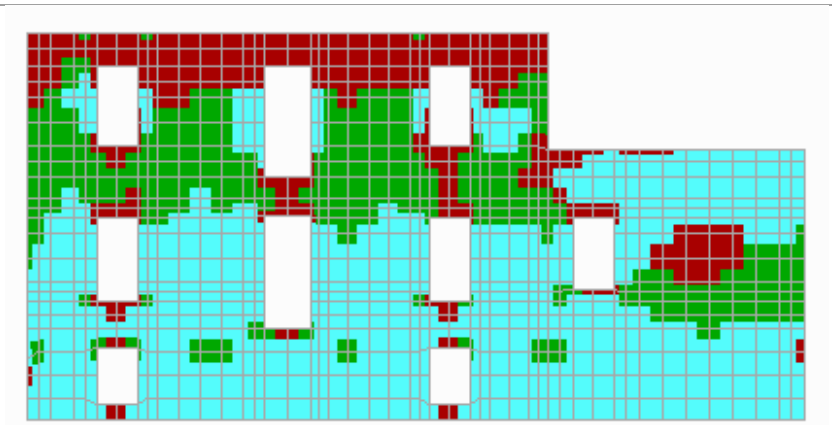	
Joints = 990 Failed = 452 Failure Percentage = 45.66%		
fwt = 250 kPa	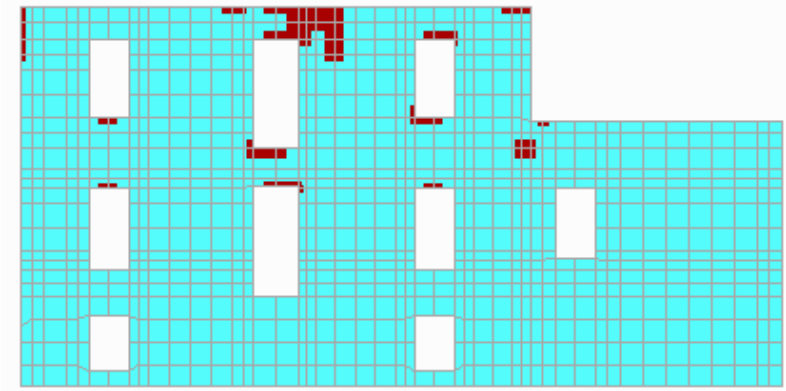	
Joints = 990 Failed = 37 Failure Percentage = 3.74%		
f_{wt} = 450 kPa	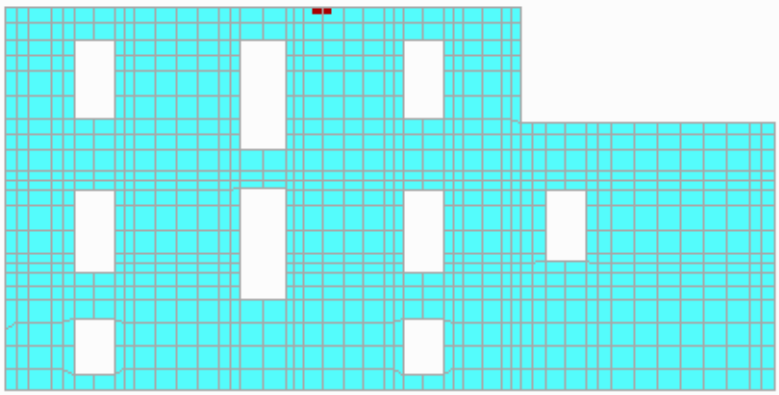	
Joints = 990 Failed = 1 Failure Percentage = 0.10%		

Failure		
wall : **8_2topmax** **Load Cases :** **0.24g**		Failure under biaxial Tension/Tension
		Failure under biaxial Tension/ Compression
		Failure under biaxial Compression /Tension
		Failure under biaxial Compression/ Compression
		NON Failure
fwt = 50 kPa Joints = 990 Failed = 630 Failure Percentage = 63.64%	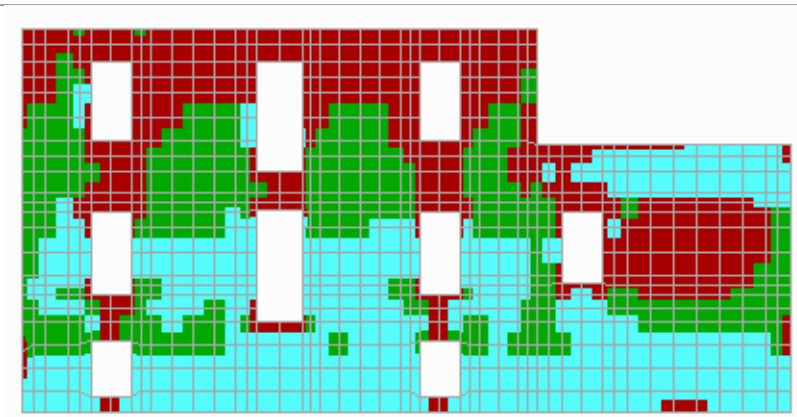	
fwt = 250 kPa Joints = 990 Failed = 124 Failure Percentage = 12.53%	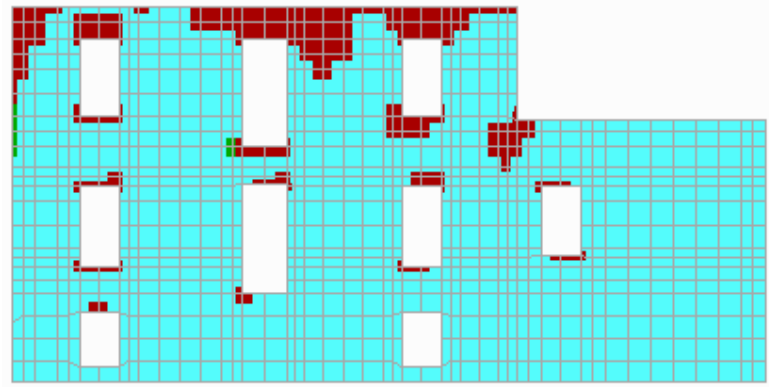	
f_{wt} = 450 kPa Joints = 990 Failed = 20 Failure Percentage = 2.02%	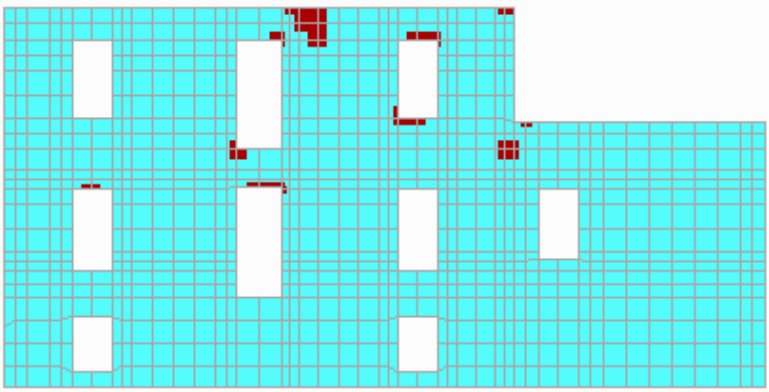	

Failure		
wall : **8_2topmax** **Load Cases :** **0.32g**		Failure under biaxial Tension/Tension
		Failure under biaxial Tension/ Compression
		Failure under biaxial Compression /Tension
		Failure under biaxial Compression/ Compression
		NON Failure
fwt = 50 kPa	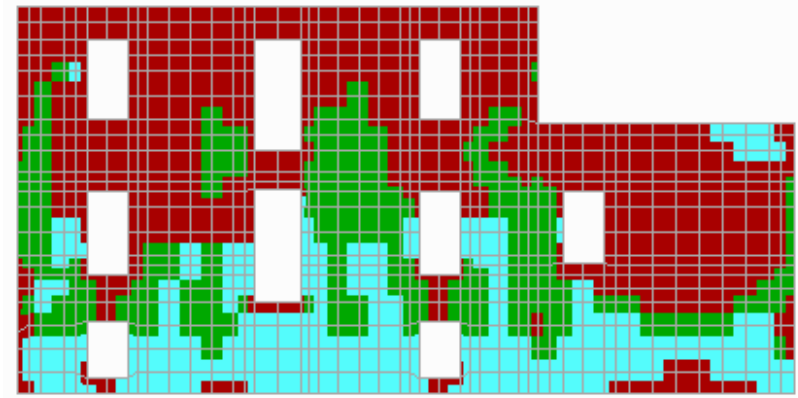	
Joints = 990 Failed = 776 Failure Percentage = 78.38%		
fwt = 250 kPa	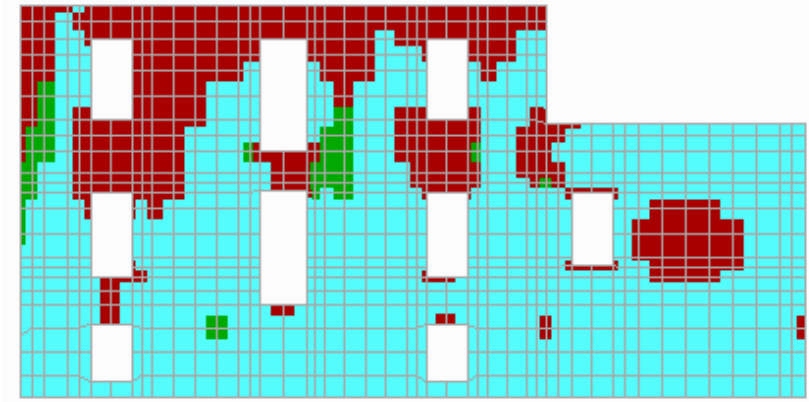	
Joints = 990 Failed = 315 Failure Percentage = 31.82%		
f_{wt} = 450 kPa	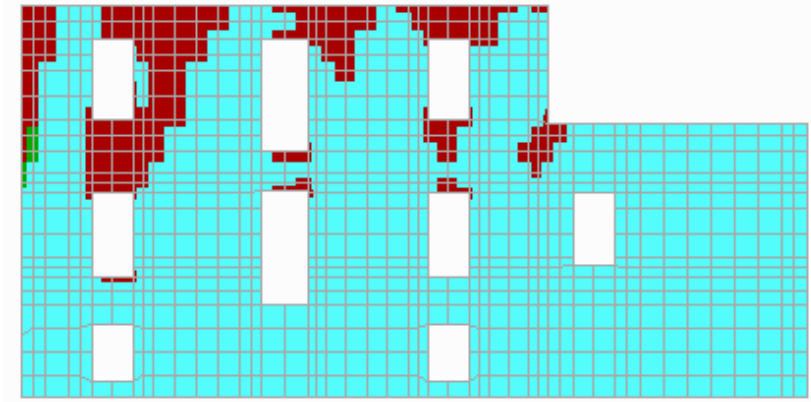	
Joints = 990 Failed = 145 Failure Percentage = 14.65%		

Failure		
wall : **8_2botmax** **Load Cases :** **0.40g**		Failure under biaxial Tension/Tension
		Failure under biaxial Tension/ Compression
		Failure under biaxial Compression /Tension
		Failure under biaxial Compression/ Compression
		NON Failure
fwt = 50 kPa	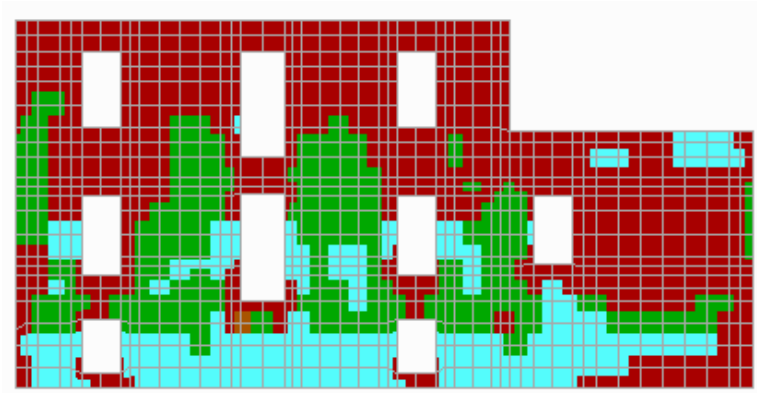	
Joints = 990 Failed = 810 Failure Percentage = 81.82%		
fwt = 250 kPa	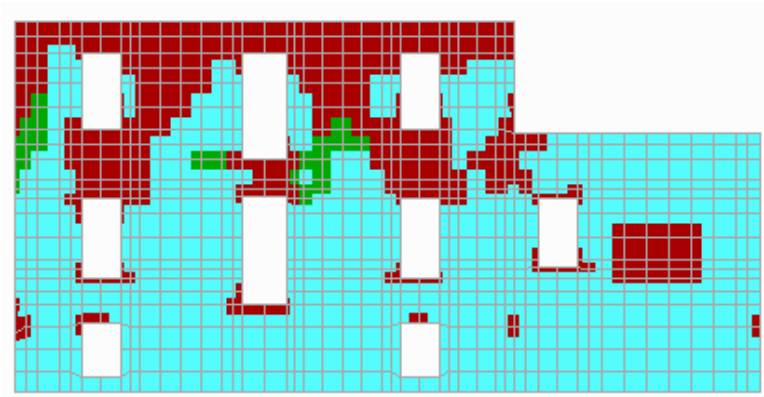	
Joints = 990 Failed = 329 Failure Percentage = 33.23%		
f_{wt} = 450 kPa	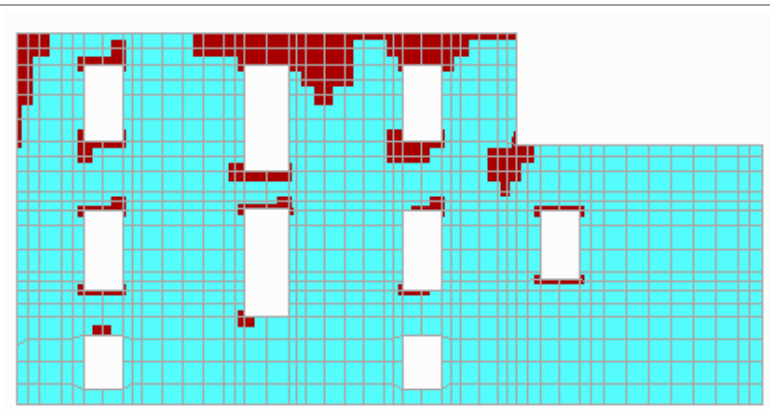	
Joints = 990 Failed = 120 Failure Percentage = 12.12%		

Failure		
wall : **D_2topmax** **Load Cases :** **0.16g**		Failure under biaxial Tension/Tension
		Failure under biaxial Tension/ Compression
		Failure under biaxial Compression /Tension
		Failure under biaxial Compression/ Compression
		NON Failure
fwt = 50 kPa Joints = 555 Failed = 377 Failure Percentage = 67.93%	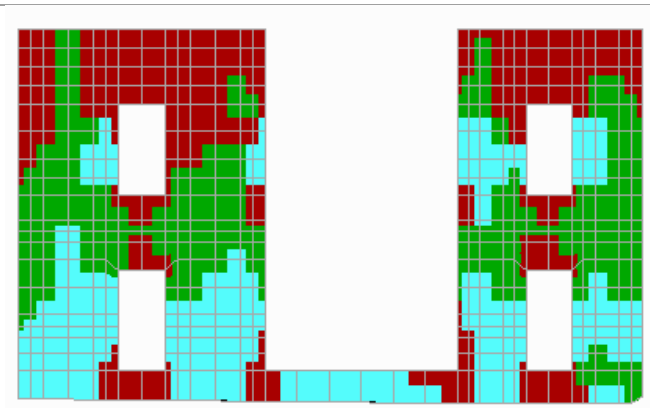	
fwt = 250 kPa Joints = 555 Failed = 73 Failure Percentage = 13.15%	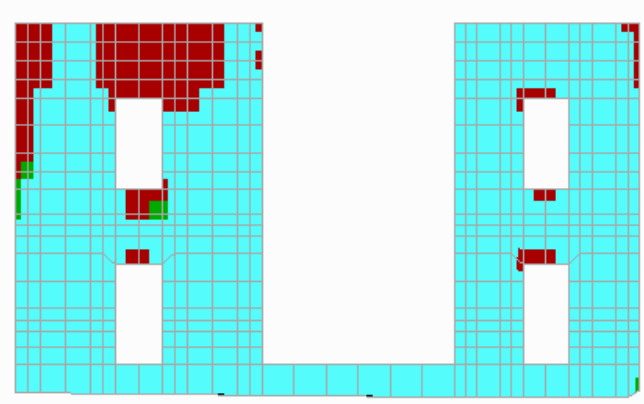	
f_{wt} = 450 kPa Joints = 555 Failed = 17 Failure Percentage = 3.06%	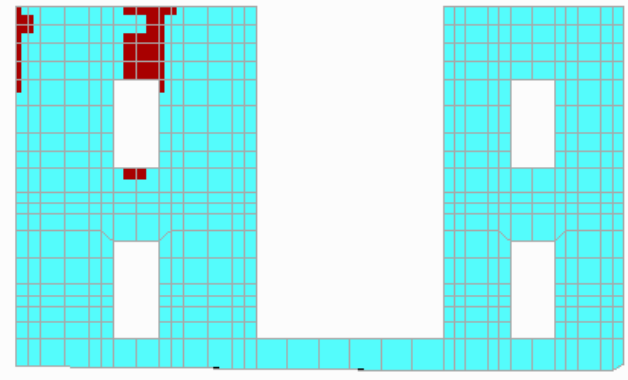	

Failure		
wall : **D_2topmax** **Load Cases :** **0.24g**		Failure under biaxial Tension/Tension
		Failure under biaxial Tension/ Compression
		Failure under biaxial Compression /Tension
		Failure under biaxial Compression/ Compression
		NON Failure
fwt = 50 kPa Joints = 555 Failed = 473 Failure Percentage = 85.23%	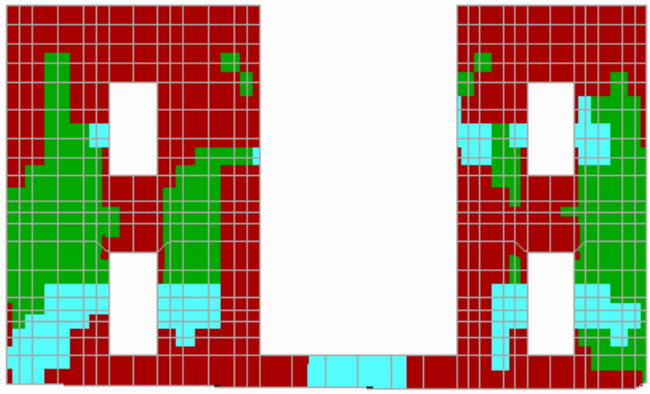	
fwt = 250 kPa Joints = 555 Failed = 165 Failure Percentage = 29.73%	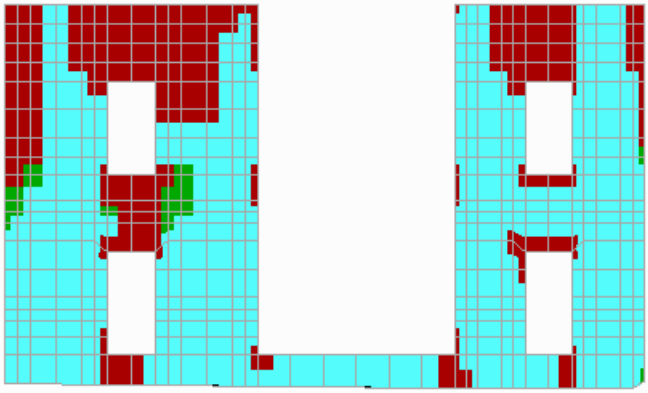	
f_{wt} = 450 kPa Joints = 555 Failed = 55 Failure Percentage = 9.91%	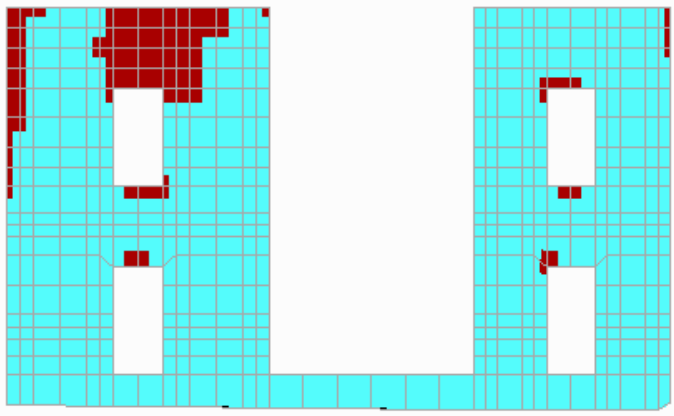	

Failure		
wall : **D_2topmax** **Load Cases :** **0.32g**		Failure under biaxial Tension/Tension
		Failure under biaxial Tension/ Compression
		Failure under biaxial Compression /Tension
		Failure under biaxial Compression/ Compression
		NON Failure
fwt = 50 kPa Joints = 555 Failed = 524 Failure Percentage = 94.41%	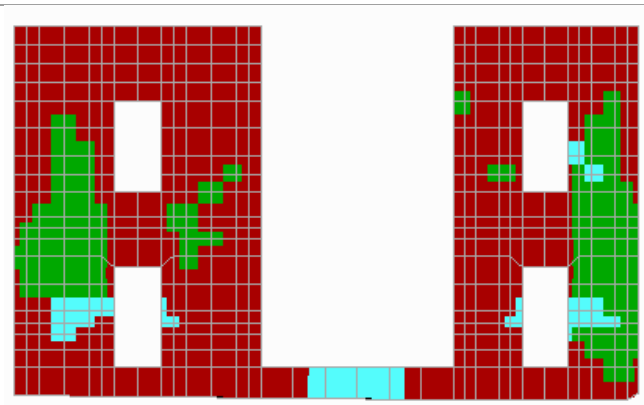	
fwt = 250 kPa Joints = 555 Failed = 268 Failure Percentage = 48.29%	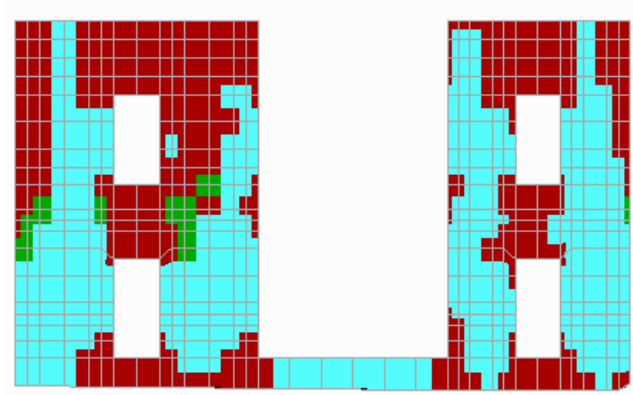	
f_{wt} = 450 kPa Joints = 555 Failed = 114 Failure Percentage = 20.54%	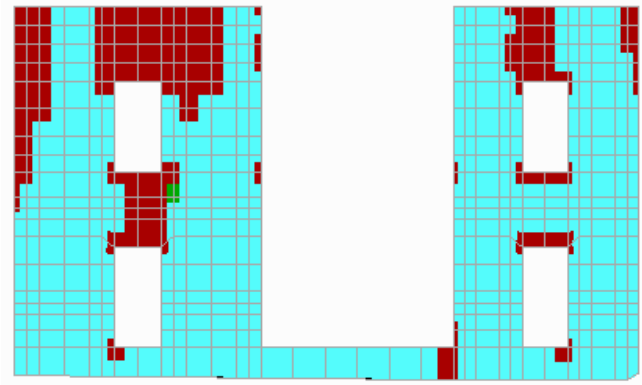	

Failure		
wall : **E_2topmax** **Load Cases :** **0.16g**		Failure under biaxial Tension/Tension
		Failure under biaxial Tension/ Compression
		Failure under biaxial Compression /Tension
		Failure under biaxial Compression/ Compression
		NON Failure
fwt = 50 kPa Joints = 558 Failed = 405 Failure Percentage = 72.58%	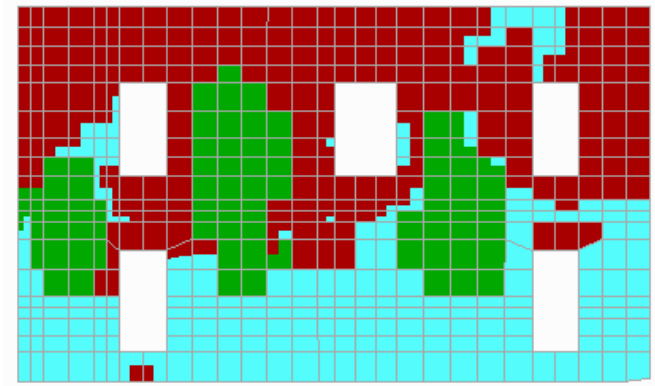	
fwt = 250 kPa Joints = 558 Failed = 243 Failure Percentage = 43.55%	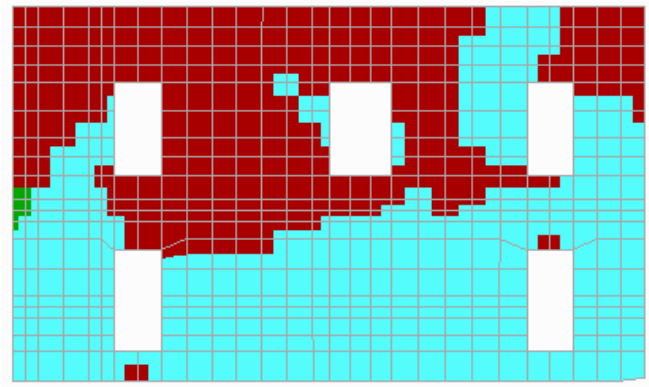	
f_{wt} = 450 kPa Joints = 558 Failed = 140 Failure Percentage = 25.09%	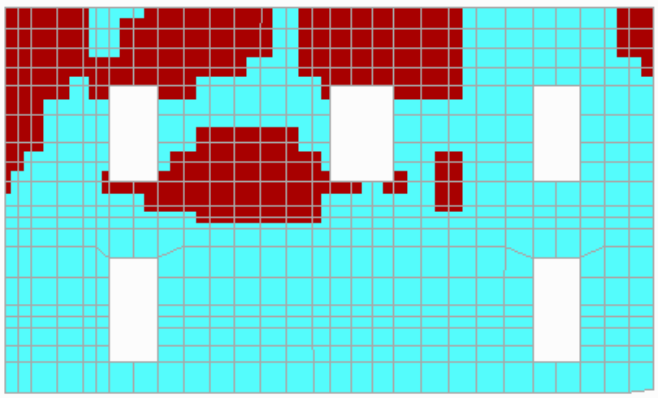	

Failure	
wall : **E_2topmax** **Load Cases :** **0.24g**	Failure under biaxial Tension/Tension
	Failure under biaxial Tension/ Compression
	Failure under biaxial Compression /Tension
	Failure under biaxial Compression/ Compression
	NON Failure
fwt = 50 kPa	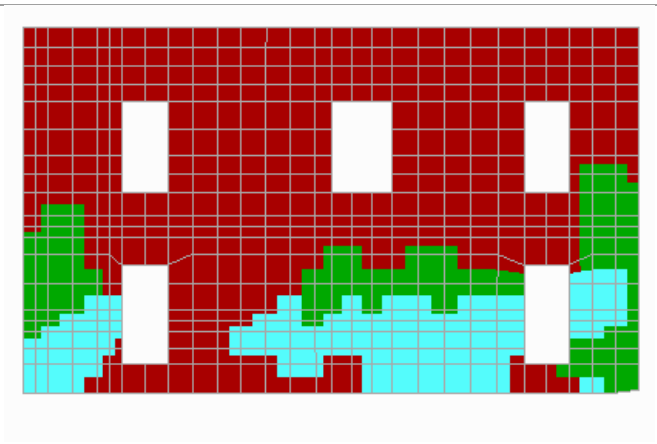
Joints = 558 Failed = 461 Failure Percentage = 82.62%	
fwt = 250 kPa	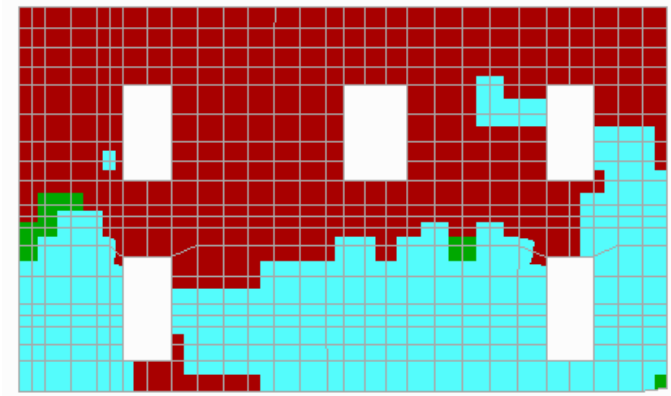
Joints = 558 Failed = 332 Failure Percentage = 59.50%	
f_{wt} = 450 kPa	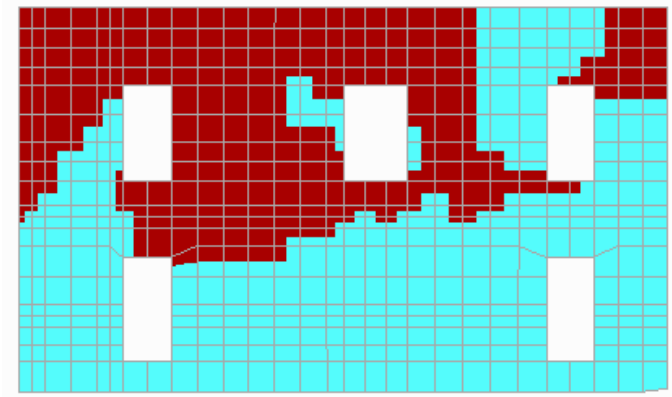
Joints = 558 Failed = 227 Failure Percentage = 40.68%	

Failure		
wall : **E_2topmax** **Load Cases :** **0.32g**		Failure under biaxial Tension/Tension
		Failure under biaxial Tension/ Compression
		Failure under biaxial Compression /Tension
		Failure under biaxial Compression/ Compression
		NON Failure
fwt = 50 kPa Joints = 558 Failed = 489 Failure Percentage = 87.63%	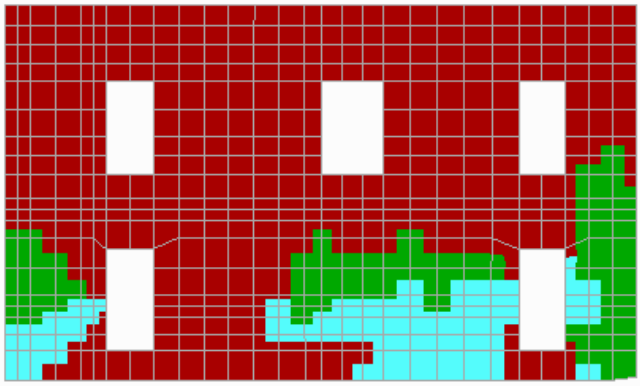	
fwt = 250 kPa Joints = 558 Failed = 365 Failure Percentage = 65.41%	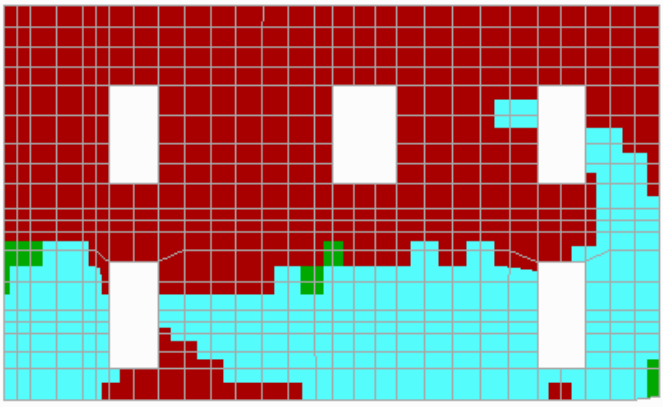	
f_{wt} = 450 kPa Joints = 558 Failed = 295 Failure Percentage = 52.87%	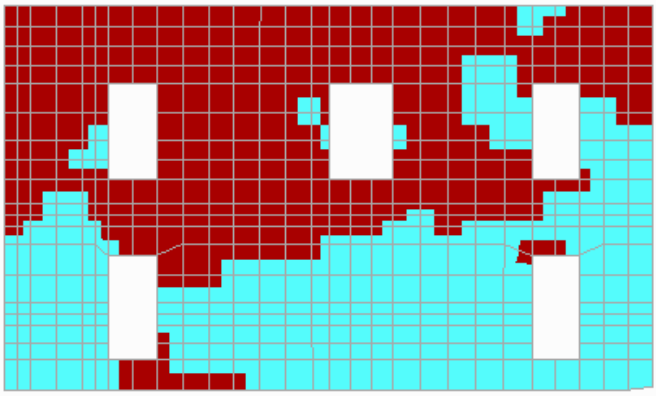	

Failure		
wall : **E_2topmax** **Load Cases :** **0.40g**		Failure under biaxial Tension/Tension
		Failure under biaxial Tension/ Compression
		Failure under biaxial Compression /Tension
		Failure under biaxial Compression/ Compression
		NON Failure
fwt = 50 kPa Joints = 558 Failed = 512 Failure Percentage = 91.76%	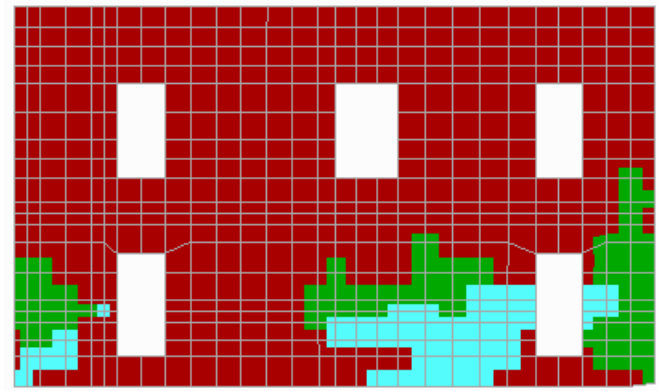	
fwt = 250 kPa Joints = 558 Failed = 410 Failure Percentage = 73.48%	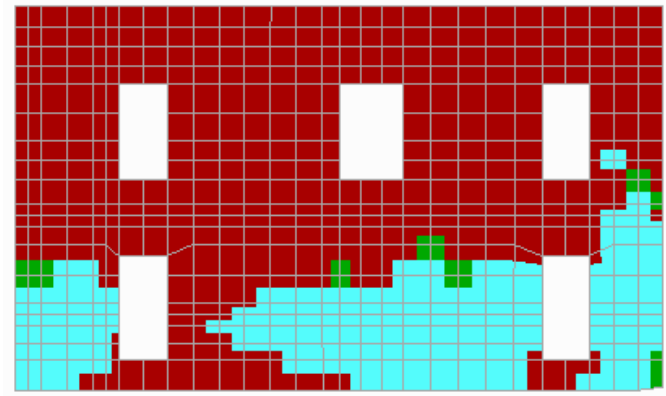	
f_{wt} = 450 kPa Joints = 558 Failed = 338 Failure Percentage = 60.57%	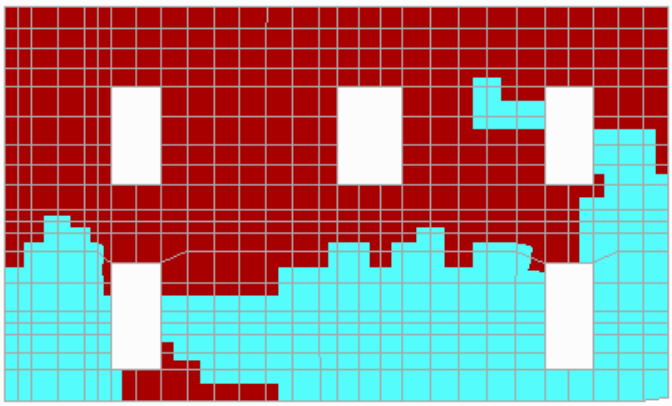	

6.9 Failure rates & Statistical elaboration of the results

For the statistical analysis of data and in order to draw conclusions concerning the type and size of the failure of the wall structure, is taken the overall rate of failure for the 15 walls of the building for different tensile strength and four ground accelerations.

Table 6.2: Total failure percentages for the building, for 9 mortars and 4 ground accelerations

f_{wt} / PGA	*0.16g*	*0.24g*	*0.36g*	*0.40g*
K50	62.84	74.12	84.89	88.47
K100	47.02	61.01	73.39	79.28
K150	37.64	48.81	62.74	71.02
K200	27.25	39.83	52.60	61.85
K250	20.12	31.83	44.47	54.44
K300	16.01	26.59	38.19	47.25
K350	12.01	22.31	33.17	41.46
K400	9.05	18.43	28.72	36.32
K450	6.39	15.96	24.91	31.68

At the stage of statistical analysis are used specific probability density functions describing the distributions with which we will process the results of the failure surfaces of the masonry. The distributions used in this study are the Normal and the lognormal distribution, which have been presented in preceding section. The calculation of the values for probability density functions and cumulative probability was performed using the program Excel. The cumulative probability is obtained by completing the p.d.f. to the desired, at each case, time. For the distributions was realized the audit of good fitting $\chi^2$with a level of significance (l.s.) 0,01. This means that the use of these distributions to describe the sample, requires the acceptance of the probability of 1% that these distributions do not reliably describe the sample (Type I error).

Here are the results of the statistical analysis of the data for the two distributions and the four ground accelerations.

Normal Distribution

The distribution is described from the below function:

$$f(x)=\frac{1}{\sigma\sqrt{2\pi}}\exp\left[-\frac{1}{2\sigma^2}(x-\mu)^2\right] \quad \text{, for interval} \quad -\infty < x < +\infty$$

The cumulative probability results by completing the *f(x)*:

$$F(x)=\int_{-\infty}^{+\infty} f(x)dx$$

So for the 4 different seismic parameters we will take the graphs below.

- **Ground acceleration PGA = 0.16g**

Tensile strength fwt	*(%)*
50	62.84
100	47.02
150	37.64
200	27.25
250	20.12
300	16.01
350	12.01
400	9.05
450	6.39
Total elements	9
Mean value	26.48
Standard deviation	19.16

x	*f(x)*	*F(x)*
0	0.00801045	0.08343736
5	0.01110584	0.13107678
10	0.01438339	0.19480766
15	0.01740150	0.27448148
20	0.01966651	0.36756311
25	0.02076267	0.46918683
30	0.02047644	0.57287020
35	0.01886432	0.67172688
40	0.01623466	0.75980859
45	0.01305150	0.83314982
50	0.00980151	0.89021789
55	0.00687608	0.93171523
60	0.00450614	0.95991395
65	0.00275857	0.97782083
70	0.00157753	0.98844735
75	0.00084273	0.99434044
80	0.00042054	0.99739448
85	0.00019604	0.99887353
90	0.00008537	0.99954292
95	0.00003473	0.99982601
100	0.00001320	0.99993790

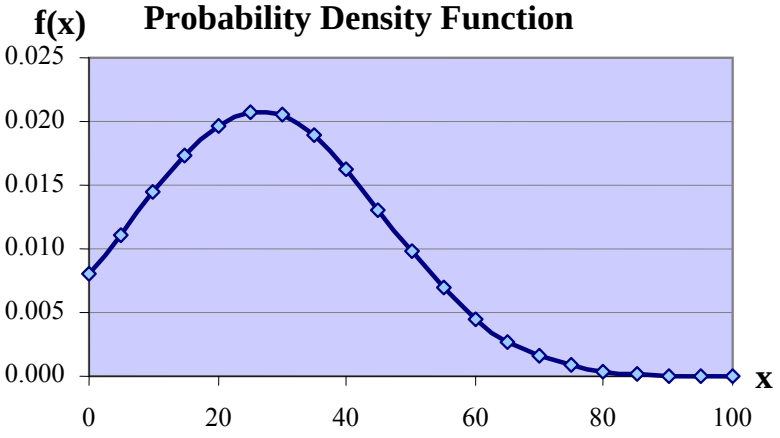

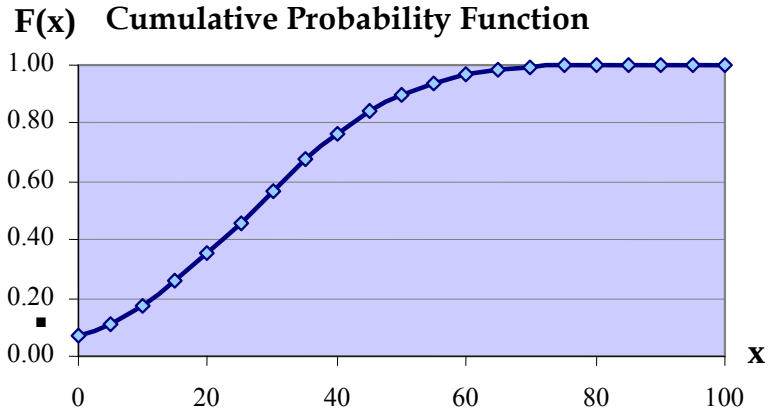

- **Ground AccelerationPGA = 0.24g**

Tensile Strength fwt	*(%)*
50	74.12
100	61.01
150	48.81
200	39.83
250	31.83
300	26.59
350	22.31
400	18.43
450	15.96
Total elements	9
Mean value	37.65
Standard deviation	20.11

x	*f(x)*	*F(x)*
0	0.00343855	0.03059655
5	0.00530970	0.05224038
10	0.00770773	0.08457824
15	0.01051829	0.13001292
20	0.01349354	0.19004218
25	0.01627303	0.26462489
30	0.01844902	0.35176397
35	0.01966257	0.44750273
40	0.01970014	0.54641780
45	0.01855497	0.64252087
50	0.01642909	0.73032439
55	0.01367504	0.80576176
60	0.01070055	0.86670997
65	0.00787128	0.91301571
70	0.00544311	0.94609896
75	0.00353843	0.96832595
80	0.00216240	0.98236869
85	0.00124229	0.99071167
90	0.00067092	0.99537277
95	0.00034063	0.99782157
100	0.00016258	0.99903137

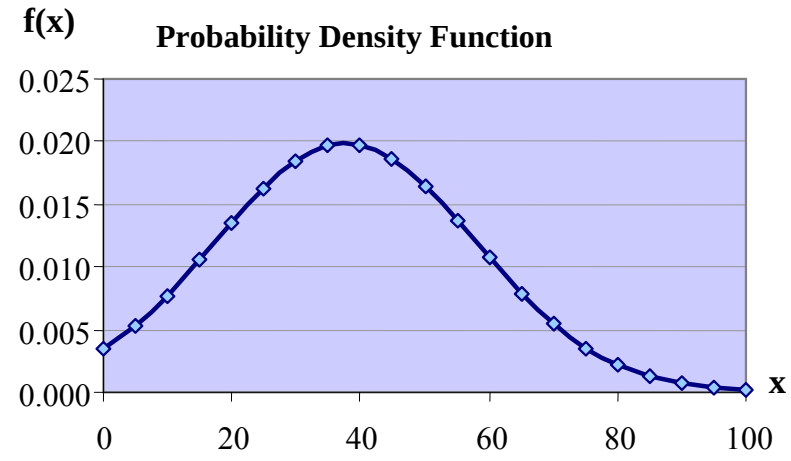

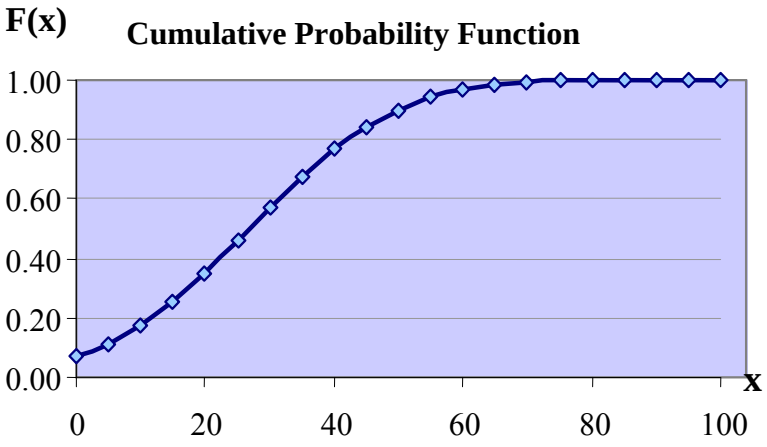

- **Ground AccelerationPGA = 0.32g**

Tensile Strength fwt	*(%)*
50	84.89
100	73.39
150	62.74
200	52.60
250	44.47
300	38.19
350	33.17
400	28.72
450	24.91
Total elements	9
Mean value	49.23
Standard deviation	20.81

x	*f(x)*	*F(x)*
0	0.00116717	0.00899161
5	0.00200218	0.01676530
10	0.00324186	0.02968925
15	0.00495461	0.04997574
20	0.00714740	0.08004077
25	0.00973219	0.12210952
30	0.01250827	0.17768734
35	0.01517427	0.24701191
40	0.01737568	0.32865452
45	0.01878019	0.41943465
50	0.01915940	0.51473816
55	0.01844963	0.60920323
60	0.01676939	0.69760844
65	0.01438702	0.77572240
70	0.01165059	0.84088879
75	0.00890531	0.89221776
80	0.00642501	0.93038979
85	0.00437545	0.95719207
90	0.00281252	0.97496019
95	0.00170644	0.98608146
100	0.00097726	0.99265365

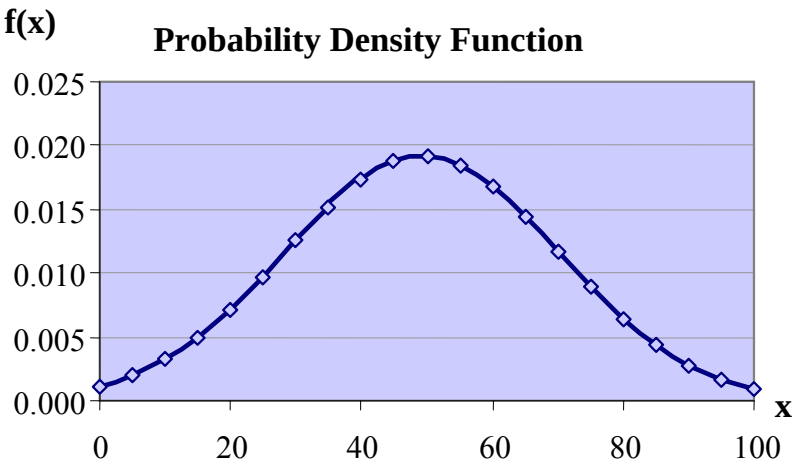

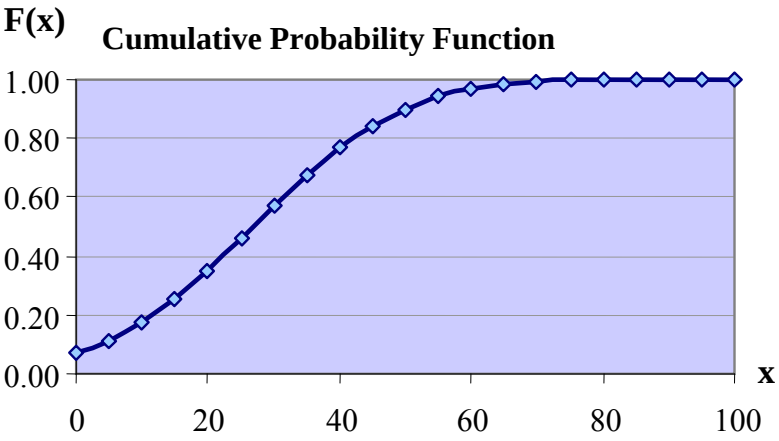

- **Ground AccelerationPGA = 0.40g**

Tensile Strength fwt	*(%)*
50	88.47
100	79.28
150	71.02
200	61.85
250	54.44
300	47.25
350	41.46
400	36.32
450	31.68
Total elements	9
Mean value	56.86
Standard deviation	19.74

x	*f(x)*	*F(x)*
0	0.00031937	0.00198801
5	0.00064140	0.00430942
10	0.00120811	0.00880853
15	0.00213418	0.01698927
20	0.00353594	0.03094504
25	0.00549445	0.05328123
30	0.00800741	0.08682090
35	0.01094479	0.13407113
40	0.01403041	0.19652284
45	0.01686867	0.27396555
50	0.01902125	0.36406303
55	0.02011615	0.46240542
60	0.01995255	0.56311368
65	0.01856092	0.65987138
70	0.01619378	0.74708858
75	0.01325087	0.82084753
80	0.01016924	0.87937008
85	0.00731948	0.92293404
90	0.00494105	0.95335878
95	0.00312829	0.97329402
100	0.00185755	0.98554894

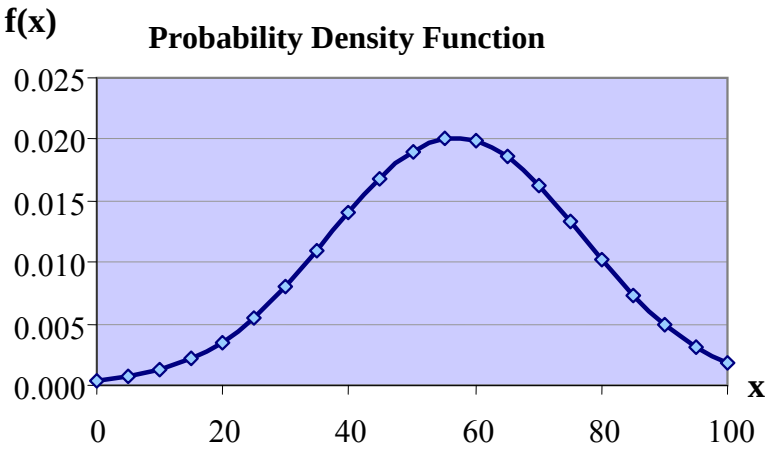

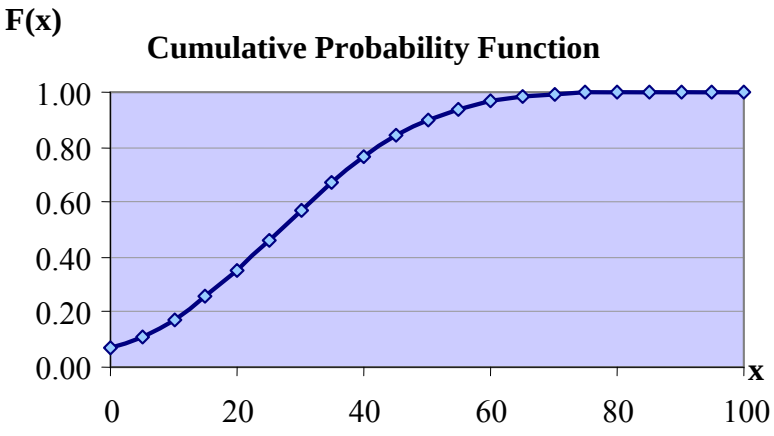

Lognormal Distribution

The distribution is described by the following equation:

$$f(x)=\begin{cases}\dfrac{1}{\sigma x\sqrt{2\pi}}\exp\left[-\dfrac{1}{2\sigma^2}\left(\ln(x)-\mu\right)^2\right] & ,\gamma\iota\alpha\ x>0\\ 0 & ,\gamma\iota\alpha\ x<0\end{cases}$$

The cumulative probability results by completing the *f(x)*:

$$F(x)=\int_{-\infty}^{+\infty} f(x)dx$$

So for the 4 different seismic parameters we will take the graphs below.

- **Ground AccelerationPGA = 0.16g**

Tensile Strength fwt	*(%)*
50	4.14
100	3.85
150	3.63
200	3.31
250	3.00
300	2.77
350	2.49
400	2.20
450	1.85
Total elements	9
Mean value	3.03
Standard deviation	0.77

x	*f(x)*	*F(x)*
0.00000000	0.00000000	0.00000000
1.60943791	0.01915582	0.03317781
2.30258509	0.03327502	0.17406641
2.70805020	0.03163192	0.33978871
2.99573227	0.02581534	0.48387891
3.21887582	0.02004019	0.59816697
3.40119738	0.01531490	0.68607555
3.55534806	0.01168089	0.75314498
3.68887945	0.00894497	0.80438144
3.80666249	0.00689552	0.84373657
3.91202301	0.00535685	0.87418556
4.00733319	0.00419512	0.89793135
4.09434456	0.00331165	0.91659907
4.17438727	0.00263450	0.93139064
4.24849524	0.00211133	0.94319992
4.31748811	0.00170394	0.95269634
4.38202663	0.00138427	0.96038511
4.44265126	0.00113161	0.96665047
4.49980967	0.00093052	0.97178698
4.55387689	0.00076941	0.97602217
4.60517019	0.00063953	0.97953303

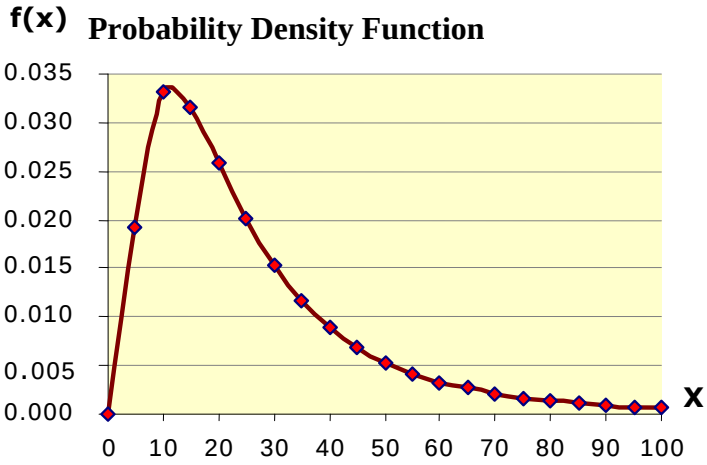

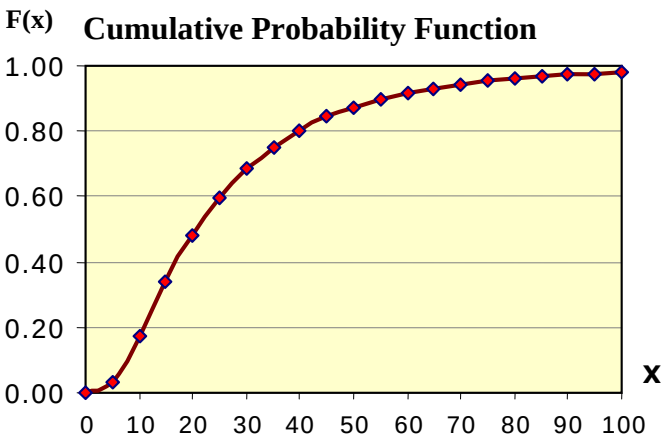

- **Ground AccelerationPGA = 0.24g**

Tensile Strength fwt	*(%)*
50	4.31
100	4.11
150	3.89
200	3.68
250	3.46
300	3.28
350	3.11
400	2.91
450	2.77
Total elements	9
Mean value	3.50
Standard deviation	0.53

x	*f(x)*	*F(x)*
0.00000000	0.00000000	0.00000000
1.60943791	0.00028503	0.00020126
2.30258509	0.00603340	0.01246181
2.70805020	0.01651833	0.06882936
2.99573227	0.02382165	0.17188464
3.21887582	0.02592967	0.29820283
3.40119738	0.02442197	0.42515389
3.55534806	0.02120411	0.53961324
3.68887945	0.01754336	0.63649166
3.80666249	0.01409443	0.71542116
3.91202301	0.01112156	0.77824046
4.00733319	0.00868126	0.82752934
4.09434456	0.00673483	0.86587788
4.17438727	0.00520899	0.89557882
4.24849524	0.00402515	0.91853731
4.31748811	0.00311205	0.93628091
4.38202663	0.00240982	0.95000864
4.44265126	0.00187025	0.96064966
4.49980967	0.00145546	0.96891863
4.55387689	0.00113612	0.97536293
4.60517019	0.00088975	0.98040113

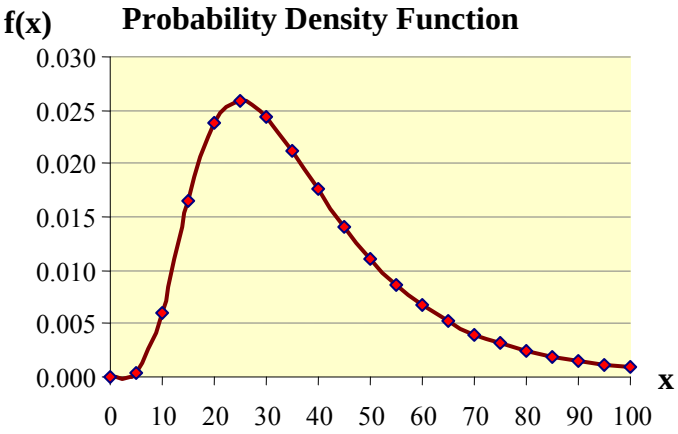

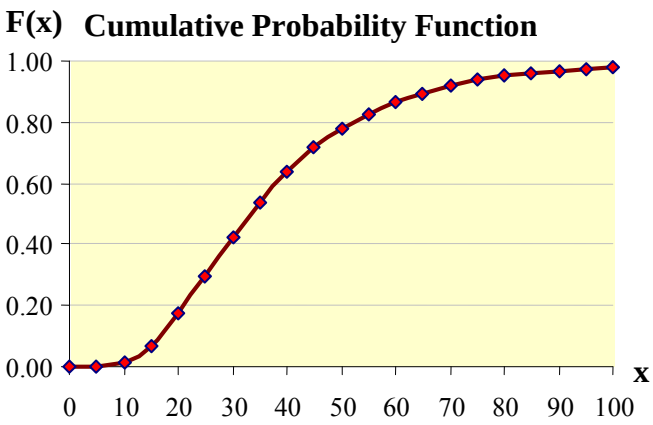

- **Ground AccelerationPGA = 0.32g**

Tensile Strength fwt	*(%)*
50	4.44
100	4.30
150	4.14
200	3.96
250	3.79
300	3.64
350	3.50
400	3.36
450	3.22
Total elements	9
Mean value	3.82
Standard deviation	0.43

x	*f(x)*	*F(x)*
0.00000000	0.00000000	0.00000000
1.60943791	0.00000027	0.00000011
2.30258509	0.00016618	0.00018564
2.70805020	0.00209324	0.00457394
2.99573227	0.00728008	0.02679370
3.21887582	0.01397052	0.07992710
3.40119738	0.01939912	0.16430020
3.55534806	0.02218575	0.26942947
3.68887945	0.02241125	0.38185349
3.80666249	0.02083604	0.49053926
3.91202301	0.01829306	0.58861295
4.00733319	0.01542396	0.67293999
4.09434456	0.01263332	0.74299407
4.17438727	0.01013289	0.79976396
4.24849524	0.00800462	0.84494734
4.31748811	0.00625413	0.88044185
4.38202663	0.00484807	0.90806348
4.44265126	0.00373742	0.92941504
4.49980967	0.00287049	0.94584367
4.55387689	0.00219949	0.95844612
4.60517019	0.00168319	0.96809599

f(x) Probability Density Function

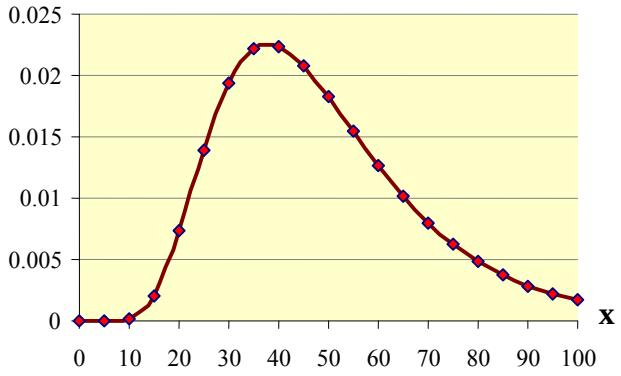

F(x) Cumulative Probability Function

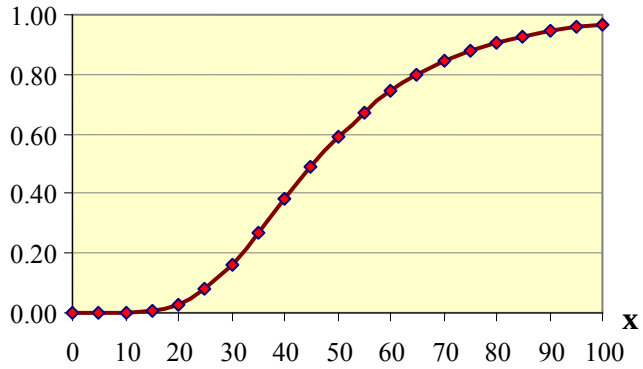

- **Ground AccelerationPGA = 0.40g**

Tensile Strength fwt	*(%)*
50	4.48
100	4.37
150	4.26
200	4.12
250	4.00
300	3.86
350	3.72
400	3.59
450	3.46
Total elements	9
Mean value	3.99
Standard deviation	0.36

x	*f(x)*	*F(x)*
0.00000000	0.00000000	0.00000000
1.60943791	0.00000000	0.00000000
2.30258509	0.00000158	0.00000114
2.70805020	0.00011967	0.00016667
2.99573227	0.00117595	0.00271920
3.21887582	0.00441434	0.01565650
3.40119738	0.00971844	0.05040310
3.55534806	0.01543516	0.11352921
3.68887945	0.01980336	0.20245031
3.80666249	0.02195282	0.30781069
3.91202301	0.02194033	0.41834728
4.00733319	0.02033540	0.52455492
4.09434456	0.01782199	0.62019432
4.17438727	0.01497409	0.70222804
4.24849524	0.01218315	0.77003978
4.31748811	0.00967046	0.82453030
4.38202663	0.00753090	0.86737070
4.44265126	0.00577874	0.90048738
4.49980967	0.00438390	0.92575466
4.55387689	0.00329666	0.94483929
4.60517019	0.00246252	0.95914291

f(x) Probability Density Function

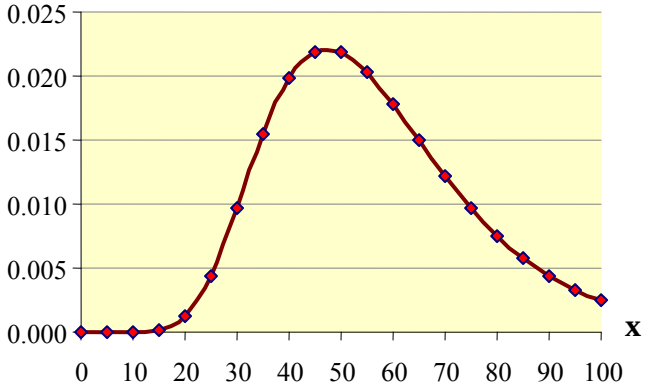

F(x) Cumulative Probability Function

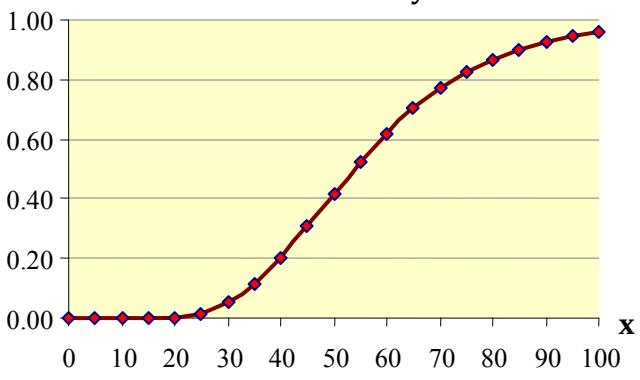

Distributions comparison for different PGA

- **Ground AccelerationPGA = 0.16g**

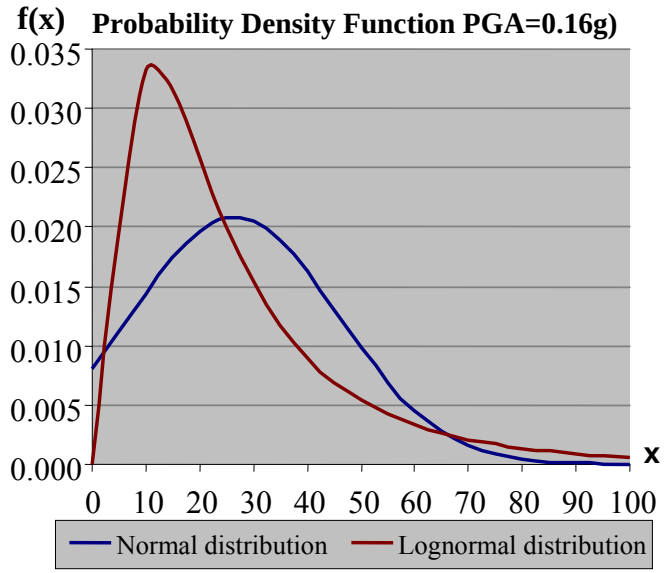

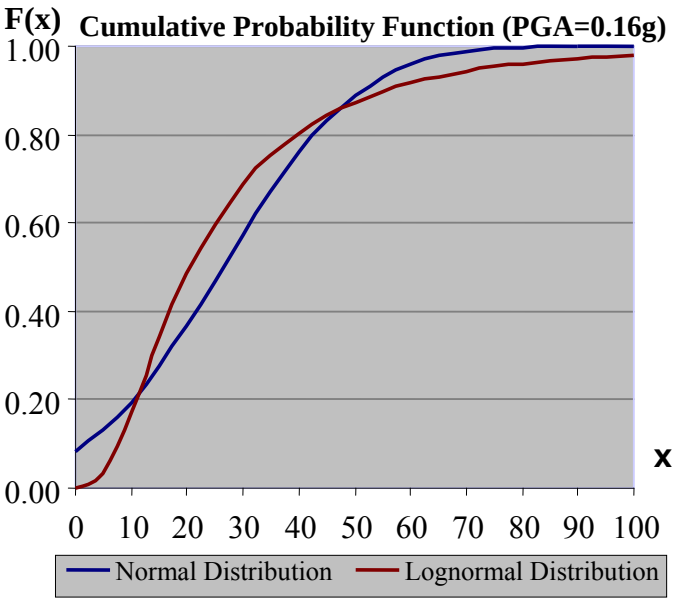

- **Ground Acceleration PGA = 0.24g**

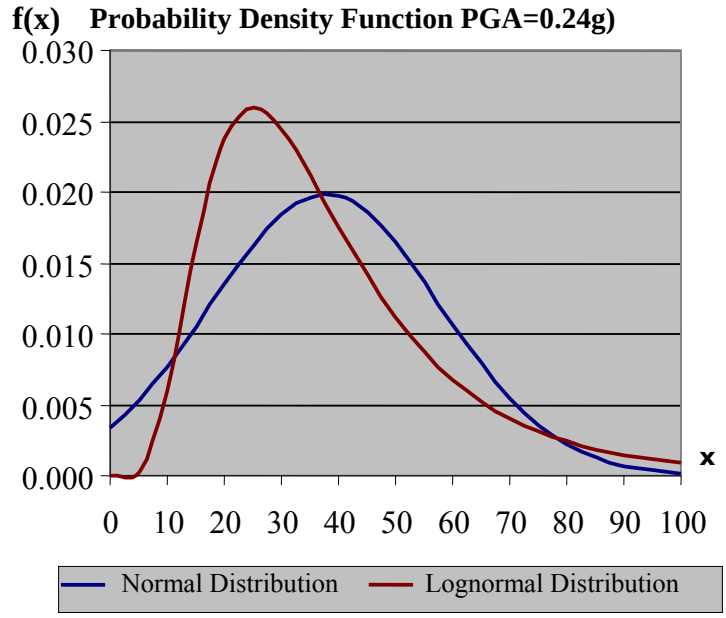

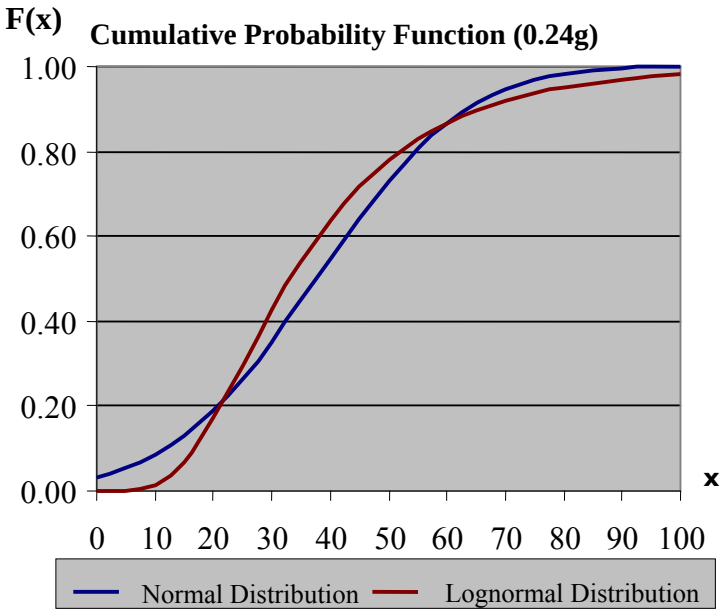

- **Ground Acceleration PGA = 0.32g**

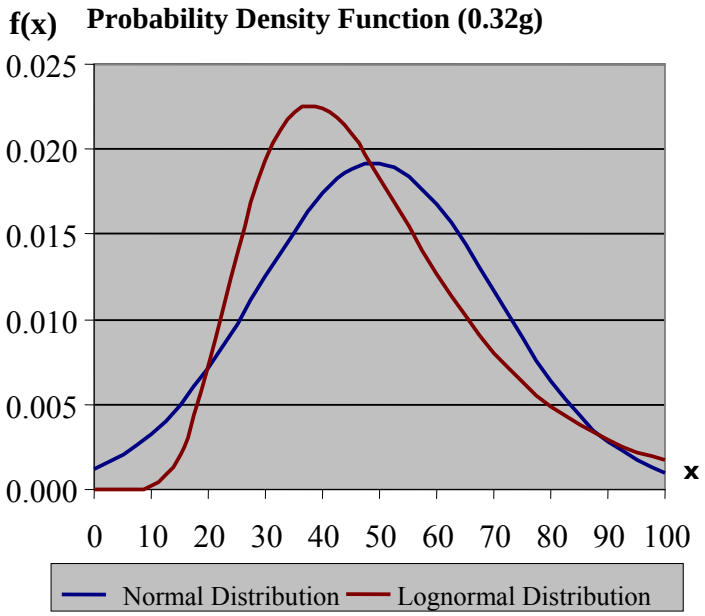

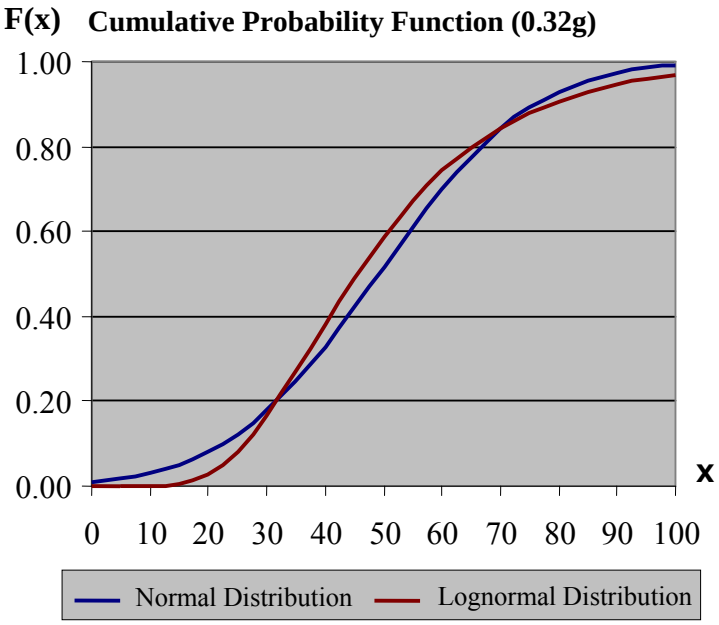

- **Ground Acceleration PGA = 0.40g**

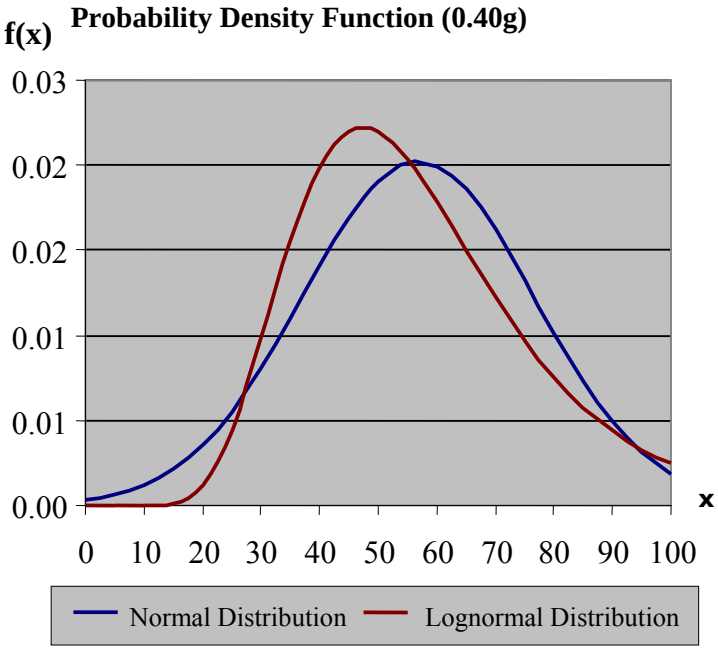

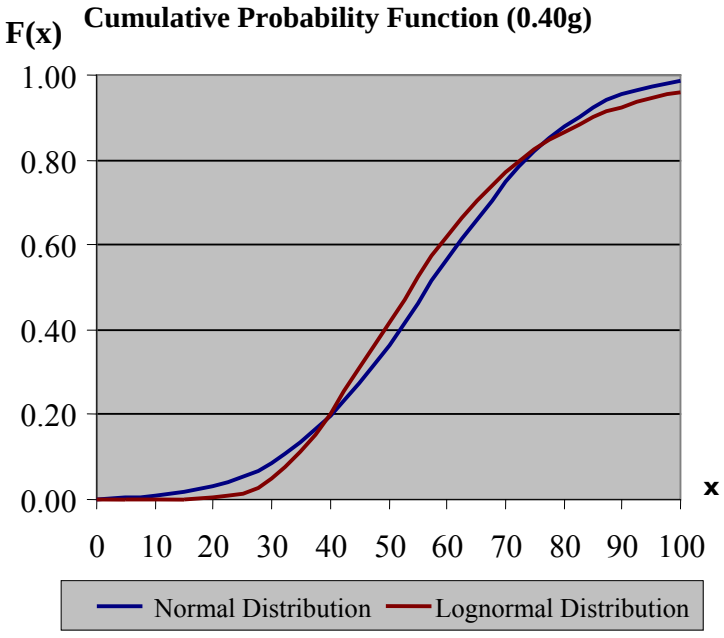

6.10 Export of fragility curves

After the statistical processing and the analysis of the failure rates of the wall structure and having set the levels of damage in a previous chapter, we can draw the fragility curves. The fragility curves reflect the probability of exceeding certain levels of damage produced by the cumulative probability, by the integral of the probability density function (p.d.f.) between the limits of each level of damage. The number of values' exceedance probability level of damage "coincides with the number of levels of damage presented. In this study, result three height specified locations per PGA, per probability density function and per type of rating levels. So for a given p.d.f. and for grading type of levels of damage is created a family of fragility curves in association of height points identified by level of damage.

Table 6.3: Values of failure levels, for the fragility curves

	No failures (%)	***Small failures (%)***	***Medium failures (%)***	***Large failures (%)***
Level of failure type a	0 - 5	5 - 15	15 - 25	> 25
Level of failure Type b	0 - 10	10 - 20	20 - 30	> 30
Level of failure type c	0 - 15	15 - 35	35 - 45	> 45

Normal Distribution

- **Graduation of failures, type a**

(%) PGA	0	0.16	0.24	0.36	0.40
Small	0	0.8689	0.9478	0.9832	0.9957
Medium	0	0.7255	0.8700	0.9500	0.9830
Large	0	0.5308	0.7354	0.8779	0.9467

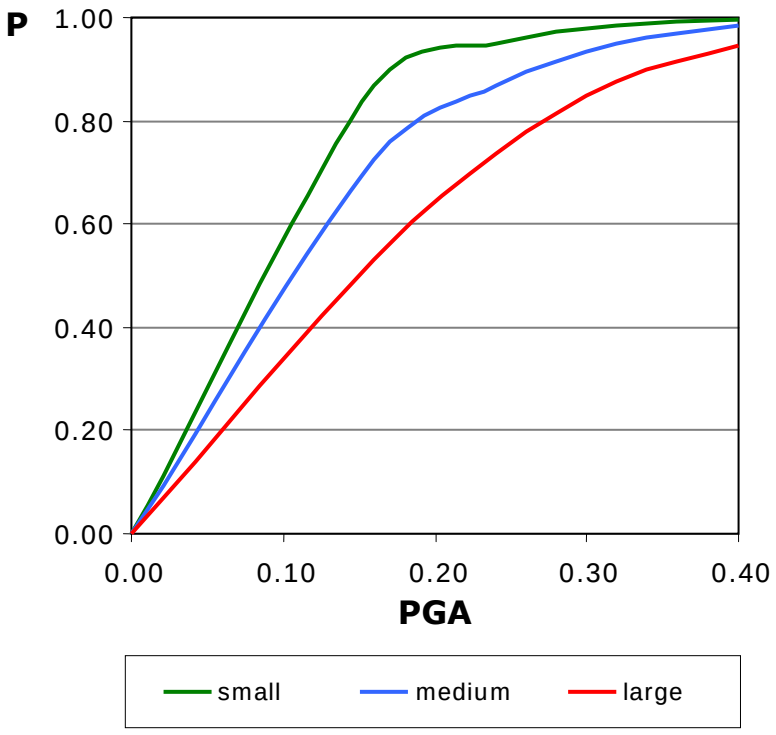

➢ **Graduation of failures, type b**

(%) PGA	0	0.16	0.24	0.36	0.40
Small	0	0.8052	0.9154	0.9703	0.9912
Medium	0	0.6324	0.8100	0.9200	0.9691
Large	0	0.4271	0.6482	0.8223	0.9132

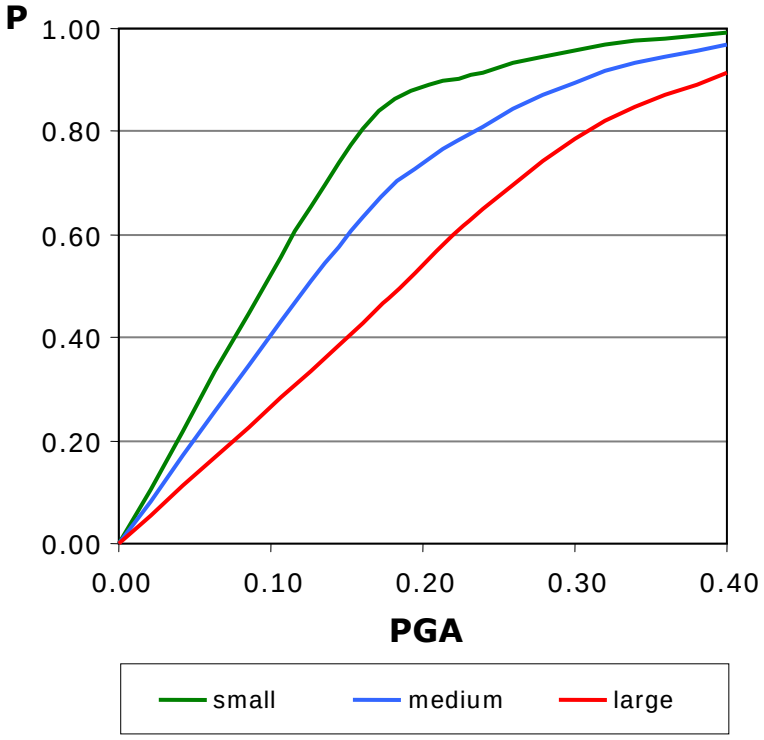

➢ **Graduation of failure, type c**

(%) PGA	0	0.16	0.24	0.36	0.40
Small	0	0.7255	0.8700	0.9500	0.9830
Medium	0	0.3283	0.5525	0.7530	0.8659
Large	0	0.1669	0.3575	0.5806	0.7260

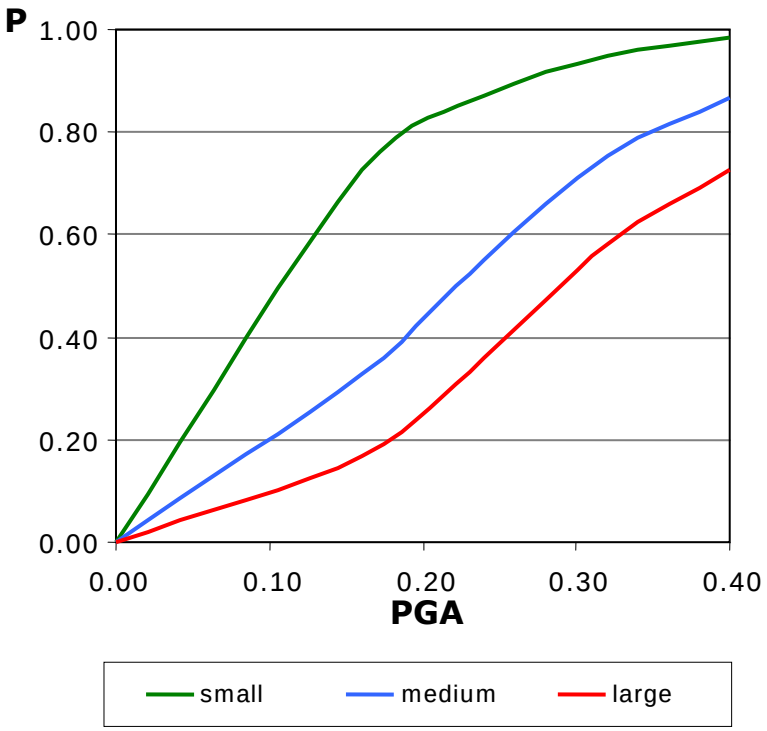

Lognormal Distribution

- **Graduation of failures, type a**

(%) PGA	0	0.16	0.24	0.36	0.40
Small	0	0.9668	0.9998	1.0000	1.0000
Medium	0	0.6602	0.9312	0.9954	0.9998
Large	0	0.4018	0.7018	0.9201	0.9843

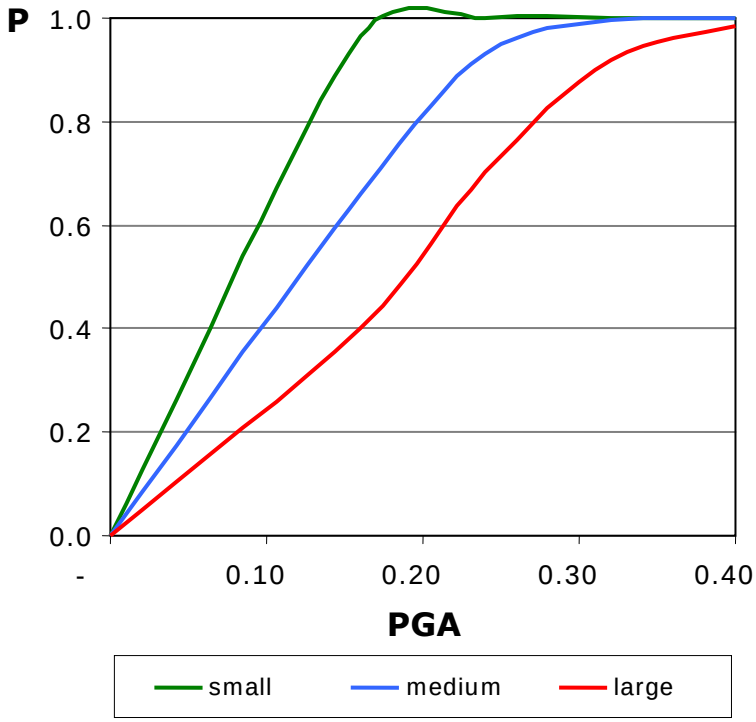

➢ **Graduation of failures, type b**

(%) PGA	0	0.16	0.24	0.36	0.40
Small	0	0.8259	0.9875	0.9998	1.0000
Medium	0	0.5161	0.8281	0.9732	0.9973
Large	0	0.3139	0.5748	0.8357	0.9496

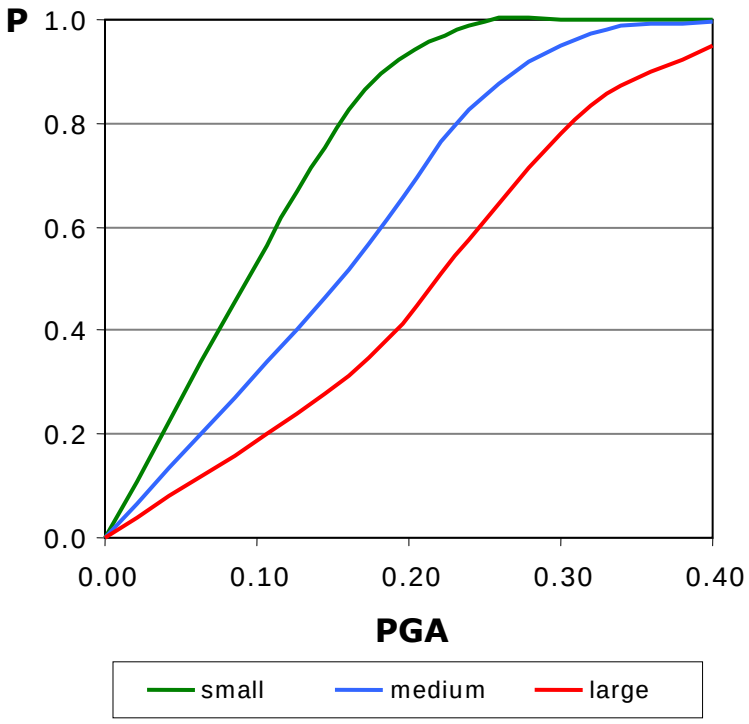

➢ **Graduation of failures, type c**

(%) PGA	0	0.16	0.24	0.36	0.40
Small	0	0.6602	0.8281	0.9732	0.9973
Medium	0	0.2469	0.5748	0.8357	0.9496
Large	0	0.1563	0.2218	0.4114	0.5817

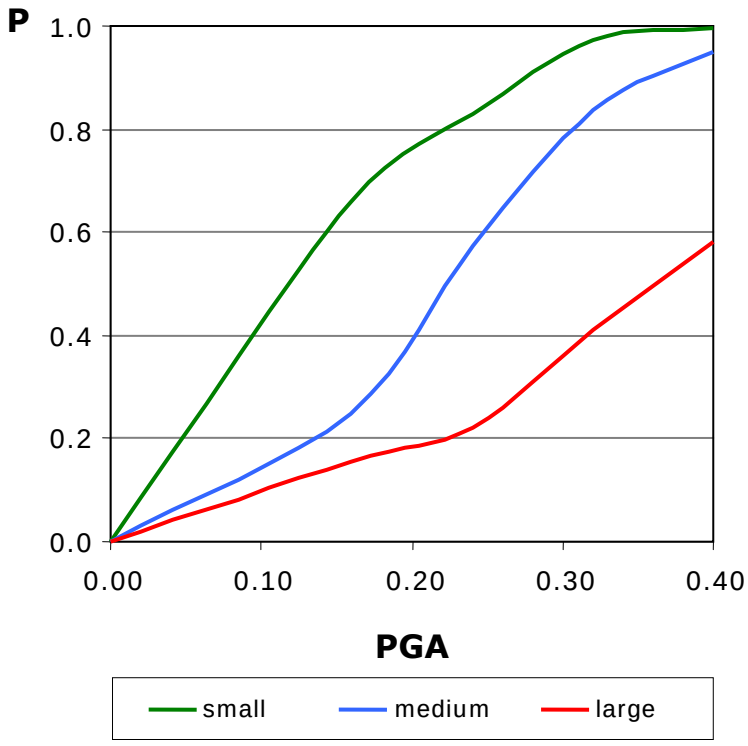

6.11 Comparison between the three failure levels of the two distributions

- ***Small failure***

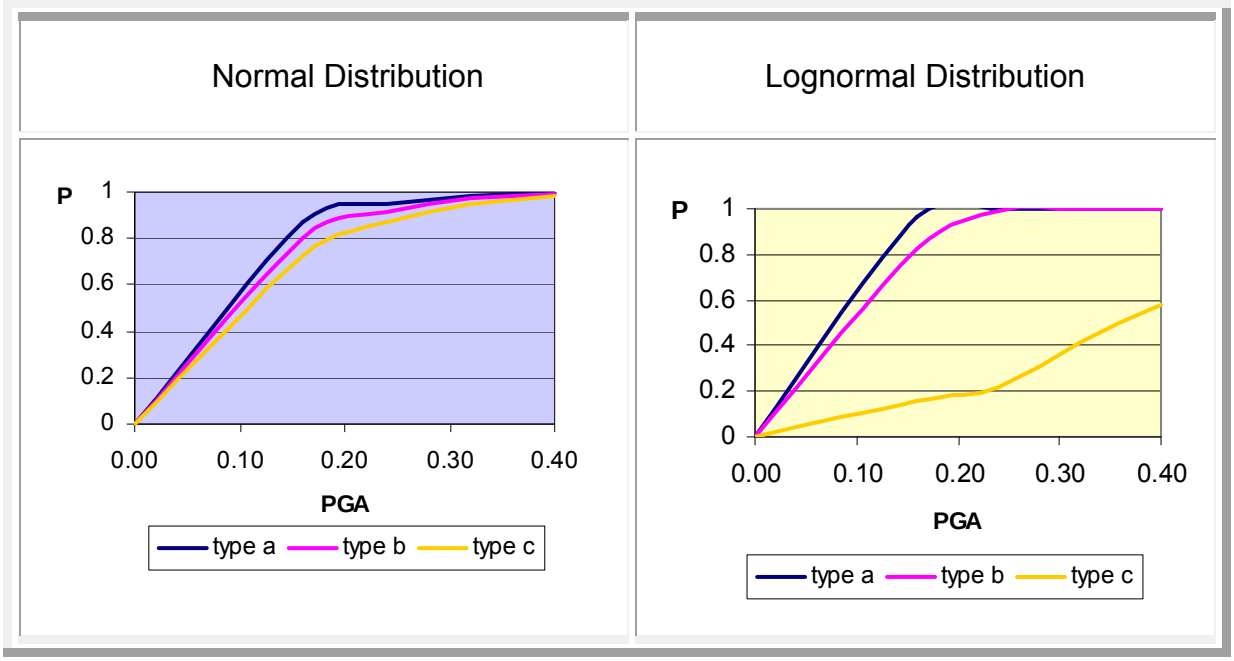

- ***Medium failure***

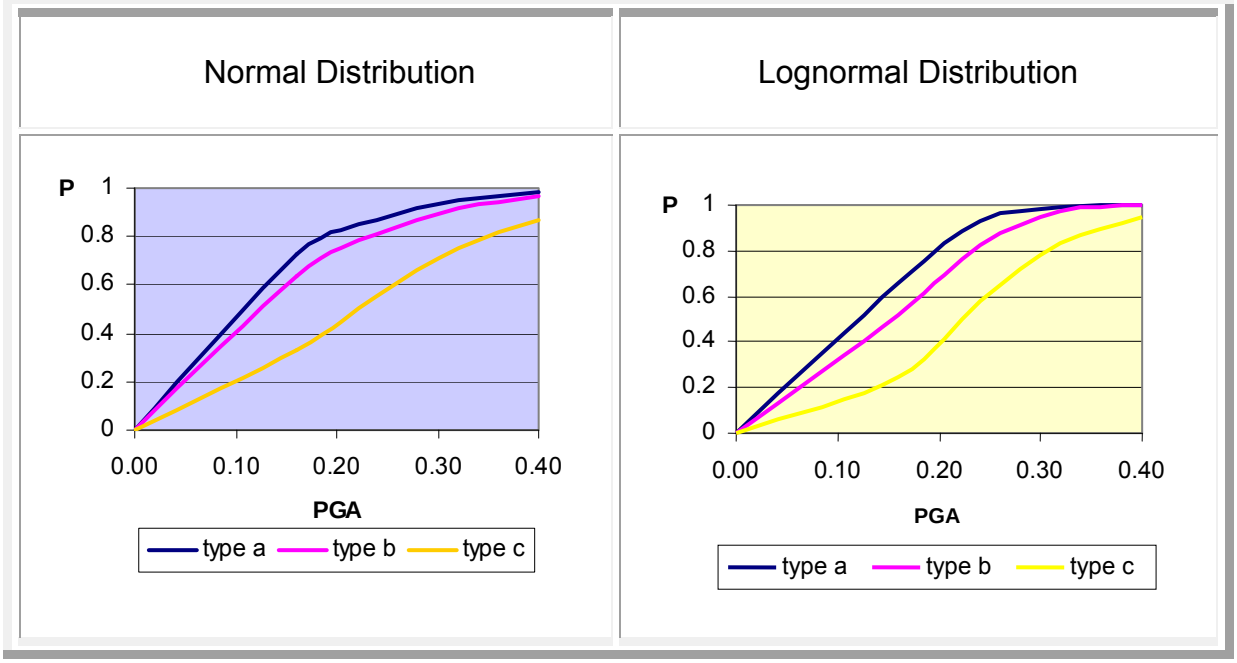

- ***Large failure***

Normal Distribution	Lognormal Distribution
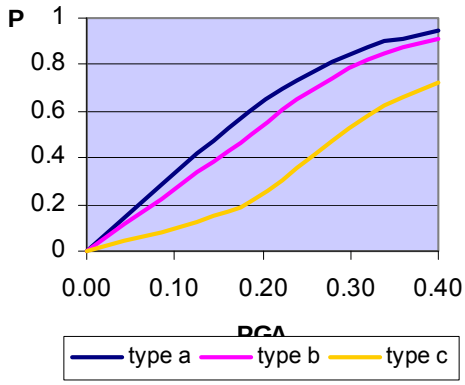	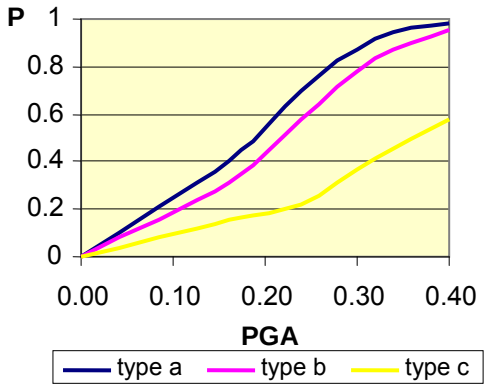

6.12 Comparison of the fragility curves of the two distributions

Here are the charts comparing the two distributions for three different levels of damage.

- **Graduation of failures, type a**

Comparison between small failures, type a

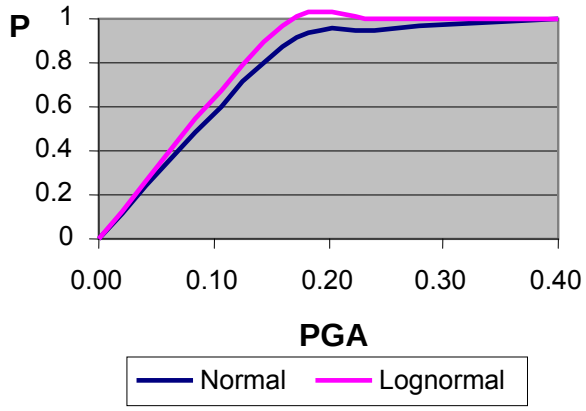

Comparison between medium failures, type a

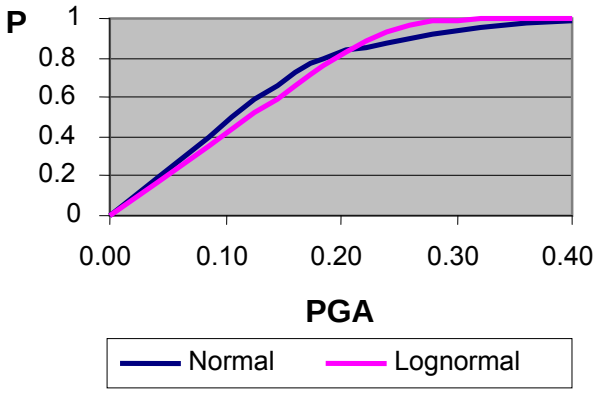

Comparison between large failures, type a

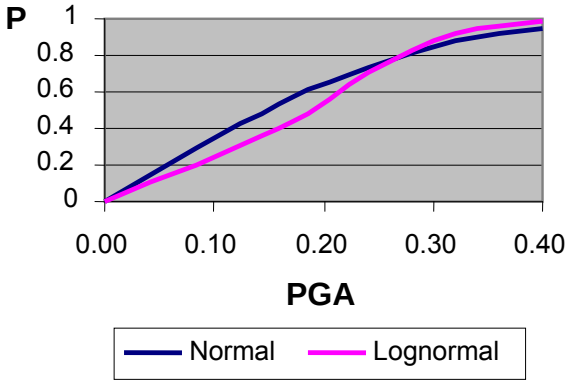

- **Graduation of failures, type b**

Comparison between small failures, type b

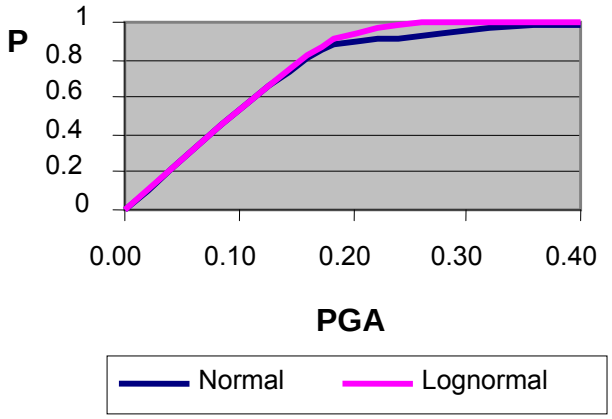

Comparison between medium failures, type b

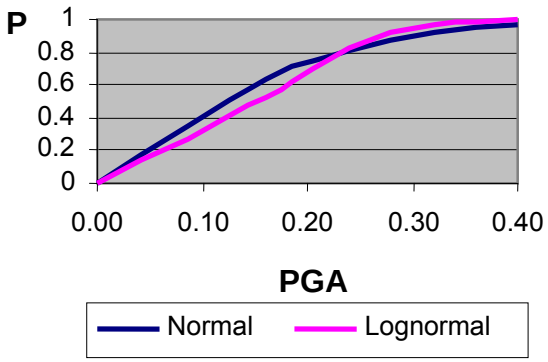

Comparison between large failures, type b

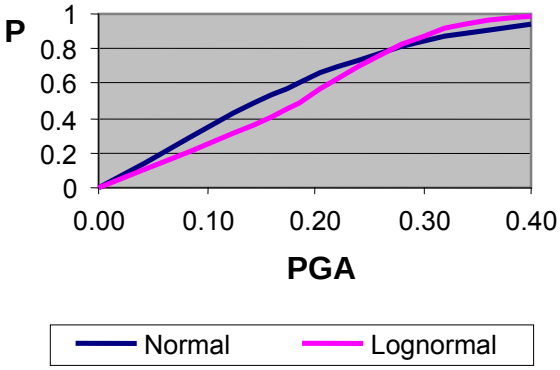

- **Graduation of failures, type c**

Comparison between small failures, type c

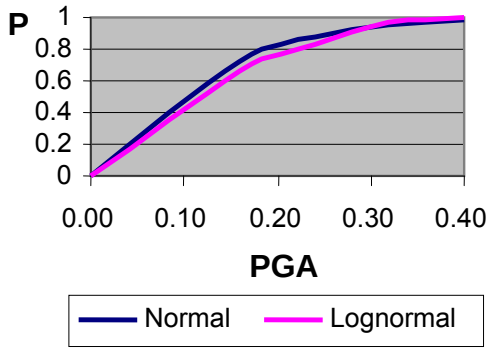

Comparison between medium failures, type c

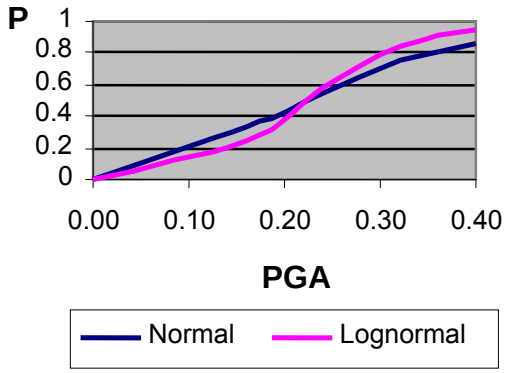

Comparison between large failures, type c

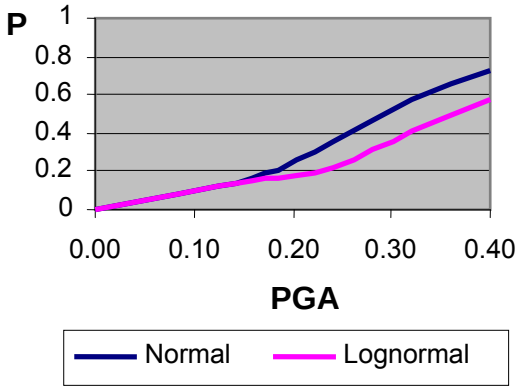

CHAPTER 7

REPAIR AND REINFORCEMENT OF EXISTING MASONRY (Reinforcement A)

7.1 Introduction

The reinforcement of an existing masonry construction is designed to increase its strength so that it can take static and dynamic loads with minimal damage, so as to meet a higher safety index.

If there is already damage, priority is to repair them and where is possible to restore the building to its original condition. To achieve this, it is necessary to identify the faults and reasons that caused them. When there is reinforcement to be done in a structure that has escaped damage, then analytical methods are used in certain actions to identify the more vulnerable points of construction and to best estimate its behavior.

Modern analytical requirements dictate the use of software programs that provide the opportunity to develop a spatial model with the properties of the materials that make up the building and the imposition of certain actions (both static and dynamic) to which it will be submitted to. Through these analytical methods is feasible to carry out multiple tests to identify vulnerabilities that lead to decisions in order to take the necessary measures. As developed in the previous chapters, special attention must be given by the user (engineer) of the program in the assumptions to be made in order for the analytical results to be closer to reality.

In the process of decision should be taken into account several factors that will influence the choice of the ideal decision. For conventional stone construction, the most important parameter is the cost function of intervention, the importance of the construction and the effectiveness of the reinforcement. But when it comes to monuments of cultural value then the decision is more difficult and requires an answer the following ‘trilimma’:

- Re-erection of the monument to its original form, which runs the risk of a new collapse, especially for seismic regions where the causes cannot be removed.

- Strong reinforcement, ensuring the proper response of the structure, greatly increasing its strength. In this case the cultural track is lost since the intervention is large and in fact it is about a new building we are dealing with.

- No intervention and maintenance of the monument to its failure condition, where the building is reminiscent of its original form, but is based on the rationale that failure is part of its history.

[12]

Apart from the above factors that play a clear role in deciding on whether to make reinforcement and in what extent, the choice can be judged by seemingly minor factors such as knowledge and experience of available technical resources, and the possibility of obtaining appropriate equipment.

7.2 Description of ways to reinforce the structure

In this chapter we will present three techniques of reinforcement stone structures as suggestions for improving the strength of the residence of Prince George in Chania, Crete. The following solutions were chosen, were simulated to the spatial model, were analyzed and their results were compared with a view to obtain the optimal solution for the given criterion. These ways of reinforcing the construction are:

- **Reinforcement A (RA):** pointing.

- **Reinforcement B (RB):** pointing, reinforced concrete slab at the ground floor and the first floor level and reinforced concrete bond beam at the roof level.

- **Reinforcement C (RC):** pointing, horizontal prestressing along the lintels with steel tendons.

7.3 Pointing (Reinforcement A)

Pointing is called the replacement of the joints with new mortar to the permitted depth from the surface of the masonry. The mortar is chosen either to replace old mortar that has been damaged by erosion, or to strengthen masonry mortar with greater strength than the existing one. The demolition of the old mortar can be done by hand and by mechanical means (water jet or air pressure). The new mortar is needed to have a reduced rate of contraction and increased workability so adding lime is necessary, but as a result to reduce the strength. Attention should be given to the new mortar which should have strength weaker than that of the resistance of natural stones and not to be harder than the existing mortar, so as to avoid brittle failure. This restricts the content of the cement in the mixture in less than 20% of the calcium / cement. When observed during launching, extremely low strength mortar, restoration of the masonry should be done very carefully to avoid possible loosening of cohesion or even detachment of natural stones.

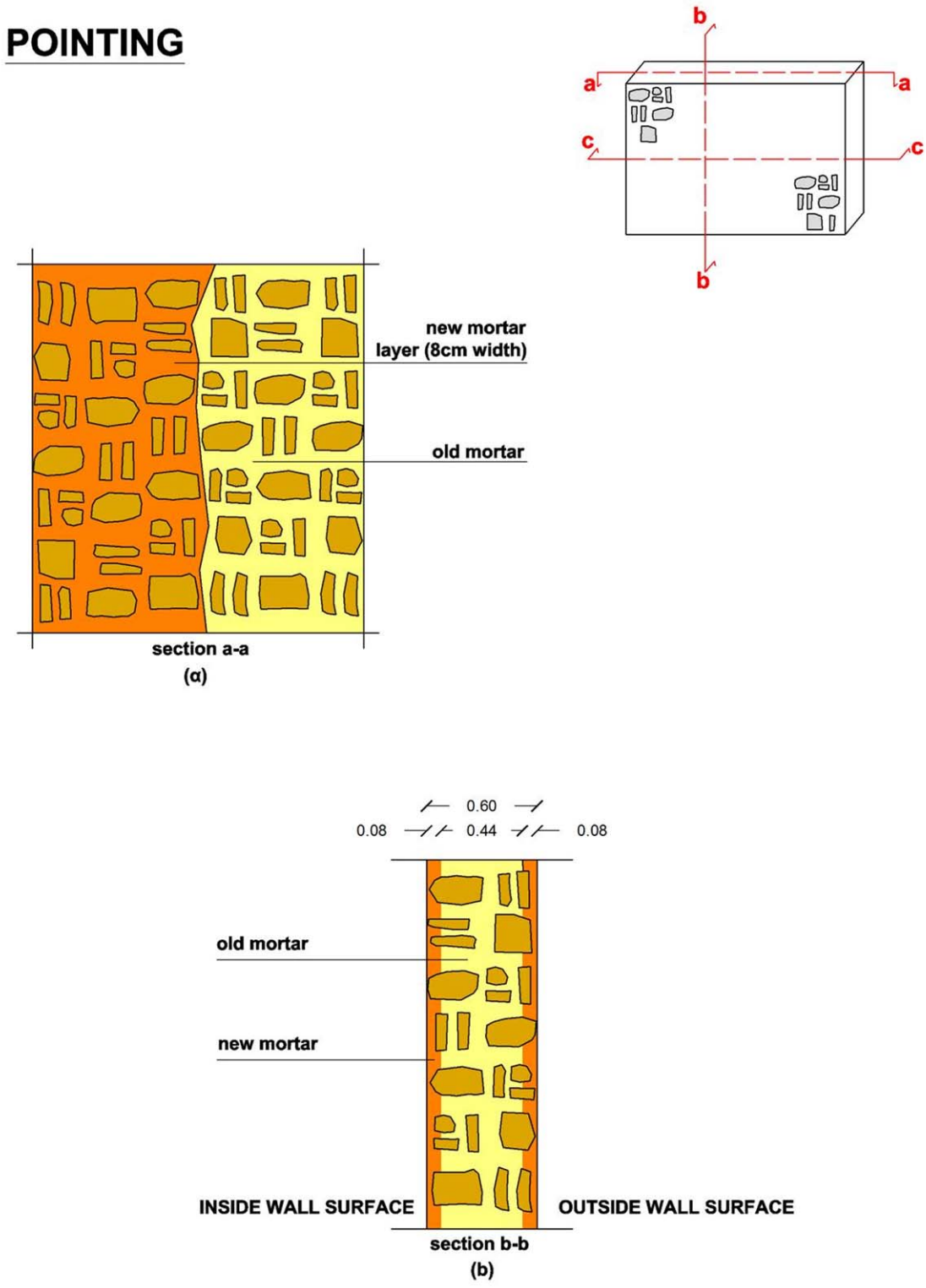

Figure 7.1 Mortar on both sides

7.3.1 Stages of work and modeling of reinforcement A

- Coating removal.
- Detachment of weak mortar and loose stones with water under pressure except of the points where there is wood, where the demolition is done by air.
- Sealing joints with mortar, with properties similar to the existing (if possible the composition of the new to consist of the same material with the old).

[13]

For the purposes of the analysis was considered mortar on both sides of the masonry at a depth of 8cm on each side (Figure 8.1). After the process of pointing, the strength of the building improves with the compressive strength and modulus to increase depending on the depth and quality of the mixture.

Thickness of external masonry =0.60m

Intervention thickness 0.08+0.08= 0.16m

Mortar replacement rate 26.67%

After applying the pointing technique, the new compressive strength of masonry is given by the following formula:

$$f_{\text{wc}} = \frac{1}{\gamma_{Rd}} \cdot \zeta \cdot f_{wc,o}$$ where:

$\frac{1}{\gamma_{Rd}} = 0.80$

ζ= empirical factor calculated,

$$\zeta = 1 + 3\frac{V_{\text{νέουκονιάματος}}}{V_{\text{παλαιούκονιάματος}}}$$

$f_{wc,o}$ = Initial compressive strength = 3.05MPa

Therefore, the compressive strength and modulus of the masonry after mortar:

$$f_{wc} = 4.34MPa$$

E=1000 x 4.34= 4340MPa

The reinforcement of the mortar was attributed to the modeling with the increase of modulus of elasticity as shown above.

Fundamental mode (transferational) of the building T= 0.096sec, mass participation ratio 24% at 'Y' direction.

TABLE: Modal Participating Mass Ratios						
OutputCase	**StepType**	**StepNum**	**Period**	**UX**	**UY**	**RZ**
Text	Text	Unitless	Sec	Unitless	Unitless	Unitless
MODAL	Mode	1	0,184285	0,05126	6,26E-06	0,00935
MODAL	Mode	2	0,128552	0,00414	0,00051	0,00804
MODAL	Mode	3	0,127868	0,01091	0,00187	0,0036
MODAL	Mode	4	0,126968	1,07E-05	0,00435	0,00296
MODAL	Mode	5	0,123536	0,0749	0,00522	0,00246
MODAL	Mode	6	0,0959	0,0022	0,24162	0,0364
MODAL	Mode	7	0,092865	0,01821	0,08761	0,14805
MODAL	Mode	8	0,090788	0,05627	0,00075	0,03551
MODAL	Mode	9	0,090424	0,03113	0,02218	0,02213
MODAL	Mode	10	0,088246	0,01373	0,01361	0,00131

Table 7.1 First ten modes after pointing

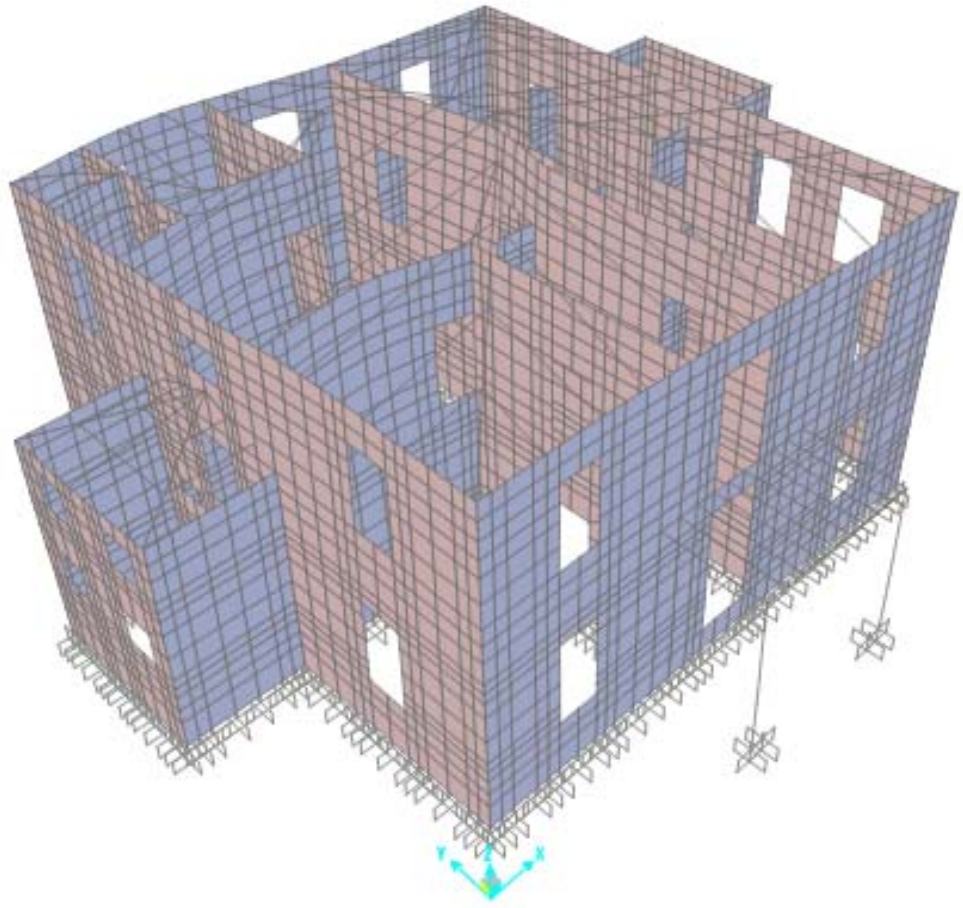

Figure 7.2 fundamental modal T= 0.096sec

7.3.2 Walls failure results from software FAILURE

As it has been mentioned in paragraph 7.2, software FAILURE has been used in order to draw the percentages of failure for each wall, for a given tensile strength and seismic acceleration. The failures are represented by different colors depends on Von Mises criteria.

Below are illustrated indicatively, the failures of four walls (w1,w8,WD,wE) of reinforcement A, for the most severe loading combination, for PGA= 0.16 and 0.40 and for tensile strength 50kPa, 250kPa, 450kPa.

Failure

wall : **1_2topmax** **Load Cases :** **0.16g**		Failure under biaxial Tension/Tension
		Failure under biaxial Tension/ Compression
		Failure under biaxial Compression /Tension
		Failure under biaxial Compression/ Compression
		NON Failure
fwt = 50 kPa	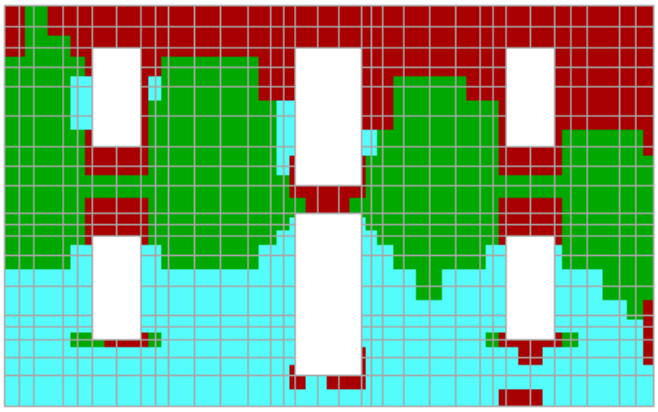	
Joints = 640 Failed = 413 Failure Percentage = 64.53%		
fwt = 250 kPa	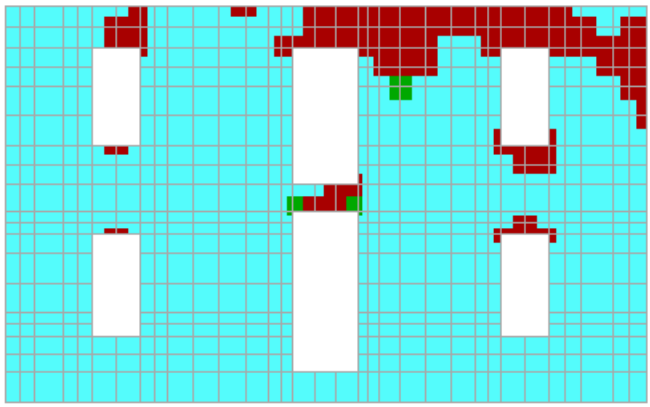	
Joints = 640 Failed = 82 Failure Percentage = 12.81%		
f_{wt} = 450 kPa	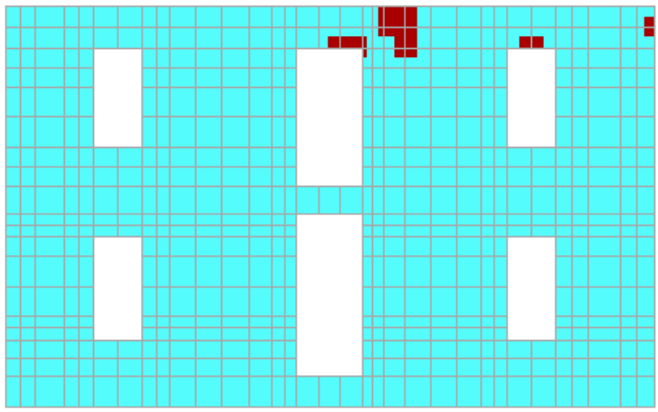	
Joints = 640 Failed = 9 Failure Percentage = 1.41%		

Failure

wall : **1_2topmax** **Load Cases :** **0.40g**		Failure under biaxial Tension/Tension
		Failure under biaxial Tension/ Compression
		Failure under biaxial Compression /Tension
		Failure under biaxial Compression/ Compression
		NON Failure
fwt = 50 kPa	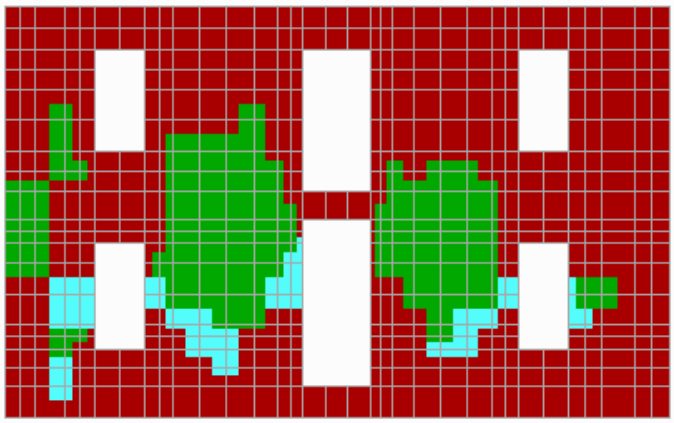	
Joints = 640 Failed = 607 Failure Percentage = 94.84%		
fwt = 250 kPa	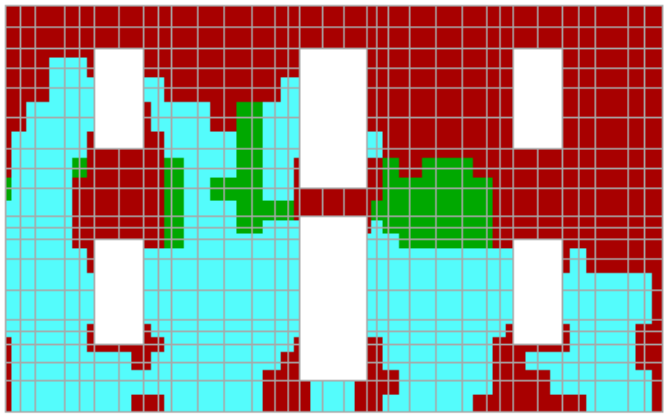	
Joints = 640 Failed = 379 Failure Percentage = 59.22%		
f_{wt} = 450 kPa	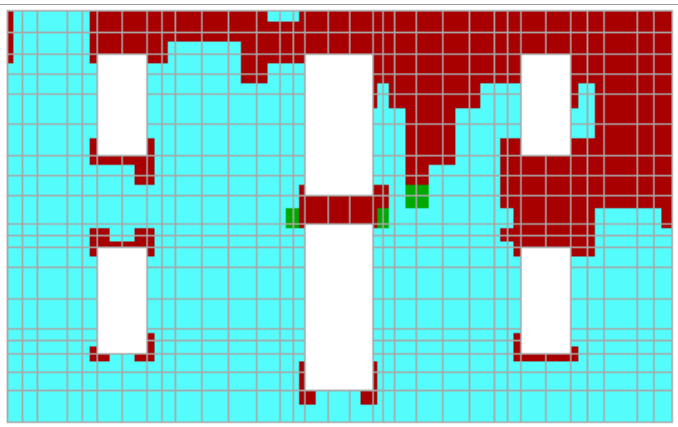	
Joints = 640 Failed = 193 Failure Percentage = 30.16%		

Failure		
wall : **8_2topmax** **Load Cases :** **0.16g**		Failure under biaxial Tension/Tension
		Failure under biaxial Tension/ Compression
		Failure under biaxial Compression /Tension
		Failure under biaxial Compression/ Compression
		NON Failure
fwt = 50 kPa	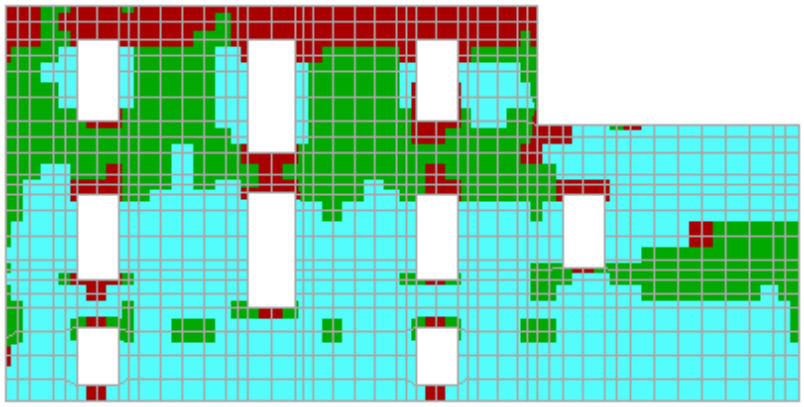	
Joints = 990 Failed = 439 Failure Percentage = 44.34%		
fwt = 250 kPa	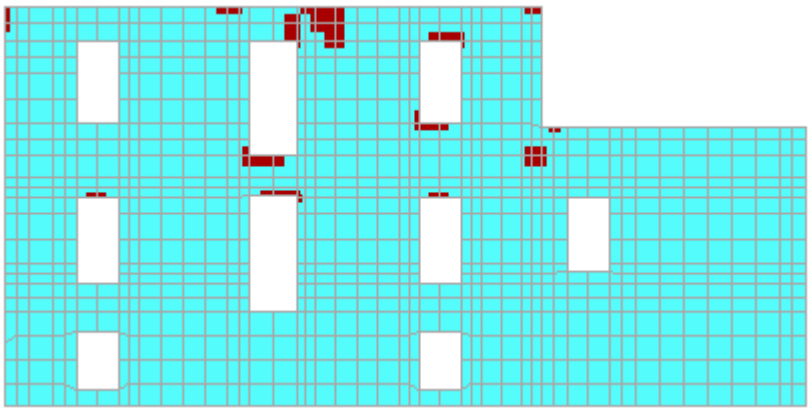	
Joints = 990 Failed = 27 Failure Percentage = 2.73%		
f_{wt} = 450 kPa	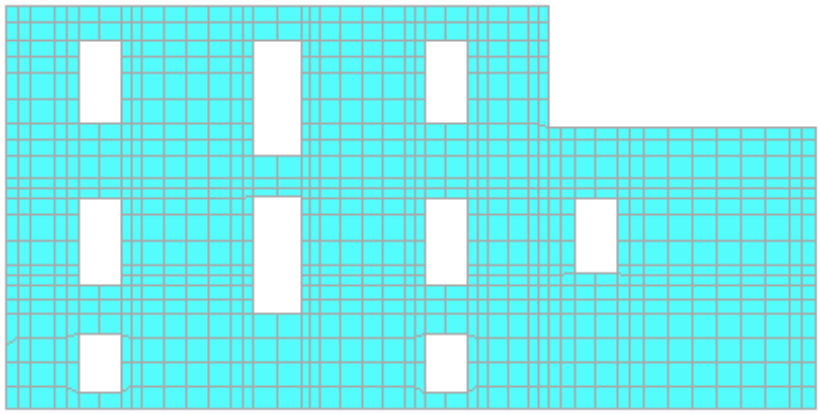	
Joints = 990 Failed = 0 Failure Percentage = 0.00%		

Failure

wall : **8_2topmax** **Load Cases :** **0.40g**		Failure under biaxial Tension/Tension
		Failure under biaxial Tension/ Compression
		Failure under biaxial Compression /Tension
		Failure under biaxial Compression/ Compression
		NON Failure
fwt = 50 kPa	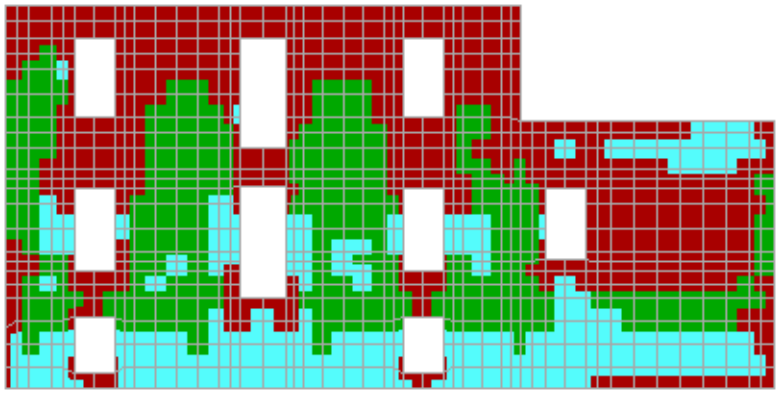	
Joints = 990 Failed = 788 Failure Percentage = 79.60%		
fwt = 250 kPa	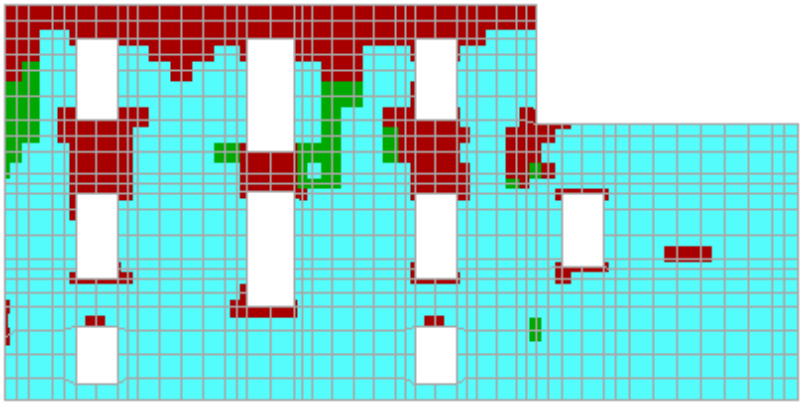	
Joints = 990 Failed = 257 Failure Percentage = 25.96%		
f_{wt} = 450 kPa	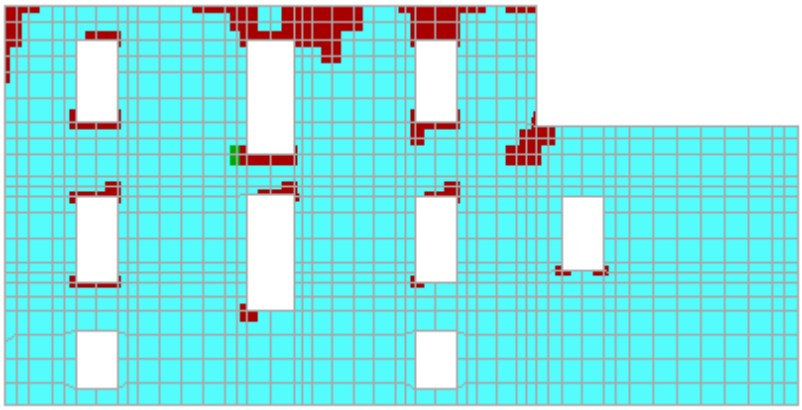	
Joints = 990 Failed = 85 Failure Percentage = 8.59%		

Failure		
wall : **D_2topmax** **Load Cases :** **0.16g**		Failure under biaxial Tension/Tension
		Failure under biaxial Tension/ Compression
		Failure under biaxial Compression /Tension
		Failure under biaxial Compression/ Compression
		NON Failure
fwt = 50 kPa	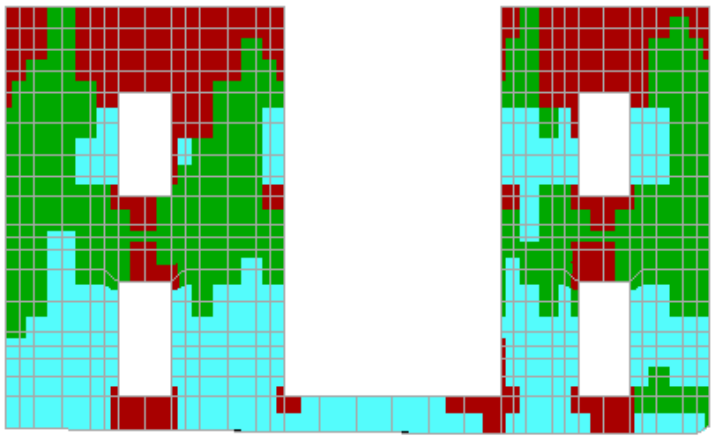	
Joints = 555 Failed = 348 Failure Percentage = 62.70%		
fwt = 250 kPa	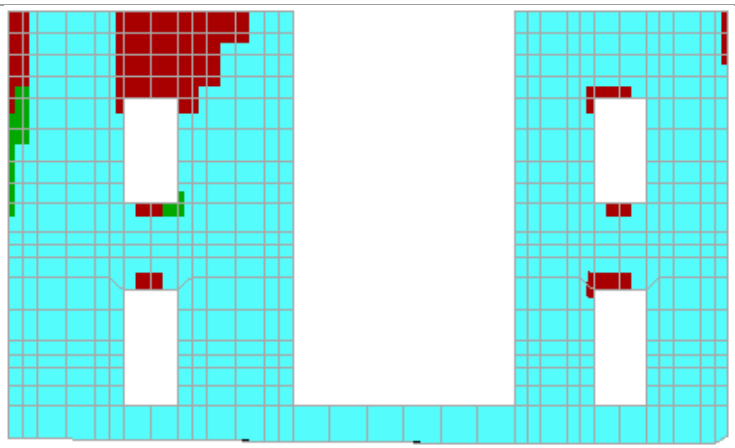	
Joints = 555 Failed = 52 Failure Percentage = 9.37%		
f_{wt} = 450 kPa	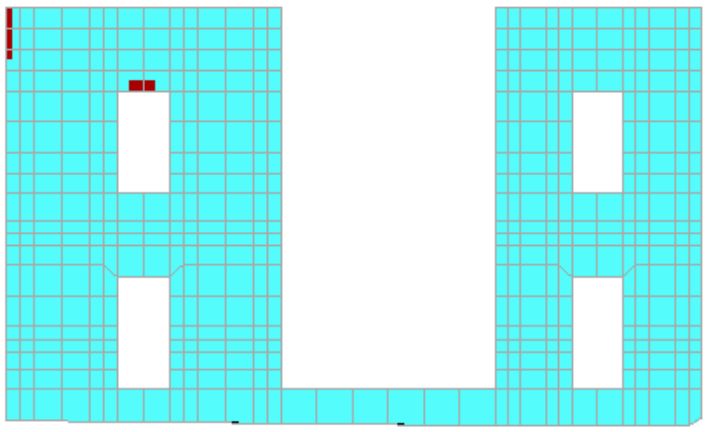	
Joints = 555 Failed = 4 Failure Percentage = 0.72%		

Failure		
wall : **D_2topmax** **Load Cases :** **0.40g**		Failure under biaxial Tension/Tension
		Failure under biaxial Tension/ Compression
		Failure under biaxial Compression /Tension
		Failure under biaxial Compression/ Compression
		NON Failure
fwt = 50 kPa	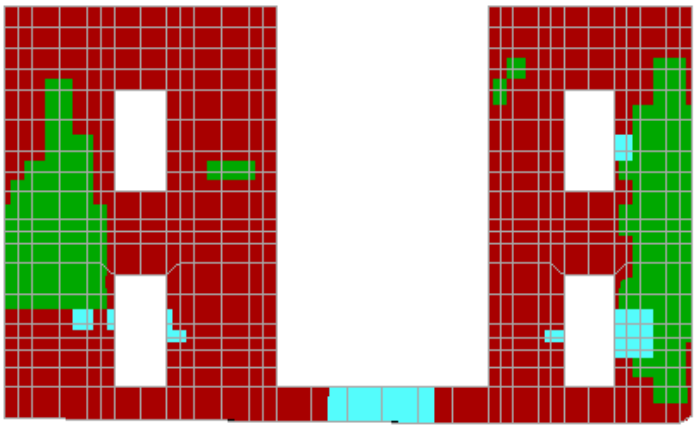	
Joints = 555 Failed = 530 Failure Percentage = 95.50%		
fwt = 250 kPa	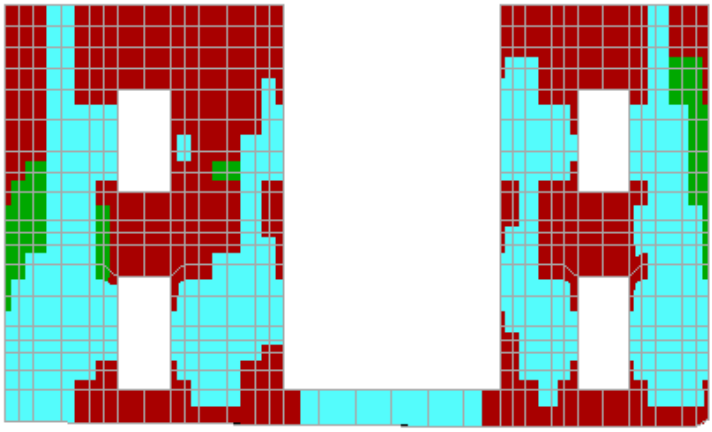	
Joints = 555 Failed = 311 Failure Percentage = 56.04%		
f_{wt} = 450 kPa	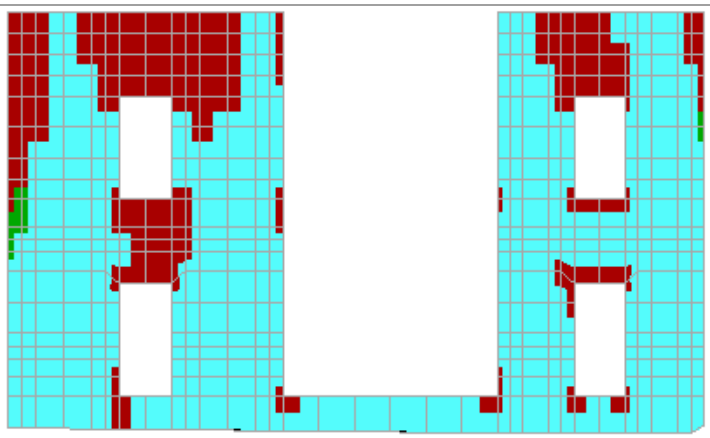	
Joints = 555 Failed = 137 Failure Percentage = 24.68%		

Failure

wall : **E_2topmax** **Load Cases :** **0.16g**		Failure under biaxial Tension/Tension
		Failure under biaxial Tension/ Compression
		Failure under biaxial Compression /Tension
		Failure under biaxial Compression/ Compression
		NON Failure

fwt = 50 kPa

Joints = 558
Failed = 406

Failure
Percentage = 72.76%

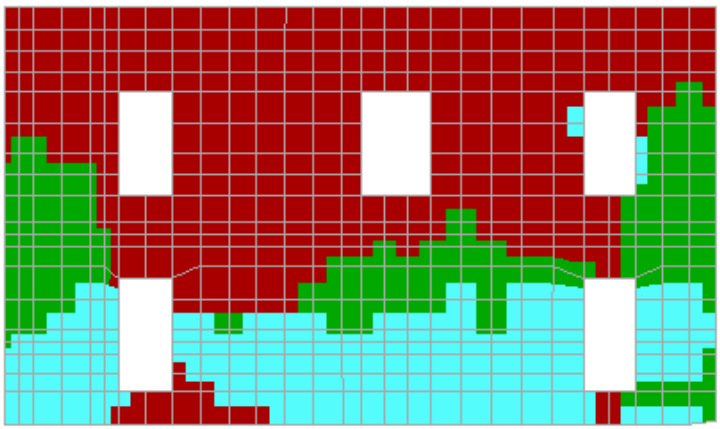

fwt = 250 kPa

Joints = 558
Failed = 227

Failure
Percentage = 40.68%

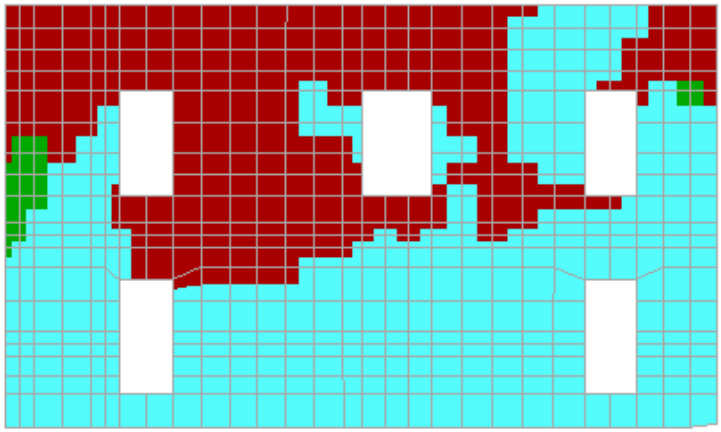

f_{wt} = 450 kPa

Joints = 558
Failed = 122

Failure
Percentage = 21.86%

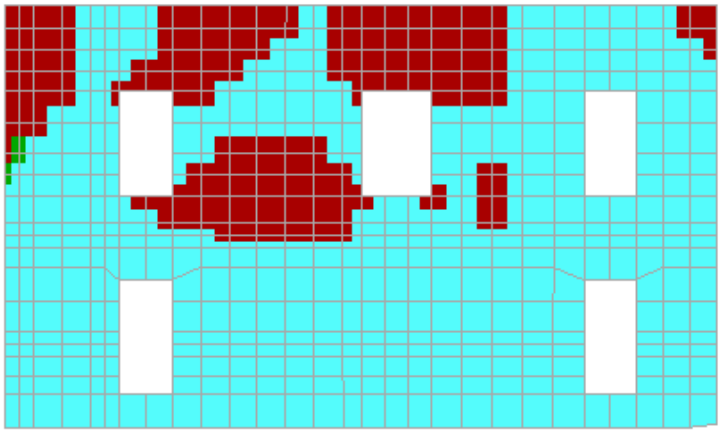

Failure		
wall : **E_2topmax** **Load Cases :** **0.40g**		Failure under biaxial Tension/Tension
		Failure under biaxial Tension/ Compression
		Failure under biaxial Compression /Tension
		Failure under biaxial Compression/ Compression
		NON Failure
fwt = 50 kPa	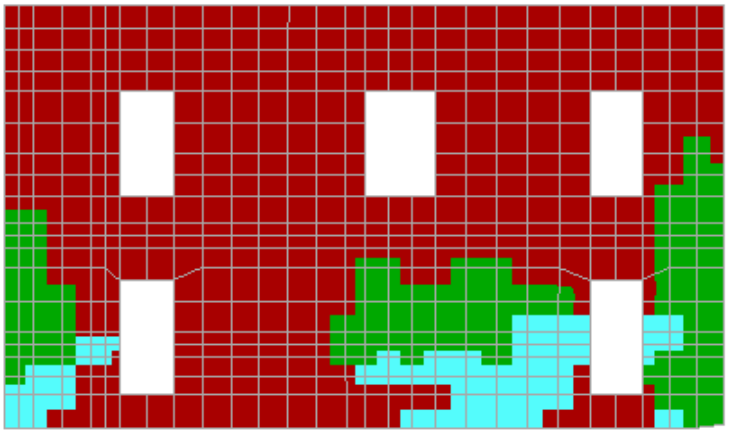	
Joints = 558 Failed = 509 Failure Percentage = 91.22%		
fwt = 250 kPa	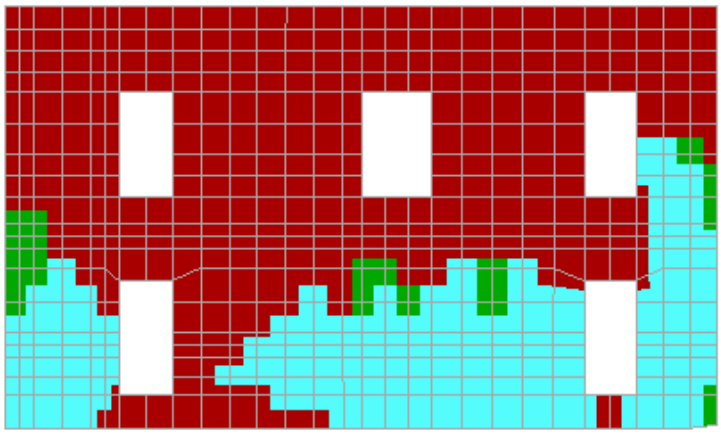	
Joints = 558 Failed = 388 Failure Percentage = 69.53%		
f_{wt} = 450 kPa	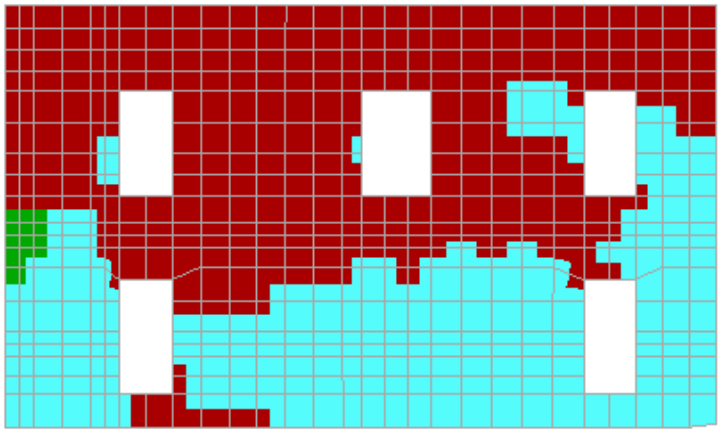	
Joints = 558 Failed = 317 Failure Percentage = 56.81%		

7.3.3 Failure rates & Statistical elaboration of the results

For the statistical analysis of data and in order to draw conclusions concerning the type and size of the failure of the wall structure, is taken the overall rate of failure for the 15 walls of the building for different tensile strength and four ground accelerations.

f_{wt} \ PGA	*0.16g*	*0.24g*	*0.36g*	*0.40g*
K50	61.08	71.20	76.98	90.29
K100	51.02	56.02	65.90	77.60
K150	42.10	43.90	55.03	70.54
K200	25.03	35.40	44.20	61.32
K250	16.40	27.02	36.50	52.69
K300	20.60	22.20	31.05	46.06
K350	15.91	17.93	25.98	41.00
K400	11.01	14.01	21.00	35.71
K450	6.00	10.90	16.35	30.06

Table 7.2: Total failure percentages for the building, for 9 mortars and 4 ground accelerations

Below are illustrated the results of the statistic analysis for the two distributions and all ground accelerations.

Normal Distribution

- **Ground acceleration PGA = 0.16g**

Tensile Strength fwt	*Failure Rate (%)*
50	61.08
100	51.00
150	40.00
200	25.00
250	16.40
300	20.00
350	16.00
400	11.00
450	6.00
Total elements	9
Mean value	27.39
Standard deviation	19.00

x	*f(x)*	*F(x)*
0	0.00743086	0.07475159
5	0.01048848	0.11936808
10	0.01381385	0.18009195
15	0.01697643	0.25724000
20	0.01946734	0.34873391
25	0.02083032	0.45002269
30	0.02079766	0.55469520
35	0.01937590	0.65566837
40	0.01684373	0.74659298
45	0.01366292	0.82302209
50	0.01034137	0.88299262
55	0.00730367	0.92691830
60	0.00481320	0.95695139
65	0.00295975	0.97611964
70	0.00169827	0.98753960
75	0.00090925	0.99389066
80	0.00045425	0.99718772
85	0.00021175	0.99878546
90	0.00009211	0.99950820
95	0.00003738	0.99981338
100	0.00001416	0.99993367

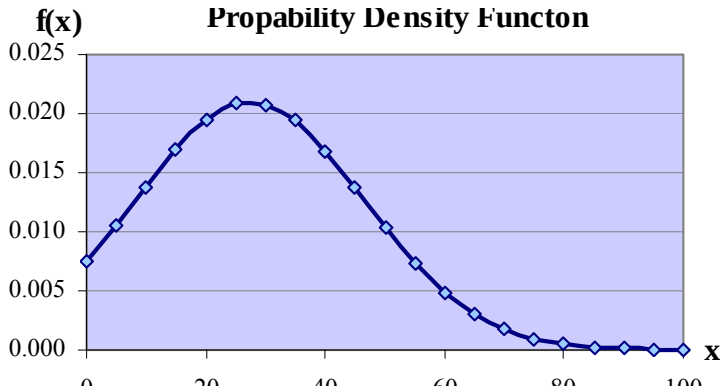

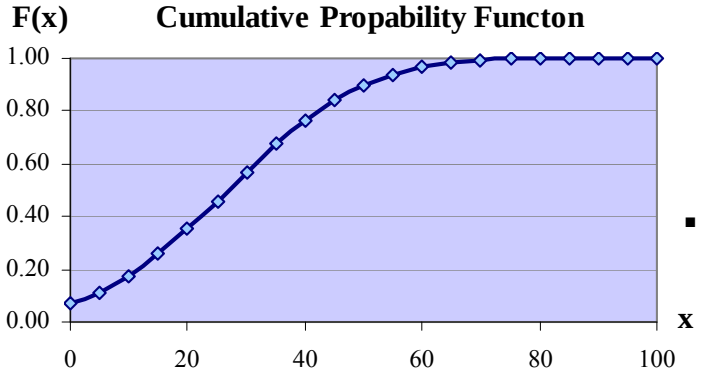

- **Ground acceleration PGA = 0.24g**

Tensile strength fwt	*Failure Rate(%)*
50	70
100	57.00
150	44.00
200	35.00
250	27.00
300	22.00
350	18.00
400	14.00
450	11.00
Total elements	9
Mean value	33.11
Standard deviation	20.30

x	*f(x)*	*F(x)*
0	0.00519664	0.05144016
5	0.00753385	0.08306472
10	0.01027935	0.12746648
15	0.01319984	0.18615624
20	0.01595239	0.25918793
25	0.01814417	0.34474330
30	0.01942240	0.43909947
35	0.01956694	0.53706662
40	0.01855228	0.63282524
45	0.01655487	0.72094280
50	0.01390301	0.79727963
55	0.01098869	0.85953729
60	0.00817405	0.90733843
65	0.00572246	0.94189021
70	0.00377036	0.96540217
75	0.00233796	0.98046454
80	0.00136441	0.98954868
85	0.00074939	0.99470641
90	0.00038737	0.99746330
95	0.00018845	0.99885058
100	0.00008628	0.99950778

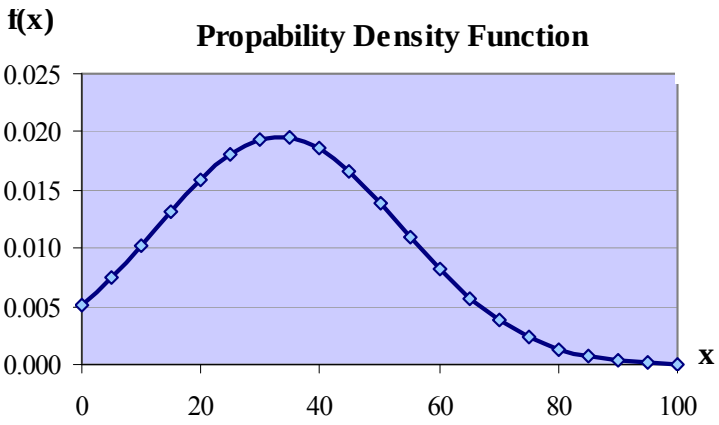

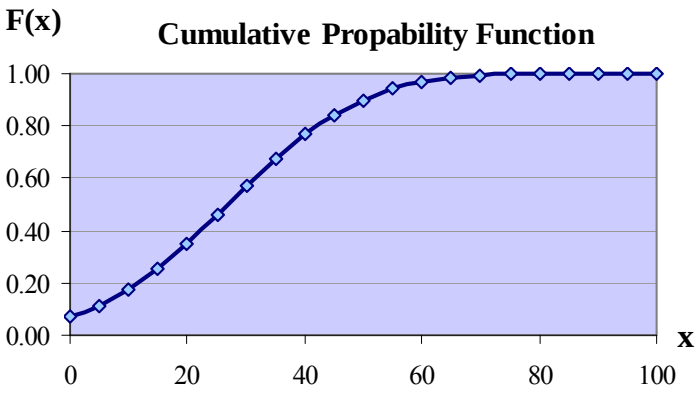

- **Ground acceleration PGA = 0.36g**

Tensile strength fwt	*Failure Rate(%)*
50	77
100	66.00
150	55.00
200	45.00
250	37.00
300	31.00
350	26.00
400	21.00
450	17.00
Total elements	9
Mean value	41.67
Standard deviation	20.75

x	*f(x)*	*F(x)*
0	0.00256212	0.02234317
5	0.00403686	0.03864061
10	0.00600182	0.06353330
15	0.00842008	0.09942046
20	0.01114663	0.14825439
25	0.01392405	0.21097638
30	0.01641277	0.28701488
35	0.01825544	0.37402365
40	0.01916007	0.46799782
45	0.01897563	0.56379877
50	0.01773330	0.65598098
55	0.01563785	0.73970312
60	0.01301245	0.81147419
65	0.01021728	0.86954719
70	0.00757017	0.91389934
75	0.00529262	0.94587140
80	0.00349164	0.96762552
85	0.00217362	0.98159652
90	0.00127682	0.99006544
95	0.00070774	0.99491099
100	0.00037018	0.99752779

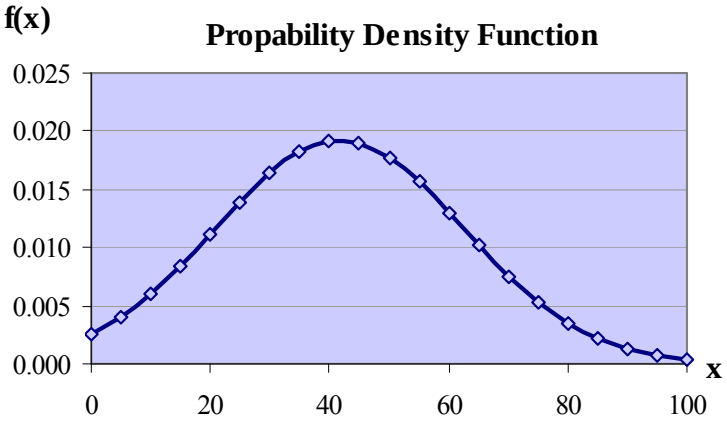

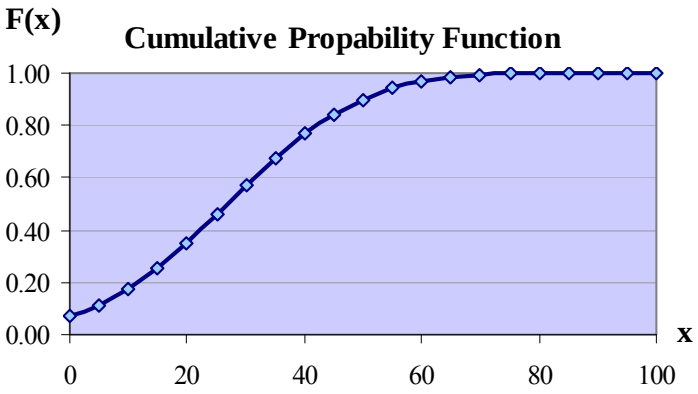

- **Ground acceleration PGA = 0.40g**

Tensile strength fwt	*Failure Rate(%)*
50	90.29
100	78.00
150	70.00
200	60.00
250	52.69
300	46.00
350	40.00
400	35.00
450	30.06
Total elements	9
Mean value	55.78
Standard deviation	20.47

x	*f(x)*	*F(x)*
0	0.00047564	0.00321457
5	0.00089824	0.00655451
10	0.00159808	0.01265836
15	0.00267852	0.02317031
20	0.00422941	0.04023034
25	0.00629150	0.06632142
30	0.00881694	0.10392431
35	0.01164047	0.15499449
40	0.01447812	0.22035730
45	0.01696457	0.29919090
50	0.01872677	0.38879123
55	0.01947475	0.48475900
60	0.01907964	0.58162222
65	0.01760992	0.67375413
70	0.01531207	0.75633490
75	0.01254294	0.82608829
80	0.00967952	0.88161080
85	0.00703716	0.92325842
90	0.00481982	0.95269777
95	0.00310994	0.97230802
100	0.00189044	0.98461792

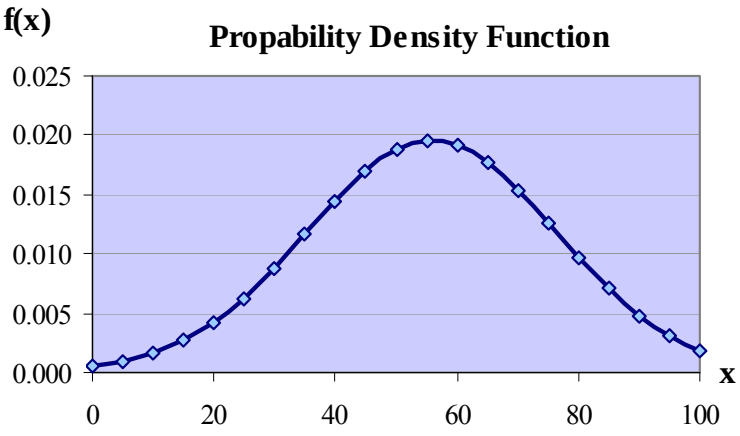

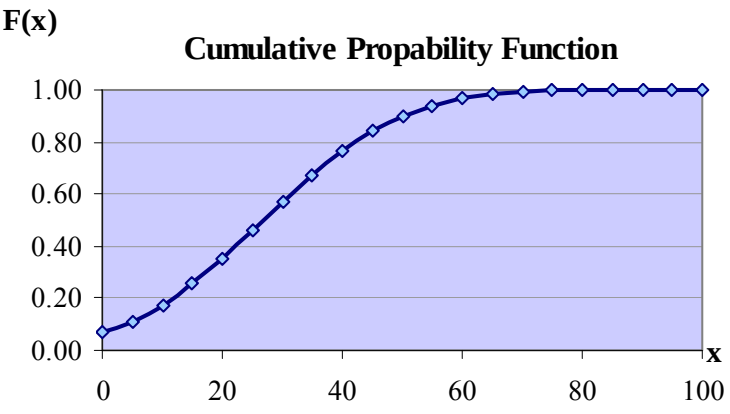

Lognormal Distribution

- **Ground acceleration PGA = 0.16g**

Tensile strength fwt	*Failure Rate(%)*
50	4.11
100	3.93
150	3.69
200	3.22
250	2.80
300	3.00
350	2.77
400	2.40
450	1.79
Total elements	9
Mean value	3.08
Standard deviation	0.75

x	*f(x)*	*F(x)*
0.00000000	0.00000000	0.00000000
1.60943791	0.01555788	0.02490570
2.30258509	0.03114278	0.15008129
2.70805020	0.03142132	0.31040425
2.99573227	0.02647117	0.45597090
3.21887582	0.02093614	0.57430819
3.40119738	0.01618226	0.66668962
3.55534806	0.01242756	0.73781170
3.68887945	0.00955427	0.79243684
3.80666249	0.00737933	0.83451711
3.91202301	0.00573544	0.86711326
4.00733319	0.00448903	0.89253217
4.09434456	0.00353886	0.91249585
4.17438727	0.00280976	0.92828810
4.24849524	0.00224637	0.94086882
4.31748811	0.00180792	0.95095946
4.38202663	0.00146430	0.95910567
4.44265126	0.00119315	0.96572296
4.49980967	0.00097778	0.97112993
4.55387689	0.00080562	0.97557260
4.60517019	0.00066718	0.97924222

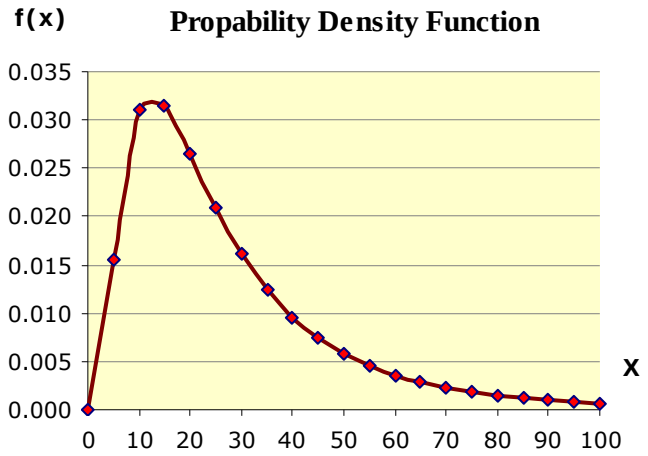

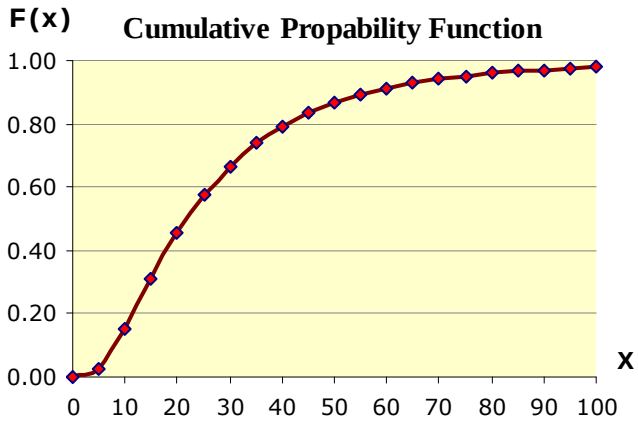

- **Ground acceleration PGA = 0.24g**

Tensile strength fwt	*Failure Rate(%)*
50	4.25
100	4.04
150	3.78
200	3.56
250	3.30
300	3.09
350	2.89
400	2.64
450	2.40
Total elements	9
Mean value	3.33
Standard deviation	0.63

x	*f(x)*	*F(x)*
0.00000000	0.00000000	0.00000000
1.60943791	0.00317627	0.00333176
2.30258509	0.01700785	0.05278654
2.70805020	0.02603911	0.16403645
2.99573227	0.02746938	0.30027042
3.21887582	0.02483783	0.43204173
3.40119738	0.02086091	0.54648664
3.55534806	0.01687194	0.64067486
3.68887945	0.01338183	0.71605767
3.80666249	0.01051239	0.77553566
3.91202301	0.00822633	0.82215637
4.00733319	0.00643441	0.85862271
4.09434456	0.00504090	0.88716383
4.17438727	0.00396053	0.90955273
4.24849524	0.00312304	0.92717309
4.31748811	0.00247271	0.94109435
4.38202663	0.00196630	0.95213953
4.44265126	0.00157054	0.96094134
4.49980967	0.00126004	0.96798672
4.55387689	0.00101539	0.97365124
4.60517019	0.00082180	0.97822554

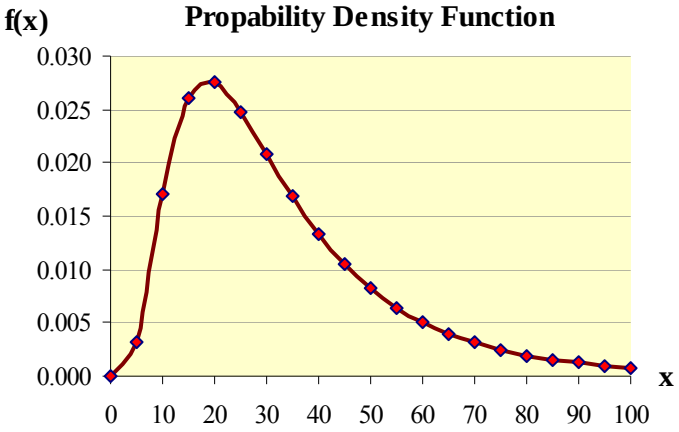

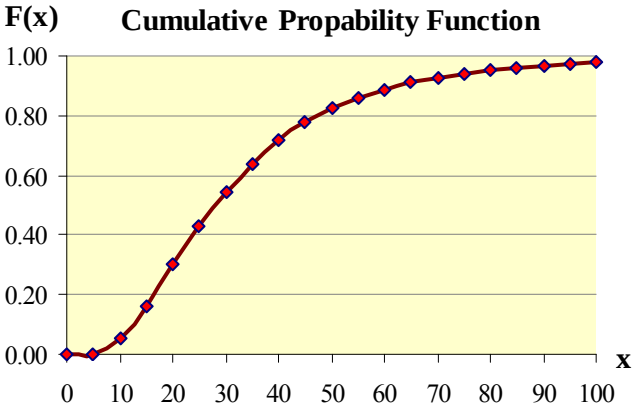

- **Ground acceleration PGA = 0.36g**

Tensile strength fwt	*Failure Rate(%)*
50	4.34
100	4.19
150	4.01
200	3.81
250	3.61
300	3.43
350	3.26
400	3.04
450	2.83
Total elements	9
Mean value	3.61
Standard deviation	0.52

x	*f(x)*	*F(x)*
0.00000000	0.00000000	0.00000000
1.60943791	0.00008672	0.00005481
2.30258509	0.00312966	0.00568955
2.70805020	0.01112737	0.04018926
2.99573227	0.01888228	0.11635374
3.21887582	0.02301672	0.22277358
3.40119738	0.02357971	0.34051010
3.55534806	0.02185149	0.45476210
3.68887945	0.01904539	0.55725339
3.80666249	0.01596646	0.64478204
3.91202301	0.01305263	0.71720659
4.00733319	0.01049719	0.77591320
4.09434456	0.00835338	0.82286827
4.17438727	0.00660370	0.86010542
4.24849524	0.00520050	0.88948312
4.31748811	0.00408773	0.91259433
4.38202663	0.00321147	0.93075423
4.44265126	0.00252432	0.94502374
4.49980967	0.00198665	0.95624612
4.55387689	0.00156625	0.96508530
4.60517019	0.00123746	0.97206099

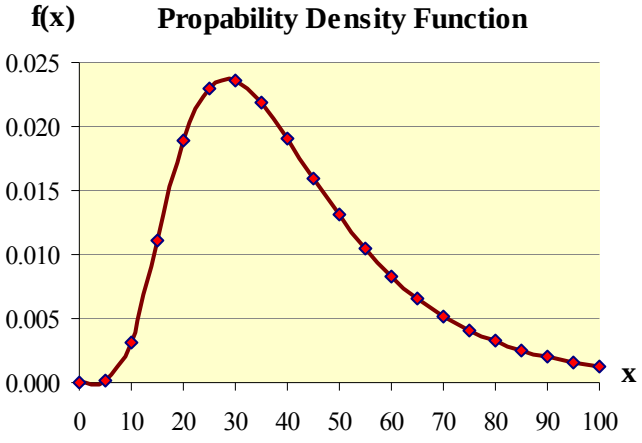

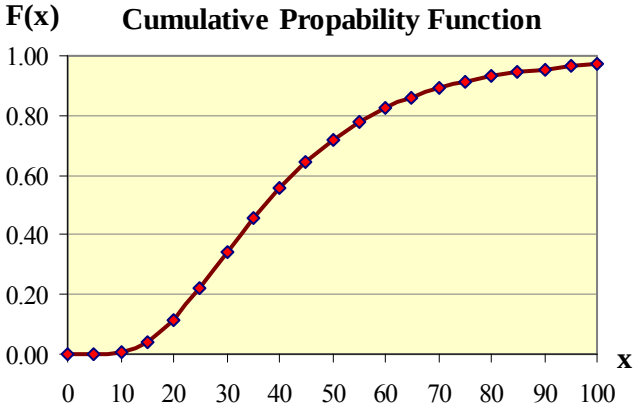

- **Ground acceleration PGA = 0.40g**

Tensile strength fwt	*Failure Rate(%)*
50	4.50
100	4.36
150	4.25
200	4.09
250	3.96
300	3.83
350	3.69
400	3.56
450	3.40
Total elements	9
Mean value	3.96
Standard deviation	0.37

x	*f(x)*	*F(x)*
0.00000000	0.00000000	0.00000000
1.60943791	0.00000000	0.00000000
2.30258509	0.00000573	0.00000462
2.70805020	0.00026035	0.00040443
2.99573227	0.00191211	0.00493677
3.21887582	0.00597169	0.02366466
3.40119738	0.01162369	0.06737244
3.55534806	0.01695556	0.13933477
3.68887945	0.02049570	0.23387944
3.80666249	0.02179268	0.34050952
3.91202301	0.02116507	0.44858208
4.00733319	0.01924967	0.55001542
4.09434456	0.01667884	0.63999548
4.17438727	0.01393539	0.71652618
4.24849524	0.01132688	0.77958244
4.31748811	0.00901517	0.83029522
4.38202663	0.00706072	0.87033294
4.44265126	0.00546223	0.90149740
4.49980967	0.00418606	0.92549311
4.55387689	0.00318527	0.94381701
4.60517019	0.00241090	0.95772294

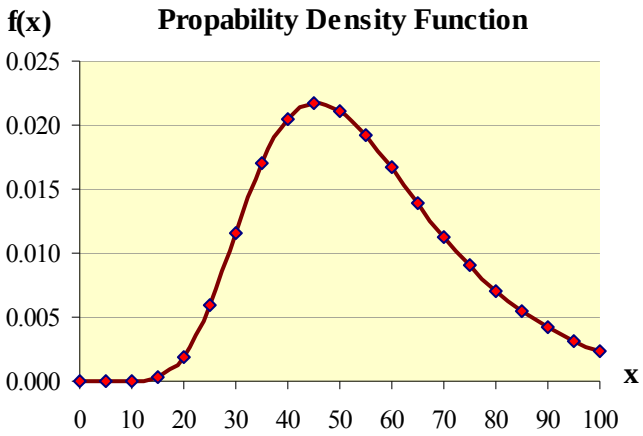

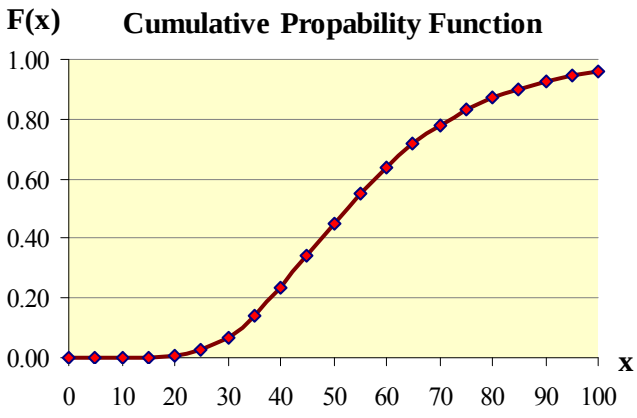

7.3.4 Export of fragility curves

After the statistical processing and the analysis of the failure rates of the wall structure and having set the levels of damage in a previous chapter, we can draw the fragility curves.

Normal Distribution

- **Graduation of failures, type a**

(%) PGA	0	0.16	0.24	0.36	0.40
Small	0	0.8806	0.9169	0.9614	0.9934
Medium	0	0.7428	0.8138	0.9006	0.9768
Large	0	0.5500	0.6553	0.7890	0.9337

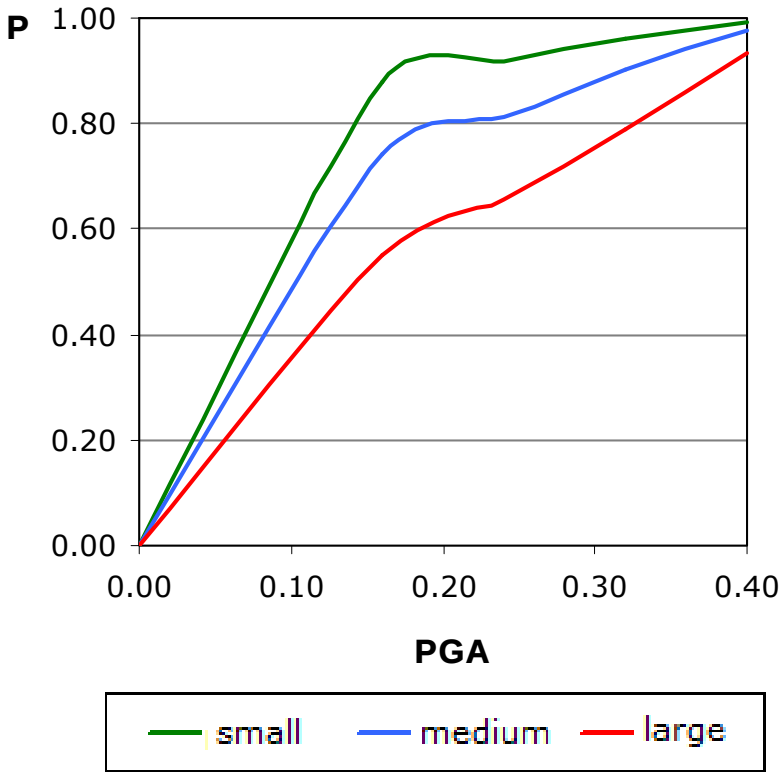

➢ **Graduation of failures, type b**

(%) PGA	0	0.16	0.24	0.36	0.40
Small	0	0.8199	0.8725	0.9365	0.9873
Medium	0	0.6513	0.7408	0.8517	0.9598
Large	0	0.4453	0.5609	0.7130	0.8961

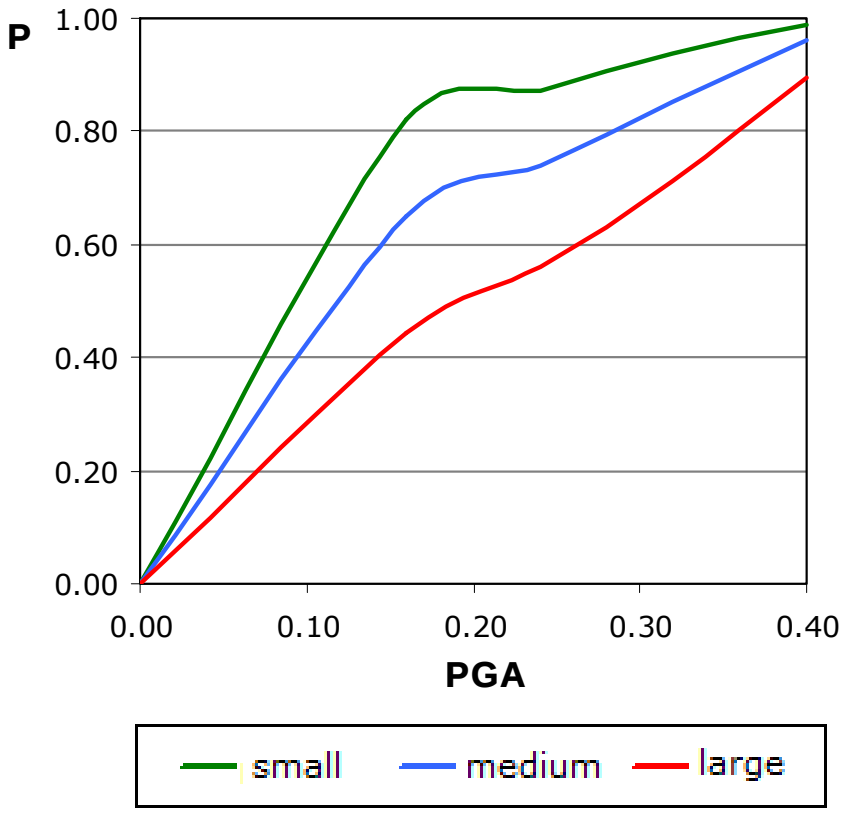

➢ **Graduation of failures, type c**

(%) PGA	0	0.16	0.24	0.36	0.40
Small	0	0.7428	0.8138	0.9006	0.9768
Medium	0	0.3443	0.4629	0.6260	0.8450
Large	0	0.1770	0.2791	0.4362	0.7008

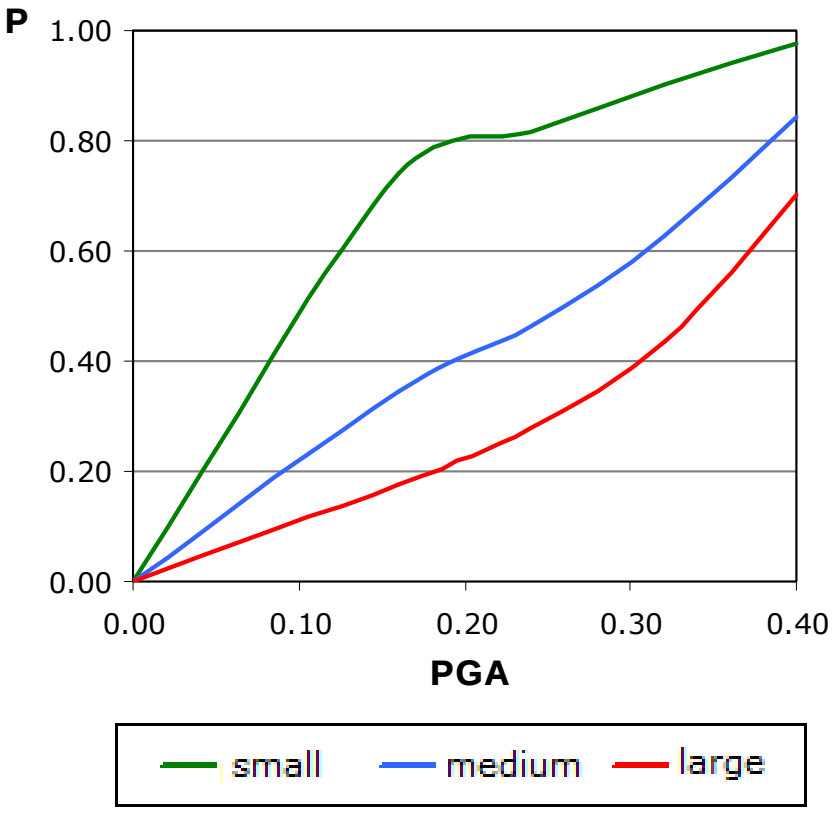

Lognormal Distribution

- **Graduation of failures, type a**

(%) PGA	0	0.16	0.24	0.36	0.40
Small	0	0.9751	0.9967	0.9999	1.0000
Medium	0	0.6896	0.8360	0.9598	0.9996
Large	0	0.4257	0.5680	0.7772	0.9763

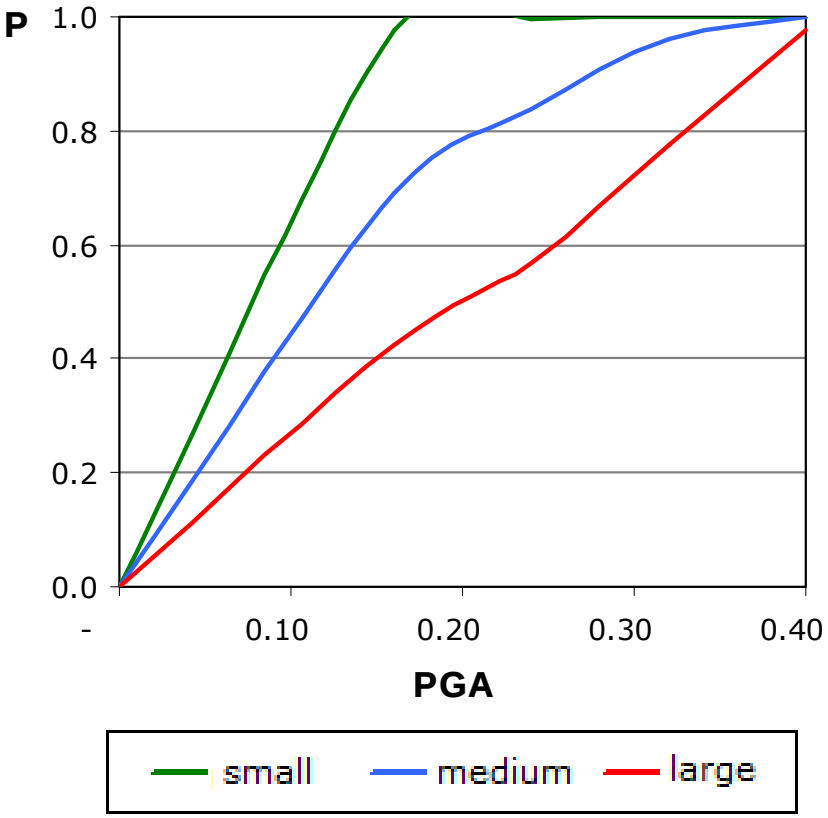

- **Graduation of failures, type b**

(%) PGA	0	0.16	0.24	0.36	0.40
Small	0	0.8499	0.9472	0.9943	1.0000
Medium	0	0.5440	0.6997	0.8836	0.9951
Large	0	0.3333	0.4535	0.6595	0.9326

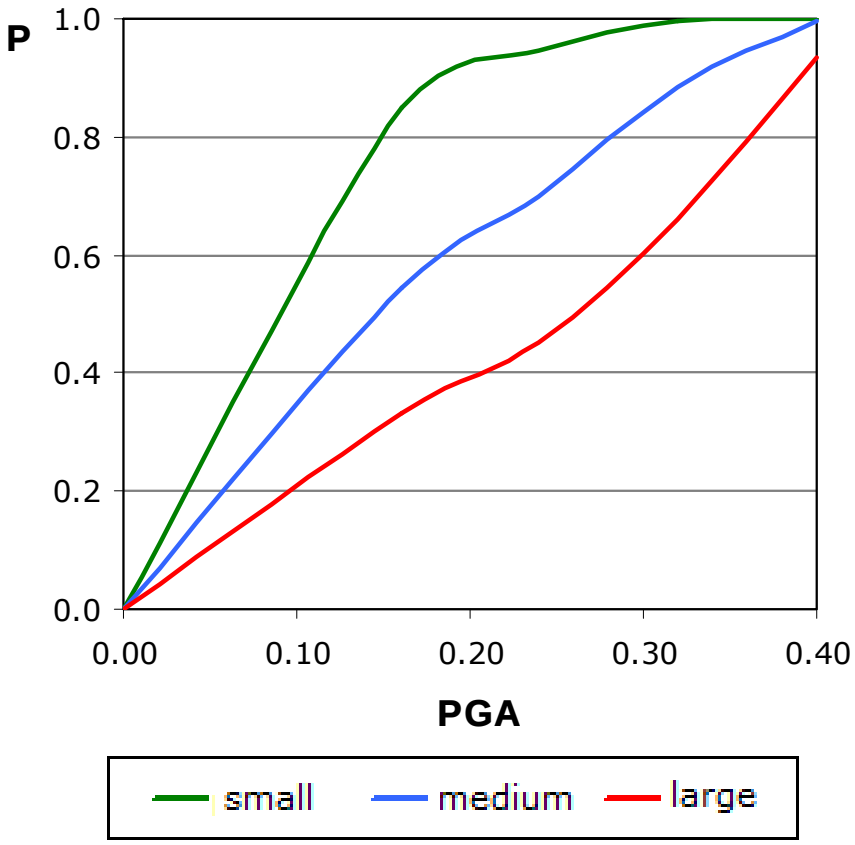

- **Graduation of failures, type c**

(%) PGA	0	0.16	0.24	0.36	0.40
Small	0	0.6896	0.6997	0.8836	0.9951
Medium	0	0.2622	0.4535	0.6595	0.9326
Large	0	0.1655	0.1778	0.2828	0.5514

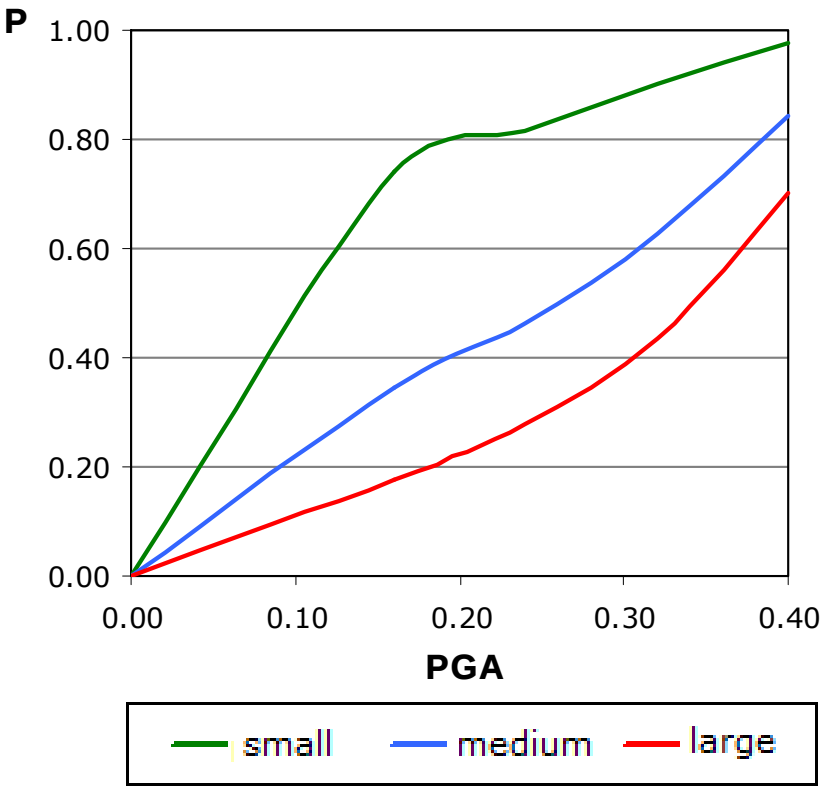

7.3.5 Comparison between the three failure levels of the two distributions

- ***Small failure***

Normal Distribution	Lognormal distribution
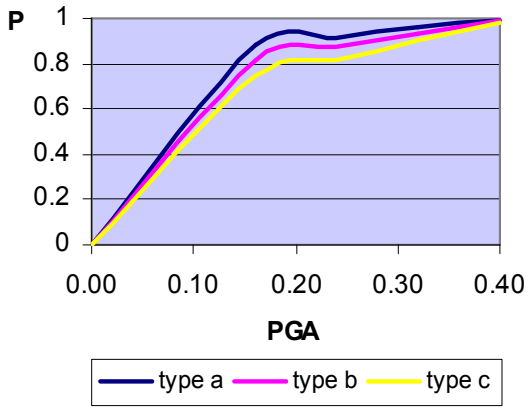	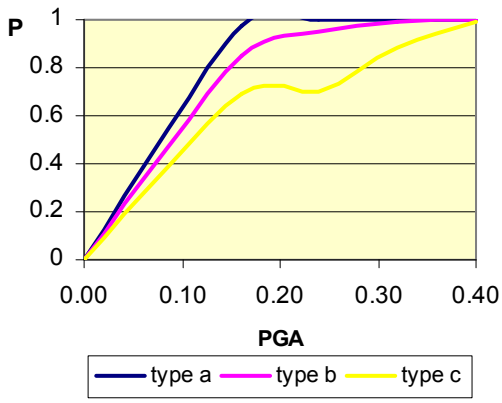

- ***Medium failure***

Normal Distribution	Lognormal distribution
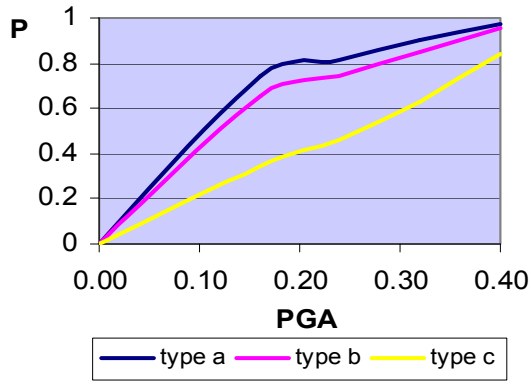	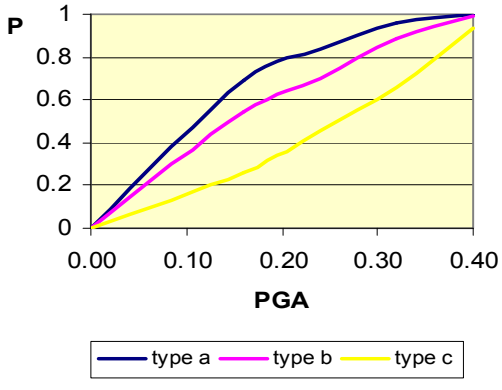

- ***Large failure***

Normal Distribution	Lognormal distribution
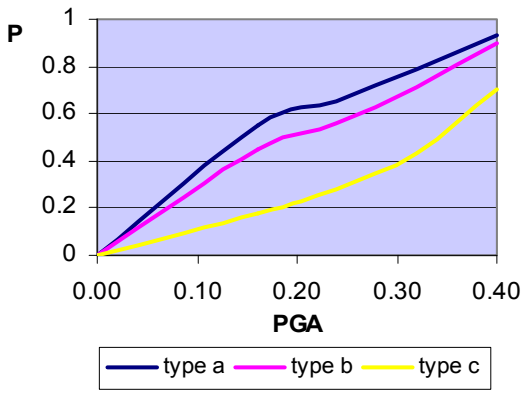	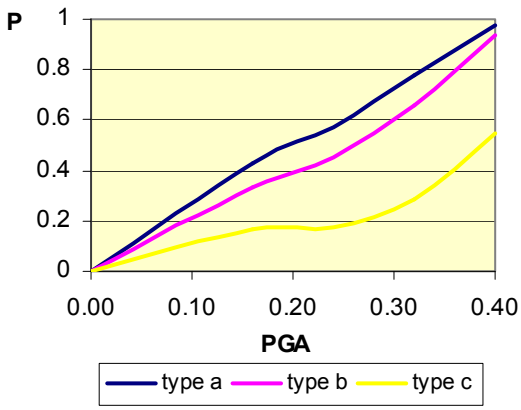

CHAPTER 8

REPAIR AND REINFORCEMENT OF EXISTING MASONRY (Reinforcement A)

8.1 Pointing, reinforced concrete slab at the ground and the first floor level and reinforced concrete bond beam at the roof level (Reinforcement B)

Important factor on the behavior of the bearing masonry can play the creation of horizontal diaphragms of reinforced concrete, because of their high stiffness they ensure a uniform distribution of horizontal forces on the walls of their base and they also reduce the bending height and due to their weight they give vertical compressive forces, thus increasing the shear strength.

Alternative methods for creating a certain degree of diaphragmatic function are:

- Diagonal tie rods that anchor on the outer surface of the walls.
- Vertical wall anchor and parallel to them floor beams
- Placing of second sheathing perpendicular to the existing and parallel to the joists.

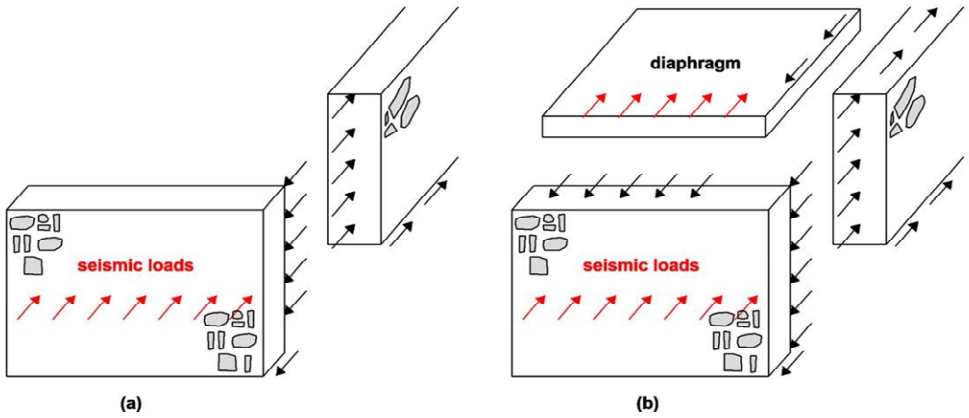

Figure 8.1 Transfer of seismic forces lack of diaphragm (a) and presence of diaphragm (b)

The ensuring of the diaphragmatic function at the top of the construction is perfect and could be achieved with the concrete slab of reinforced concrete in

order to ensure equal movements of the walls and thus reduce the tension of the construction and to prevent the deflection of the walls as a cantilever. Nevertheless this solution is avoided, because in addition to the large component of costs, results a large mass concentration at the top of the building, where due to the stiffness of the floors in their plane, significant inertial forces are transferred to the perimeter walls.

The optimal solution is presented to create a horizontal bond beam of reinforced concrete on top of the building causing the walls to have a common move at the corners, at the height of the crest, reducing the size of the deformation sufficiently. The bond beam of reinforced concrete is one of the most effective, as well as the lowest cost way, to increase the strength of the wall against fatal actions such as the earthquake.

8.2 Stages of work and modeling of reinforcement B

The construction of the bond beam at level of the roof does not present particular difficulties in contrast to intermediate levels. If there is a steep roof, the pouring of the concrete is easy, the removal of some tiles and the placing of side molds is enough. In this construction, however, the slope of the roof is low and therefore requires the rising and the temporary support like shown in Figure 8.4. Attention should be paid to the temporary support where it has to reach up to the ground.

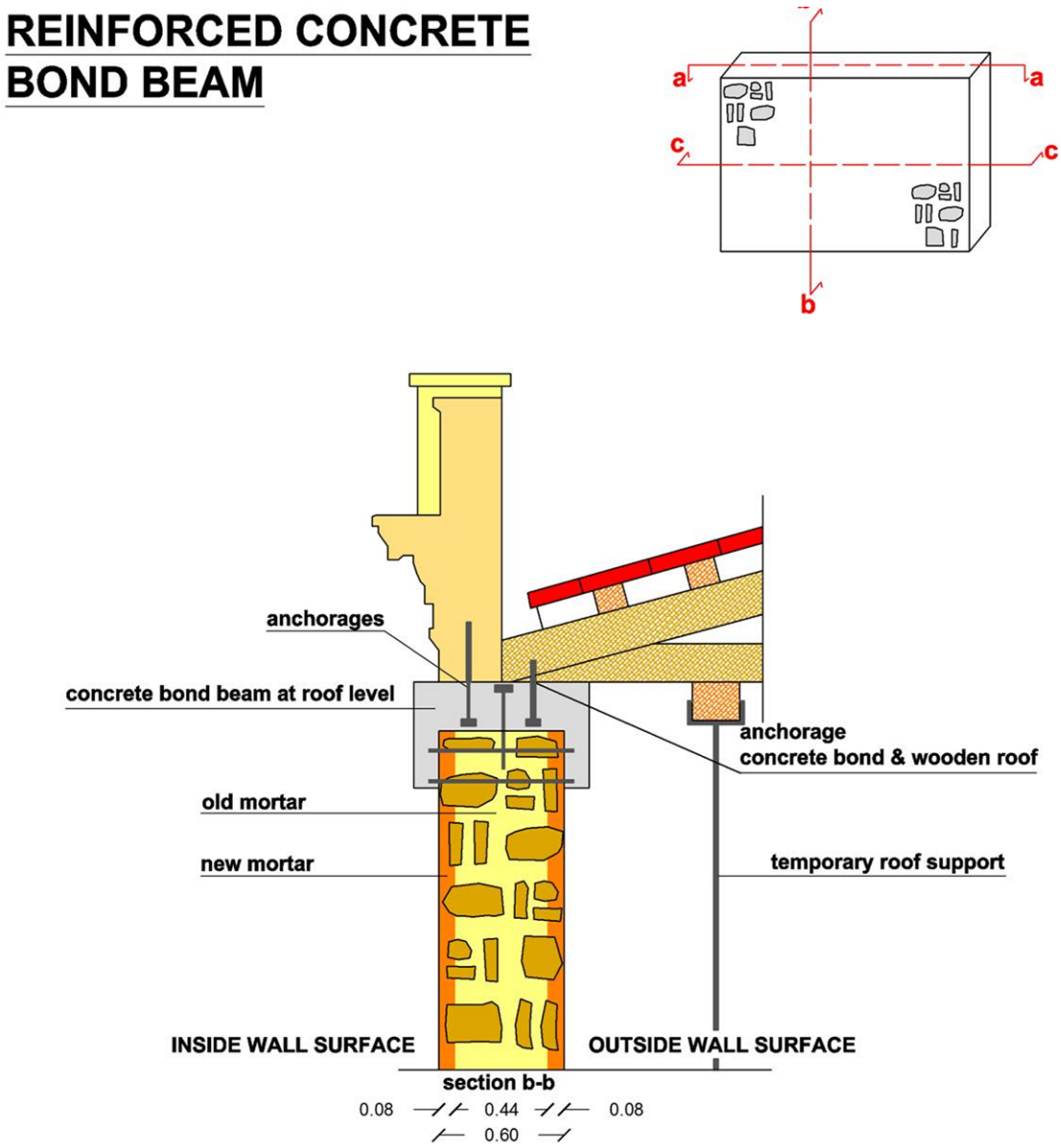

Figure 7.4 Bond beam R.C. on the crest

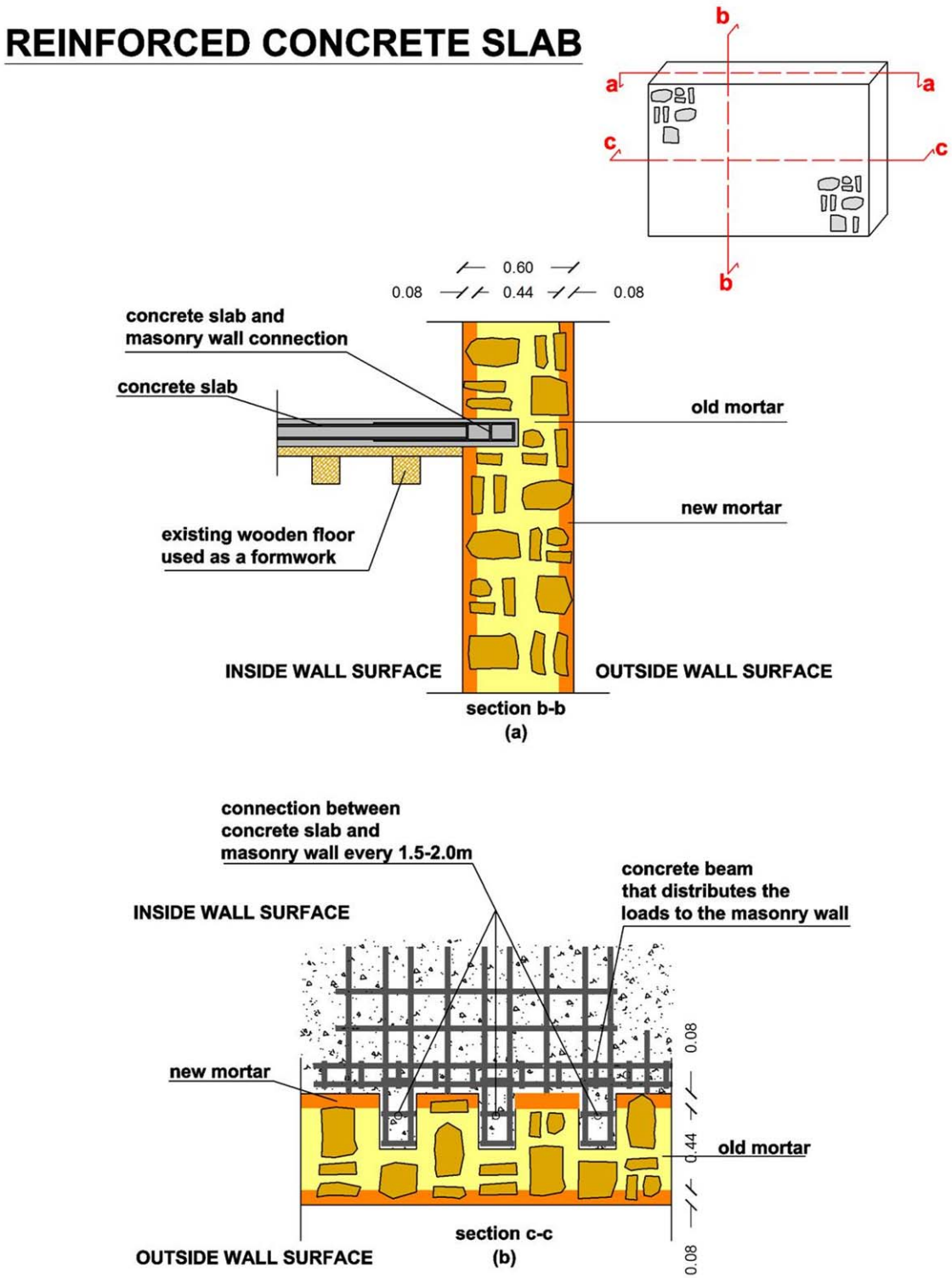

Figure 8.2 Slab R.C.at the levels of the basement and ground floor slabs
For the construction of reinforced concrete slabs the existing floors will be used

as formwork. The support of the plate at the walls will be by 1.5-2m as shown in Figure 8.5 while a perimeter beam will transfer the loads evenly.

For the modeling of the bond beam and the slab was chosen such concrete quality of C20/25 (W = 25KN.m3 / E = 29GPa / v = 0.2). The thickness of the bond beam protrudes from both sides of the wall 15cm creating two panels that hug the top of the wall, the height of the bond beam is up to 30cm. The modeling of slabs R.C. was achieved with kinematic commitment of the horizontal transfers and the turning on the vertical axis of the nodes in the levels of the floors. The bond beam on the crest of the stone wall was simulated with the performance of the properties of concrete as described above, to the corresponding finite elements of the wall.

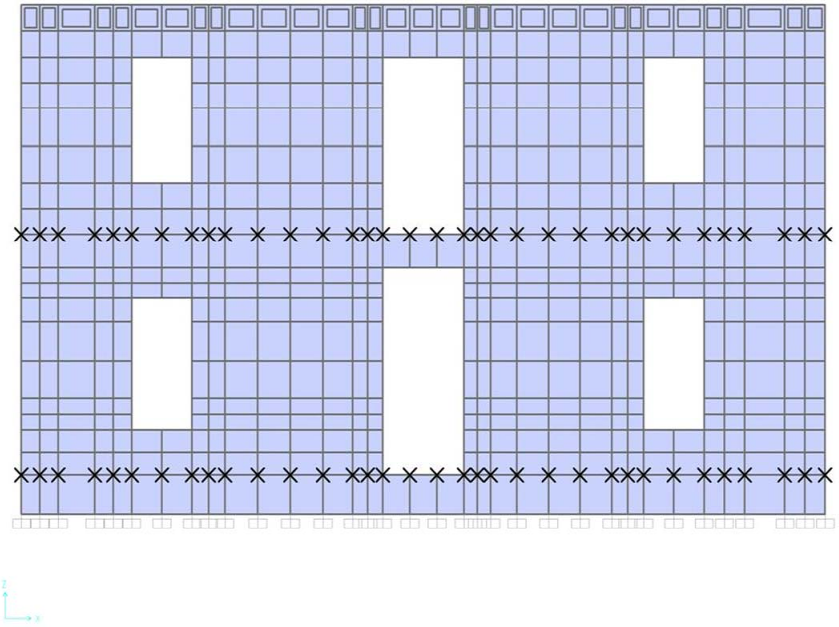

Figure 8.3 Indicative façade where are visible the levels of reinforced concrete slabs and the bond beam as simulated

Fundamental mode (transferational) of the building T= 0.086sec, mass participation ratio 36% at 'Y' direction.

TABLE: Modal Participating Mass Ratios						
OutputCase	**StepType**	**StepNum**	**Period**	**UX**	**UY**	**RZ**
Text	Text	Unitless	Sec	Unitless	Unitless	Unitless
MODAL	Mode	1	0,14531	0,03569	4,29E-07	0,00753
MODAL	Mode	2	0,108186	0,00569	2,89E-05	0,00887
MODAL	Mode	3	0,092947	0,15107	0,00118	0,02628
MODAL	Mode	4	0,086281	2,23E-07	0,36117	0,25201
MODAL	Mode	5	0,082596	0,00608	0,02049	0,0055
MODAL	Mode	6	0,077405	0,00807	0,154	0,01015
MODAL	Mode	7	0,075139	5,63E-05	0,00012	9,43E-09
MODAL	Mode	8	0,074921	0,00909	0,01691	0,00063
MODAL	Mode	9	0,072173	0,09667	0,02063	0,00031
MODAL	Mode	10	0,067894	0,01699	0,04094	0,01459

Table 8.1 first ten modes after the reinforcement with concrete slab at the ground and 1st floor levels, bond beam on the crest and pointing.

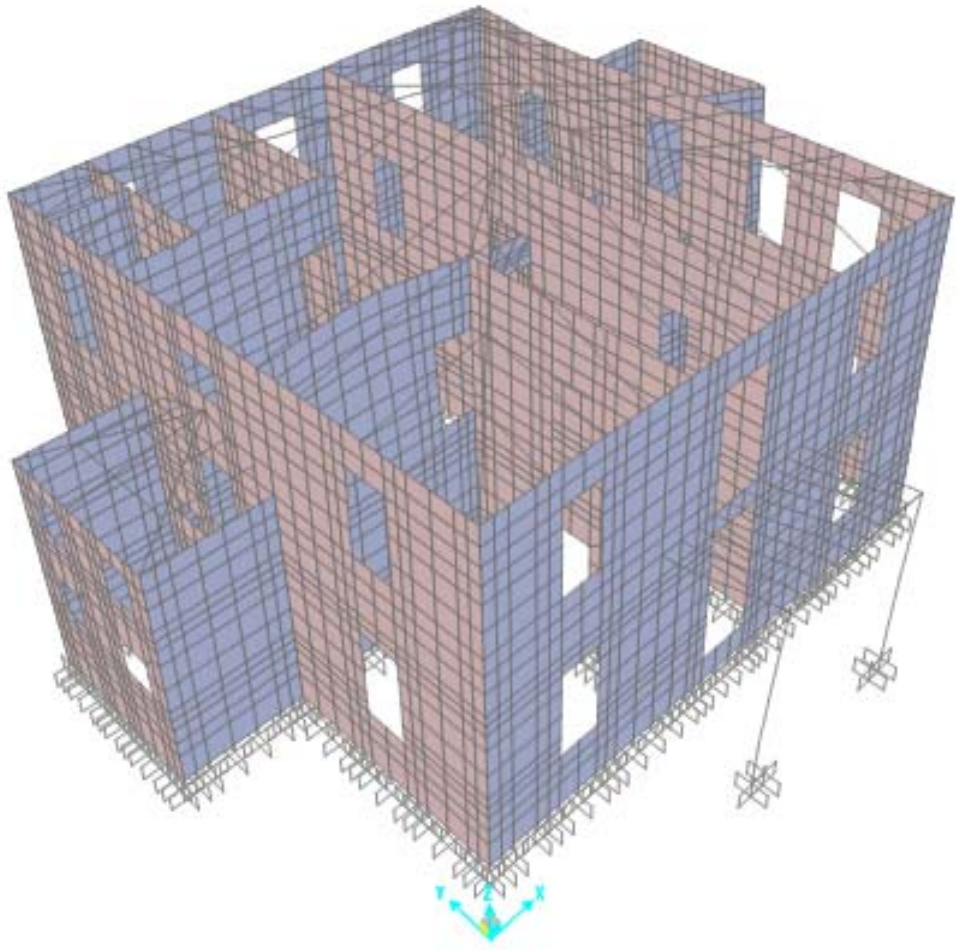

Figure 8.4 fundamental mode T= 0.086sec

8.3 Walls failure results from software FAILURE

As in chapter 9, In this chapter are illustrated indicatively, the failures of four walls (w1,w8,WD,wE) of reinforcement B for the most severe loading combination, for PGA= 0.16 and 0.40 and for tensile strength 50kPa, 250kPa, 450kPa.

Failure

wall : **1_2topmax** **Load Cases :** **0.16g**	Failure under biaxial Tension/Tension
	Failure under biaxial Tension/ Compression
	Failure under biaxial Compression /Tension
	Failure under biaxial Compression/ Compression
	NON Failure

fwt = 50 kPa

Joints = 640
Failed = 182

Failure
Percentage = 28.44%

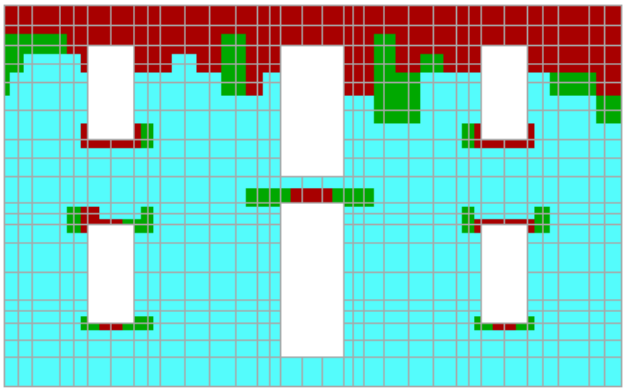

fwt = 250 kPa

Joints = 640
Failed = 60

Failure
Percentage = 9.38%

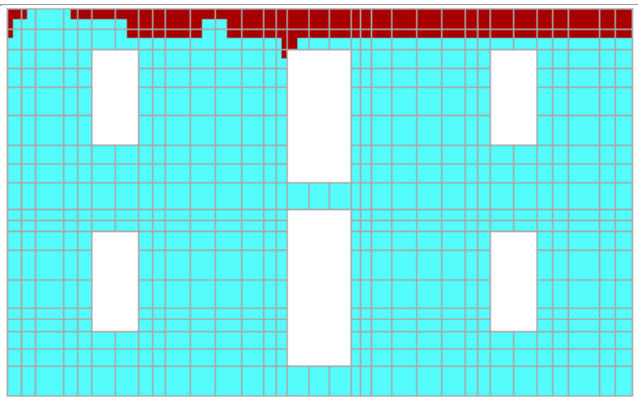

f_{wt} = 450 kPa

Joints = 640
Failed = 24

Failure
Percentage = 3.75%

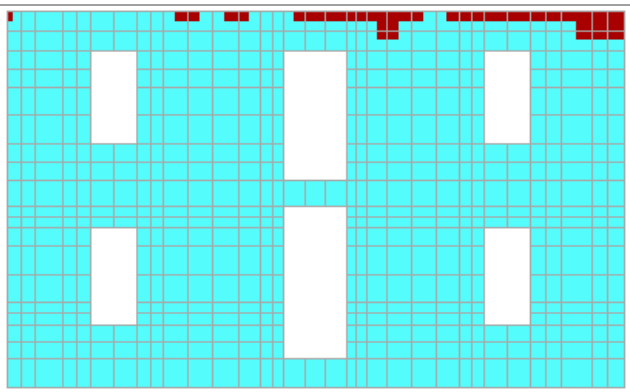

Failure

wall : **1_2topmax** **Load Cases :** **0.40g**		Failure under biaxial Tension/Tension
		Failure under biaxial Tension/ Compression
		Failure under biaxial Compression /Tension
		Failure under biaxial Compression/ Compression
		NON Failure
fwt = 50 kPa	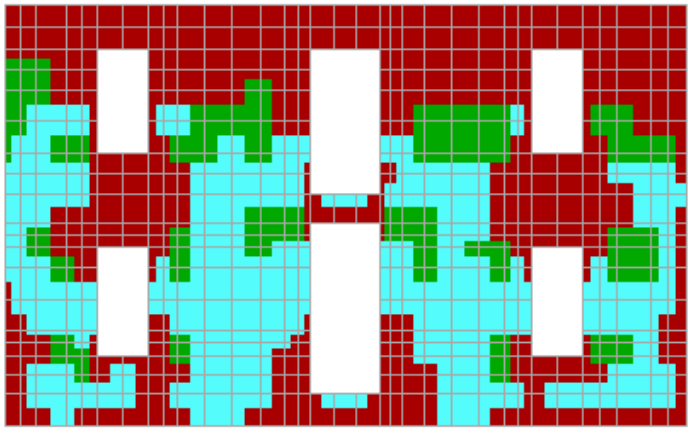	
Joints = 640 Failed = 441 Failure Percentage = 68.91%		
fwt = 250 kPa	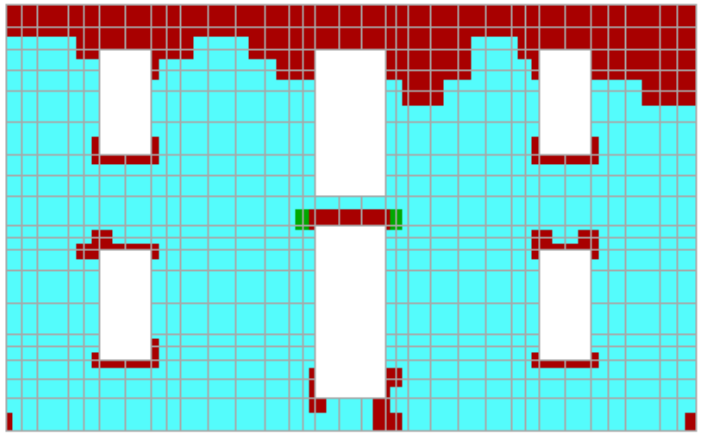	
Joints = 640 Failed = 153 Failure Percentage = 23.91%		
f_{wt} = 450 kPa	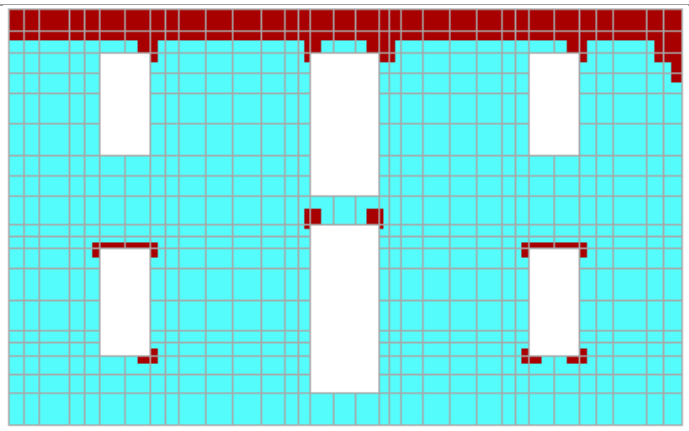	
Joints = 640 Failed = 87 Failure Percentage = 13.59%		

Failure

wall : **8_2topmax** **Load Cases :** **0.16g**		Failure under biaxial Tension/Tension
		Failure under biaxial Tension/ Compression
		Failure under biaxial Compression /Tension
		Failure under biaxial Compression/ Compression
		NON Failure
fwt = 50 kPa	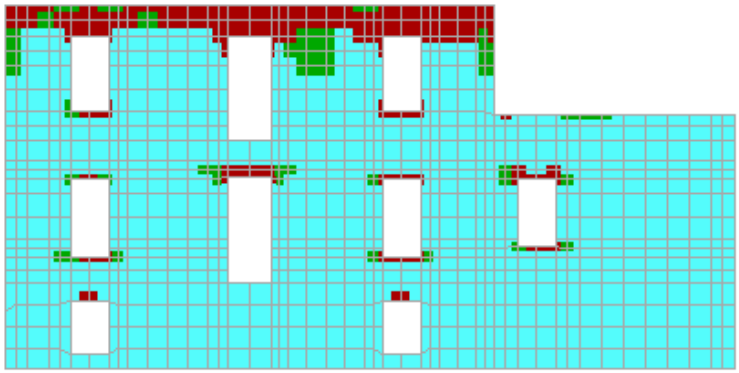	
Joints = 990 Failed = 161 Failure Percentage = 16.26%		
fwt = 250 kPa	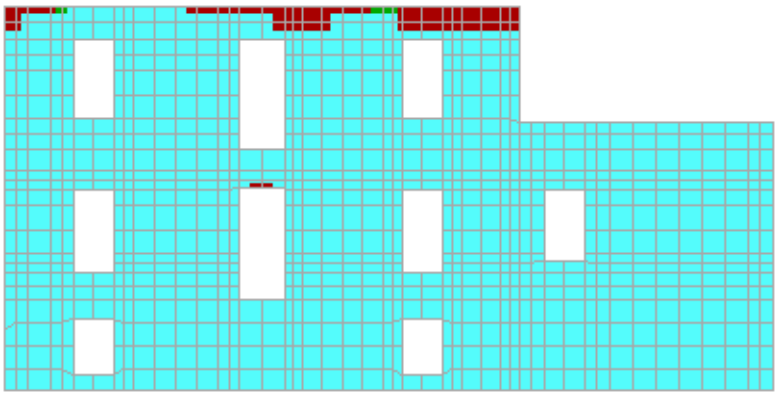	
Joints = 990 Failed = 43 Failure Percentage = 4.34%		
f_{wt} = 450 kPa	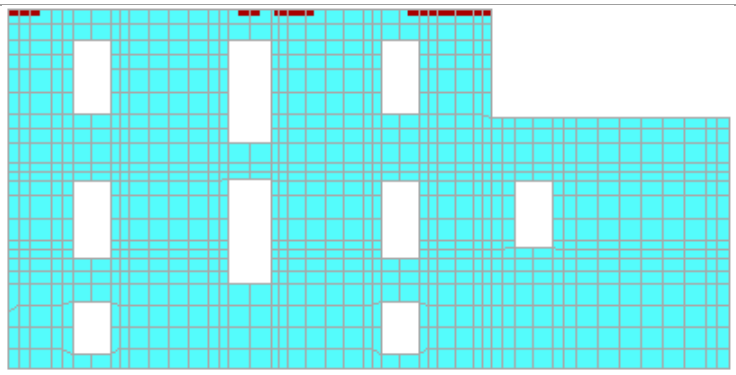	
Joints = 990 Failed = 14 Failure Percentage = 1.41%		

Failure		
wall : **8_2topmax** **Load Cases :** **0.40g**		Failure under biaxial Tension/Tension
		Failure under biaxial Tension/ Compression
		Failure under biaxial Compression /Tension
		Failure under biaxial Compression/ Compression
		NON Failure
fwt = 50 kPa	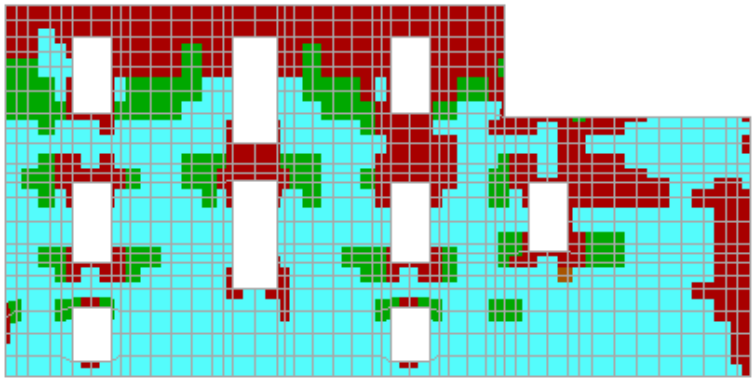	
Joints = 990 Failed = 476 Failure Percentage = 48.08%		
fwt = 250 kPa	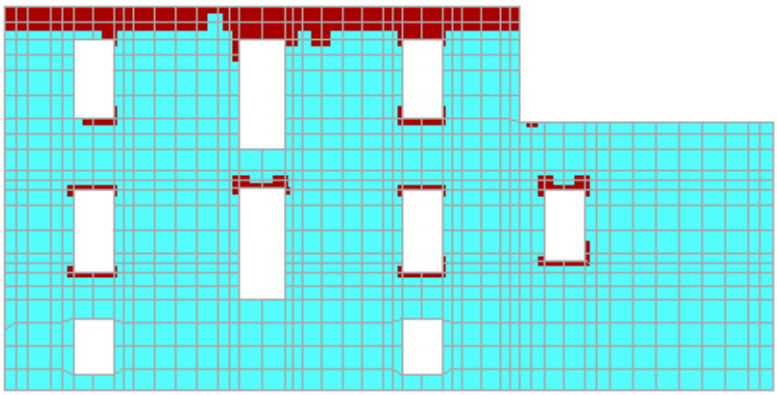	
Joints = 990 Failed = 110 Failure Percentage = 11.11%		
f_{wt} = 450 kPa	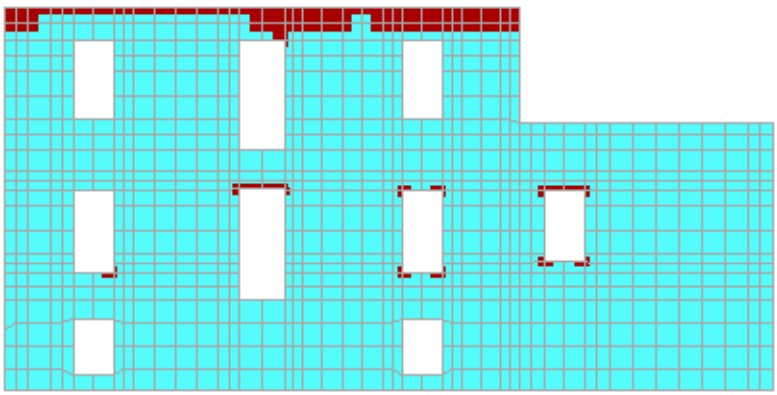	
Joints = 990 Failed = 68 Failure Percentage = 6.87%		

Failure		
wall : **D_2topmax** **Load Cases :** **0.16g**		Failure under biaxial Tension/Tension
		Failure under biaxial Tension/ Compression
		Failure under biaxial Compression /Tension
		Failure under biaxial Compression/ Compression
		NON Failure
fwt = 50 kPa	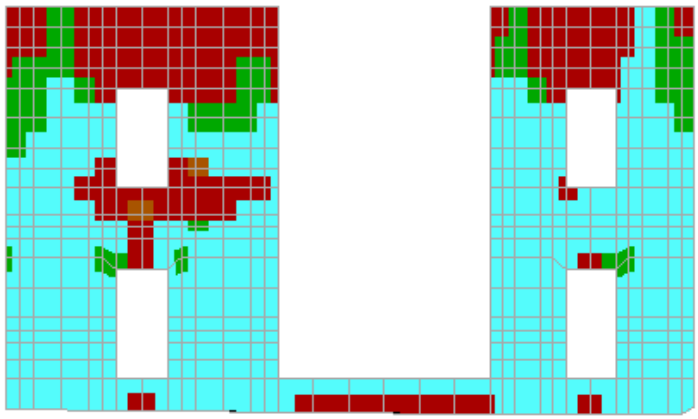	
Joints = 555 Failed = 181 Failure Percentage = 32.61%		
fwt = 250 kPa	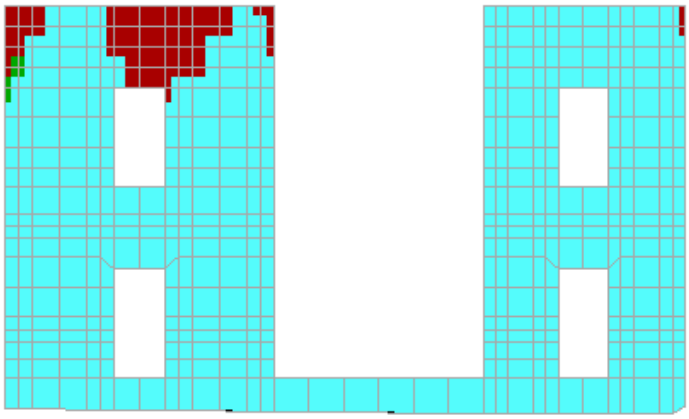	
Joints = 555 Failed = 40 Failure Percentage = 7.21%		
f_{wt} = 450 kPa	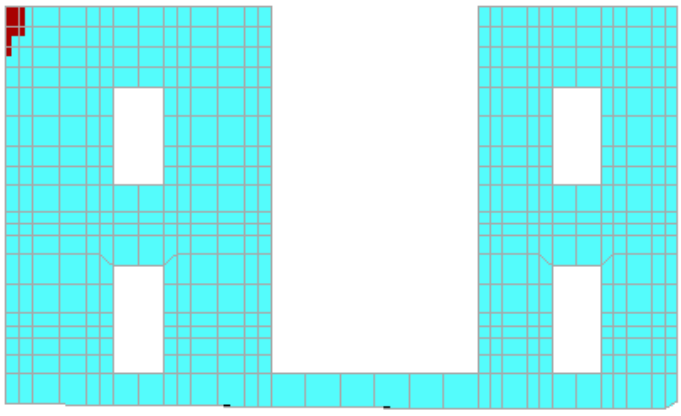	
Joints = 555 Failed = 4 Failure Percentage = 0.90%		

Failure

wall : **D_2topmax** **Load Cases :** **0.40g**		Failure under biaxial Tension/Tension
		Failure under biaxial Tension/ Compression
		Failure under biaxial Compression /Tension
		Failure under biaxial Compression/ Compression
		NON Failure
fwt = 50 kPa	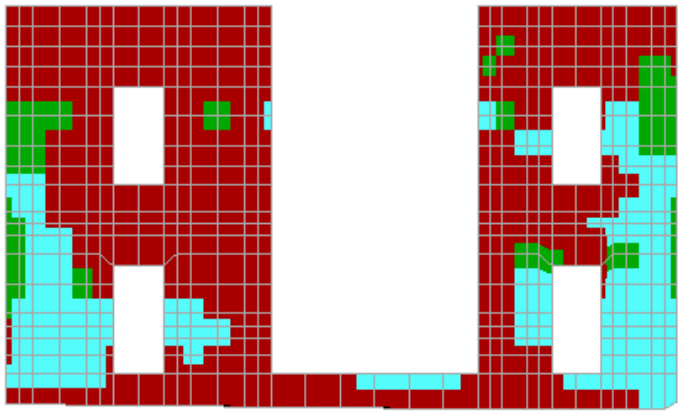	
Joints = 555 Failed = 417 Failure Percentage = 75.14%		
fwt = 250 kPa	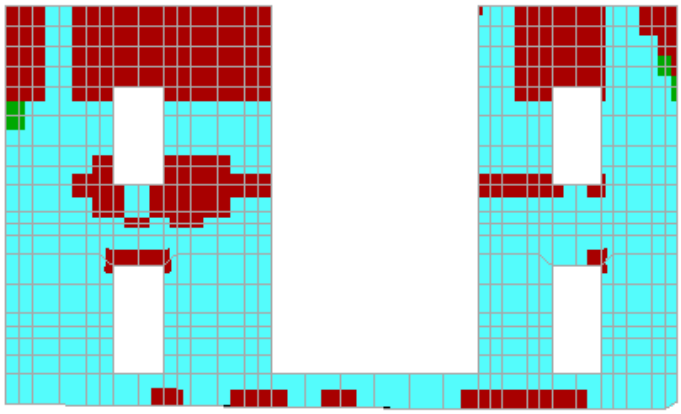	
Joints = 555 Failed = 158 Failure Percentage = 28.47%		
f_{wt} = 450 kPa	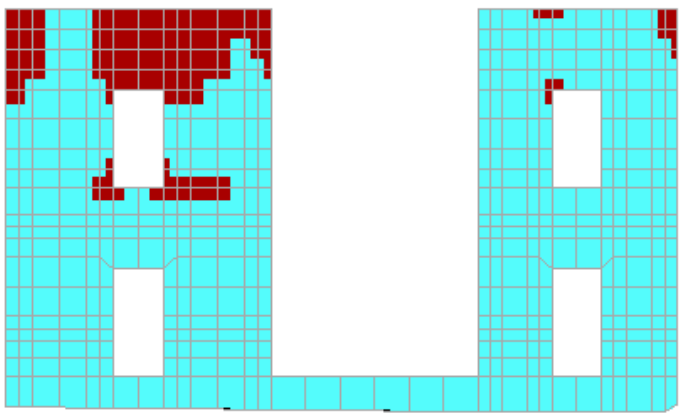	
Joints = 555 Failed = 72 Failure Percentage = 12.97%		

Failure		
wall : **E_2topmax** **Load Cases :** **0.16g**		Failure under biaxial Tension/Tension
		Failure under biaxial Tension/ Compression
		Failure under biaxial Compression /Tension
		Failure under biaxial Compression/ Compression
		NON Failure
fwt = 50 kPa	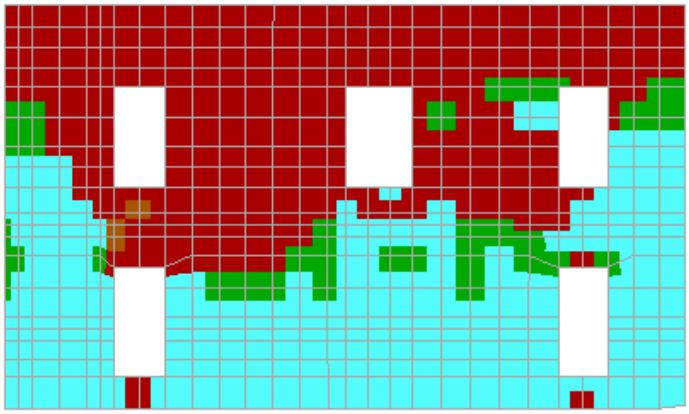	
Joints = 558 Failed = 298 Failure Percentage = 53.41%		
fwt = 250 kPa	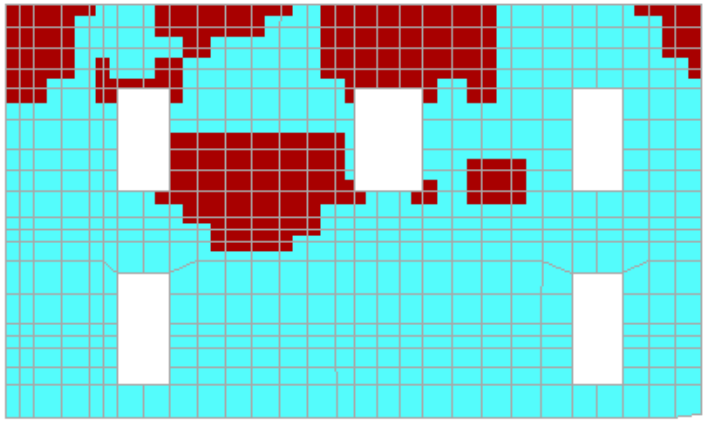	
Joints = 558 Failed = 116 Failure Percentage = 20.79%		
f_{wt} = 450 kPa	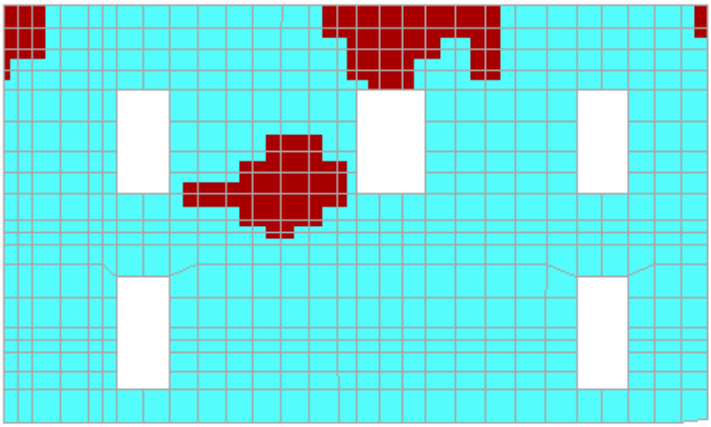	
Joints = 558 Failed = 53 Failure Percentage = 9.50%		

Failure

wall : **E_2topmax** **Load Cases :** **0.40g**		Failure under biaxial Tension/Tension
		Failure under biaxial Tension/ Compression
		Failure under biaxial Compression /Tension
		Failure under biaxial Compression/ Compression
		NON Failure
fwt = 50 kPa	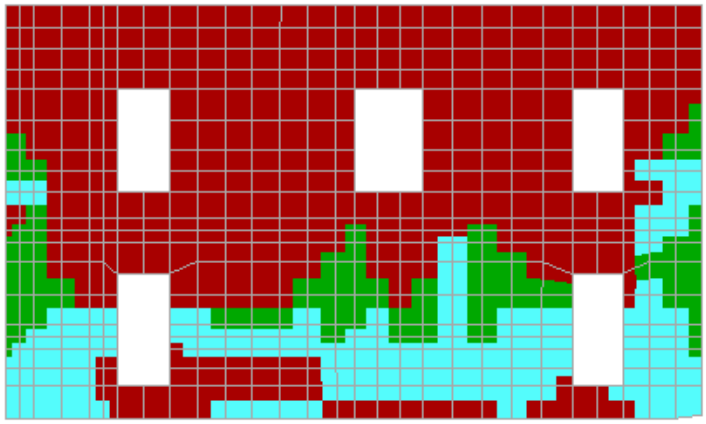	
Joints = 558 Failed = 431 Failure Percentage = 77.24%		
fwt = 250 kPa	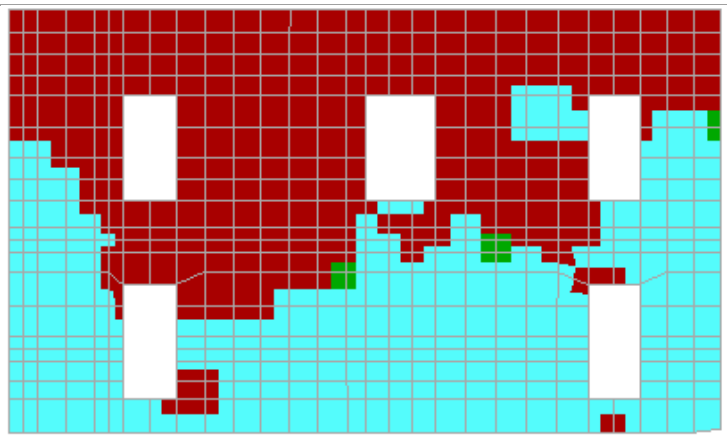	
Joints = 558 Failed = 283 Failure Percentage = 50.72%		
f_{wt} = 450 kPa	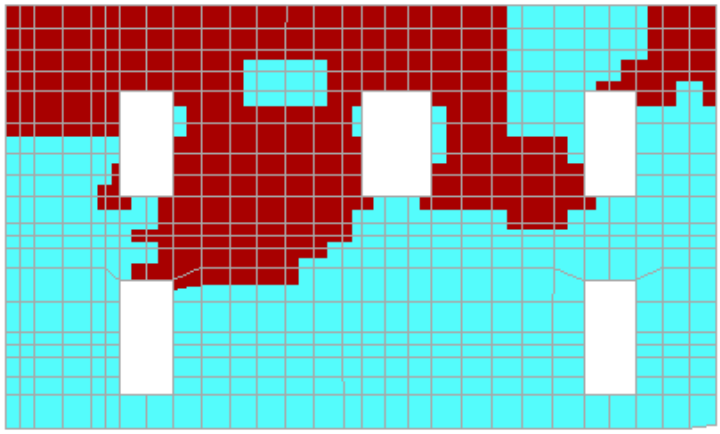	
Joints = 558 Failed = 203 Failure Percentage = 36.38%		

8.4 Failure rates & Statistical elaboration of the results

For the statistical analysis of data and in order to draw conclusions concerning the type and size of the failure of the wall structure, is taken the overall rate of failure for the 15 walls of the building for different tensile strength and four ground accelerations.

f_{wt} / PGA	*0.16g*	*0.24g*	*0.36g*	*0.40g*
K50	32.68	44.23	55.79	67.34
K100	25.87	35.08	44.29	53.5
K150	16.29	26.80	37.31	47.82
K200	13.5	20.87	28.23	35.6
K250	10.43	16.47	22.51	28.55
K300	8.5	14.03	19.57	25.1
K350	6.89	11.96	17.03	22.1
K400	4.58	9.45	14.33	19.2
K450	3.89	8.41	12.93	17.45

Table 8.2: Total failure percentages for the building, for 9 mortars and 4 ground accelerations

Below are illustrated the results of the statistic analysis for the two distributions and all ground accelerations.

Normal distribution

- **Ground acceleration PGA = 0.16g**

Tensile Strength fwt	*Failure Rate (%)*
50	32.68
100	25.87
150	16.29
200	13.5
250	10.43
300	8.5
350	6.89
400	4.58
450	3.89
Total elements	9
Mean value	13.63
Standard deviation	9.87

x	*f(x)*	*F(x)*
0	0.01557982	0.08361136
5	0.02759317	0.19096452
10	0.03779880	0.35661856
15	0.04004903	0.55540272
20	0.03282037	0.74091177
25	0.02080331	0.87554365
30	0.01019903	0.95152565
35	0.00386743	0.98486981
40	0.00113429	0.99624679
45	0.00025731	0.99926448
50	0.00004515	0.99988662
55	0.00000613	0.99998630
60	0.00000064	0.99999870
65	0.00000005	0.99999990
70	0.00000000	0.99999999
75	0.00000000	1.00000000
80	0.00000000	1.00000000
85	0.00000000	1.00000000
90	0.00000000	1.00000000
95	0.00000000	1.00000000
100	0.00000000	1.00000000

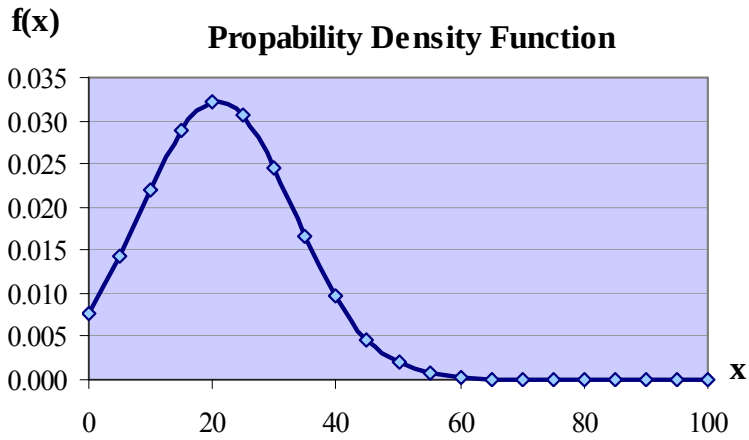

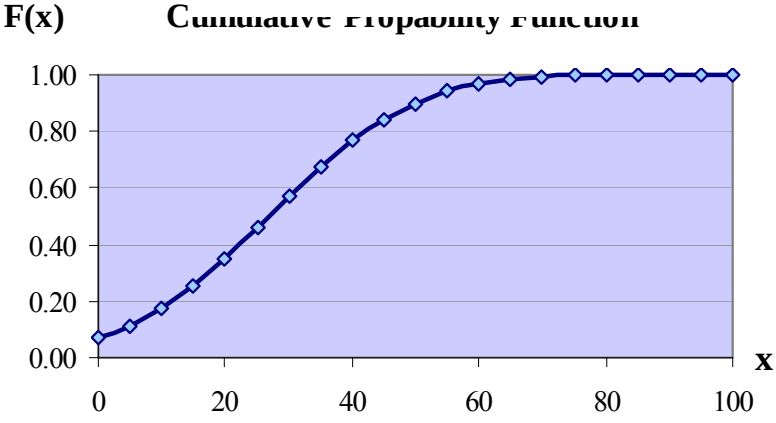

- **Ground acceleration PGA = 0.24g**

Tensile strength fwt	*Failure Rate(%)*
50	44.23
100	35.08
150	26.80
200	20.87
250	16.47
300	14.03
350	11.96
400	9.45
450	8.41
Total elements	9
Mean value	20.81
Standard deviation	12.32

x	*f(x)*	*F(x)*
0	0.00777225	0.04556516
5	0.01420968	0.09964534
10	0.02203299	0.19005738
15	0.02897435	0.31853667
20	0.03231509	0.47372691
25	0.03056670	0.63306633
30	0.02452127	0.77212878
35	0.01668356	0.87529137
40	0.00962689	0.94034261
45	0.00471123	0.97520864
50	0.00195539	0.99109239
55	0.00068831	0.99724269
60	0.00020549	0.99926671
65	0.00005203	0.99983282
70	0.00001117	0.99996738
75	0.00000203	0.99999456
80	0.00000031	0.99999923
85	0.00000004	0.99999991
90	0.00000000	0.99999999
95	0.00000000	1.00000000
100	0.00000000	1.00000000

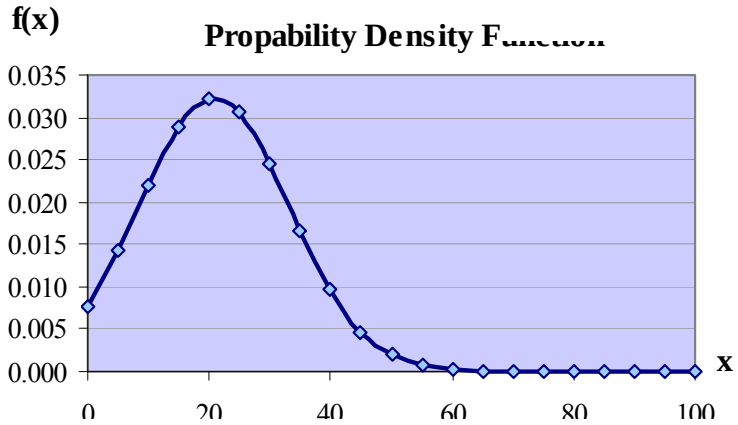

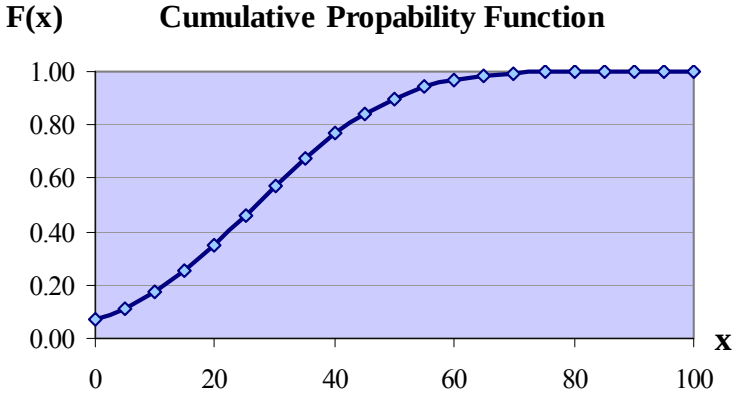

- **Ground acceleration PGA = 0.36g**

Tensile strength fwt	*Failure Rate(%)*
50	55.79
100	44.29
150	37.31
200	28.23
250	22.51
300	19.57
350	17.03
400	14.33
450	12.93
Total elements	9
Mean value	28.00
Standard deviation	14.83

x	*f(x)*	*F(x)*
0	0.00452817	0.02953248
5	0.00808385	0.06049923
10	0.01288124	0.11247261
15	0.01832068	0.19041454
20	0.02325788	0.29485497
25	0.02635378	0.41990242
30	0.02665386	0.55368227
35	0.02406146	0.68156639
40	0.01938778	0.79079901
45	0.01394372	0.87416656
50	0.00895104	0.93101901
55	0.00512877	0.96566134
60	0.00262299	0.98452247
65	0.00119736	0.99369794
70	0.00048786	0.99768621
75	0.00017743	0.99923515
80	0.00005759	0.99977264
85	0.00001669	0.99993928
90	0.00000432	0.99998545
95	0.00000100	0.99999687
100	0.00000021	0.99999940

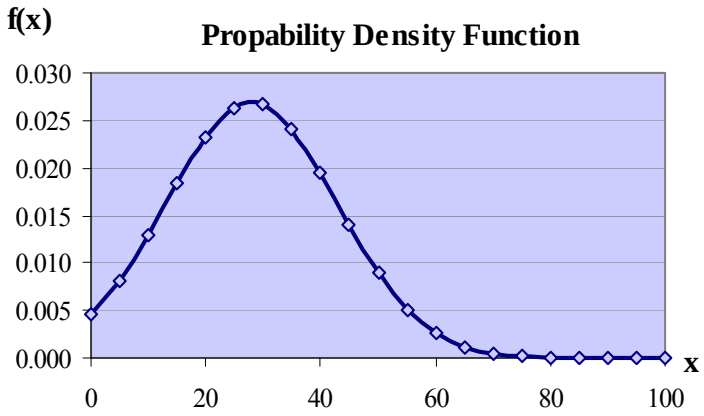

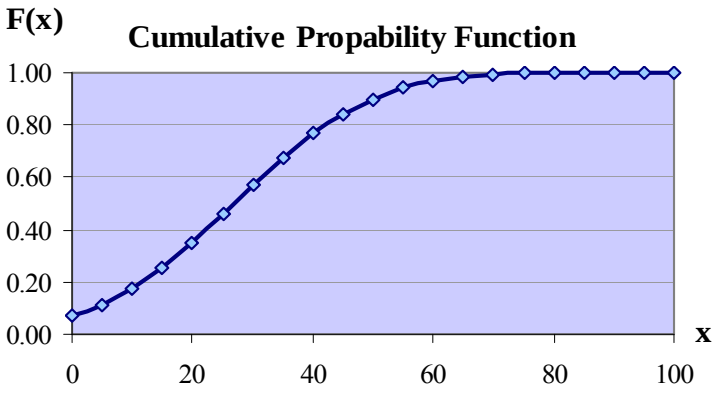

- **Ground acceleration PGA = 0.40g**

Tensile strength fwt	*Failure Rate(%)*
50	67.34
100	53.5
150	47.82
200	35.6
250	28.55
300	25.1
350	22.1
400	19.2
450	17.45
Total elements	9
Mean value	35.18
Standard deviation	17.38

x	*f(x)*	*F(x)*
0	0.00295693	0.02145655
5	0.00507964	0.04120693
10	0.00803297	0.07364884
15	0.01169422	0.12273212
20	0.01567175	0.19113238
25	0.01933370	0.27892934
30	0.02195655	0.38272981
35	0.02295432	0.49576604
40	0.02209104	0.60914557
45	0.01957129	0.71389467
50	0.01596151	0.80303298
55	0.01198340	0.87290072
60	0.00828204	0.92334207
65	0.00526922	0.95688443
70	0.00308607	0.97742898
75	0.00166386	0.98901929
80	0.00082581	0.99504194
85	0.00037731	0.99792446
90	0.00015869	0.99919517
95	0.00006144	0.99971113
100	0.00002190	0.99990409

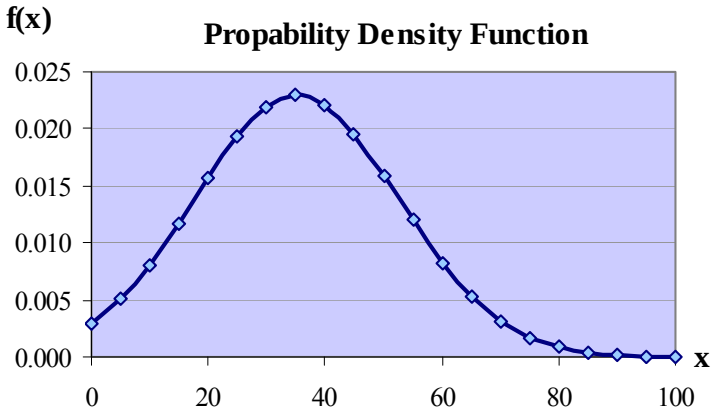

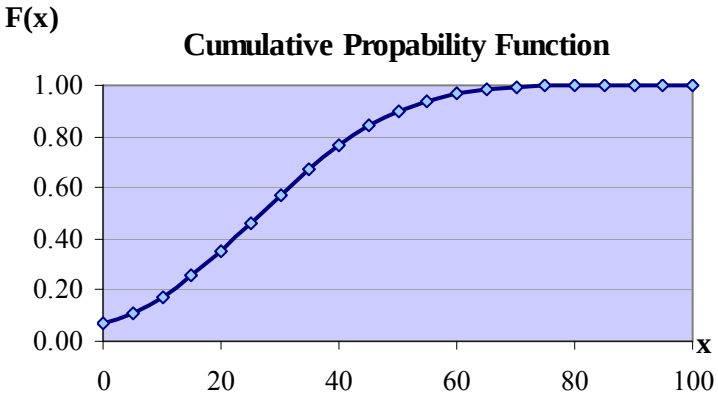

Lognormal distribution

- **Ground acceleration PGA = 0.16g**

Tensile strength fwt	*Failure Rate(%)*
50	3.49
100	3.25
150	2.79
200	2.60
250	2.34
300	2.14
350	1.93
400	1.52
450	1.36
Total elements	9
Mean value	2.38
Standard deviation	0.73

x	*f(x)*	*F(x)*
0.00000000	0.00000000	0.00000000
1.60943791	0.06251863	0.14484333
2.30258509	0.05443898	0.45720649
2.70805020	0.03300241	0.67329192
2.99573227	0.01917597	0.80062654
3.21887582	0.01130419	0.87495336
3.40119738	0.00684654	0.91929674
3.55534806	0.00426712	0.94651103
3.68887945	0.00273244	0.96368881
3.80666249	0.00179345	0.97481758
3.91202301	0.00120365	0.98219961
4.00733319	0.00082415	0.98720144
4.09434456	0.00057457	0.99065588
4.17438727	0.00040716	0.99308309
4.24849524	0.00029282	0.99481531
4.31748811	0.00021344	0.99606916
4.38202663	0.00015750	0.99698855
4.44265126	0.00011755	0.99767070
4.49980967	0.00008864	0.99818235
4.55387689	0.00006749	0.99856998
4.60517019	0.00005184	0.99886639

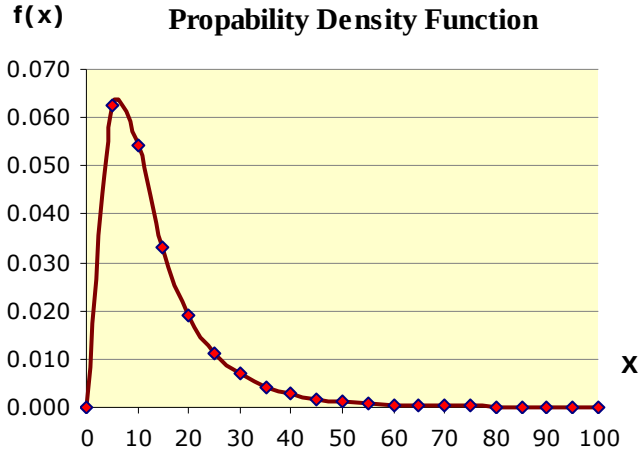

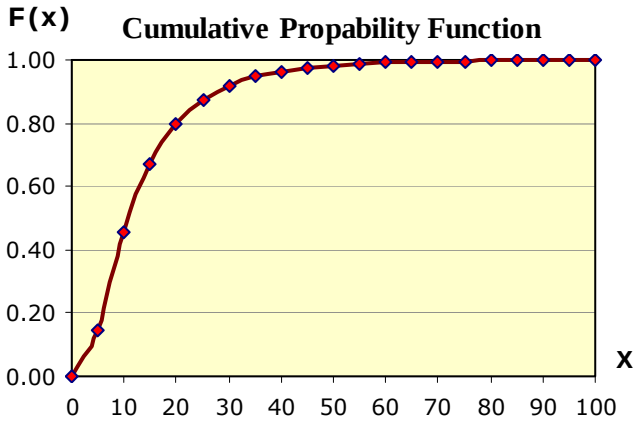

- **Ground acceleration PGA = 0.24g**

Tensile strength fwt	*Failure Rate(%)*
50	3.79
100	3.56
150	3.29
200	3.04
250	2.80
300	2.64
350	2.48
400	2.25
450	2.13
Total elements	9
Mean value	2.89
Standard deviation	0.58

x	*f(x)*	*F(x)*
0.00000000	0.00000000	0.00000000
1.60943791	0.01197334	0.01348429
2.30258509	0.04146999	0.15602829
2.70805020	0.04394518	0.37891054
2.99573227	0.03394434	0.57540027
3.21887582	0.02341343	0.71796057
3.40119738	0.01546943	0.81399448
3.55534806	0.01008040	0.87693864
3.68887945	0.00656622	0.91791700
3.80666249	0.00430338	0.94467580
3.91202301	0.00284662	0.96228573
4.00733319	0.00190327	0.97399187
4.09434456	0.00128692	0.98185971
4.17438727	0.00088003	0.98720782
4.24849524	0.00060846	0.99088405
4.31748811	0.00042520	0.99343866
4.38202663	0.00030018	0.99523251
4.44265126	0.00021399	0.99650479
4.49980967	0.00015396	0.99741576
4.55387689	0.00011175	0.99807396
4.60517019	0.00008179	0.99855360

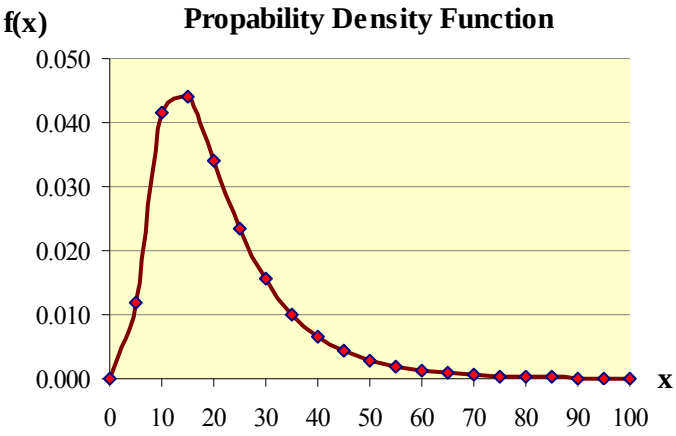

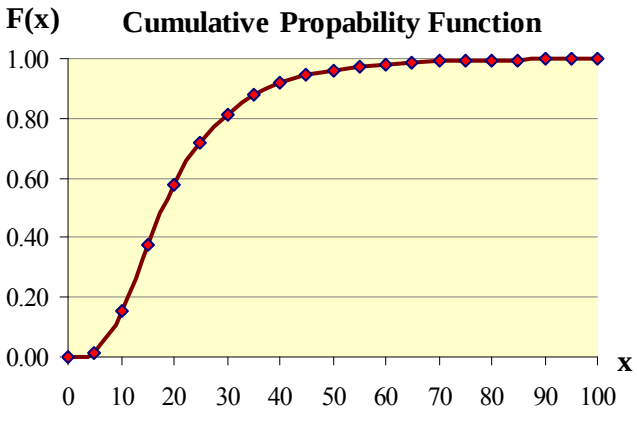

- **Ground acceleration PGA = 0.36g**

Tensile strength fwt	*Failure Rate(%)*
50	4.02
100	3.79
150	3.62
200	3.34
250	3.11
300	2.97
350	2.83
400	2.66
450	2.56
Total elements	9
Mean value	3.21
Standard deviation	0.51

x	*f(x)*	*F(x)*
0.00000000	0.00000000	0.00000000
1.60943791	0.00118502	0.00089546
2.30258509	0.01613699	0.03811831
2.70805020	0.03194109	0.16273083
2.99573227	0.03552268	0.33613800
3.21887582	0.03107603	0.50460874
3.40119738	0.02421502	0.64305233
3.55534806	0.01777320	0.74756374
3.68887945	0.01264079	0.82301062
3.80666249	0.00884824	0.87621781
3.91202301	0.00615057	0.91331873
4.00733319	0.00426862	0.93908019
4.09434456	0.00296760	0.95696978
4.17438727	0.00207088	0.96942720
4.24849524	0.00145238	0.97814017
4.31748811	0.00102450	0.98426720
4.38202663	0.00072716	0.98860167
4.44265126	0.00051943	0.99168740
4.49980967	0.00037345	0.99389837
4.55387689	0.00027023	0.99549282
4.60517019	0.00019678	0.99665006

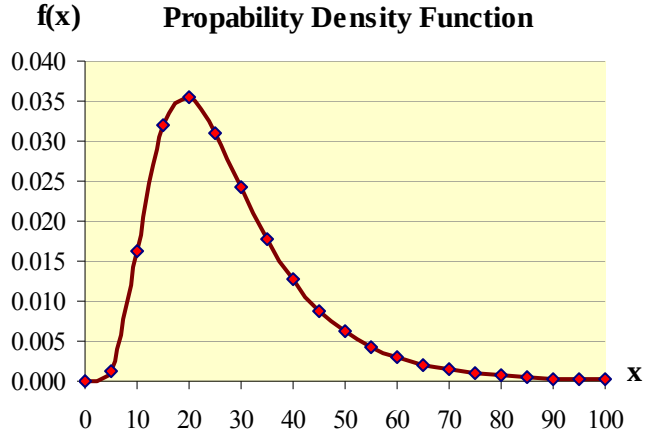

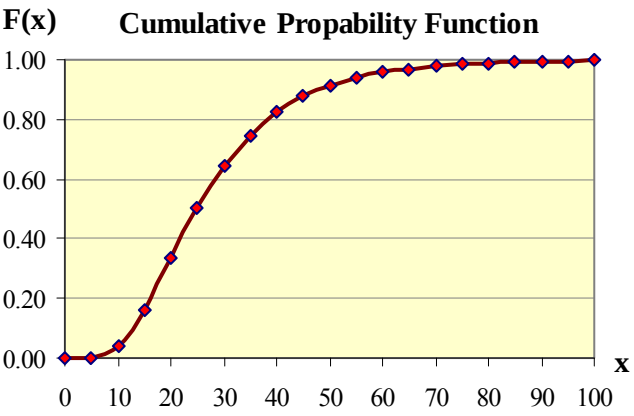

- **Ground acceleration PGA = 0.40g**

Tensile strength fwt	*Failure Rate(%)*
50	4.21
100	3.98
150	3.87
200	3.57
250	3.35
300	3.22
350	3.10
400	2.95
450	2.86
Total elements	9
Mean value	3.46
Standard deviation	0.48

x	*f(x)*	*F(x)*
0.00000000	0.00000000	0.00000000
1.60943791	0.00009494	0.00005537
2.30258509	0.00451379	0.00785648
2.70805020	0.01629784	0.05853850
2.99573227	0.02619319	0.16721121
3.21887582	0.02948915	0.30911469
3.40119738	0.02763412	0.45347356
3.55534806	0.02334980	0.58146362
3.68887945	0.01855196	0.68617133
3.80666249	0.01419511	0.76775214
3.91202301	0.01061206	0.82942864
4.00733319	0.00782223	0.87520118
4.09434456	0.00571894	0.90879660
4.17438727	0.00416373	0.93330338
4.24849524	0.00302698	0.95113001
4.31748811	0.00220145	0.96409052
4.38202663	0.00160378	0.97352313
4.44265126	0.00117142	0.98040293
4.49980967	0.00085838	0.98543546
4.55387689	0.00063129	0.98912943
4.60517019	0.00046611	0.99185118

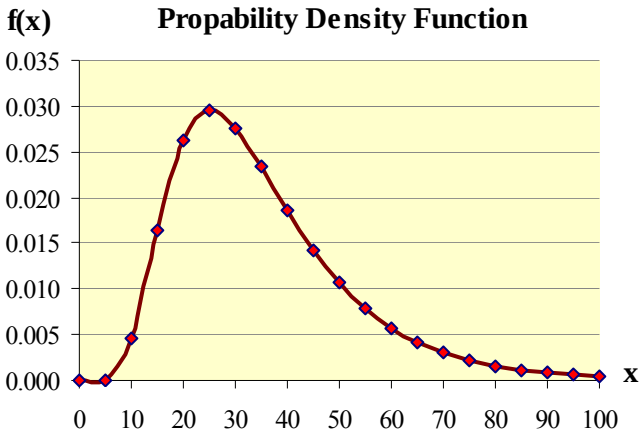

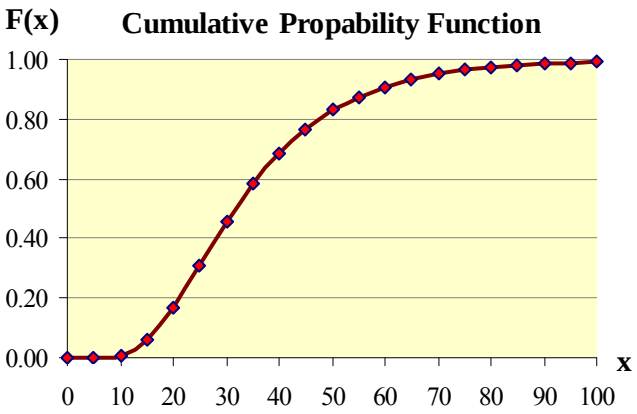

8.5 Export of fragility curves

After the statistical processing and the analysis of the failure rates of the wall structure and having set the levels of damage in a previous chapter, we can draw the fragility curves.

Normal distribution

- **Graduation of failures, type a**

(%) PGA	0	0.16	0.24	0.36	0.40
Small	0	0.8552	0.9998	0.9991	0.9999
Medium	0	0.3267	0.9312	0.8373	0.9415
Large	0	0.1250	0.7018	0.4954	0.6909

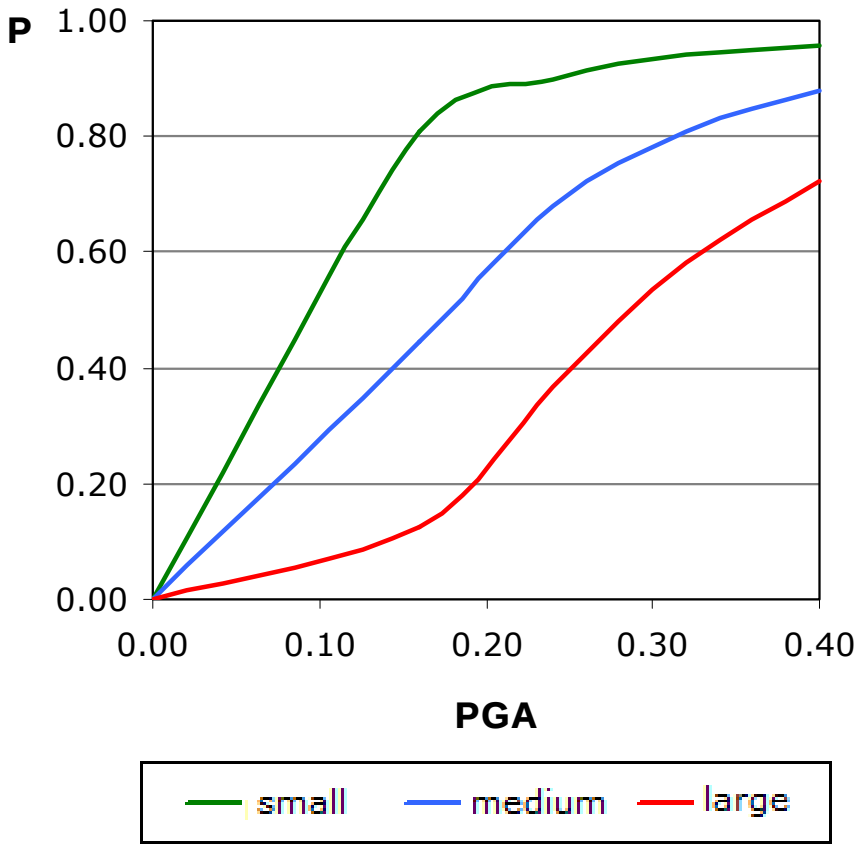

➢ **Graduation of failures, type b**

(%) PGA	0	0.16	0.24	0.36	0.40
Small	0	0.6434	0.8099	0.8875	0.9264
Medium	0	0.2591	0.5263	0.7051	0.8089
Large	0	0.0485	0.2279	0.4463	0.6173

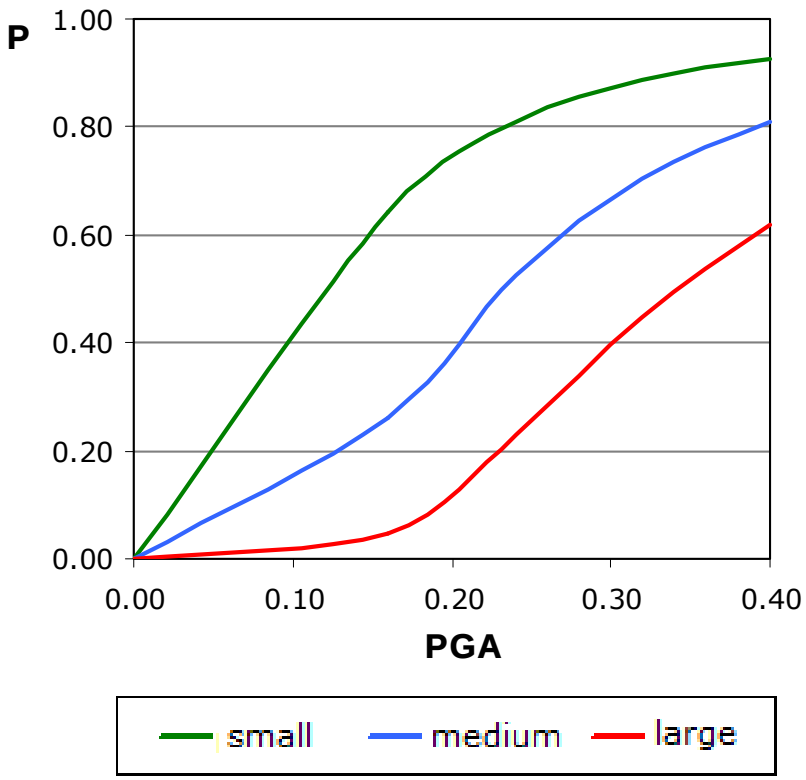

- **Graduation of failures, type c**

(%) PGA	0	0.16	0.24	0.36	0.40
Small	0	0.4446	0.6815	0.8096	0.8773
Medium	0	0.0151	0.1247	0.3184	0.5042
Large	0	0.0007	0.0248	0.1258	0.2861

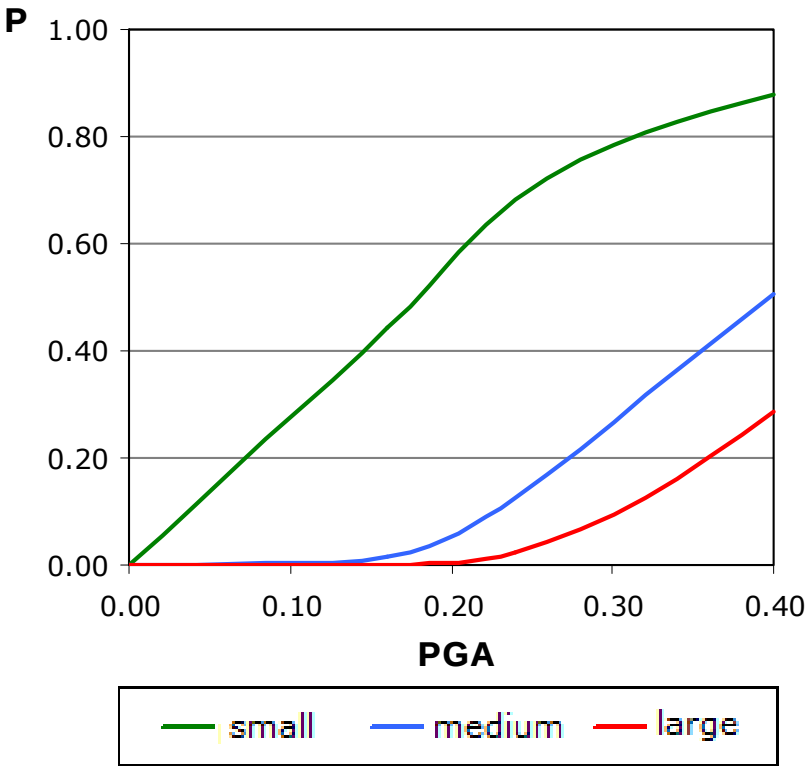

Lognormal distribution

- **Graduation of failures, type a**

(%) PGA	0	0.16	0.24	0.36	0.40
Small	0	0.9751	0.9967	0.9999	1.0000
Medium	0	0.6896	0.8360	0.9598	0.9996
Large	0	0.4257	0.5680	0.7772	0.9763

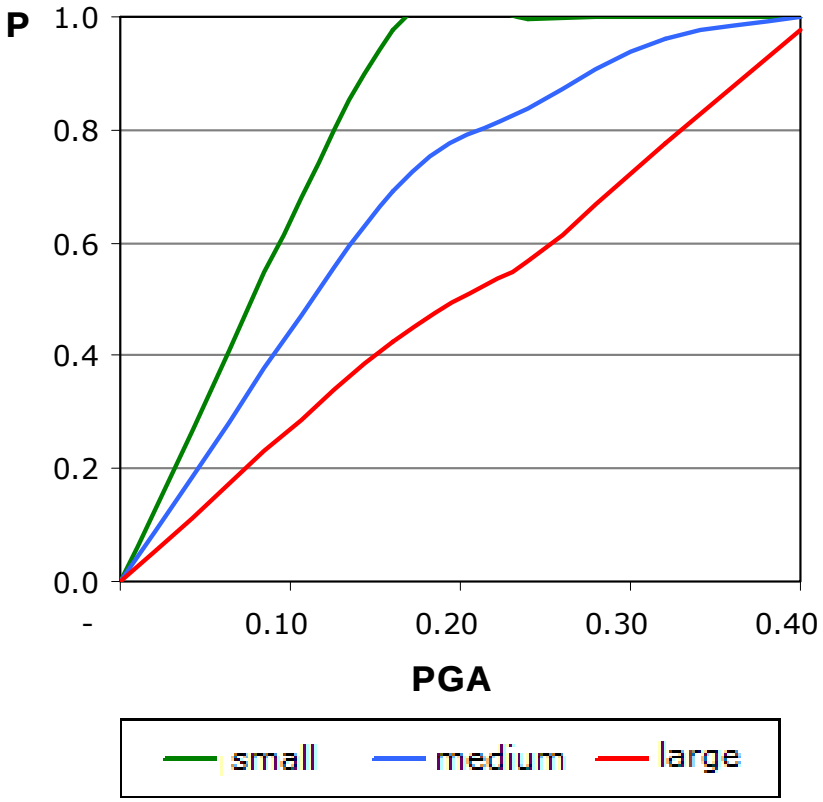

- **Graduation of failures, type b**

(%) PGA	0	0.16	0.24	0.36	0.40
Small	0	0.8499	0.9472	0.9943	1.0000
Medium	0	0.5440	0.8200	0.9300	0.9951
Large	0	0.3333	0.4535	0.6595	0.9326

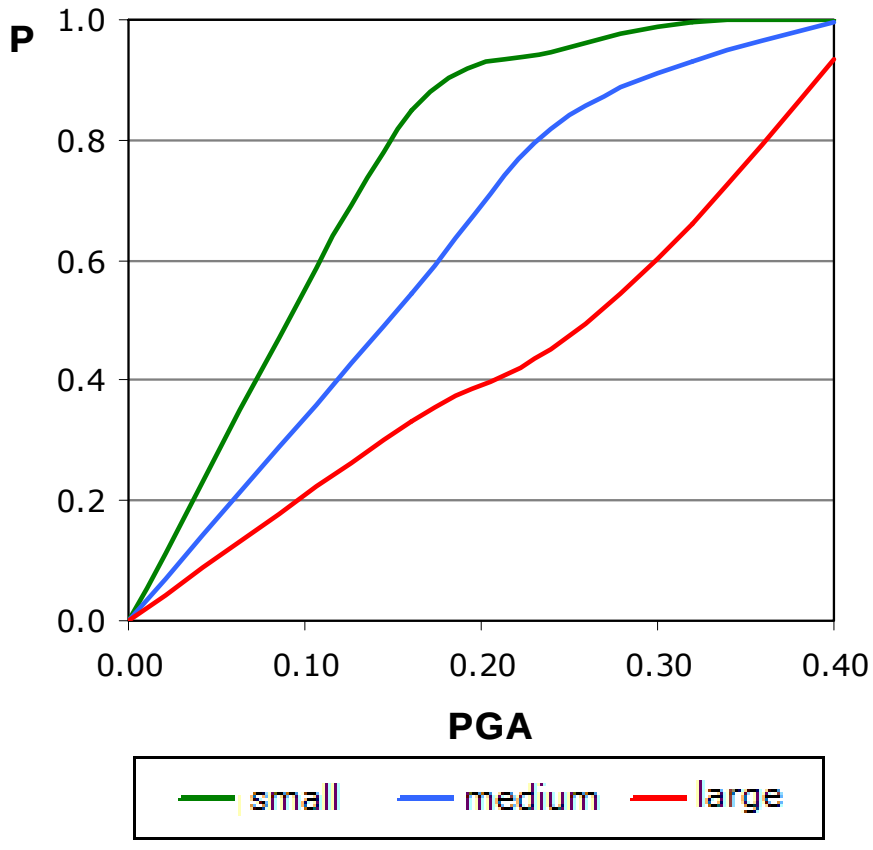

➢ **Graduation of failures, type c**

(%) PGA	0	0.16	0.24	0.36	0.40
Small	0	0.6896	0.8200	0.9300	0.9951
Medium	0	0.2622	0.4535	0.6595	0.9326
Large	0	0.1655	0.2000	0.3000	0.5514

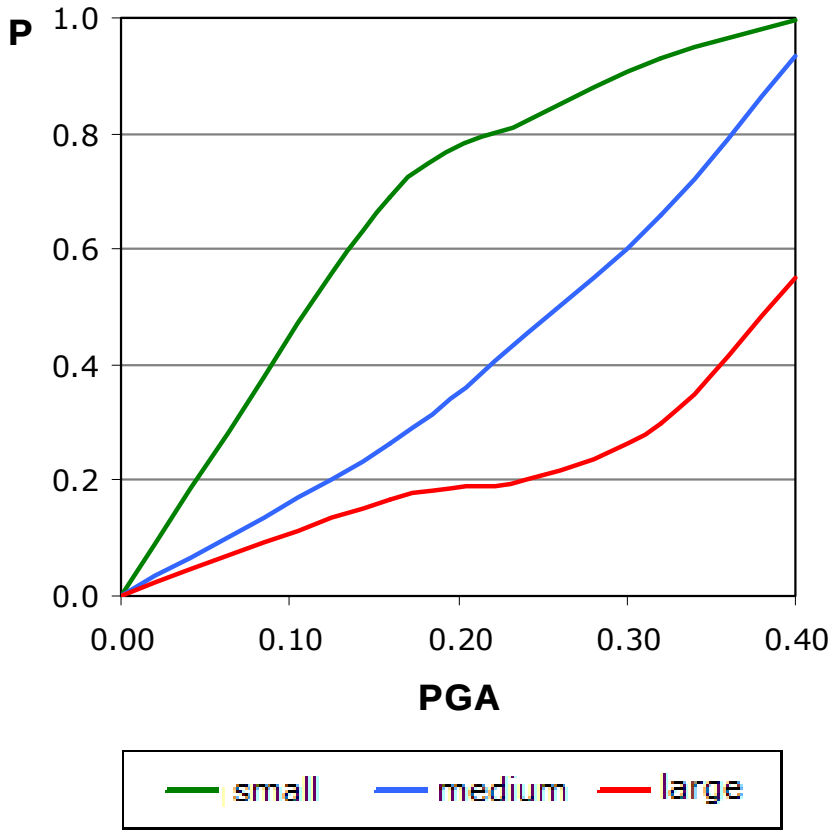

8.6 Comparison between the three failure levels of the two distributions

- ***Small failure***

Normal distribution	Lognormal distribution
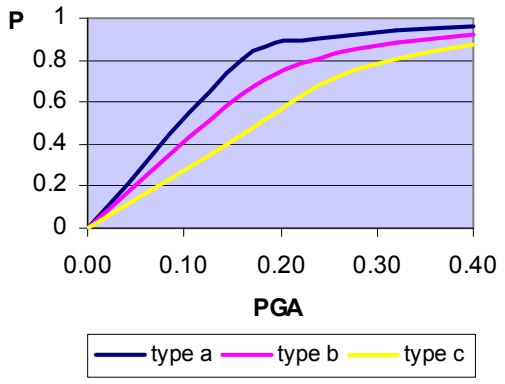	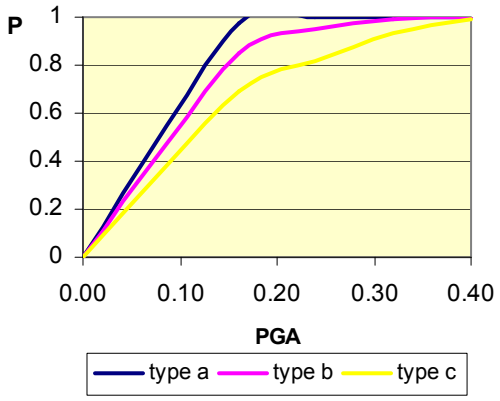

- ***Medium failure***

Normal distribution	Lognormal distribution
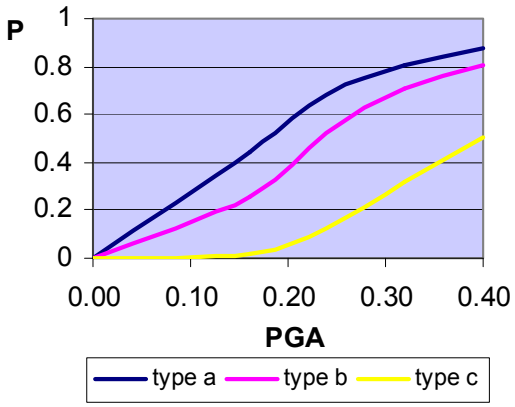	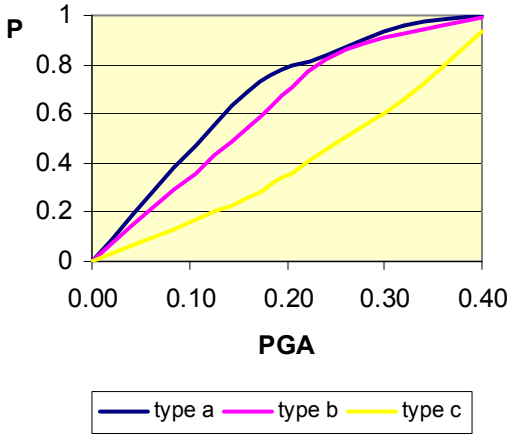

- ***Large failure***

Normal distribution	Lognormal distribution
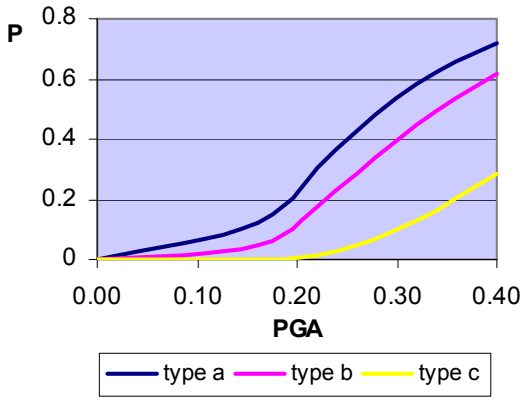	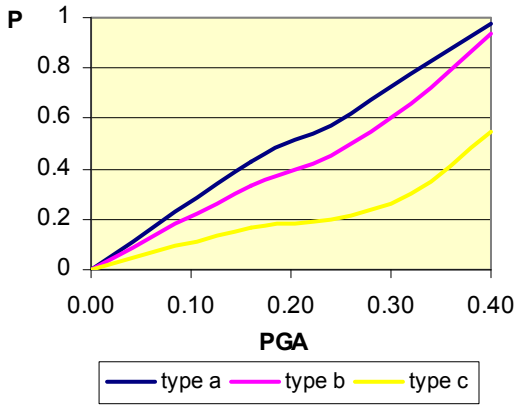

CHAPTER 9

REPAIR AND REINFORCEMENT OF EXISTING MASONRY (Reinforcement C)

9.1 Pointing and horizontal prestressing (Reinforcement C)

Prestressed masonry is not a widely used and well known technique of strengthening compared to the previous reinforcements (A and B); this happens because there are still uncertainties about the interaction between masonry and materials that are used nowadays for prestressing; therefore engineers feel safer with other ways of strengthening. However, this method concentrates important advantages. Firstly it can be applied to the structure very fast and that makes it a high speed and low cost technique, moreover it is reversible since it does not cause great interferences to the structure and that is the reason that is qualified as an excellent reinforcement method for buildings with cultural value. On the other hand prestressing is not suited for every structure but is a function of the layout of openings and piers, as well as the size of the wall. Small and thin wall areas are not suited to prestressing due to the high compression introduced by the tendons, consequently the alignment of openings must be considered so as to ensure the smooth flow of stresses along the lintels or piers. For prestressing strengthening can be used both bar tendons or strands. Bar tendons have slight advantage in most of the cases because they are less expensive, more available and come in a variety of lengths while strands offer the best corrosion protection as they are covered with a plastic sheath. Finally, regarding reinforced masonry, larger tendons at a wider spacing tend to be more economical solution but they cause locally high stresses and difficulties during installation.

9.2Stages of works and modeling of reinforcement C

The tendons can be installed either vertically or horizontally depending on the format of the structure and the needs of reinforcement. In this case, the alignment of the openings is good enough (figure 8.9) and the tendons can be installed

continuously without any offsets that would give an additional expense. Therefore two tendons are installed horizontally along the lintels, in both sides (inside and outside) of the wall in a way that the resultant force of the two tendons passes from the centroid of the wall (figure 8.8).

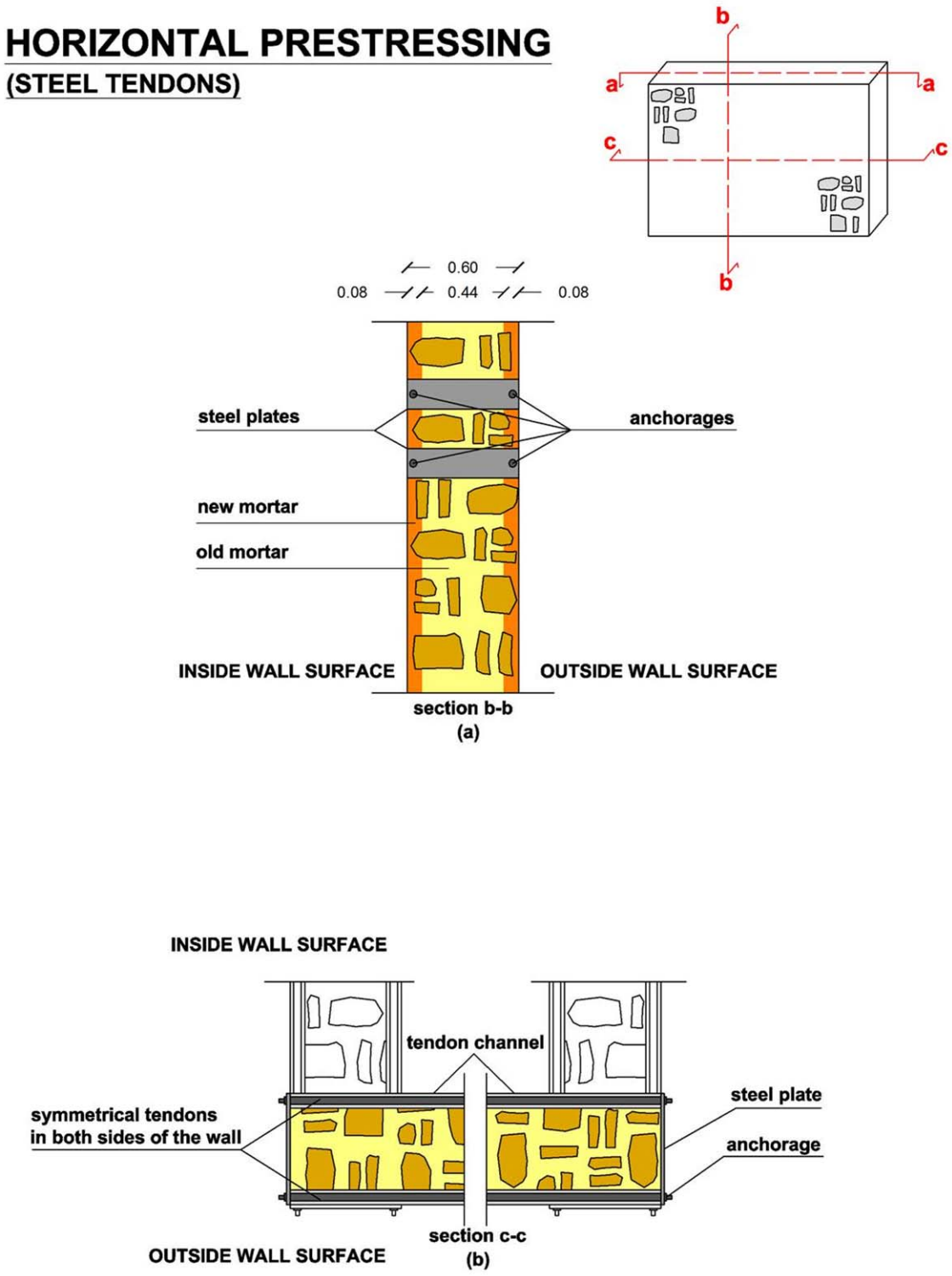

Figure 7.8 Horizontal prestressing along the lintels

For this building, steel tendon bars were chosen as reinforcement. The tendons

are placed in channels that have been made in the wall and they are covered with shotcrete. The loads are distributed to the structure by bearing plates which are connected at the edges of the tendons. The plate distributes the tension created by its anchor point and stabilizes the connected wall. Since the building is made by rubble masonry the bearing plates can be placed in recesses which can be filled with mortar or covered with stones, for fully restoration of the facades.

Prestressing modeled as the horizontal stress on the lintels that corresponds to the pressure of the tendons. This force, for each lintel, was calculated equals to the 10% of the wall compressive strength after pointing (where: F_{wc}=4340MPa) multiplied by the vertical cross section area of the lintel. The force of the tendons shared to the joints match to each lintel as shown in figure 8.9 below.

The axial prestressing force depends on the vertical cross section area of the lintel. At this point we assume an average cross section of a lintel so as to keep constant the size of the tendons. We remind that the walls width is equal to 0.60m, therefore is assumed only the height of the lintel.

A= lintel height × lintel width= 0.50m×0.60m=0.30m^2

Horizontal Stress = 0.1× 4.34MPa= 0.434Mpa

Cross section area of the lintel: A= 0.30m^2=300000mm^2

Axial force: N= 0.434×300000= 130200N= 130.2kN

Since we have a pair of tendons (inside and outside of wall surface), each of them needs to carry half of the axial force N_T= 130.2/2= 65.1kN.

Therefore, if tendons yield strength: f_y= 355MPa, then:

$$N_T = \frac{A_s \times f_y}{\gamma_m} \Rightarrow A_S = \frac{N \times \gamma_m}{f_y} (1) \qquad \Rightarrow A_S = 183 mm^2$$

Where:

N_T: Axial prestressing force

A_s: Tendons cross section area

f_y: Yield strength

γ_m: Safety factor (is taken equal to 1)

Finally the tendos diameter is: D= $(4\times N_T/\pi)^{1/2}$= 15.26mm= 1.53cm

The reinforcement is decided to be: 1.60cm tendons diameter every 0.50m.

Consequently whenever the cross section is greater than 0.30m^2 they would be needed two pairs of tendons instead of one.

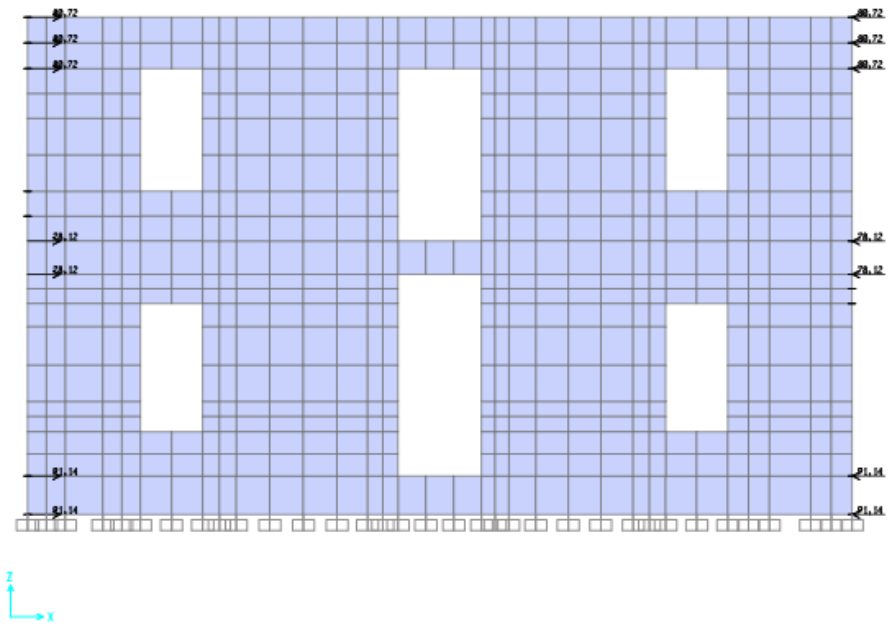

Figure 7.9 Modeling of horizontal prestressing along the lintels

Fundamental mode (transferational) of the building T=0.096sec, participating mass ratio 24%, in 'Y' direction.

TABLE: Modal Participating Mass Ratios						
OutputCase	**StepType**	**StepNum**	**Period**	**UX**	**UY**	**RZ**
Text	Text	Unitless	Sec	Unitless	Unitless	Unitless
MODAL	Mode	1	0,184285	0,05126	6,26E-06	0,00935
MODAL	Mode	2	0,128552	0,00414	0,00051	0,00804
MODAL	Mode	3	0,127868	0,01091	0,00187	0,0036
MODAL	Mode	4	0,126968	1,07E-05	0,00435	0,00296
MODAL	Mode	5	0,123536	0,0749	0,00522	0,00246
MODAL	Mode	6	0,0959	0,0022	0,24162	0,0364
MODAL	Mode	7	0,092865	0,01821	0,08761	0,14805
MODAL	Mode	8	0,090788	0,05627	0,00075	0,03551
MODAL	Mode	9	0,090424	0,03113	0,02218	0,02213
MODAL	Mode	10	0,088246	0,01373	0,01361	0,00131

Table 7.3 First ten modes after pointing and horizontal prestressing along the lintels

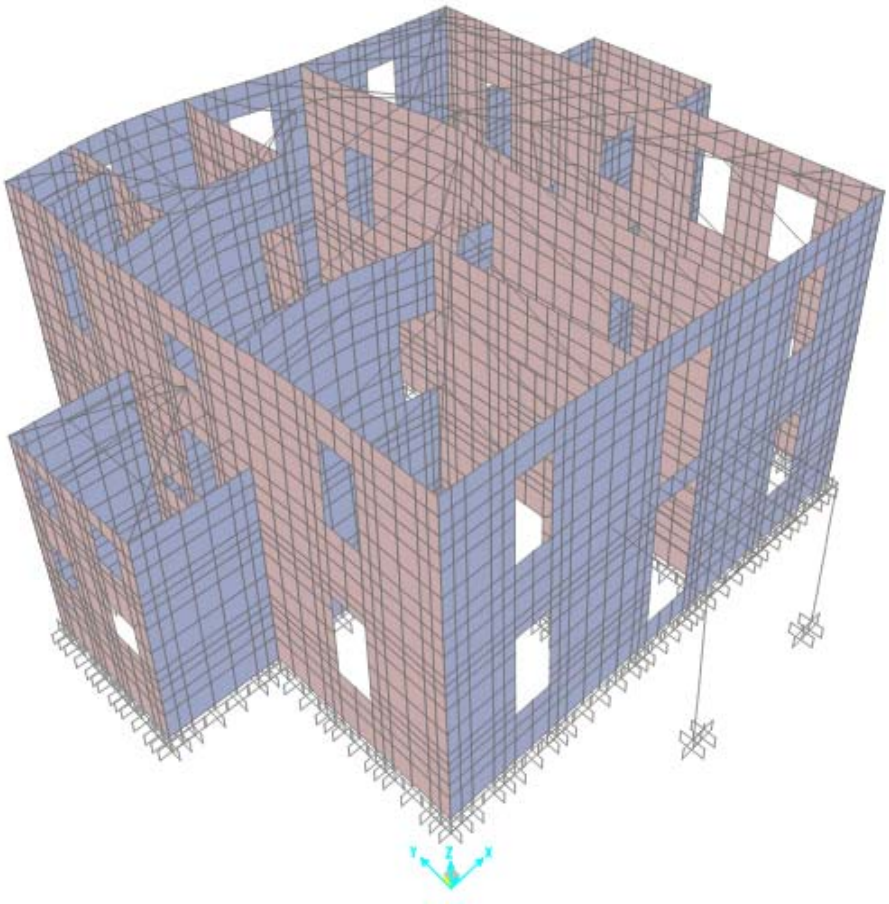

Figure 7.10 fundamental mode T= 0.096sec

9.3 Walls failure results from software FAILURE

As in chapter 9 and 10, In this chapter are illustrated indicatively, the failures of four walls (w1,w8,WD,wE) of reinforcement C, for the most severe loading combination, for PGA= 0.16 and 0.40 and for tensile strength 50kPa, 250kPa, 450kPa.

Failure		
wall : **1_2topmax** **Load Cases :** **0.16g**		Failure under biaxial Tension/Tension
		Failure under biaxial Tension/ Compression
		Failure under biaxial Compression /Tension
		Failure under biaxial Compression/ Compression
		NON Failure
fwt = 50 kPa	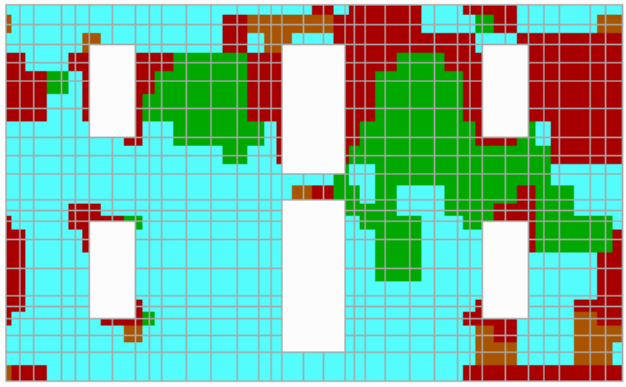	
Joints = 640 Failed = 277 Failure Percentage = 43.28%		
fwt = 250 kPa	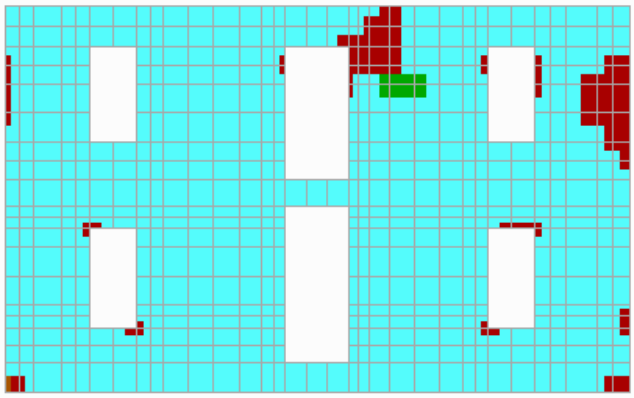	
Joints = 640 Failed = 43 Failure Percentage = 6.72%		
f_{wt} = 450 kPa	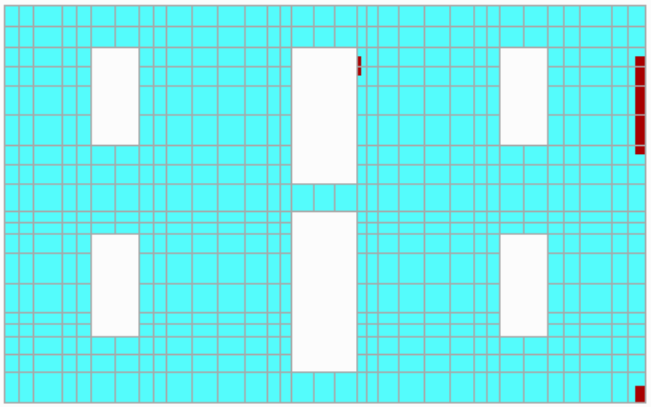	
Joints = 640 Failed = 6 Failure Percentage = 0.94%		

Failure

wall : **1_2topmax** **Load Cases :** **0.40g**		Failure under biaxial Tension/Tension
		Failure under biaxial Tension/ Compression
		Failure under biaxial Compression /Tension
		Failure under biaxial Compression/ Compression
		NON Failure
fwt = 50 kPa	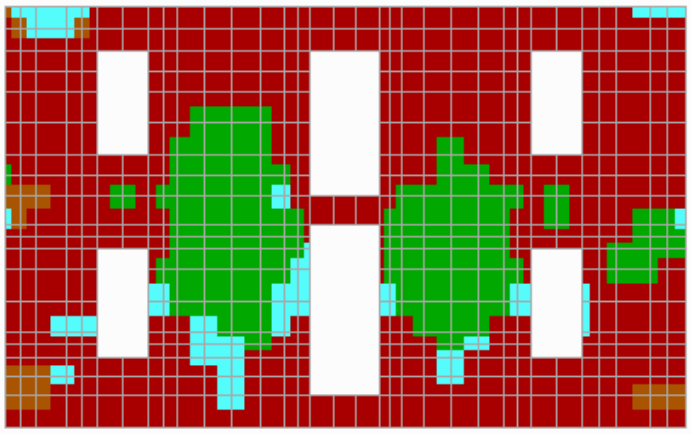	
Joints = 640 Failed = 599 Failure Percentage = 93.59%		
fwt = 250 kPa	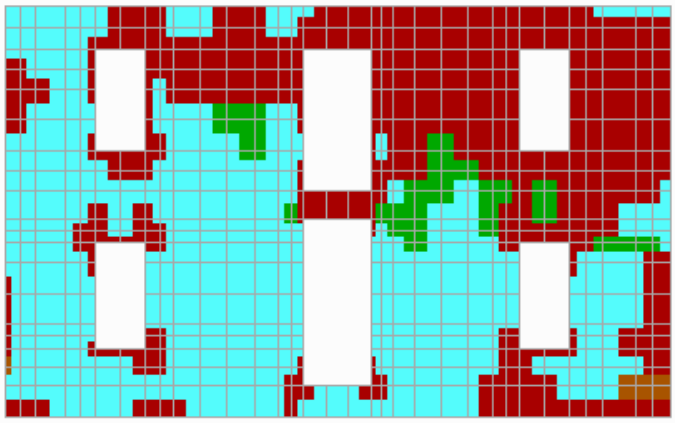	
Joints = 640 Failed = 315 Failure Percentage = 49.22%		
f_{wt} = 450 kPa	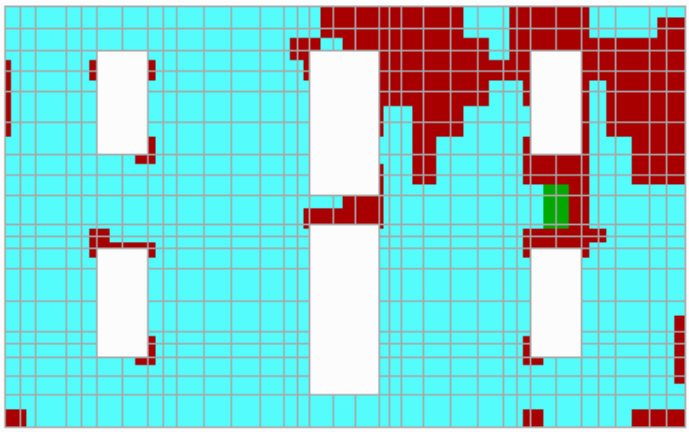	
Joints = 640 Failed = 134 Failure Percentage = 20.94%		

Failure		
wall : **8_2topmax** **Load Cases :** **0.16g**		Failure under biaxial Tension/Tension
		Failure under biaxial Tension/ Compression
		Failure under biaxial Compression /Tension
		Failure under biaxial Compression/ Compression
		NON Failure
fwt = 50 kPa Joints = 990 Failed = 223 Failure Percentage = 22.53%	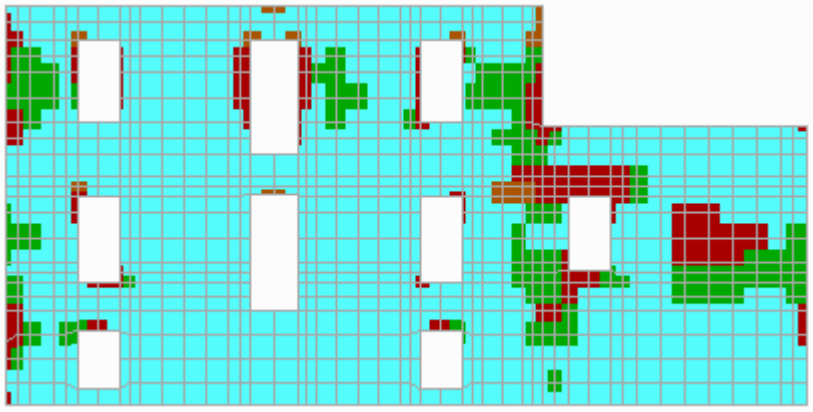	
fwt = 250 kPa Joints = 990 Failed = 17 Failure Percentage = 1.72%	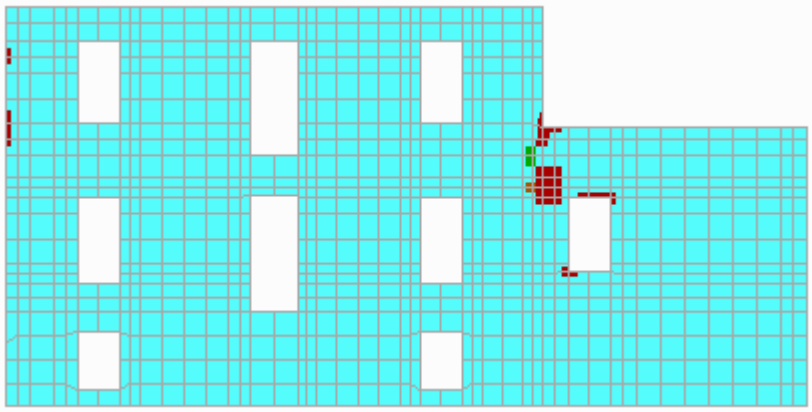	
f_{wt} = 450 kPa Joints = 990 Failed = 4 Failure Percentage = 0.40%	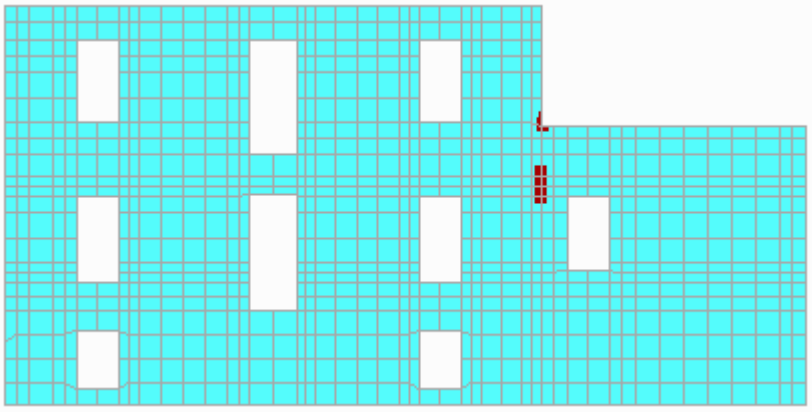	

Failure	
wall : **8_2topmax** **Load Cases :** **0.40g**	Failure under biaxial Tension/Tension
	Failure under biaxial Tension/ Compression
	Failure under biaxial Compression /Tension
	Failure under biaxial Compression/ Compression
	NON Failure
fwt = 50 kPa	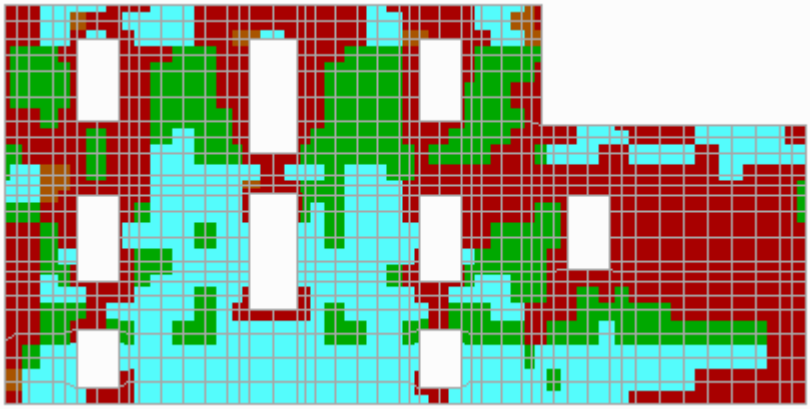
Joints = 990 Failed = 679 Failure Percentage = 68.59%	
fwt = 250 kPa	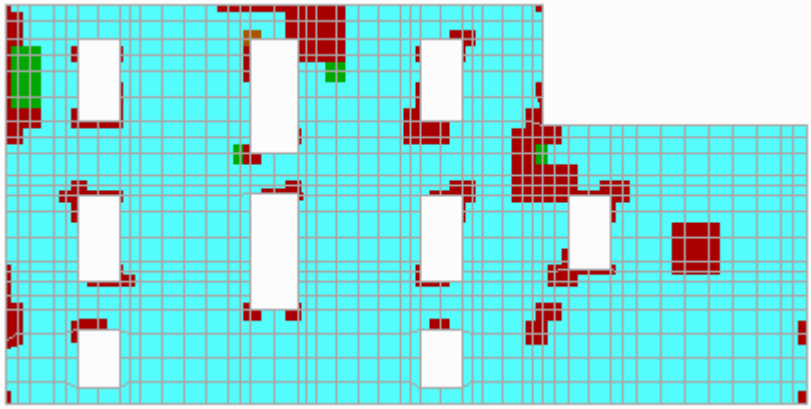
Joints = 990 Failed = 150 Failure Percentage = 15.15%	
f_{wt} = 450 kPa	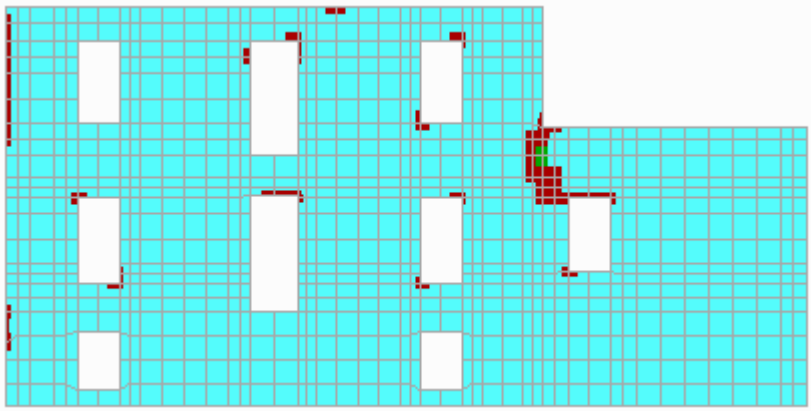
Joints = 990 Failed = 39 Failure Percentage = 3.94%	

Failure		
wall : **D_2topmax** **Load Cases :** **0.16g**		Failure under biaxial Tension/Tension
		Failure under biaxial Tension/ Compression
		Failure under biaxial Compression /Tension
		Failure under biaxial Compression/ Compression
		NON Failure
fwt = 50 kPa	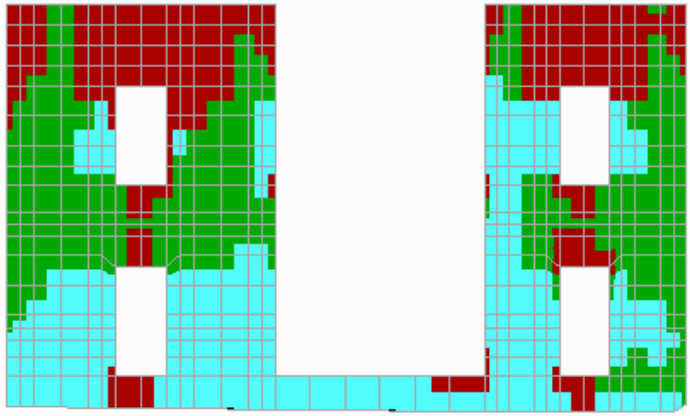	
Joints = 555 Failed = 337 Failure Percentage = 60.72%		
fwt = 250 kPa	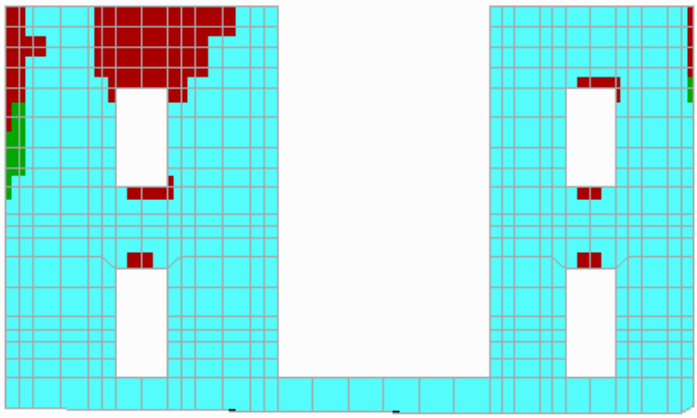	
Joints = 555 Failed = 60 Failure Percentage = 10.81%		
f_{wt} = 450 kPa	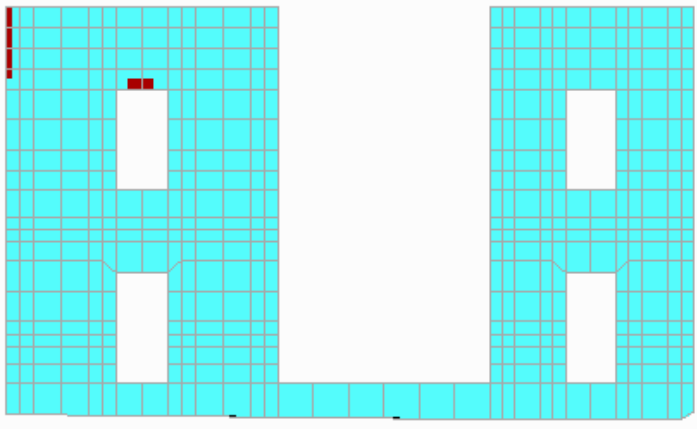	
Joints = 555 Failed = 5 Failure Percentage = 0.90%		

Failure		
wall : **D_2topmax** **Load Cases :** **0.40g**		Failure under biaxial Tension/Tension
		Failure under biaxial Tension/ Compression
		Failure under biaxial Compression /Tension
		Failure under biaxial Compression/ Compression
		NON Failure
fwt = 50 kPa	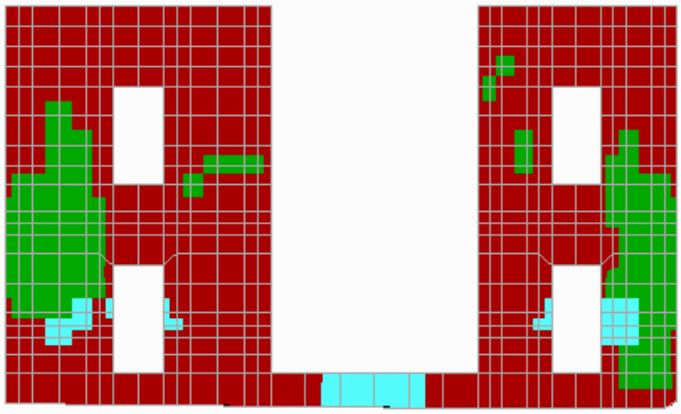	
Joints = 555 Failed = 528 Failure Percentage = 95.14%		
fwt = 250 kPa	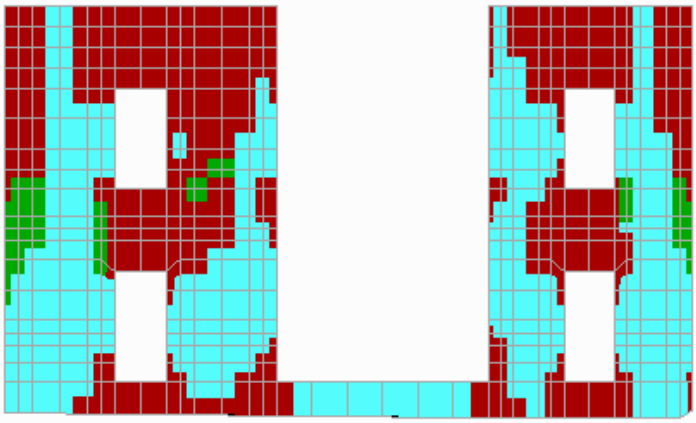	
Joints = 555 Failed = 298 Failure Percentage = 53.69%		
f_{wt} = 450 kPa	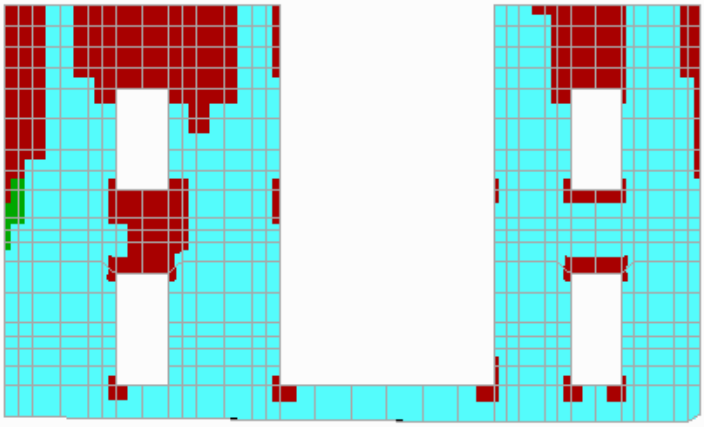	
Joints = 555 Failed = 138 Failure Percentage = 24.86%		

Failure

wall : **E_2topmax** **Load Cases :** **0.16g**		Failure under biaxial Tension/Tension
		Failure under biaxial Tension/ Compression
		Failure under biaxial Compression /Tension
		Failure under biaxial Compression/ Compression
		NON Failure
fwt = 50 kPa	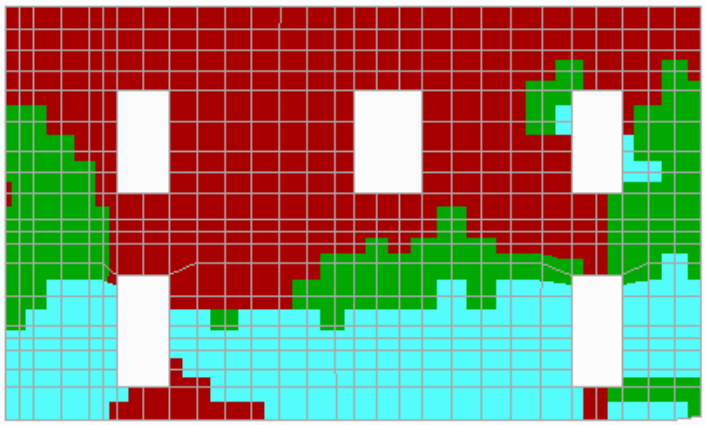	
Joints = 558 Failed = 396 Failure Percentage = 70.97%		
fwt = 250 kPa	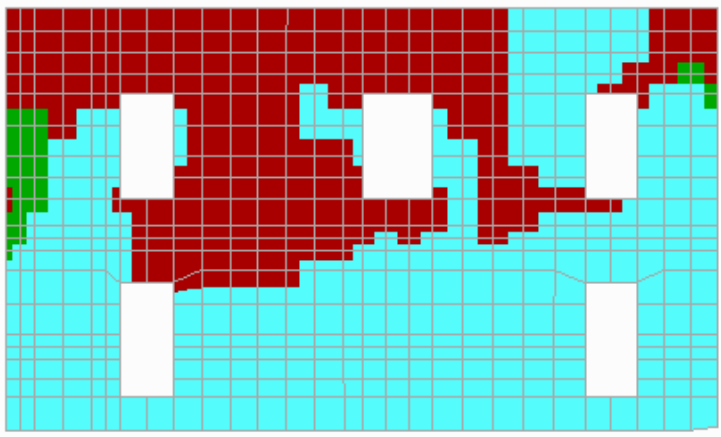	
Joints = 558 Failed = 218 Failure Percentage = 39.07%		
f_{wt} = 450 kPa	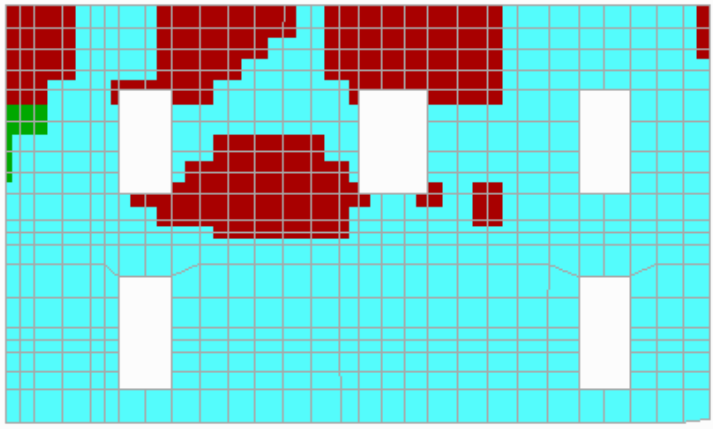	
Joints = 558 Failed = 116 Failure Percentage = 20.79%		

Failure		
wall : **E_2topmax** **Load Cases :** **0.40g**		Failure under biaxial Tension/Tension
		Failure under biaxial Tension/ Compression
		Failure under biaxial Compression /Tension
		Failure under biaxial Compression/ Compression
		NON Failure
fwt = 50 kPa	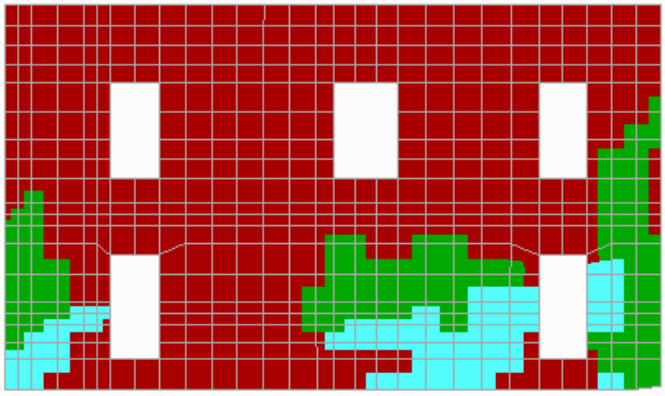	
Joints = 558 Failed = 503 Failure Percentage = 90.14%		
fwt = 250 kPa	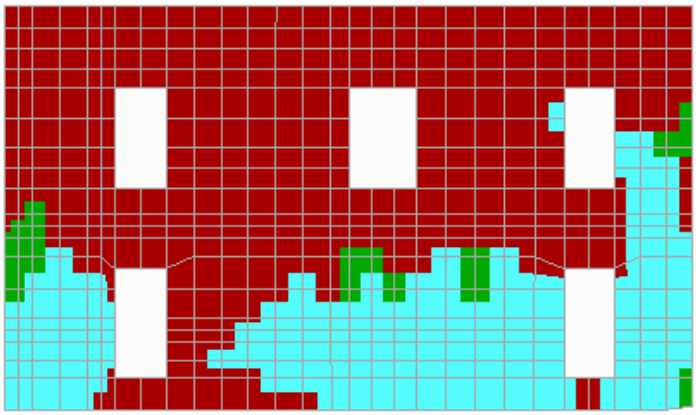	
Joints = 558 Failed = 387 Failure Percentage = 69.35%		
f_{wt} = 450 kPa	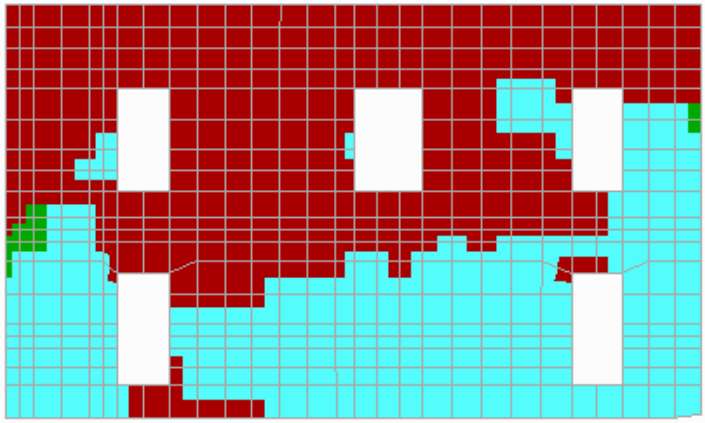	
Joints = 558 Failed = 311 Failure Percentage = 55.73%		

9.4 Failure rates & Statistical elaboration of the results

For the statistical analysis of data and in order to draw conclusions concerning the type and size of the failure of the wall structure, is taken the overall rate of failure for the 15 walls of the building for different tensile strength and four ground accelerations.

f_{wt} / PGA	*0.16g*	*0.24g*	*0.36g*	*0.40g*
K50	32.68	44.23	55.79	67.34
K100	25.87	35.08	44.29	53.5
K150	16.29	26.80	37.31	47.82
K200	13.5	20.87	28.23	35.6
K250	10.43	16.47	22.51	28.55
K300	8.5	14.03	19.57	25.1
K350	6.89	11.96	17.03	22.1
K400	4.58	9.45	14.33	19.2
K450	3.89	8.41	12.93	17.45

Table 9.1: Total failure percentages for the building, for 9 mortars and 4 ground accelerations

Below are illustrated the results of the statistic analysis for the two distributions and all ground accelerations.

.

Normal distribution

- **Ground acceleration PGA = 0.16g**

Tensile Strength fwt	*Failure Rate (%)*
50	49.37
100	38.78
150	30.89
200	22.14
250	14.58
300	12.56
350	10.3
400	7.86
450	5.76
Total elements	9
Mean value	21.36
Standard deviation	15.21

x	*f(x)*	*F(x)*
0	0.00978514	0.08012749
5	0.01470827	0.14107257
10	0.01984417	0.22758872
15	0.02403151	0.33793342
20	0.02612197	0.46437874
25	0.02548635	0.59456093
30	0.02231959	0.71498079
35	0.01754452	0.81505955
40	0.01237866	0.88978736
45	0.00783939	0.93991967
50	0.00445623	0.97013634
55	0.00227368	0.98649948
60	0.00104128	0.99446061
65	0.00042804	0.99794053
70	0.00015793	0.99930714
75	0.00005231	0.99978930
80	0.00001555	0.99994214
85	0.00000415	0.99998566
90	0.00000099	0.99999680
95	0.00000021	0.99999935
100	0.00000004	0.99999988

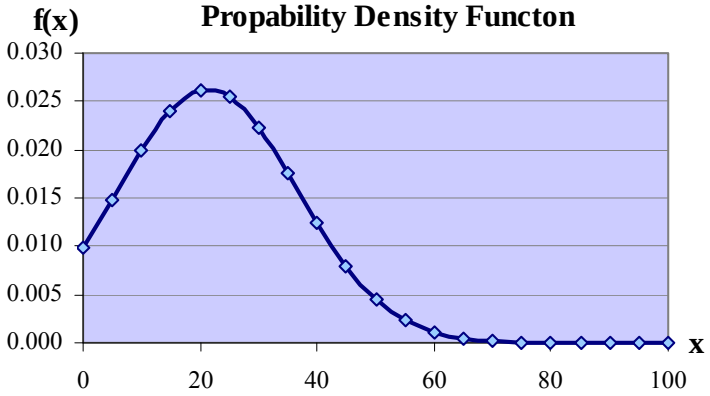

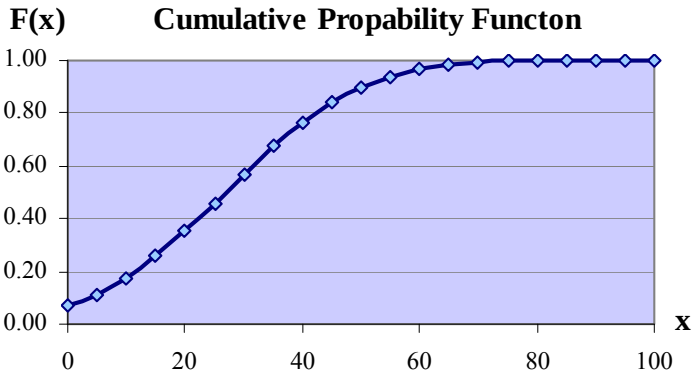

- **Ground acceleration PGA = 0.24g**

Tensile Strength fwt	*Failure Rate(%)*
50	61.87
100	51.20
150	41.50
200	33.89
250	25.34
300	21.77
350	18.95
400	15.60
450	12.63
Total elements	9
Mean value	31.42
Standard deviation	17.01

x	*f(x)*	*F(x)*
0	0.00426186	0.03239334
5	0.00702370	0.06023372
10	0.01061735	0.10403290
15	0.01472144	0.16727515
20	0.01872267	0.25108597
25	0.02184081	0.35302604
30	0.02336972	0.46682607
35	0.02293622	0.58342448
40	0.02064780	0.69307122
45	0.01704941	0.78770618
50	0.01291304	0.86267139
55	0.00897080	0.91717433
60	0.00571633	0.95354330
65	0.00334108	0.97581700
70	0.00179119	0.98833696
75	0.00088080	0.99479590
80	0.00039728	0.99785409
85	0.00016436	0.99918306
90	0.00006237	0.99971310
95	0.00002171	0.99990711
100	0.00000693	0.99997229

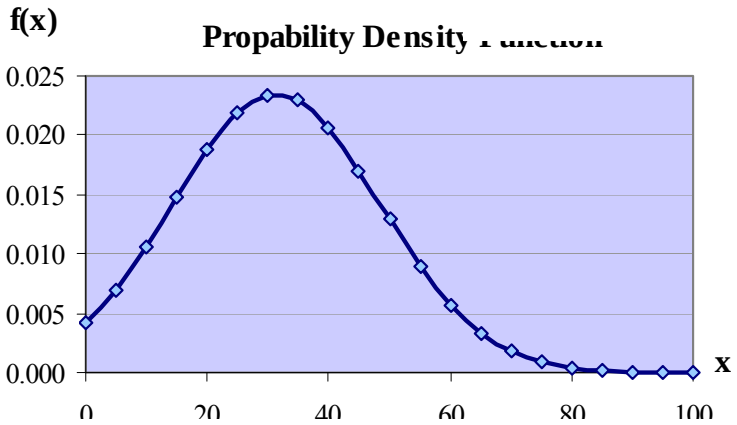

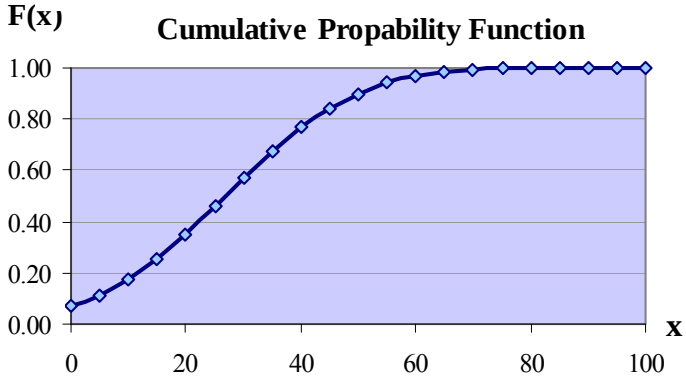

- **Ground acceleration PGA = 0.36g**

Tensile Strength fwt	*Failure Rate(%)*
50	74.37
100	63.11
150	58.16
200	47.67
250	36.10
300	31.88
350	27.81
400	23.20
450	19.50
Total elements	9
Mean value	42.42
Standard deviation	19.31

x	*f(x)*	*F(x)*
0	0.00185026	0.01401994
5	0.00316002	0.02632318
10	0.00504700	0.04658647
15	0.00753809	0.07780746
20	0.01052872	0.12280926
25	0.01375229	0.18349130
30	0.01679811	0.26003997
35	0.01918807	0.35037636
40	0.02049688	0.45010862
45	0.02047528	0.55311316
50	0.01912747	0.65263651
55	0.01670979	0.74259487
60	0.01365117	0.81866352
65	0.01042929	0.87883872
70	0.00745118	0.92337118
75	0.00497829	0.95420184
80	0.00311044	0.97416988
85	0.00181739	0.98626845
90	0.00099303	0.99312616
95	0.00050741	0.99676253
100	0.00024246	0.99856638

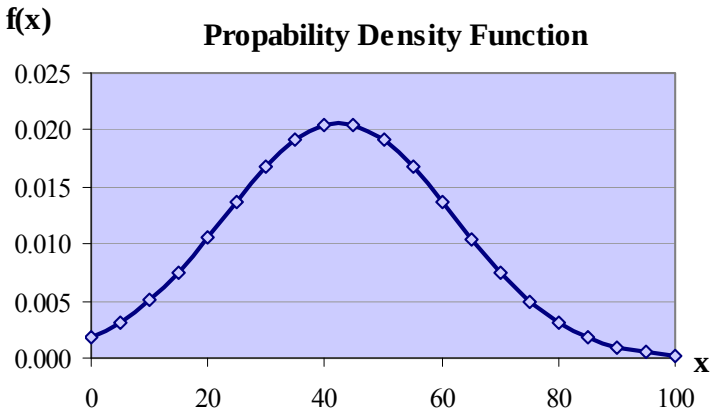

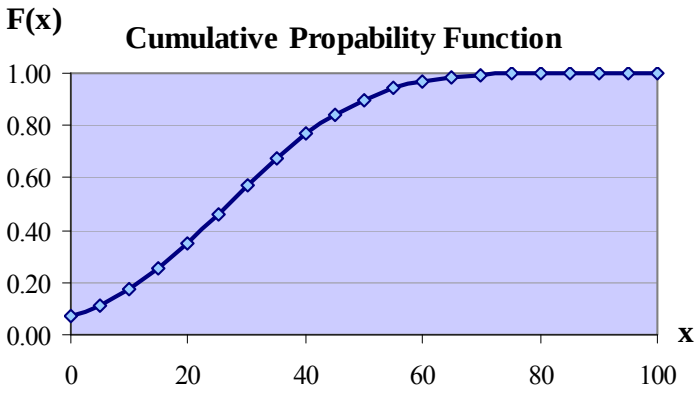

- **Ground acceleration PGA = 0.40g**

Tensile Strength fwt	*Failure Rate(%)*
50	86.86
100	71.69
150	63.43
200	54.26
250	46.85
300	41.94
350	36.15
400	31.01
450	26.37
Total elements	9
Mean value	50.95
Standard deviation	20.02

x	*f(x)*	*F(x)*
0	0.00078104	0.00545913
5	0.00142963	0.01085122
10	0.00245856	0.02038962
15	0.00397232	0.03624731
20	0.00602997	0.06102437
25	0.00859989	0.09740802
30	0.01152331	0.14762021
35	0.01450671	0.21274689
40	0.01715803	0.29213504
45	0.01906657	0.38308442
50	0.01990604	0.48100889
55	0.01952558	0.58009894
60	0.01799409	0.67433484
65	0.01557984	0.75856159
70	0.01267368	0.82931235
75	0.00968611	0.88516699
80	0.00695509	0.92660838
85	0.00469206	0.95550560
90	0.00297393	0.97444317
95	0.00177094	0.98610693
100	0.00099080	0.99285840

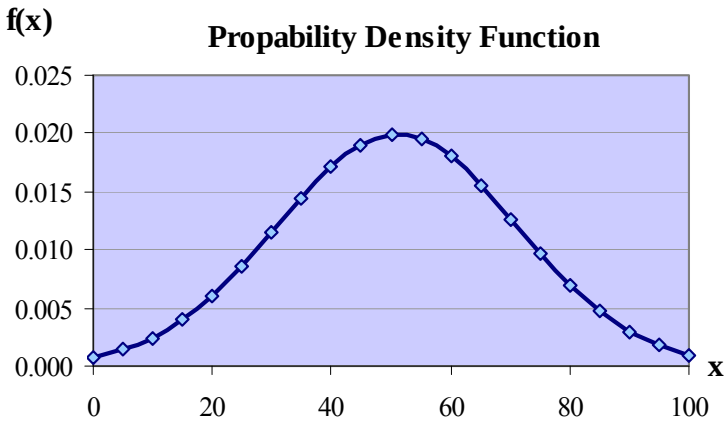

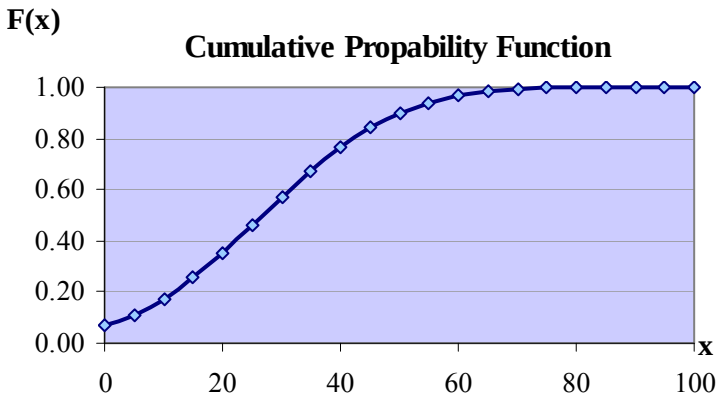

Lognormal distribution

- **Ground acceleration PGA = 0.16g**

Tensile Strength fwt	*Failure Rate(%)*
50	3.90
100	3.66
150	3.43
200	3.10
250	2.68
300	2.53
350	2.33
400	2.06
450	1.75
Total elements	9
Mean value	2.83
Standard deviation	0.74

x	*f(x)*	*F(x)*
0.00000000	0.00000000	0.00000000
1.60943791	0.02785121	0.04991725
2.30258509	0.04196450	0.23931227
2.70805020	0.03549901	0.43631260
2.99573227	0.02627296	0.59041919
3.21887582	0.01874476	0.70205326
3.40119738	0.01329634	0.78136608
3.55534806	0.00948510	0.83774395
3.68887945	0.00683479	0.87814494
3.80666249	0.00498246	0.90741557
3.91202301	0.00367544	0.92887385
4.00733319	0.00274275	0.94479077
4.09434456	0.00206936	0.95673152
4.17438727	0.00157753	0.96578566
4.24849524	0.00121429	0.97272026
4.31748811	0.00094318	0.97808154
4.38202663	0.00073881	0.98226289
4.44265126	0.00058329	0.98555075
4.49980967	0.00046391	0.98815583
4.55387689	0.00037152	0.99023472
4.60517019	0.00029945	0.99190480

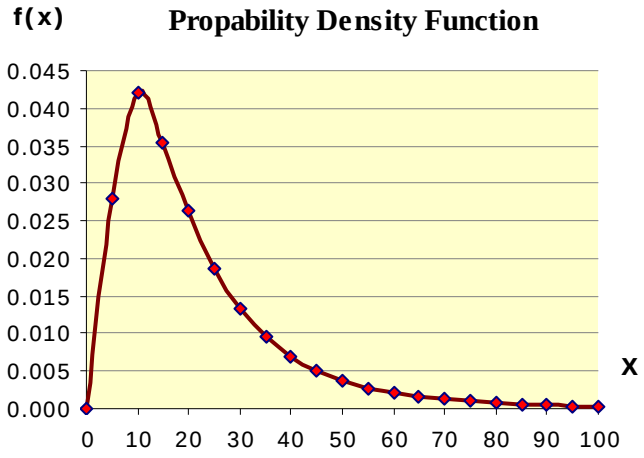

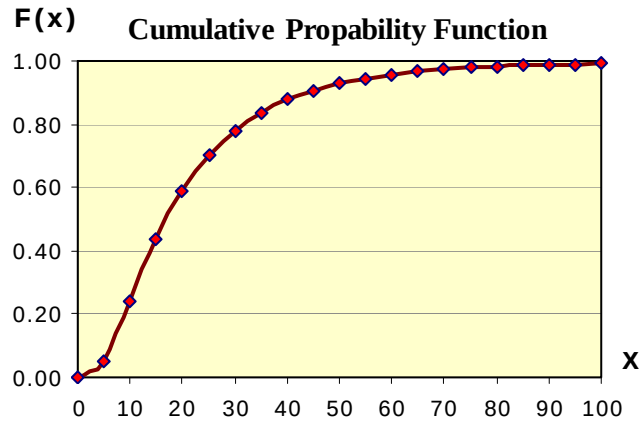

- **Ground acceleration PGA = 0.24g**

Tensile Strength fwt	*Failure Rate(%)*
50	4.13
100	3.94
150	3.73
200	3.52
250	3.23
300	3.08
350	2.94
400	2.75
450	2.54
Total elements	9
Mean value	3.32
Standard deviation	0.55

x	*f(x)*	*F(x)*
0.00000000	0.00000000	0.00000000
1.60943791	0.00110042	0.00088300
2.30258509	0.01302673	0.03164125
2.70805020	0.02618465	0.13255001
2.99573227	0.03075131	0.27846611
3.21887582	0.02877072	0.42911770
3.40119738	0.02406884	0.56173892
3.55534806	0.01897299	0.66922449
3.68887945	0.01447579	0.75250474
3.80666249	0.01085012	0.81545073
3.91202301	0.00805933	0.86240235
4.00733319	0.00596409	0.89720370
4.09434456	0.00441178	0.92294693
4.17438727	0.00326908	0.94200261
4.24849524	0.00242976	0.95614192
4.31748811	0.00181302	0.96667004
4.38202663	0.00135885	0.97454218
4.44265126	0.00102330	0.98045557
4.49980967	0.00077441	0.98491915
4.55387689	0.00058899	0.98830513
4.60517019	0.00045019	0.99088648

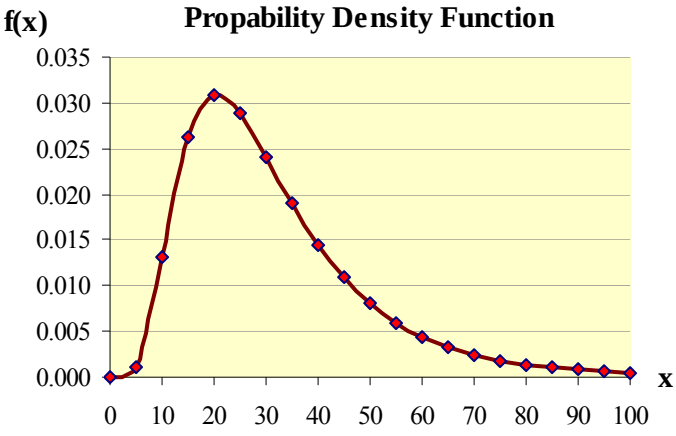

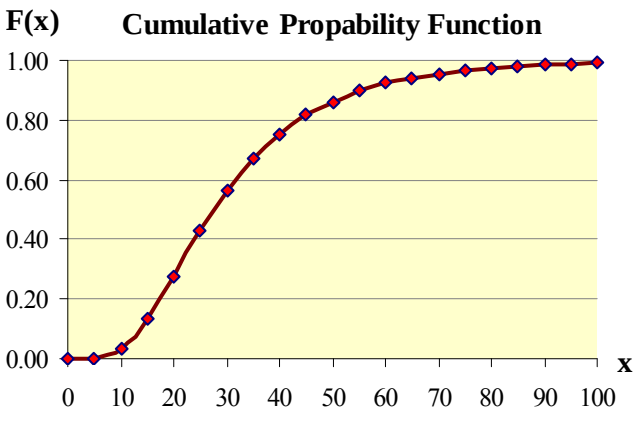

- **Ground acceleration PGA = 0.36g**

Tensile Strength fwt	*Failure Rate(%)*
50	4.31
100	4.14
150	4.06
200	3.86
250	3.59
300	3.46
350	3.33
400	3.14
450	2.97
Total elements	9
Mean value	3.65
Standard deviation	0.47

x	*f(x)*	*F(x)*
0.00000000	0.00000000	0.00000000
1.60943791	0.00001284	0.00000659
2.30258509	0.00135067	0.00199729
2.70805020	0.00746841	0.02201793
2.99573227	0.01596508	0.08073632
3.21887582	0.02220674	0.17769624
3.40119738	0.02457814	0.29622253
3.55534806	0.02379932	0.41820041
3.68887945	0.02120803	0.53121217
3.80666249	0.01791009	0.62912752
3.91202301	0.01459522	0.71030395
4.00733319	0.01161201	0.77564440
4.09434456	0.00909031	0.82719968
4.17438727	0.00703973	0.86733565
4.24849524	0.00541351	0.89830521
4.31748811	0.00414498	0.92206689
4.38202663	0.00316620	0.94023750
4.44265126	0.00241631	0.95410981
4.49980967	0.00184428	0.96469648
4.55387689	0.00140899	0.97278004
4.60517019	0.00107807	0.97895989

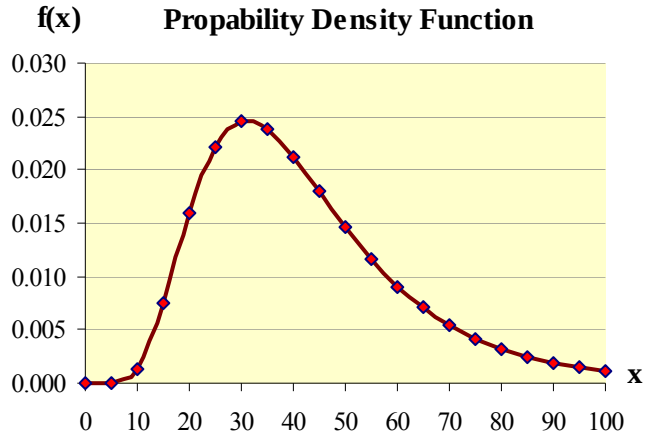

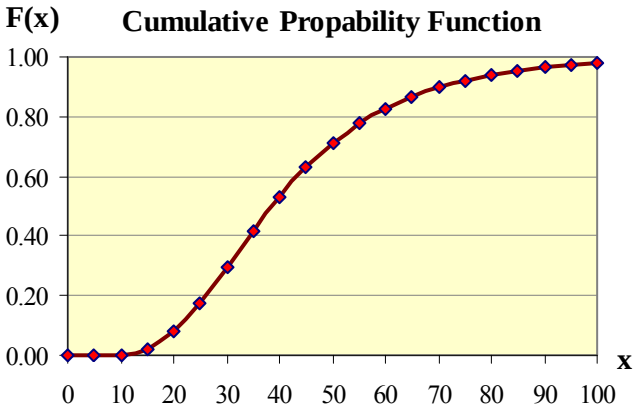

- **Ground acceleration PGA = 0.40g**

Tensile Strength fwt	*Failure Rate(%)*
50	4.46
100	4.27
150	4.15
200	3.99
250	3.85
300	3.74
350	3.59
400	3.43
450	3.27
Total elements	9
Mean value	3.86
Standard deviation	0.40

x	*f(x)*	*F(x)*
0.00000000	0.00000000	0.00000000
1.60943791	0.00000002	0.00000001
2.30258509	0.00004304	0.00004088
2.70805020	0.00095978	0.00177871
2.99573227	0.00459752	0.01432560
3.21887582	0.01077220	0.05212602
3.40119738	0.01706106	0.12220669
3.55534806	0.02132965	0.21927816
3.68887945	0.02289614	0.33093748
3.80666249	0.02217666	0.44440910
3.91202301	0.01999476	0.55027118
4.00733319	0.01712875	0.64322969
4.09434456	0.01413854	0.72136472
4.17438727	0.01135609	0.78497106
4.24849524	0.00893884	0.83554043
4.31748811	0.00693151	0.87504602
4.38202663	0.00531575	0.90550969
4.44265126	0.00404369	0.92877683
4.49980967	0.00305812	0.94642397
4.55387689	0.00230335	0.95974232
4.60517019	0.00173018	0.96975967

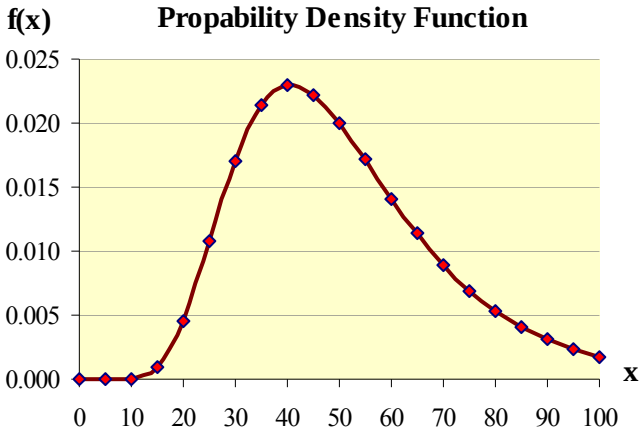

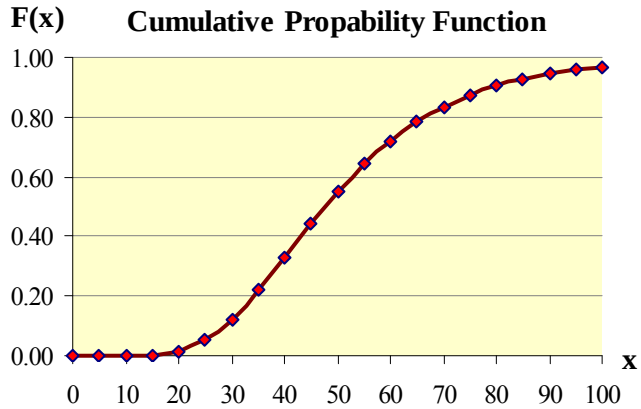

9.5 Export of fragility curves

After the statistical processing and the analysis of the failure rates of the wall structure and having set the levels of damage in a previous chapter, we can draw the fragility curves.

Normal distribution

- **Graduation of failures, type a**

(%) PGA	0	0.16	0.24	0.36	0.40
Small	0	0.8589	0.9398	0.9737	0.9891
Medium	0	0.6621	0.8327	0.9222	0.9638
Large	0	0.4054	0.6470	0.8165	0.9026

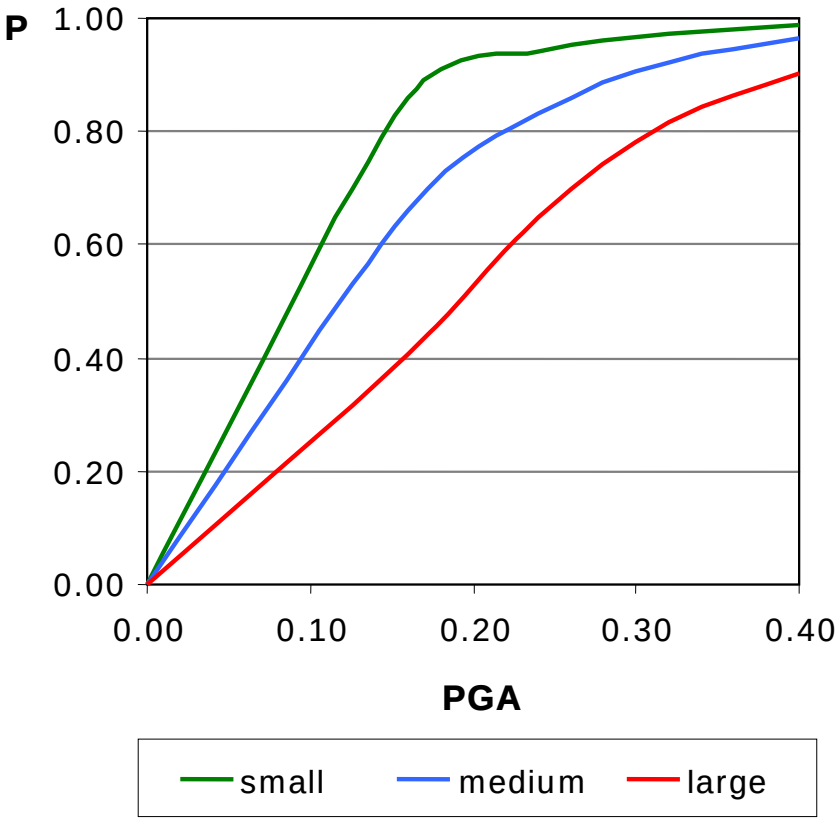

➢ **Graduation of failures, type b**

(%) PGA	0	0.16	0.24	0.36	0.40
Small	0	0.7724	0.8960	0.9534	0.9796
Medium	0	0.5356	0.7489	0.8772	0.9390
Large	0	0.2850	0.5332	0.7400	0.8524

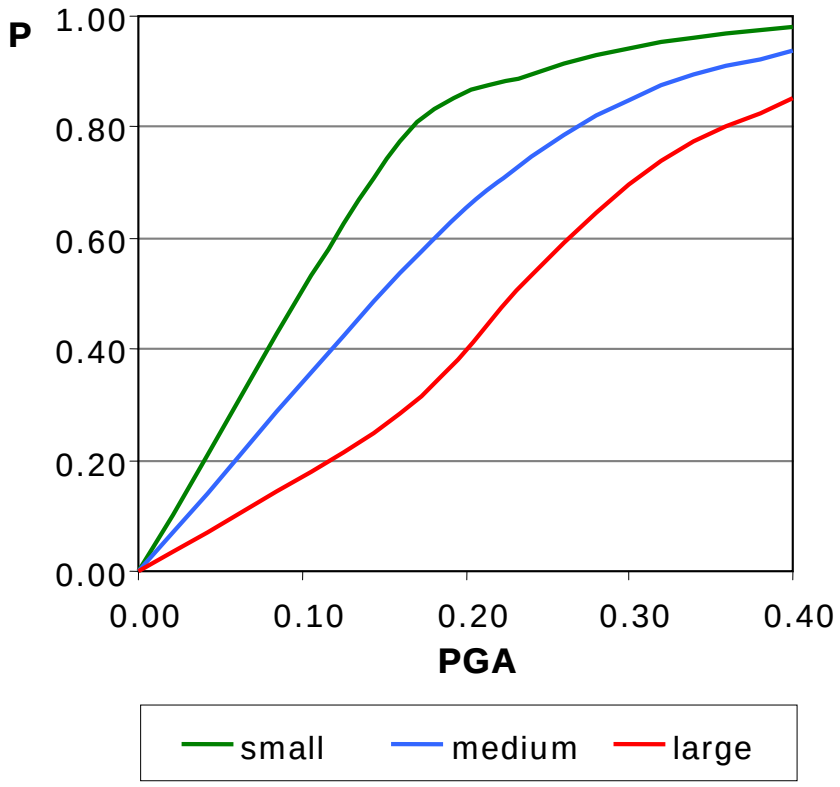

- **Graduation of failures, type c**

(%) PGA	0	0.16	0.24	0.36	0.40
Small	0	0.6621	0.8327	0.9222	0.9638
Medium	0	0.1849	0.4166	0.6496	0.7873
Large	0	0.0601	0.2123	0.4469	0.6169

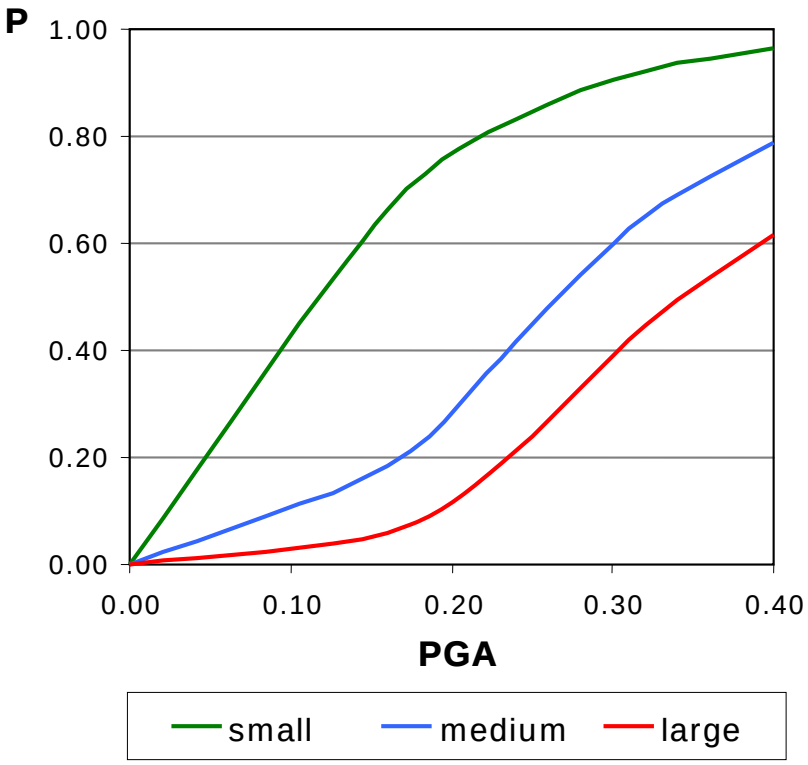

Lognormal distribution

- **Graduation of failures, type a**

(%) PGA	0	0.16	0.24	0.36	0.40
Small	0	0.9501	0.9991	1.0000	1.0000
Medium	0	0.5637	0.8674	0.9780	0.9982
Large	0	0.2979	0.5709	0.8223	0.9479

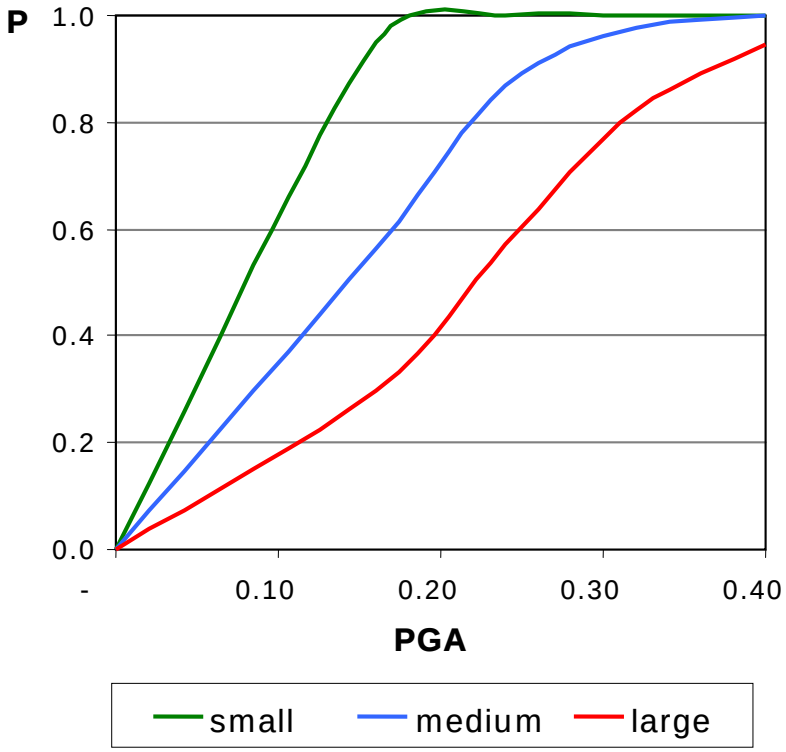

- **Graduation of failures, type b**

(%) PGA	0	0.16	0.24	0.36	0.40
Small	0	0.7607	0.9684	0.9980	1.0000
Medium	0	0.4096	0.7215	0.9193	0.9857
Large	0	0.2186	0.4383	0.7038	0.8778

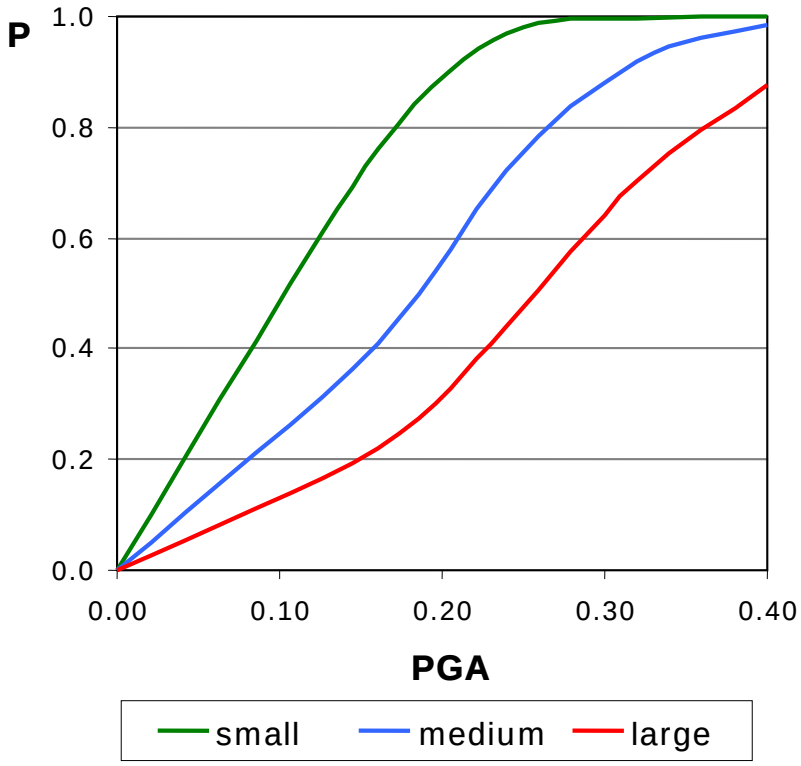

➢ **Graduation of failures, type c**

(%) PGA	0	0.16	0.24	0.36	0.40
Small	0	0.5637	0.7215	0.9193	0.9857
Medium	0	0.1623	0.4383	0.7038	0.8778
Large	0	0.0926	0.1376	0.2897	0.4497

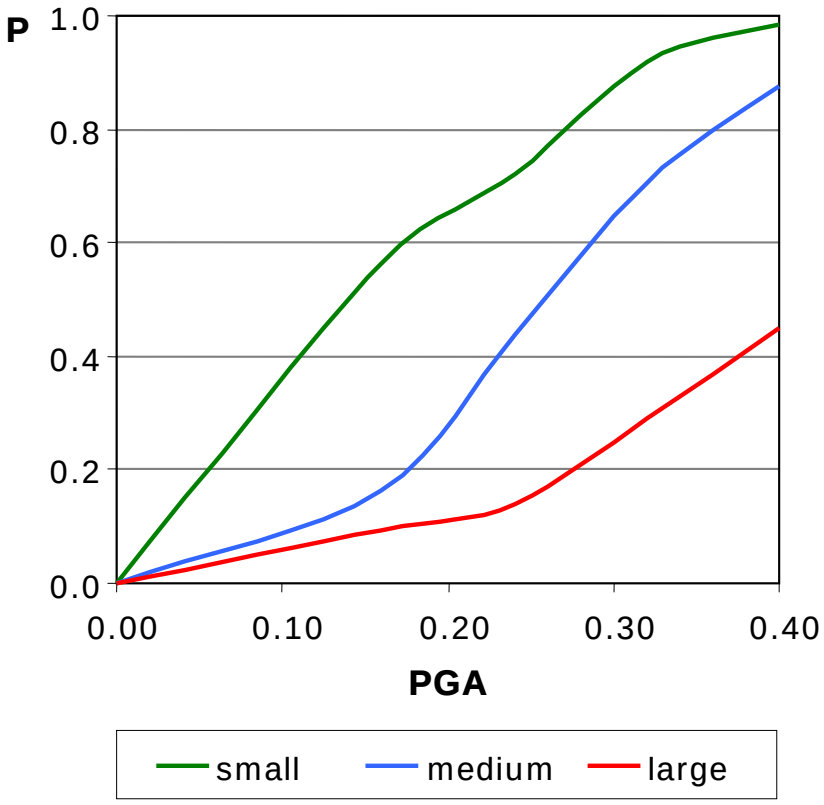

9.5 Comparison between the three failure levels of the two distributions

- ***Small failure***

Normal distribution	Lognormal distribution
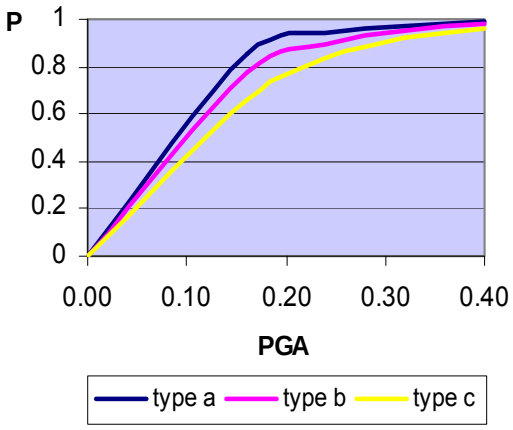	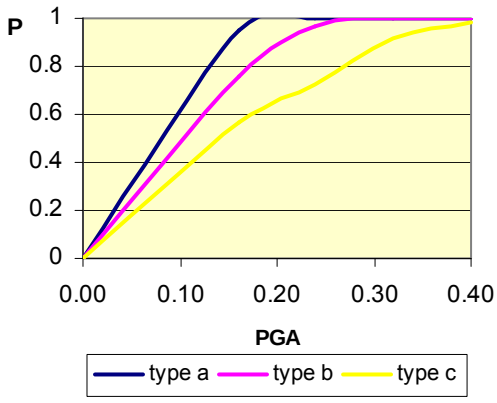

- ***Medium failure***

Normal distribution	Lognormal distribution
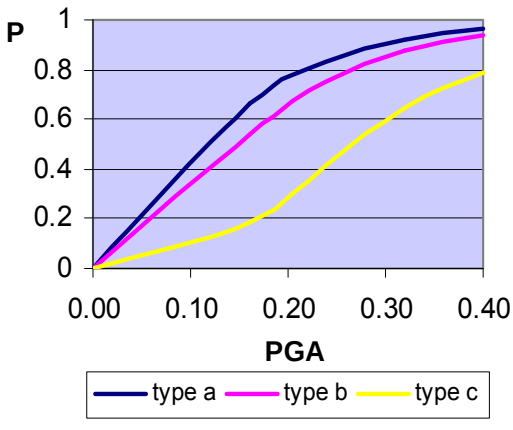	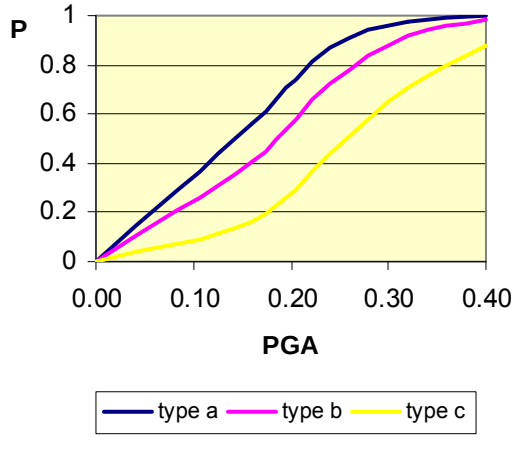

- ***Large failure***

Normal distribution	Lognormal distribution
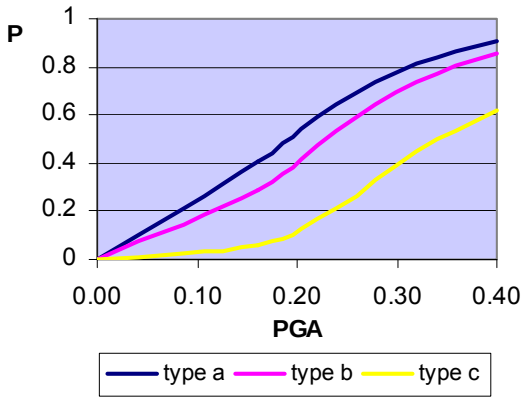	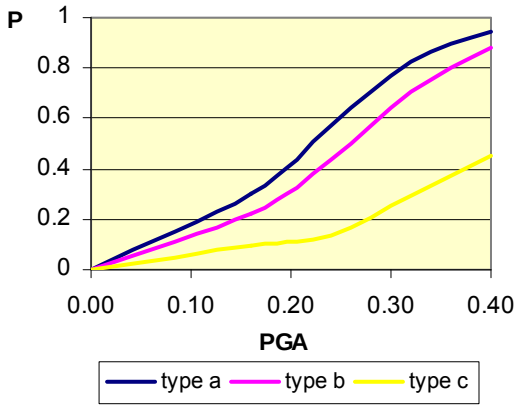

CHAPTER 10

COMPARISONS – CONCLUSIONS

10.1 Introduction

In the previous paragraphs were presented three techniques that can be applied for reinforcing the structure. In this chapter we will compare and comment on the results of these three reinforcements in order to emerge the best reinforcement solution.

The purpose of all proposed reinforcements is to restore the damage and prevent their progression to the next stage. All the techniques are considered to be compatible since they have been used in the past and there is a workforce with knowledge and experience and technical means for their proper implementation. Nevertheless, any proposal approaches the problem differently, but always taking into account the context of cost-effectiveness-intervention.

The effectiveness of any reinforcement is reflected in fragility curves, but also in failures that appear in pictures of some indicative facades based on the failure criterion, which was presented in detail in a previous chapter, and after multiple solutions with the software SAP 2000 14.

The cost of each reinforcement was approximately estimated based on proportionality arising from the analytical construction work invoice (ATOE - AICW) with official rates of the third quarter of 1994 listed in the book "Design of masonry structures, design and repair / Fyllitsa B. Karantoni / Athens 2004.

Lastly, the degree of intervention came from the stages of work required for each one of the reinforcements as outlined in Chapter 8 of this study.

10.1.1 Pointing (Reinforcement A)

The pointing is not just a reinforcement method, but rather a method to restore the building to its original condition. Essentially the pointing method attempts to recover the building's lost, over time, mechanical characteristics which had the first years after its construction. The technique is proposed for all current proposed reinforcements because apart from the mechanical properties, the construction retrieves its form, correcting the defects which expose its vulnerability areas. For the proper application of the method and to achieve the above, the replacement mortar is required to be composed of similar materials (if possible the same) as the original, so that neither the form nor the mechanical features of the masonry to deteriorate. Even mortar with great strength, which is apparently preferable, it could cause unwanted and uncontrolled brittle failure.

From the above it is clear that the method not only intervenes in the construction but corrects the damage from environmental conditions. As for the cost, compared with the other two proposed reinforcements, it can only be cheaper, since as mentioned above the pointing of the masonry is included in all of them. Finally, its effectiveness is limited because the recovery of the properties of the masonry implies that the same damage can occur again.

10.1.2 Pointing, reinforced concrete slab at the ground and the first floor level and reinforced concrete bond beam at the roof level (Reinforcement B)

The horizontal concrete bond beams and concrete slabs are both very effective reinforcements, especially in taking seismic horizontal tensile stresses. Both take over the decline of the cross-walls preventing their possible separation and overturning; while significantly reduce any movement even on the walls parallel to the earthquake. Despite these advantages, their application in the building is not always as easy and does not end with the

same cost. Bond beam in an intermediate level (e.g. 1st floor level) has difficulties in constructing, risk of collapse during the work and high cost due to the need to purchase steel beams for the temporary support of the above wall.

On the other hand, the concrete slab at the higher levels is not recommended because of its large mass that loads the structure during the earthquake. But combination of the two methods can give very good results since the two reinforcements overlap their weaknesses. Choosing the reinforced concrete slab construction on the levels of the ground floor and first floor, is reached the full diaphragmatic function, the increase of the shear strength and the reduce of the amount of masonry flexural height up to the level of the slab. So, it is achieved a better result from the bond beam application and with lower cost. This is because although the slab needs more concrete, the bond beam construction shows the difficulties mentioned above. Moreover, the way the slab was applied, i.e. with the support on the perimeter walls per 1.5-2m and the use of the existing floor as forUMork, more money were saved. On the other hand, better choice is the construction of the bond beam on the roof as it ensures partial diaphragmatic function without loading the construction with large concentrated mass at high altitude. For the construction of the bond beam at this level, the use of beams is not necessary, so the manufacturing cost drops to 50%. The effectiveness of this reinforcement is more than satisfactory and the cost is within reasonable limits. Compared with the other two proposals this alters the form of the building to the greatest extent, but within acceptable limits.

10.1.3 Pointing and horizontal prestressing (Reinforcement C)

Horizontal prestressing can be applied easily compared to the vertical one, since the anchorage of the tendons can be simply installed at the edges of the

walls by the use of steel plates (as described in chapter 8). Moreover, an extra advantage is that the tendons work in the direction of horizontal forces, which is more critical for the structure. Actually, tendons keep the wall glued together as a unit in order to prevent tensile types of failure during an earthquake. However, because of the uncertainties about masonry strength, the pressure of the tendons applied conservatively, 10% of the walls compressive strength after pointing (where: F_{wc}=4340MPa), so as to ensure that compressive failure will not occur at the areas where the lintels are short or the wall is weak. This type of failure could probably take place especially when a seismic applies an extra horizontal compressive load parallel to the tendons pressure. On the other hand, since the pressure of the tendons is small the effectiveness of the method reduces considerably.

Taking everything into account, this type of reinforcement does not causes important intervention to the structure, is easy to apply and its cost is significant low (it could cost 5 to 6 times less than reinforcement B) although its strengthening results are insufficient compared to reinforcement B.

10.2 Conclusions from the modal analysis

Table 12.1 presents the fundamental modes, such as they derived from the modal analysis of the model of the construction for the four cases (unreinforced masonry and three reinforcements), using the software SAP 2000 14. Overall, the building has a uniform geometry and distribution of rigidities (Annex 2 / architectural building plans) attached to a certain convergence of the pole shift and the center of the mass of the building, thus preventing large rotational movements.

TABLE: Modal Participating Mass Ratios	MODE	Period	UX	UY	RZ
CASE	Text	Sec	Unitless	**Unitless**	Unitless
UNREINFORCEMENT MASONRY	6	0.115	0.003	**0.273**	0.045
REINFORCEMENT 1	6	0.096	0.002	**0.242**	0.036
REINFORCEMENT 2	4	0.086	$2.23*10^{-7}$	**0.361**	0.252
REINFORCEMENT 3	6	0.096	0.002	**0.242**	0.036

Table 10.1 Fundamental modes for all cases

As fundumental is taken mode that has the largest mass participation, and as we see this is observed in all cases at the axis y-y (transferational mode). This behavior of the body is due to the existence of two additions that have been constructed along the axis x-x, which restrict its oscillation to that direction.

Because of the nature of the masonry, characterized by unevenness, it took 300 modes to concentrate about 90% of the total oscillating mass in both directions (axis x-x, y-y / Annex 1). Observing the first modes small contributions of high-level masses are distinguished, because they oscillate first the linear elements of the roof and interior walls of small thickness section.

As shown in the table above (Table 12.1), the reinforcements cause reduction to the period, as expected, since their purpose is to reduce displacements by increasing the stiffness of the building.

From the three suggested methods, reinforcement B is the only that minimize drastically the period of the structure. Moreover it is worth to be mentioned that the modal participating mass ratios (UR and RZ) are greater than any other case and that is explained from the existence of concrete slabs that they order diaphragmatic function. Finally an important note is that results from modal analysis are the same for reinforcement A and C. This might happened because the tendons were modeled as a horizontal force and the software could not take into account the tying that the tendons offer at the transverse walls.

10.3 Comparison between fragility curves

At this point we can compare the results come from the analysis. Below, from figure 12.1 to figure 12.3, are shown the fragility curves for all types (a,b and c). Each type represents the curves only for one level of failure (small, medium, large) but for all the reinforcement cases (Unreinforced masonry and reinforcement A,B,C).

Code	Name	Description
MW	Masonry Wall	No reinforcement
RA	Reinforcement A	Pointing
RB	Reinforcement B	Pointing – Concrete Slab at the ground and the first floor - Concrete Bond at the roof level
RC	Reinforcement C	Pointing – Horizontal Prestressing along the lintels

Table 10.2 Masonry wall and Reinforcements A,B & C

Type a	Small failure	MW, RA,RB,RC
Type b	Medium failure	MW, RA,RB,RC
Type c	Large failure	MW, RA,RB,RC

Table 10.3 Way that represents graphs presentation

From the graphs below, it is obvious that for small failures all the curves have very similar shape. As the failure level increases (from small to large) the curves starts to behave differently. Therefore is understood that the reinforcements start working and prove their efficiency as the failures getting greater. Moreover it is observed, that all reinforcements represent a very high percentage in small failures while their performance improves significantly in large failures. From that is realized that a successful reinforcement might not stops small cracks but has many possibilities to prevent structure from severe damages.

Small failure: MW, RA and RC have almost the same behavior and possibilities to present small cracks while RB has slightly the best

performance. The differences between the curves are very little and that confirms that no matter how proficient is the reinforcement small cracks will definitely occur.

Medium failure: The curves of MW, RA and RC are still alike and only RB curve follows a different shape. At this level, most of the reinforcements strengthening the structure insignificantly and only RB minimize considerably the possibilities of medium failures.

Large failure: At this failure level, the effectiveness of each technique is clear (figure 12.3). For small seismic acceleration all of the methods perform efficiently, especial RB that shows almost zero possibilities of large damages. Also, taking into account the most severe case (PGA =0.40) there is only a 30% possibility for RB having large failures while for the rest of reinforcements the possibilities are the double (the percentage fluctuates from 60 to75%).

The results that outcome from the fragility curves shows that pointing (RA) contributes a little to the strengthening of the structure. However this is not so accurate because the efficacy of pointing cannot be modeled. Actually there is no possible way to model the damaged areas of the building, which are the most likely to fail if they do not gain back their strength by the help of a new mortar, after pointing.

Horizontal prestressing (RC) was also barely effective for the structure, giving slightly better results in comparison with pointing (RA). A fair excuse could be that the prestressing force was decide conservatively (10% of wall compressive strength times the cross section area of each lintel) with concern not to exceed the compressive strength in areas were the wall is either weak or very thin.

Finally from the curves is established that reinforcement B (RB) is the most effective method to take horizontal forces and minimize medium and large failures. Also it is verified that diaphragmatic function is a first-class method for a high-quality performance of a building.

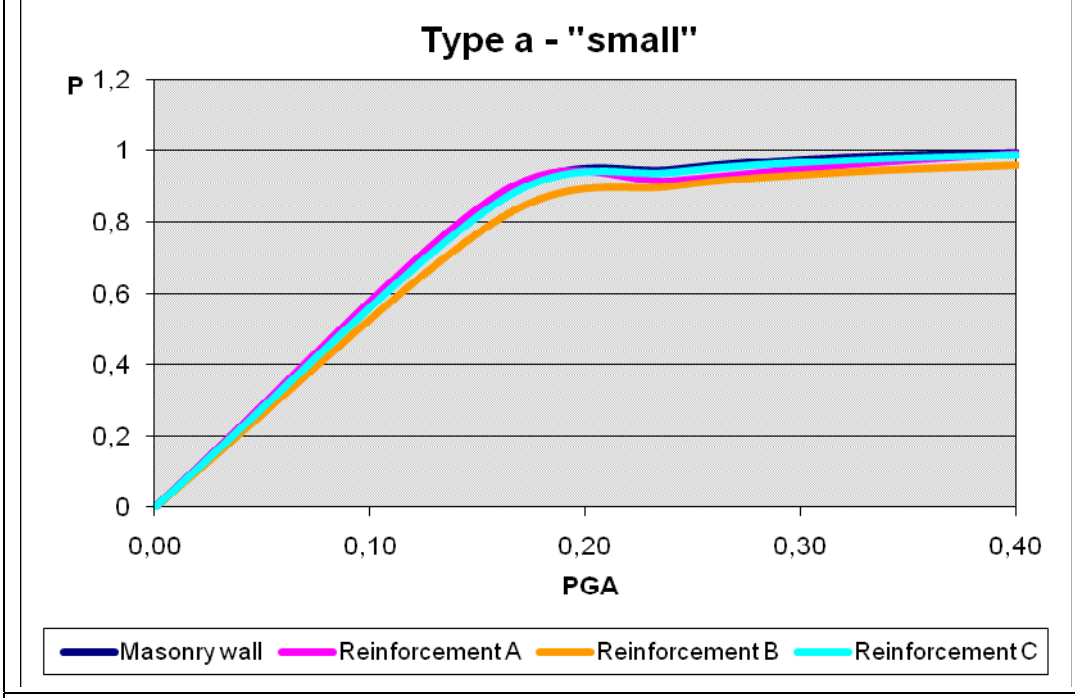

Figure 10.1: Fragility curves – type a "small failures"

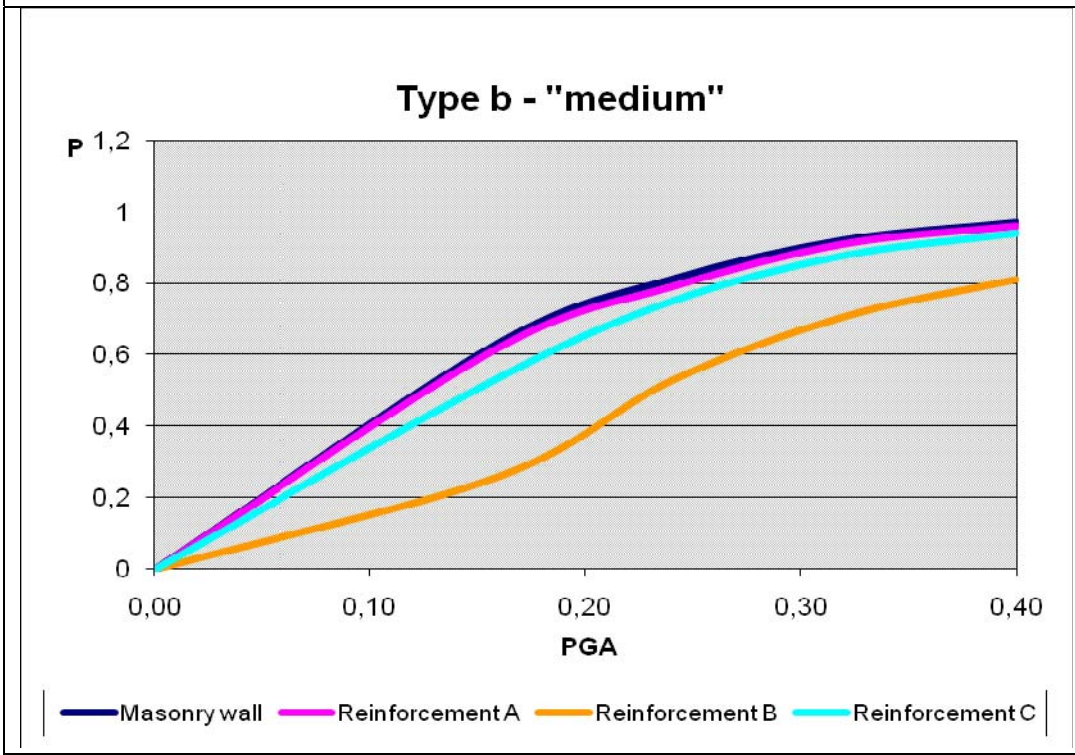

Figure 10.2: Fragility curves – type b "medium failures"

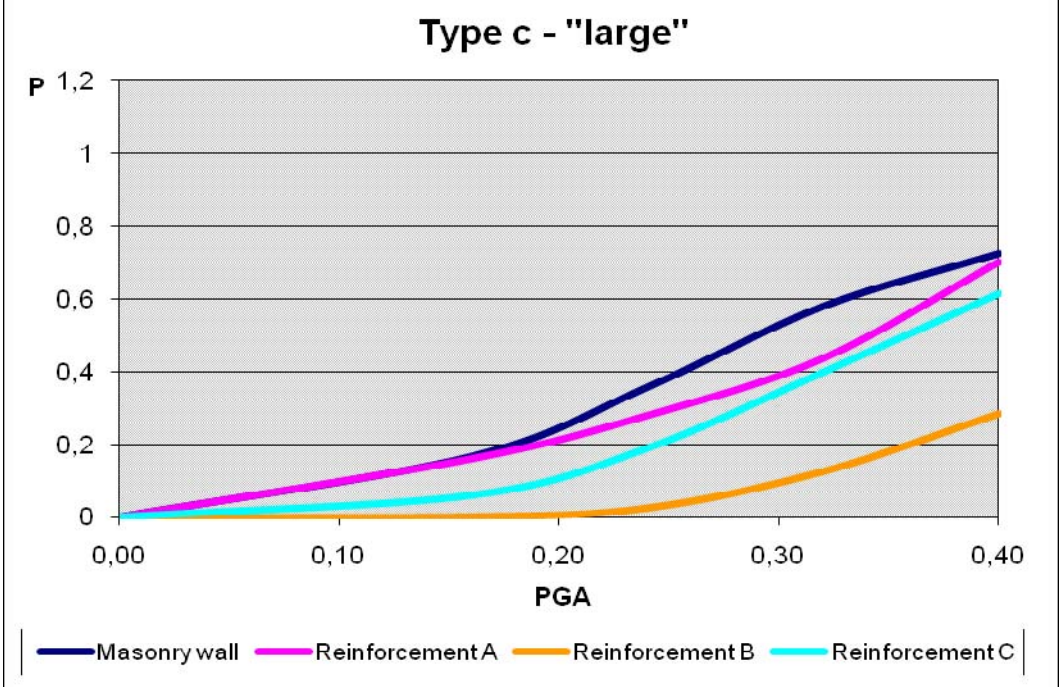

Figure 10.3: Fragility curves – type c "large failures"

10.4 Comparison between failure results of all the reinforcement cases

Below are illustrated the failure results of the main façade of the building for all reinforcement cases, for different tensile strengths and for seismic acceleration equals to 0.40g. At this point is needed to be mentioned that tensile strength is the parameter of observation in order to study the walls behavior under seismic loading.

Masonry wall

Biaxial tension - tension is the main reason of failure for masonry while quit many piers fail under biaxial tension - compression when the tensile strength is very low. For low tensile strength, failure will occur almost in all walls surface whereas when the tensile strength is increases failures are minimized and gathered around the openings and the corners where the walls are connected.

Reinforcement A

Since the only parameter has changed in the model, compared to masonry wall, is the modulus of elasticity by 40%, the failures appear at the same areas; with the only difference to be that the results are to some extent better than before.

Reinforcement B

This reinforcement has the best performance in comparison with the rest of reinforcements, under severe dynamic loads and for any tensile strength. For low tensile strength the wall failures mainly appear at the top of the structure and around the opening while as the tensile strength increases the damages are extensively decreased and the failures concentrate at the top of the wall. The concentration of failures at the top of the structure happens because there was not a satisfactory way to model the partial diaphragmatic function that concrete bond offers at the top of the structure (the way of modeling of this reinforcement is described extensively in paragraph 8.2.2.1). Therefore, for a real building the failures would be even less at this area.

Reinforcement C

This reinforcement has similar behavior with the Masonry Wall and reinforcement A. Although the failure under biaxial tension- tension is barely less likely to happen whereas failures under biaxial tension - compression is more or less as possible as before. However, as the tensile strength increases, the tendons seem to work more efficient.

Failure – Masonry Wall		
wall : **1_2topmax** **Load Cases :** **0.40g**		Failure under biaxial Tension/Tension
		Failure under biaxial Tension/ Compression
		Failure under biaxial Compression /Tension
		Failure under biaxial Compression/ Compression
		NON Failure
fwt = 50 kPa	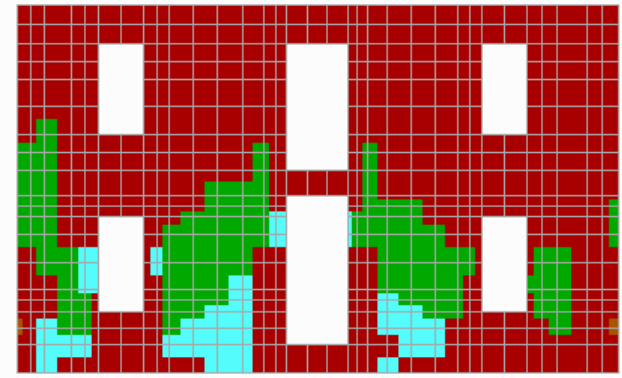	
Joints = 640 Failed = 629 Failure Percentage = 98.27%		
fwt = 250 kPa	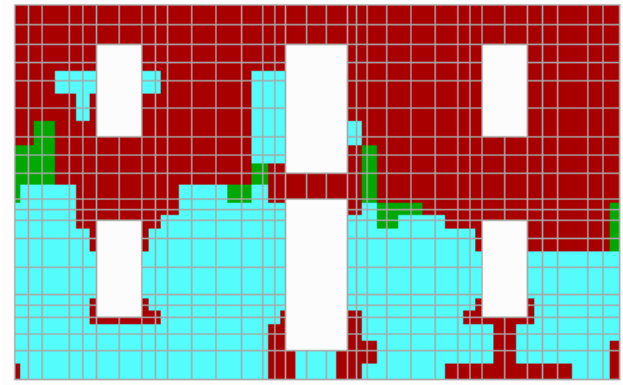	
Joints = 640 Failed = 444 Failure Percentage = 69.38%		
f_{wt} = 450 kPa	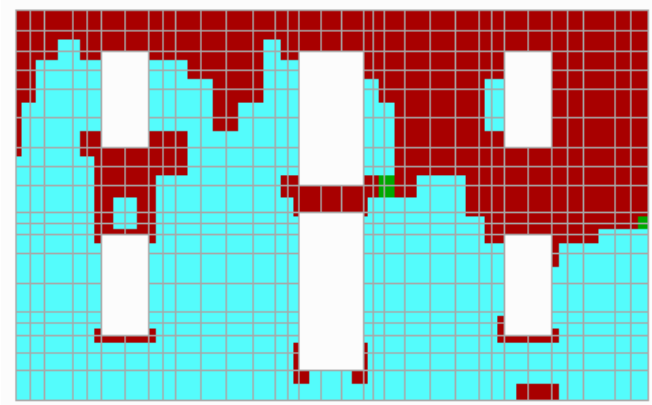	
Joints = 640 Failed = 260 Failure Percentage = 40.63%		

Failure – Reinforcement A

wall : **1_2topmax** **Load Cases :** **0.40g**		Failure under biaxial Tension/Tension
		Failure under biaxial Tension/ Compression
		Failure under biaxial Compression /Tension
		Failure under biaxial Compression/ Compression
		NON Failure
fwt = 50 kPa	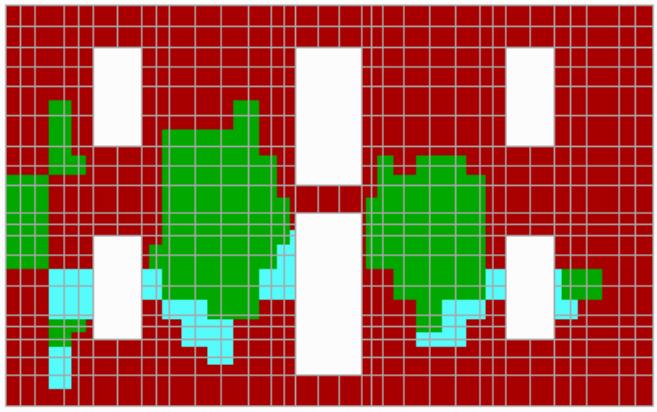	
Joints = 640 Failed = 607 Failure Percentage = 94.84%		
fwt = 250 kPa	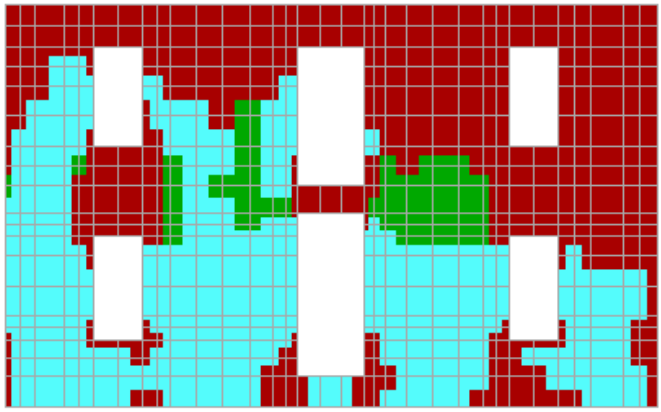	
Joints = 640 Failed = 379 Failure Percentage = 59.22%		
f_{wt} = 450 kPa	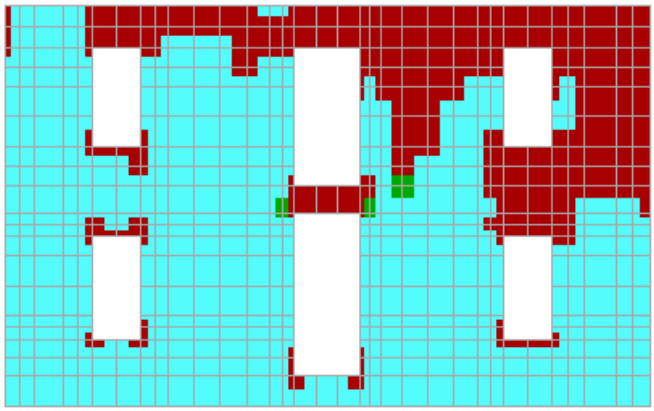	
Joints = 640 Failed = 193 Failure Percentage = 30.16%		

Failure - Reinforcement B

wall : **1_2topmax** **Load Cases :** **0.40g**	Failure under biaxial Tension/Tension
	Failure under biaxial Tension/ Compression
	Failure under biaxial Compression /Tension
	Failure under biaxial Compression/ Compression
	NON Failure

fwt = 50 kPa

Joints = 640
Failed = 441

Failure
Percentage = 68.91%

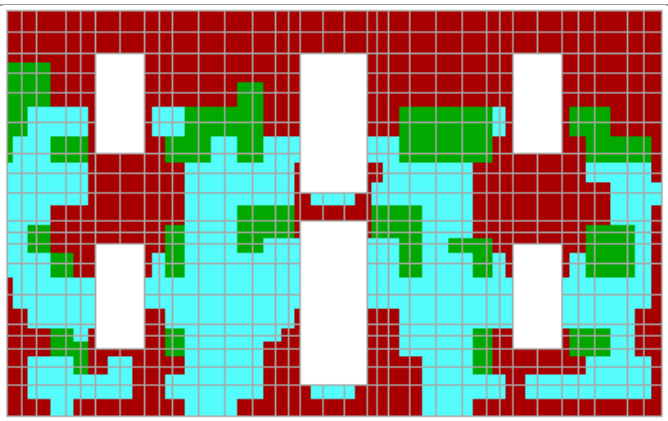

fwt = 250 kPa

Joints = 640
Failed = 153

Failure
Percentage = 23.91%

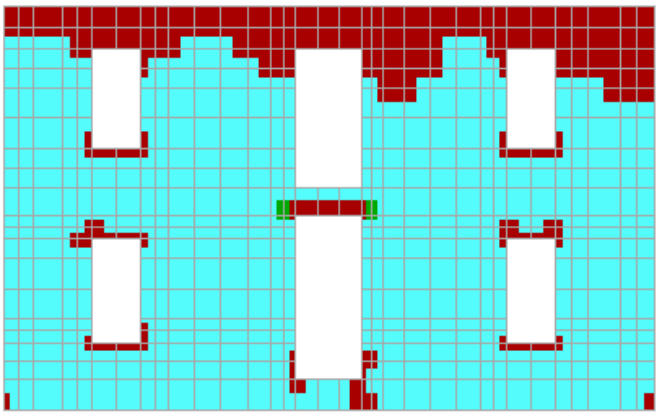

f_{wt} = 450 kPa

Joints = 640
Failed = 87

Failure
Percentage = 13.59%

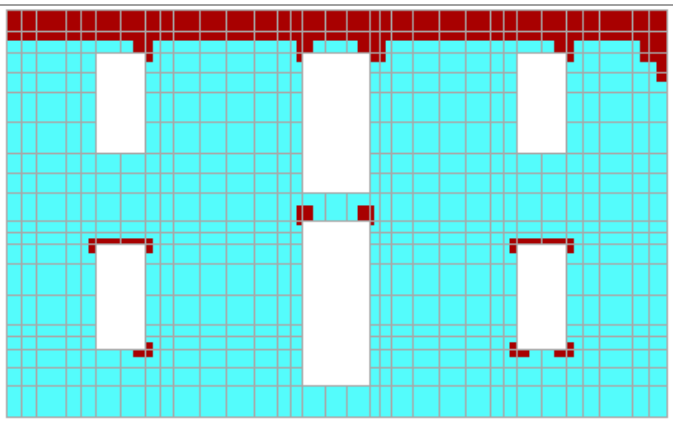

Failure - Reinforcement C

wall : **1_2topmax** **Load Cases :** **0.40g**	Failure under biaxial Tension/Tension
	Failure under biaxial Tension/ Compression
	Failure under biaxial Compression /Tension
	Failure under biaxial Compression/ Compression
	NON Failure

fwt = 50 kPa	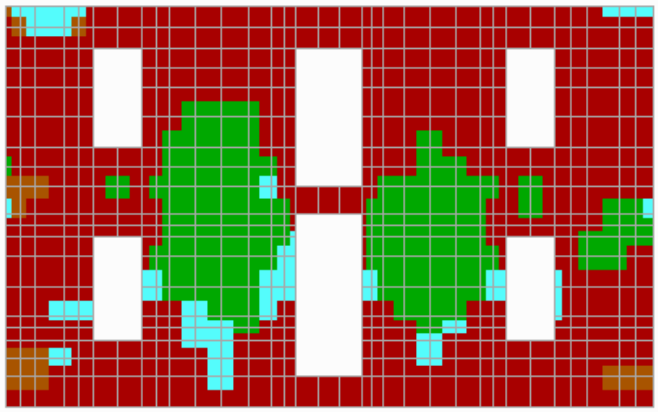
Joints = 640 Failed = 599 Failure Percentage = 93.59%	
fwt = 250 kPa	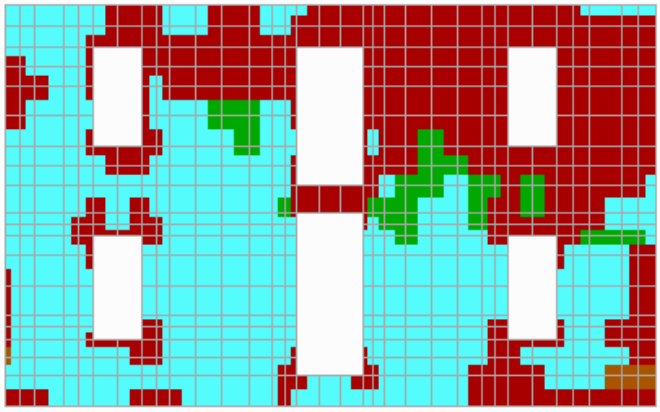
Joints = 640 Failed = 315 Failure Percentage = 49.22%	
f_{wt} = 450 kPa	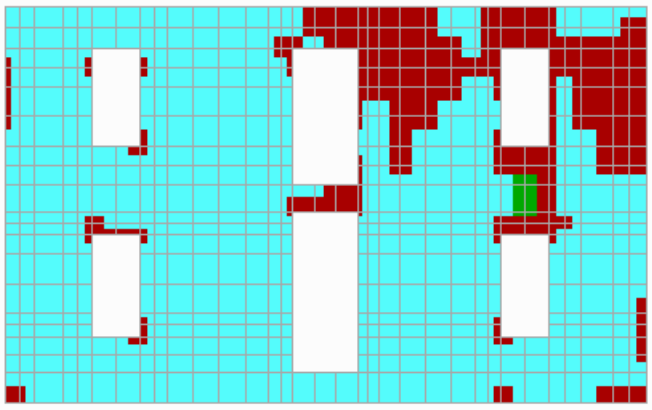
Joints = 640 Failed = 134 Failure Percentage = 20.94%	

10.5 Reinforcement evaluation criterion

At this point, data will be listed for each reinforcement case regarding the function cost-efficiency- intervention, which will determine the final decision to which reinforcement will prevail as the most appropriate. It should be noted that each of the above factors affect the function with a varying rate of importance. This factor results from the responsible engineer who in collaboration with the relevant agencies, evaluates the parameters and quantify their influence to the decision making.

Cost

As mentioned in the introduction of this chapter the cost, of each reinforcement method, was approximately estimated based on the proportionality arising from the construction work itemized bill (ATOE).

Effectiveness

The effectiveness of the reinforcements was assessed based on the fragility curves, for the worst ground acceleration (PGA = 0.40) and for large failures - type C.

Intervention

The intervention of each reinforcement case was assessed subjectively, taking into account existing bibliography and after contact with technical agencies with experience in reinforcement of masonry structures.

The degree of evaluation of each case, results from the following function:

0.15×cost + 0.60×effectiveness + 0.25×intervention= Grade

	Factor	Cost	Factor	Effectiveness	Factor	Intervention	Grade
Masonry wall	**0,15**	20	**0,6**	5	**0,25**	20	***11***
Reinforcement A		19		7		18	***11,55***
Reinforcement B		13		14		12	***13,35***
Reinforcement C		17		9		16	***11,95***

Table 10.3: Cost-Effectiveness-Intervention function

From Table 10.3 results as the best reinforcement, the construction of the bond beam at the crest of the walls and the concrete slab on the ground floor and first floor levels (grade = 13.35). While this reinforcement is the most invasive and most expensive than any other, it prevailed as the most appropriate due to the high efficiency to undertake horizontal seismic loads, but also because of the high rate of importance has given to this parameter (0.6). The results of the remaining three cases are among a small value range (between 11 and 11.95) which is quite natural, since in all three cases, all parameters affecting the result are not very different.

In the specific assessment plays an important role the effectiveness of the reinforcement to undertake seismic action while the influence of cost and intervention is limited. The factors which guide the choice of reinforcement are objective and not fixed but depend on parameters such as:

- The cultural value of the construction.
- The economic prosperity at the time which is decided to carry out the work
- The subjective judgment of people who take the decisions.

Taking into account the above, we conclude that the method is more recommended rather than imposed in order to help the ones responsible in the decision making, especially when choices are many.

BIBLIOGRAPHY

[1] Christos Ignatakis (1994), "Bearing bodies of masonry buildings, Conservation restoration rehabilitation, p.190, Thessaloniki.

[2] Dimitris Bikas (1994), "Wooden floors. Assets, vulnerabilities, traditional and modern construction solutions, «Conservation restoration rehabilitation, p.337, Thessaloniki.

[3] “Pathology and rehabilitation of the components of the skeleton of traditional buildings "Paul Lutus (these pages were created and maintained by the program "Arachnophilia" by Paul Lutus with the help of "HTML Reference Library" of principal Stephen Le Hunte, The transfer of this study at the Internet is done by Charalambos Paspallis).

[4] Fyllitsa B. Karantoni (2004), "Construction of Masonry - Design and Repairs”, Athens.

[5] Christos Ignatakis (1994), "Structures of Bearing Masonry Regulation - Damages - Restoration”, 1st Lecture: Mechanics of masonry - Composition of bearing body - Response and damage typology under vertical and seismic loads, Thessaloniki.

[6] Costas A. Syrmakezis & Athanasios K. Antonopoulos (2008), "Use of fragility curves in Seismic Design of Masonry Structures", 3rd National Conference on Earthquake Engineering and Earthquake Technology, Article 1844, 5-7 November.

[7] Syrmakezis C.A., Antonopoulos A.K. & Mavrouli O.A. (2005b) "Analysis of Historical Masonry Structures using three dimensional Solid Elements", in Proceedings of the 10th International Conference on Civil Structural and Environmental Engineering Computing, Rome, Italy, August 29-September 2.

[8] Shinozuka M., Feng Q.M., Lee J.H., Nagamura T. (2003) “Statistical analysis of fragility curves”, in Proceedings of the Asian-Pacific Symposium on Structural Reliability and its Application (APSSRA 99).

[9] Spyridon N. Asimakopoulos (2007), Master Thesis, "Evaluation of seismic vulnerability of Byzantine churches with the development of methodology of fragility curves", Athens.

[10] Bavellas Christos & Bouzoukou Marianna (2005), "Comparative Study of masonry reinforcement with composite materials of organic and inorganic matrices", University of Patra School of Civil Engineering Department of Mechanical Engineering Department and Materials Technology, Patra.

[11] Christos Ignatakis (1994) "Mechanics of Masonry - Composition of skeleton-Response and damage typology under vertical and seismic loads", 1st Lecture, Technical Chamber of Greece, Department of Central Macedonia.

[12] Costas A. Syrmakezis (2010-11), "Analysis of Historical Constructions", Athens.

[13] "Restoration of Damaged Stonework", "Seminar of Maintenance and Rehabilitation of Monuments and Traditional Building (May 1999), K.E.K. development of Crete, Sitia.

APPENDIX 1

MODAL PARTICIPATION MASS RATIOS OF MASONRY WALL

TABLE: Modal Participating Mass Ratios															
OutputCase	StepType	StepNum	Period	UX	UY	UZ	SumUX	SumUY	SumUZ	RX	RY	RZ	SumRX	SumRY	SumRZ
Text	Text	Unitless	Sec	Unitless	Unitless	Unitless	Unitless	Unitless	Unitless	Unitless	Unitless	Unitless	Unitless	Unitless	Unitless
MODAL	Mode	1	0,222751	0,05091	0,000004547	1,859E-07	0,05091	0,000004547	1,859E-07	0,000003606	0,02676	0,00936	0,000003606	0,02676	0,00936
MODAL	Mode	2	0,154235	0,00443	0,00009969	0,000007884	0,05534	0,0001	0,00000807	0,00005694	0,00249	0,00692	0,00006055	0,02925	0,01628
MODAL	Mode	3	0,15035	0,00409	0,00402	0,000001212	0,05942	0,00413	0,000009282	0,00096	0,00194	0,00489	0,00102	0,03119	0,02117
MODAL	Mode	4	0,149668	0,00002911	0,00439	3,957E-07	0,05945	0,00851	0,000009678	0,00128	0,00002625	0,00262	0,0023	0,03122	0,02379
MODAL	Mode	5	0,141835	0,09383	0,00556	0,00002317	0,15328	0,01407	0,00003285	0,00248	0,04544	0,00249	0,00478	0,07666	0,02628
MODAL	Mode	6	0,114667	0,00278	0,27315	0,00026	0,15606	0,28722	0,00029	0,13414	0,00071	0,04553	0,13892	0,07737	0,07182
MODAL	Mode	7	0,110921	0,02316	0,08624	0,00001105	0,17922	0,37343	0,00031	0,02752	0,01089	0,16127	0,16644	0,08826	0,23308
MODAL	Mode	8	0,107901	0,09293	0,01032	0,000001441	0,27915	0,38375	0,00031	0,00273	0,04496	0,00012	0,16917	0,13322	0,2332
MODAL	Mode	9	0,104276	0,00044	0,03816	0,00002466	0,27959	0,42191	0,00033	0,01745	0,000003838	0,02413	0,18663	0,13322	0,25733
MODAL	Mode	10	0,103586	0,03741	0,00943	0,000001012	0,31699	0,43134	0,00033	0,00521	0,01767	0,0866	0,19184	0,15089	0,34393
MODAL	Mode	11	0,101067	0,02075	0,03653	0,00003261	0,33774	0,46787	0,00036	0,01656	0,00846	0,00135	0,2084	0,15935	0,34528
MODAL	Mode	12	0,096161	0,03825	0,00202	0,000004078	0,37599	0,46989	0,00037	0,00084	0,0235	0,00053	0,20924	0,18285	0,34581
MODAL	Mode	13	0,093887	0,05288	0,10928	0,00009274	0,42887	0,57917	0,00046	0,0575	0,02828	0,00218	0,26674	0,21113	0,34799
MODAL	Mode	14	0,086186	0,11761	0,01064	0,00001245	0,54648	0,58981	0,00047	0,00387	0,039	0,19282	0,27061	0,25013	0,54081
MODAL	Mode	15	0,08471	0,00441	0,00045	0,000003894	0,55089	0,59026	0,00048	0,00032	0,00243	0,00605	0,27093	0,25257	0,54686
MODAL	Mode	16	0,083851	0,03962	0,00008958	0,00004461	0,59051	0,59035	0,00052	0,00076	0,01658	0,02072	0,27169	0,26915	0,56758
MODAL	Mode	17	0,081799	0,00573	0,00317	0,000009206	0,59624	0,59352	0,00053	0,0016	0,00002981	0,00018	0,27329	0,26918	0,56775
MODAL	Mode	18	0,079905	0,00183	0,00521	0,00001209	0,59807	0,59873	0,00054	0,00135	0,00065	0,00308	0,27464	0,26982	0,57084
MODAL	Mode	19	0,07829	0,00297	0,00482	0,00001036	0,60103	0,60354	0,00055	0,00115	0,00088	0,01926	0,27578	0,2707	0,59009
MODAL	Mode	20	0,077359	0,00303	0,00761	0,0000757	0,60406	0,61115	0,00063	0,00406	0,001	0,00958	0,27984	0,2717	0,59967
MODAL	Mode	21	0,075391	0,00672	0,00088	4,712E-07	0,61079	0,61204	0,00063	0,00002166	0,00199	0,04197	0,27986	0,27369	0,64165
MODAL	Mode	22	0,074317	0,00586	0,00018	0,00008067	0,61665	0,61221	0,00071	0,00006132	0,00188	0,00197	0,27992	0,27557	0,64362

MODAL	Mode	23	0,072641	0,00025	0,02976	0,00006144	0,6169	0,64197	0,00077	0,01245	0,00019	0,00023	0,29237	0,27576	0,64384
MODAL	Mode	24	0,071624	0,02326	0,01632	0,00003875	0,64016	0,65829	0,00081	0,0032	0,00964	0,00481	0,29557	0,2854	0,64865
MODAL	Mode	25	0,069948	0,00032	0,00744	0,00051	0,64048	0,66572	0,00132	0,00237	0,00008924	0,00372	0,29793	0,28549	0,65238
MODAL	Mode	26	0,068916	0,00129	2,916E-07	0,00001023	0,64177	0,66573	0,00133	0,00001767	0,00131	0,00026	0,29795	0,2868	0,65264
MODAL	Mode	27	0,068586	0,00002317	0,00000053	3,645E-07	0,64179	0,66573	0,00133	0,00000133	0,00004139	0,00058	0,29795	0,28684	0,65322
MODAL	Mode	28	0,068317	0,00002697	0,00324	1,751E-07	0,64182	0,66897	0,00133	0,00043	0,00033	0,00235	0,29839	0,28717	0,65557
MODAL	Mode	29	0,06811	0,00029	0,00091	0,00002251	0,64211	0,66988	0,00135	0,00007269	0,00003468	0,0027	0,29846	0,28721	0,65827
MODAL	Mode	30	0,06784	0,00258	0,000006949	0,00002811	0,6447	0,66989	0,00138	0,00085	0,00039	0,00036	0,29931	0,28759	0,65863
MODAL	Mode	31	0,066213	0,00149	0,00341	0,00001403	0,64618	0,6733	0,00139	0,00308	0,00028	0,00329	0,30239	0,28788	0,66191
MODAL	Mode	32	0,064328	0,00076	0,00073	0,000002333	0,64694	0,67403	0,00139	0,00055	0,00027	0,00117	0,30294	0,28815	0,66308
MODAL	Mode	33	0,064005	0,00587	0,00016	0,000007023	0,65281	0,67419	0,0014	0,00001354	0,00097	0,00178	0,30295	0,28912	0,66486
MODAL	Mode	34	0,062736	0,01169	0,00543	0,00012	0,66451	0,67962	0,00153	0,00277	0,00316	0,00017	0,30573	0,29228	0,66503
MODAL	Mode	35	0,061684	0,00116	0,03163	0,00031	0,66566	0,71125	0,00184	0,01999	0,00003394	0,00036	0,32572	0,29232	0,66539
MODAL	Mode	36	0,061239	0,00225	0,00016	0,00003309	0,66791	0,71142	0,00187	0,00006275	0,00064	0,00124	0,32578	0,29296	0,66663
MODAL	Mode	37	0,058981	0,00449	0,00103	0,00038	0,6724	0,71245	0,00225	0,00023	0,00275	0,00081	0,32601	0,29571	0,66743
MODAL	Mode	38	0,058439	0,01266	0,00198	0,000004346	0,68507	0,71443	0,00226	1,937E-07	0,0051	0,01467	0,32601	0,30081	0,6821
MODAL	Mode	39	0,057396	0,00044	0,00338	0,000001329	0,68551	0,71781	0,00226	0,00011	0,0013	0,00558	0,32612	0,30211	0,68768
MODAL	Mode	40	0,056849	0,00339	0,0052	0,000001412	0,6889	0,72301	0,00226	0,00186	0,0001	0,01142	0,32798	0,30221	0,6991
MODAL	Mode	41	0,05608	0,00171	0,00039	0,000003926	0,69061	0,7234	0,00226	0,00029	0,00027	0,000001381	0,32827	0,30248	0,6991
MODAL	Mode	42	0,054393	0,00089	0,00006005	0,000004058	0,6915	0,72346	0,00227	0,00008368	0,00155	0,0011	0,32836	0,30403	0,70019
MODAL	Mode	43	0,052967	0,00827	0,00029	0,00005068	0,69977	0,72374	0,00232	0,00074	0,00176	0,00019	0,3291	0,3058	0,70038
MODAL	Mode	44	0,052665	0,00551	0,0001	0,00014	0,70529	0,72385	0,00246	0,00106	0,00257	0,00111	0,33016	0,30837	0,70149
MODAL	Mode	45	0,0522	0,00018	0,00956	0,00013	0,70546	0,73341	0,00259	0,00002062	0,00002081	4,9E-12	0,33018	0,30839	0,70149
MODAL	Mode	46	0,051238	0,00046	7,206E-09	0,0000117	0,70592	0,73341	0,0026	0,00035	0,00022	0,00022	0,33053	0,30861	0,70171
MODAL	Mode	47	0,05108	0,00878	0,0046	0,00002442	0,7147	0,73801	0,00263	0,00018	0,0001	0,0017	0,33071	0,30871	0,70341
MODAL	Mode	48	0,050616	0,00126	0,00077	0,00002547	0,71596	0,73878	0,00265	9,123E-07	0,00063	1,665E-08	0,33071	0,30934	0,70341

MODAL	Mode	49	0,050149	0,00084	0,00071	0,00001302	0,7168	0,73949	0,00267	0,00003653	0,00055	0,00001309	0,33074	0,30989	0,70342
MODAL	Mode	50	0,04946	0,00004657	0,00002596	0,00036	0,71685	0,73952	0,00303	0,00613	0,00005335	0,00051	0,33687	0,30994	0,70393
MODAL	Mode	51	0,048948	0,00078	0,00041	0,00015	0,71763	0,73993	0,00318	0,00007769	0,00013	0,00019	0,33695	0,31007	0,70412
MODAL	Mode	52	0,048751	0,000004045	0,00003322	3,586E-08	0,71763	0,73996	0,00318	0,000004003	2,876E-08	0,00002466	0,33695	0,31007	0,70415
MODAL	Mode	53	0,048655	0,0017	0,00019	0,00005006	0,71933	0,74015	0,00323	0,00001958	0,00013	0,00086	0,33697	0,3102	0,70501
MODAL	Mode	54	0,048135	0,00026	0,01022	0,00028	0,71958	0,75037	0,00351	0,00194	0,00007805	0,00152	0,33892	0,31028	0,70653
MODAL	Mode	55	0,047936	0,0056	0,0005	0,0000245	0,72519	0,75087	0,00354	0,00001152	0,00009873	0,01101	0,33893	0,31038	0,71754
MODAL	Mode	56	0,047285	0,00349	0,01065	0,00006432	0,72867	0,76153	0,0036	0,00051	0,00146	0,02243	0,33944	0,31184	0,73997
MODAL	Mode	57	0,047194	0,00398	0,00007346	0,00004101	0,73265	0,7616	0,00364	0,00017	0,00211	0,00072	0,3396	0,31395	0,74069
MODAL	Mode	58	0,046647	0,00116	0,00006279	0,00043	0,73382	0,76166	0,00407	0,00057	0,000007968	0,00009763	0,34018	0,31396	0,74078
MODAL	Mode	59	0,046037	0,00007431	0,00295	0,000008047	0,73389	0,76461	0,00408	0,00015	0,000002442	0,0041	0,34032	0,31396	0,74488
MODAL	Mode	60	0,045455	0,00009705	0,0005	0,00002503	0,73399	0,76512	0,0041	0,00002873	0,00007524	0,00034	0,34035	0,31403	0,74523
MODAL	Mode	61	0,04517	0,00028	0,00259	0,00007342	0,73427	0,76771	0,00418	0,00018	0,00003839	0,00002394	0,34053	0,31407	0,74525
MODAL	Mode	62	0,044028	0,00003747	0,00000232	0,00173	0,73431	0,76771	0,00591	0,00116	0,00005656	0,00002897	0,34169	0,31413	0,74528
MODAL	Mode	63	0,043562	0,00537	0,00026	0,00319	0,73968	0,76796	0,0091	0,00064	0,00363	0,00108	0,34233	0,31776	0,74636
MODAL	Mode	64	0,043294	1,989E-07	0,00076	0,00002116	0,73968	0,76872	0,00912	0,00001845	0,00001892	0,00022	0,34235	0,31778	0,74658
MODAL	Mode	65	0,043228	0,00019	0,00158	0,00022	0,73988	0,7703	0,00933	0,00001475	0,00023	0,00082	0,34236	0,31801	0,7474
MODAL	Mode	66	0,042614	0,00832	0,00435	0,00012	0,7482	0,77465	0,00945	0,0004	0,0013	0,0001	0,34276	0,3193	0,7475
MODAL	Mode	67	0,042371	0,00535	0,00051	0,00003968	0,75355	0,77516	0,00949	0,000005234	0,00018	0,00181	0,34277	0,31948	0,74931
MODAL	Mode	68	0,04178	0,00001201	0,00283	2,688E-07	0,75356	0,77799	0,00949	0,00097	0,00145	0,00005477	0,34374	0,32093	0,74936
MODAL	Mode	69	0,041325	0,000004987	0,0041	0,00022	0,75356	0,78209	0,0097	0,00016	0,0000917	0,0000214	0,34389	0,32102	0,74939
MODAL	Mode	70	0,041095	0,00188	0,00177	0,0000598	0,75544	0,78386	0,00976	0,0000258	0,00015	0,00075	0,34392	0,32117	0,75013
MODAL	Mode	71	0,04097	0,0029	0,00218	0,00112	0,75835	0,78604	0,01088	0,00062	0,00015	0,00468	0,34453	0,32132	0,75481
MODAL	Mode	72	0,040682	0,01889	0,00119	0,00014	0,77723	0,78723	0,01103	0,00001903	0,00005764	0,01382	0,34455	0,32138	0,76863
MODAL	Mode	73	0,040444	0,00135	0,00017	0,00071	0,77858	0,78739	0,01173	0,00038	0,00005104	0,00103	0,34493	0,32143	0,76966
MODAL	Mode	74	0,039902	0,00038	0,00032	0,000002469	0,77896	0,78771	0,01174	0,000007694	0,00023	0,000002223	0,34494	0,32166	0,76967

MODAL	Mode	75	0,03917	0,00125	0,0008	0,00175	0,78021	0,78851	0,01348	0,00022	0,00404	0,00141	0,34516	0,32571	0,77108
MODAL	Mode	76	0,039133	0,0002	0,00056	0,00079	0,78041	0,78907	0,01427	0,000006029	0,00005347	0,00042	0,34516	0,32576	0,7715
MODAL	Mode	77	0,038785	0,00023	0,00003853	0,000000786	0,78063	0,78911	0,01427	0,00012	0,00007535	0,00019	0,34528	0,32584	0,77169
MODAL	Mode	78	0,038748	0,000004648	0,000005205	0,00009271	0,78064	0,78911	0,01437	0,00015	0,00007777	0,00003841	0,34543	0,32591	0,77173
MODAL	Mode	79	0,037753	0,00298	0,0001	0,00046	0,78362	0,78922	0,01483	0,00099	0,00151	0,0019	0,34643	0,32742	0,77363
MODAL	Mode	80	0,037401	0,00079	0,000009397	0,00585	0,78441	0,78923	0,02068	0,00523	0,00227	0,00036	0,35165	0,32969	0,77398
MODAL	Mode	81	0,037088	0,00001428	0,00018	0,00524	0,78442	0,7894	0,02592	0,00861	0,0027	0,00007633	0,36026	0,33239	0,77406
MODAL	Mode	82	0,036907	0,00045	0,00007017	0,00014	0,78487	0,78947	0,02606	0,0028	0,00056	0,00012	0,36306	0,33295	0,77418
MODAL	Mode	83	0,036667	0,00131	0,0000929	0,00143	0,78618	0,78957	0,02749	0,00038	0,00108	0,00269	0,36344	0,33404	0,77686
MODAL	Mode	84	0,036311	0,00044	0,00002587	0,00529	0,78662	0,78959	0,03278	0,0051	0,00419	0,00005902	0,36854	0,33822	0,77692
MODAL	Mode	85	0,03619	0,00002188	0,000002149	1,178E-07	0,78664	0,7896	0,03278	0,00005319	2,831E-09	0,000004135	0,36859	0,33822	0,77693
MODAL	Mode	86	0,036027	0,00034	0,00697	0,000001193	0,78699	0,79656	0,03278	0,0000036	0,00007993	0,0015	0,3686	0,3383	0,77842
MODAL	Mode	87	0,035732	0,00044	0,00017	0,04001	0,78743	0,79673	0,07279	0,05098	0,00759	0,00095	0,41958	0,34589	0,77937
MODAL	Mode	88	0,03554	0,00019	0,00022	0,00349	0,78762	0,79695	0,07628	0,00199	0,00102	0,00045	0,42157	0,34691	0,77982
MODAL	Mode	89	0,035395	0,00375	0,0003	0,00401	0,79137	0,79725	0,08028	0,00077	0,00315	0,00271	0,42233	0,35006	0,78253
MODAL	Mode	90	0,035243	0,00389	0,00003571	0,00591	0,79527	0,79728	0,08619	0,00494	0,00322	0,00092	0,42727	0,35329	0,78344
MODAL	Mode	91	0,035134	0,00189	0,00001356	0,00064	0,79715	0,7973	0,08683	0,000003197	9,596E-07	0,00168	0,42727	0,35329	0,78513
MODAL	Mode	92	0,035078	0,00274	0,00021	0,00301	0,79989	0,79751	0,08984	0,00275	0,00022	0,00045	0,43002	0,3535	0,78558
MODAL	Mode	93	0,034594	0,0003	0,00019	0,00588	0,8002	0,7977	0,09572	0,00153	0,00506	0,00081	0,43155	0,35856	0,78639
MODAL	Mode	94	0,034311	0,00041	0,00073	0,00028	0,80061	0,79843	0,096	0,00082	0,00276	0,00145	0,43238	0,36133	0,78785
MODAL	Mode	95	0,03419	0,00004413	0,00002012	0,00093	0,80066	0,79845	0,09692	0,00254	0,00212	0,000007897	0,43492	0,36344	0,78785
MODAL	Mode	96	0,034086	0,00026	0,00125	0,12912	0,80092	0,7997	0,22604	0,09769	0,02345	0,00055	0,53261	0,38689	0,7884
MODAL	Mode	97	0,033957	0,00005365	7,405E-07	0,00305	0,80097	0,7997	0,22909	0,004	0,00444	0,00006496	0,53661	0,39134	0,78847
MODAL	Mode	98	0,033829	0,00002039	0,00086	0,00793	0,80099	0,80056	0,23702	0,00341	0,00419	0,00002472	0,54002	0,39552	0,78849
MODAL	Mode	99	0,033105	0,00024	0,00177	0,00225	0,80123	0,80234	0,23926	0,00403	0,01116	0,0002	0,54405	0,40668	0,78869
MODAL	Mode	100	0,032981	0,00072	0,00682	0,07977	0,80195	0,80916	0,31903	0,11236	0,0323	0,00337	0,65641	0,43899	0,79207

MODAL	Mode	101	0,032695	0,00029	0,00164	0,00015	0,80224	0,8108	0,31918	0,0000561	0,00048	0,00022	0,65647	0,43947	0,79229
MODAL	Mode	102	0,032526	0,00072	0,00008322	0,00041	0,80297	0,81089	0,31959	0,00075	0,00016	0,00067	0,65722	0,43962	0,79296
MODAL	Mode	103	0,032366	0,00069	0,00031	0,00018	0,80366	0,8112	0,31977	0,00011	0,00005499	0,00017	0,65733	0,43968	0,79313
MODAL	Mode	104	0,032259	0,00019	0,00272	0,00204	0,80385	0,81392	0,32181	0,00132	0,0156	0,00084	0,65865	0,45528	0,79397
MODAL	Mode	105	0,032213	0,00001346	0,00299	0,01304	0,80386	0,8169	0,33485	0,00016	0,01353	0,00034	0,65881	0,46882	0,79431
MODAL	Mode	106	0,032051	0,00249	0,00001057	0,04643	0,80635	0,81691	0,38129	0,00442	0,01888	0,00003	0,66323	0,4877	0,79434
MODAL	Mode	107	0,031922	0,00014	0,00166	0,05494	0,80649	0,81857	0,43623	0,01971	0,03948	7,117E-07	0,68294	0,52718	0,79434
MODAL	Mode	108	0,031793	0,00067	0,00004648	0,00041	0,80716	0,81862	0,43663	1,316E-11	0,00018	0,00017	0,68294	0,52736	0,79451
MODAL	Mode	109	0,031762	0,00115	0,000004173	0,00409	0,80831	0,81862	0,44073	0,00029	0,00259	0,00026	0,68323	0,52995	0,79477
MODAL	Mode	110	0,031711	0,0004	0,00008081	0,00221	0,80871	0,8187	0,44294	0,00036	0,00139	0,00026	0,68359	0,53134	0,79503
MODAL	Mode	111	0,031523	0,0003	0,00003117	0,00162	0,80901	0,81874	0,44456	0,0008	0,00291	0,00001535	0,68438	0,53425	0,79504
MODAL	Mode	112	0,031474	0,00016	0,00008268	0,00255	0,80916	0,81882	0,44711	0,00068	0,00868	0,00014	0,68507	0,54293	0,79518
MODAL	Mode	113	0,031205	0,00006429	7,586E-07	0,00123	0,80923	0,81882	0,44834	0,00052	0,00028	0,00001319	0,68559	0,54321	0,7952
MODAL	Mode	114	0,031114	0,00057	0,00005762	0,03538	0,8098	0,81888	0,48371	0,00006572	0,01386	0,00014	0,68566	0,55708	0,79534
MODAL	Mode	115	0,030983	0,00028	0,00086	0,01139	0,81008	0,81974	0,4951	0,00001777	0,00034	0,00153	0,68567	0,55742	0,79686
MODAL	Mode	116	0,030905	0,00314	0,00085	0,00959	0,81322	0,82059	0,50469	0,00279	0,00004711	0,0021	0,68846	0,55747	0,79896
MODAL	Mode	117	0,030587	0,00011	0,00105	0,00015	0,81333	0,82164	0,50484	0,0000206	0,00027	0,00166	0,68848	0,55774	0,80062
MODAL	Mode	118	0,030458	1,691E-07	0,0000415	0,01455	0,81333	0,82168	0,51939	0,00633	0,02291	0,00008023	0,69482	0,58065	0,8007
MODAL	Mode	119	0,030407	0,00019	0,00011	0,03095	0,81352	0,82179	0,55034	0,00298	0,00086	0,00085	0,6978	0,58151	0,80155
MODAL	Mode	120	0,030266	0,00172	0,000008325	0,04626	0,81524	0,8218	0,5966	0,00478	0,049	0,00002336	0,70257	0,63051	0,80157
MODAL	Mode	121	0,030163	0,00027	0,0038	0,00064	0,81551	0,8256	0,59725	0,00073	0,0000122	0,00786	0,70331	0,63052	0,80943
MODAL	Mode	122	0,029856	0,00074	0,00169	0,00032	0,81625	0,82729	0,59756	0,00049	0,00046	0,00022	0,7038	0,63098	0,80965
MODAL	Mode	123	0,02982	0,00087	0,00012	0,00012	0,81712	0,82741	0,59768	0,000004178	0,0152	0,00012	0,7038	0,64618	0,80977
MODAL	Mode	124	0,029635	0,00239	0,00092	0,00095	0,81951	0,82833	0,59863	0,00016	0,00033	0,00114	0,70397	0,6465	0,81091
MODAL	Mode	125	0,029587	0,00083	0,00001597	0,01353	0,82035	0,82835	0,61216	0,0024	0,00023	7,558E-07	0,70636	0,64674	0,81091
MODAL	Mode	126	0,029456	0,00011	0,00074	0,01282	0,82046	0,82909	0,62498	0,00441	0,0155	0,00006501	0,71078	0,66224	0,81098

MODAL	Mode	127	0,029426	0,00046	0,000003228	0,02766	0,82092	0,82909	0,65264	0,01252	0,00949	2,96E-08	0,72329	0,67173	0,81098
MODAL	Mode	128	0,029222	0,000003509	0,00034	0,00213	0,82092	0,82943	0,65477	0,00111	0,00021	0,00079	0,72441	0,67195	0,81177
MODAL	Mode	129	0,029158	0,00072	0,000004315	0,00623	0,82164	0,82944	0,661	0,00171	0,00034	0,00255	0,72612	0,67229	0,81432
MODAL	Mode	130	0,029104	0,000001302	0,00124	0,00002593	0,82164	0,83067	0,66103	0,00003254	2,287E-07	0,00053	0,72616	0,67229	0,81485
MODAL	Mode	131	0,02897	0,00007246	0,00005168	0,00317	0,82171	0,83073	0,66419	0,00392	0,0005	0,00004078	0,73007	0,67279	0,81489
MODAL	Mode	132	0,028883	0,00001869	0,00148	0,01598	0,82173	0,8322	0,68017	0,01424	0,00522	0,00047	0,74432	0,67801	0,81536
MODAL	Mode	133	0,028658	0,00181	0,000009867	0,00398	0,82354	0,83221	0,68415	0,00132	0,00008863	0,00006716	0,74563	0,6781	0,81542
MODAL	Mode	134	0,028502	0,000004039	0,00019	0,00933	0,82355	0,8324	0,69348	0,00621	0,0008	0,000001751	0,75184	0,6789	0,81542
MODAL	Mode	135	0,028284	0,00002518	0,000007763	0,00267	0,82357	0,83241	0,69615	0,00012	0,00138	0,0001	0,75196	0,68027	0,81553
MODAL	Mode	136	0,028145	0,00209	0,0000685	0,00292	0,82566	0,83248	0,69907	0,0009	0,00075	0,00165	0,75287	0,68102	0,81718
MODAL	Mode	137	0,028062	0,00033	0,00041	0,00432	0,826	0,83288	0,70339	0,00453	0,00006226	0,00082	0,7574	0,68109	0,818
MODAL	Mode	138	0,028005	0,00074	0,00214	0,00088	0,82674	0,83503	0,70427	0,00031	0,00003565	0,0000112	0,75771	0,68112	0,81802
MODAL	Mode	139	0,027771	0,00146	0,0000699	0,00044	0,8282	0,8351	0,70471	0,00156	0,00029	0,00016	0,75927	0,68141	0,81818
MODAL	Mode	140	0,02758	0,00015	0,00085	0,00121	0,82835	0,83595	0,70593	0,00255	0,00177	0,00134	0,76182	0,68318	0,81951
MODAL	Mode	141	0,027391	0,000002088	0,00011	0,00007216	0,82835	0,83605	0,706	0,0000333	0,00008676	0,00008598	0,76185	0,68327	0,8196
MODAL	Mode	142	0,027097	0,0000809	0,00004579	0,00058	0,82844	0,8361	0,70658	0,00011	0,00085	0,00003117	0,76196	0,68412	0,81963
MODAL	Mode	143	0,026931	0,00439	0,00122	0,00073	0,83282	0,83732	0,70731	0,00094	0,00292	0,00027	0,7629	0,68704	0,81989
MODAL	Mode	144	0,026885	0,0044	0,00368	0,00112	0,83722	0,841	0,70843	0,00002242	0,00226	0,00995	0,76293	0,6893	0,82984
MODAL	Mode	145	0,026398	0,00005233	0,0000192	0,000004331	0,83728	0,84102	0,70844	0,00111	0,00049	0,00014	0,76403	0,68979	0,82998
MODAL	Mode	146	0,026385	0,00055	0,00051	0,00084	0,83782	0,84153	0,70928	0,000002731	0,00043	3,413E-07	0,76403	0,69022	0,82998
MODAL	Mode	147	0,026161	0,00052	0,00016	0,00008331	0,83835	0,84169	0,70936	0,00001045	0,00013	0,00021	0,76405	0,69035	0,83018
MODAL	Mode	148	0,026002	0,00064	4,009E-07	0,00018	0,83899	0,84169	0,70954	0,00002458	0,00034	0,0004	0,76407	0,69069	0,83059
MODAL	Mode	149	0,025929	0,00001125	0,00001206	0,00016	0,839	0,84171	0,70971	0,00012	0,00004604	0,00003421	0,76419	0,69074	0,83062
MODAL	Mode	150	0,025847	0,00015	0,0000185	0,00009952	0,83915	0,84172	0,70981	0,0002	0,00015	0,000000357	0,76439	0,69089	0,83062
MODAL	Mode	151	0,025644	0,00048	0,00124	0,00013	0,83963	0,84297	0,70994	0,00097	0,0066	0,00075	0,76536	0,69749	0,83137
MODAL	Mode	152	0,025446	0,00058	0,0000813	0,00425	0,84022	0,84305	0,71418	0,00363	0,00426	0,00032	0,76898	0,70174	0,83169

MODAL	Mode	153	0,025239	0,00226	0,000001613	0,0042	0,84247	0,84305	0,71838	0,00452	0,00584	0,00008971	0,7735	0,70759	0,83178
MODAL	Mode	154	0,025177	0,0008	0,000036	0,00422	0,84327	0,84309	0,7226	0,00269	0,00606	0,00014	0,7762	0,71364	0,83191
MODAL	Mode	155	0,025088	0,00002443	0,00031	4,451E-07	0,8433	0,8434	0,7226	0,000001785	0,0008	0,00006764	0,7762	0,71444	0,83198
MODAL	Mode	156	0,024986	0,00041	0,000003621	0,00003666	0,84371	0,84341	0,72263	0,00052	0,0007	0,00024	0,77671	0,71514	0,83223
MODAL	Mode	157	0,024856	0,00001168	0,00006903	0,00053	0,84372	0,84347	0,72317	0,00003507	0,00003086	0,00004657	0,77675	0,71517	0,83227
MODAL	Mode	158	0,024818	0,00003353	0,00119	0,00014	0,84376	0,84466	0,7233	0,00069	0,0015	0,00013	0,77744	0,71667	0,8324
MODAL	Mode	159	0,024654	0,00175	0,00178	0,00071	0,84551	0,84645	0,72401	0,00203	0,00434	0,000005001	0,77947	0,72101	0,83241
MODAL	Mode	160	0,024588	0,0006	0,00021	0,00003011	0,8461	0,84666	0,72404	0,0002	9,438E-07	0,00002156	0,77968	0,72101	0,83243
MODAL	Mode	161	0,024558	0,000001705	0,00002188	5,515E-07	0,8461	0,84668	0,72404	4,583E-07	0,000001055	0,00003022	0,77968	0,72101	0,83246
MODAL	Mode	162	0,024546	0,00083	0,00193	0,00009494	0,84693	0,84861	0,72414	0,00047	0,00001531	0,00016	0,78015	0,72103	0,83262
MODAL	Mode	163	0,024493	0,00025	0,00045	0,00266	0,84718	0,84906	0,72679	0,00299	0,00556	0,00009147	0,78314	0,72658	0,83271
MODAL	Mode	164	0,024387	0,000003374	0,00054	0,00073	0,84718	0,8496	0,72752	0,00082	0,00013	0,000045	0,78396	0,72671	0,83275
MODAL	Mode	165	0,02414	0,00036	0,00009584	0,00006474	0,84754	0,84969	0,72759	0,000001839	0,0000551	0,00007602	0,78396	0,72677	0,83283
MODAL	Mode	166	0,024012	0,00424	0,00046	0,00089	0,85178	0,85015	0,72848	0,00272	0,00174	0,00756	0,78667	0,72851	0,8404
MODAL	Mode	167	0,023986	0,00061	0,00001372	0,00204	0,85239	0,85017	0,73052	0,00563	0,00716	0,000000228	0,7923	0,73567	0,8404
MODAL	Mode	168	0,023869	0,00007959	0,00001319	0,00004303	0,85247	0,85018	0,73056	0,000009903	0,000007363	0,00002659	0,79231	0,73567	0,84042
MODAL	Mode	169	0,023793	0,000006255	0,00006277	0,00096	0,85248	0,85024	0,73153	0,00254	0,00381	0,00029	0,79486	0,73948	0,84071
MODAL	Mode	170	0,023676	0,00023	0,00002478	0,00001623	0,85271	0,85027	0,73154	0,0000345	0,00032	0,00025	0,79489	0,7398	0,84096
MODAL	Mode	171	0,023645	0,00002888	0,00009449	0,00078	0,85274	0,85036	0,73232	0,0008	0,00148	0,000009426	0,79569	0,74128	0,84097
MODAL	Mode	172	0,023571	0,00032	0,0021	0,00223	0,85306	0,85247	0,73455	0,00033	0,00155	0,00053	0,79602	0,74283	0,8415
MODAL	Mode	173	0,02343	0,00046	0,00068	0,00041	0,85351	0,85315	0,73496	0,00069	0,00039	0,00029	0,79671	0,74323	0,84178
MODAL	Mode	174	0,023314	0,0005	0,00292	0,00223	0,85402	0,85607	0,73719	0,00442	0,00592	0,0008	0,80113	0,74915	0,84258
MODAL	Mode	175	0,023247	0,00084	0,0000239	0,0000233	0,85486	0,85609	0,73721	0,00003063	0,00035	0,00003646	0,80116	0,74949	0,84262
MODAL	Mode	176	0,023159	0,00055	0,00019	0,00028	0,85541	0,85629	0,73749	0,00004895	0,00298	0,0042	0,80121	0,75247	0,84682
MODAL	Mode	177	0,023063	0,00028	0,00044	0,01132	0,85569	0,85673	0,74881	0,01309	0,02579	0,00077	0,8143	0,77826	0,84759
MODAL	Mode	178	0,023029	0,0012	0,00091	0,000005026	0,85689	0,85764	0,74881	0,00001551	0,00061	0,00195	0,81431	0,77887	0,84955

MODAL	Mode	179	0,02292	0,00005893	0,0012	0,00000207	0,85695	0,85884	0,74882	0,00008953	0,00002912	0,00038	0,8144	0,7789	0,84993
MODAL	Mode	180	0,022883	0,00298	0,00004239	0,00103	0,85992	0,85888	0,74985	0,00072	0,00306	0,00166	0,81513	0,78196	0,85159
MODAL	Mode	181	0,022755	0,00005142	0,00009985	0,00581	0,85997	0,85898	0,75566	0,00377	0,00655	0,00007761	0,8189	0,78851	0,85167
MODAL	Mode	182	0,022585	0,00025	0,00003484	0,00177	0,86022	0,85901	0,75743	0,00222	0,00152	0,00075	0,82112	0,79004	0,85242
MODAL	Mode	183	0,022534	0,00003328	0,0002	0,000005407	0,86025	0,85921	0,75744	0,00008607	0,00038	0,00061	0,82121	0,79042	0,85303
MODAL	Mode	184	0,022512	0,00008262	0,00024	0,00402	0,86034	0,85945	0,76145	0,00498	0,00878	0,00047	0,82619	0,7992	0,8535
MODAL	Mode	185	0,022366	0,00056	0,00113	0,00011	0,8609	0,86059	0,76156	0,00031	0,00003525	0,00074	0,82649	0,79924	0,85424
MODAL	Mode	186	0,022305	0,00021	0,0004	0,00031	0,86111	0,86099	0,76187	0,00003533	4,037E-07	0,00022	0,82653	0,79924	0,85446
MODAL	Mode	187	0,022255	0,00031	0,00113	0,00089	0,86142	0,86212	0,76276	0,00051	0,00202	0,00027	0,82704	0,80125	0,85473
MODAL	Mode	188	0,022227	0,00028	0,00013	0,00021	0,8617	0,86225	0,76298	0,00001014	0,000002535	0,00015	0,82705	0,80126	0,85488
MODAL	Mode	189	0,022149	0,00161	0,00053	0,00003902	0,86332	0,86279	0,76302	0,00036	0,000009331	0,00039	0,82741	0,80127	0,85527
MODAL	Mode	190	0,022086	0,00124	0,00025	0,00071	0,86455	0,86303	0,76373	0,0014	0,00078	0,00111	0,82881	0,80205	0,85637
MODAL	Mode	191	0,022005	0,0029	0,00418	0,0000148	0,86746	0,86721	0,76374	0,00103	4,107E-07	0,0051	0,82984	0,80205	0,86147
MODAL	Mode	192	0,021962	0,00049	0,00002725	0,00009696	0,86795	0,86724	0,76384	0,000007448	0,000009135	0,00022	0,82985	0,80206	0,86169
MODAL	Mode	193	0,021889	0,0008	0,00101	0,00071	0,86874	0,86825	0,76455	0,00009124	0,00045	0,000003797	0,82994	0,8025	0,8617
MODAL	Mode	194	0,021872	0,00004625	0,00048	0,00126	0,86879	0,86873	0,76582	0,00007042	0,0004	0,00003776	0,83001	0,8029	0,86173
MODAL	Mode	195	0,021794	0,00031	0,00206	0,00034	0,8691	0,87079	0,76616	0,00012	0,00088	0,00355	0,83013	0,80378	0,86528
MODAL	Mode	196	0,021744	0,000003467	0,00037	0,00015	0,8691	0,87116	0,7663	0,00005038	0,00253	0,00019	0,83018	0,80631	0,86547
MODAL	Mode	197	0,021721	0,0009	0,00034	0,00067	0,87	0,8715	0,76697	0,00019	0,00009344	0,00094	0,83037	0,8064	0,86641
MODAL	Mode	198	0,021679	0,0000621	0,00042	0,00001769	0,87006	0,87192	0,76699	0,00004631	0,00003775	0,00007093	0,83041	0,80644	0,86648
MODAL	Mode	199	0,02156	0,00192	0,000003318	0,000002613	0,87198	0,87192	0,76699	0,00003308	0,00006133	0,0006	0,83045	0,8065	0,86708
MODAL	Mode	200	0,021547	0,000000329	0,00072	0,00003046	0,87198	0,87264	0,76702	0,00022	0,00137	0,00044	0,83066	0,80787	0,86752
MODAL	Mode	201	0,021447	0,00018	0,00055	0,00007258	0,87215	0,87319	0,76709	2,201E-07	0,00001827	0,0002	0,83066	0,80789	0,86772
MODAL	Mode	202	0,021403	8,402E-08	0,00002003	0,00004466	0,87215	0,87321	0,76714	0,00001316	0,000008668	0,00003237	0,83068	0,8079	0,86776
MODAL	Mode	203	0,02139	0,00007698	0,000004802	0,00001512	0,87223	0,87321	0,76715	0,000005672	0,00000826	0,00017	0,83068	0,80791	0,86793
MODAL	Mode	204	0,021271	0,00097	0,0004	0,00137	0,8732	0,87361	0,76852	0,00061	0,00073	0,00003197	0,83129	0,80864	0,86796

MODAL	Mode	205	0,021206	0,0000273	0,00015	0,00064	0,87323	0,87376	0,76917	0,00053	0,00132	0,00027	0,83182	0,80996	0,86823
MODAL	Mode	206	0,02117	0,00159	0,00027	0,00009038	0,87483	0,87404	0,76926	0,000001294	0,00045	0,0016	0,83182	0,81041	0,86983
MODAL	Mode	207	0,021102	0,00003841	0,00086	0,00004607	0,87486	0,87489	0,7693	0,00023	0,00132	0,00028	0,83205	0,81173	0,87011
MODAL	Mode	208	0,021053	0,00075	0,00004059	0,00039	0,87562	0,87493	0,76969	0,00036	0,00025	0,000006273	0,83241	0,81198	0,87012
MODAL	Mode	209	0,020967	0,00028	0,00015	0,0002	0,8759	0,87508	0,76989	0,00019	0,00006891	0,00012	0,8326	0,81205	0,87023
MODAL	Mode	210	0,020884	0,00006878	0,00027	0,00004127	0,87597	0,87535	0,76993	0,00015	0,00057	0,00024	0,83275	0,81262	0,87047
MODAL	Mode	211	0,020815	0,00023	0,00003565	0,00013	0,8762	0,87539	0,77006	0,00004368	0,00009452	0,00007315	0,8328	0,81272	0,87054
MODAL	Mode	212	0,020815	0,0000291	0,00003565	5,793E-08	0,87623	0,87542	0,77006	1,577E-08	0,00002159	0,000004566	0,8328	0,81274	0,87055
MODAL	Mode	213	0,020799	0,00096	0,00119	0,00029	0,87719	0,87661	0,77035	8,074E-07	0,00009123	0,001	0,8328	0,81283	0,87155
MODAL	Mode	214	0,020595	0,000003737	0,00008729	0,00035	0,87719	0,8767	0,7707	0,00063	0,0023	0,000001191	0,83343	0,81513	0,87155
MODAL	Mode	215	0,020546	0,00002393	0,00026	0,00001076	0,87722	0,87696	0,77071	0,00004324	0,00001272	0,00002441	0,83348	0,81515	0,87158
MODAL	Mode	216	0,020433	0,00037	0,00018	0,00319	0,87758	0,87714	0,7739	0,00173	0,00763	0,00036	0,8352	0,82278	0,87194
MODAL	Mode	217	0,020377	0,00015	0,00045	0,00143	0,87773	0,87759	0,77533	0,00114	0,00119	0,00013	0,83635	0,82397	0,87207
MODAL	Mode	218	0,020289	0,00078	0,00037	0,00008685	0,87851	0,87797	0,77542	0,000001814	0,00001969	0,00095	0,83635	0,82399	0,87302
MODAL	Mode	219	0,020247	0,00009482	0,00183	0,0001	0,87861	0,87979	0,77552	0,00013	0,00008114	0,00002003	0,83648	0,82407	0,87304
MODAL	Mode	220	0,020161	0,00023	0,0005	0,00027	0,87883	0,88029	0,77579	0,00002236	0,00026	0,00004919	0,8365	0,82433	0,87309
MODAL	Mode	221	0,020137	0,000000267	0,00173	0,00067	0,87883	0,88202	0,77646	0,00102	0,00224	0,00013	0,83753	0,82657	0,87322
MODAL	Mode	222	0,02009	0,00002098	8,758E-07	0,00004474	0,87885	0,88202	0,7765	0,00001264	0,00001749	0,00001027	0,83754	0,82659	0,87323
MODAL	Mode	223	0,020019	0,00044	0,00001396	0,00262	0,87929	0,88204	0,77912	0,00202	0,00588	0,0000737	0,83956	0,83247	0,8733
MODAL	Mode	224	0,019995	0,00144	0,00147	0,00018	0,88073	0,8835	0,7793	0,00077	0,00136	0,00002438	0,84033	0,83382	0,87332
MODAL	Mode	225	0,019888	0,00072	0,00025	0,00014	0,88145	0,88376	0,77944	0,00012	0,0000644	0,00101	0,84045	0,83389	0,87434
MODAL	Mode	226	0,019806	0,000004906	0,00086	0,00003871	0,88145	0,88462	0,77947	0,00033	0,00025	0,00015	0,84078	0,83414	0,87448
MODAL	Mode	227	0,019686	0,0002	3,479E-07	0,00004077	0,88166	0,88462	0,77951	0,00004992	0,00003664	0,00005404	0,84083	0,83417	0,87454
MODAL	Mode	228	0,019651	0,00017	0,00021	0,00005674	0,88183	0,88483	0,77957	0,00025	0,00012	0,00018	0,84109	0,83429	0,87472
MODAL	Mode	229	0,019575	0,00025	0,00042	0,00003965	0,88208	0,88525	0,77961	0,00027	0,00025	0,00051	0,84136	0,83454	0,87523
MODAL	Mode	230	0,019467	0,00045	0,00002653	0,000001243	0,88253	0,88528	0,77961	0,00001873	0,00113	0,00061	0,84137	0,83567	0,87584

MODAL	Mode	231	0,019374	0,00021	0,000004221	0,00019	0,88274	0,88528	0,7798	0,00009002	0,00001743	0,00004502	0,84146	0,83568	0,87588
MODAL	Mode	232	0,019356	0,00015	0,00001517	0,00007937	0,88289	0,8853	0,77988	0,00002657	0,00006952	0,00003851	0,84149	0,83575	0,87592
MODAL	Mode	233	0,019332	0,00119	0,00016	0,00038	0,88408	0,88546	0,78027	0,00029	0,00203	0,00071	0,84178	0,83779	0,87663
MODAL	Mode	234	0,019257	0,00106	0,00032	0,0019	0,88514	0,88578	0,78217	0,00149	0,00132	0,00084	0,84328	0,83911	0,87747
MODAL	Mode	235	0,019228	0,00176	0,00001258	0,000001099	0,88691	0,88579	0,78217	0,00007398	0,00054	0,00104	0,84335	0,83964	0,87851
MODAL	Mode	236	0,019189	0,00191	0,00059	0,00062	0,88881	0,88638	0,78279	0,0000209	0,00043	0,0005	0,84337	0,84007	0,87901
MODAL	Mode	237	0,019173	0,00004588	0,0000018	0,00004447	0,88886	0,88638	0,78284	0,00007671	0,00017	0,00012	0,84345	0,84024	0,87913
MODAL	Mode	238	0,019122	0,00207	0,00002985	0,00019	0,89092	0,88641	0,78302	0,00016	0,00016	0,00036	0,8436	0,8404	0,87949
MODAL	Mode	239	0,018995	0,00004488	0,00015	0,00047	0,89097	0,88656	0,7835	0,00035	0,00075	0,00026	0,84396	0,84116	0,87975
MODAL	Mode	240	0,018987	0,00031	0,00008377	0,00168	0,89128	0,88664	0,78518	0,00183	0,00066	0,00145	0,84579	0,84182	0,8812
MODAL	Mode	241	0,018906	0,00005659	0,00004034	0,00089	0,89134	0,88668	0,78606	0,00031	0,00001903	0,00005608	0,8461	0,84184	0,88125
MODAL	Mode	242	0,018885	0,000001658	0,00004582	0,000009846	0,89134	0,88673	0,78607	0,000007746	0,00001394	0,000004305	0,84611	0,84185	0,88126
MODAL	Mode	243	0,018847	0,000003204	0,00002159	0,00021	0,89134	0,88675	0,78629	0,00004336	0,00006302	0,000006827	0,84615	0,84192	0,88126
MODAL	Mode	244	0,01876	0,00008179	0,00034	0,00239	0,89142	0,88708	0,78868	0,00088	0,0000116	0,00015	0,84703	0,84193	0,88142
MODAL	Mode	245	0,018688	0,00044	0,00027	0,00044	0,89186	0,88735	0,78912	0,00029	0,00008868	0,00035	0,84732	0,84202	0,88176
MODAL	Mode	246	0,018602	0,00052	0,00048	0,00206	0,89238	0,88783	0,79118	0,00175	0,00015	0,00013	0,84908	0,84217	0,88189
MODAL	Mode	247	0,018528	0,00003258	0,00142	0,00422	0,89242	0,88925	0,7954	0,00129	0,000003968	0,00018	0,85037	0,84217	0,88208
MODAL	Mode	248	0,018483	0,00054	0,00004127	0,00036	0,89295	0,88929	0,79576	0,00012	0,00038	0,00073	0,85048	0,84256	0,88281
MODAL	Mode	249	0,018436	0,00001044	0,00036	0,00089	0,89296	0,88965	0,79665	0,00068	0,00184	0,00054	0,85116	0,84439	0,88334
MODAL	Mode	250	0,018419	0,00001579	0,000009039	0,00051	0,89298	0,88966	0,79717	0,00028	0,00057	0,00005148	0,85144	0,84497	0,88339
MODAL	Mode	251	0,018359	0,00049	0,00033	0,00152	0,89347	0,88998	0,79868	0,00059	0,00026	0,00111	0,85204	0,84522	0,88451
MODAL	Mode	252	0,018337	0,00187	0,0005	0,00083	0,89534	0,89049	0,79952	0,00068	0,00021	0,00023	0,85271	0,84544	0,88474
MODAL	Mode	253	0,01831	0,00038	0,00022	0,00006447	0,89572	0,89071	0,79958	1,531E-07	0,00036	0,00098	0,85271	0,8458	0,88572
MODAL	Mode	254	0,018267	0,00004306	0,00004703	0,00022	0,89576	0,89076	0,7998	0,00031	0,00099	0,00001198	0,85302	0,84679	0,88573
MODAL	Mode	255	0,018234	0,00005741	0,00006805	0,00005753	0,89582	0,89083	0,79986	0,00002471	0,00006189	0,000002426	0,85305	0,84685	0,88573
MODAL	Mode	256	0,018162	8,648E-07	0,00038	0,00012	0,89582	0,89121	0,79998	0,00001189	0,00095	0,00048	0,85306	0,84779	0,88621

MODAL	Mode	257	0,01814	0,00052	0,0013	0,0000193	0,89634	0,89252	0,8	0,000004554	0,00036	0,00091	0,85307	0,84816	0,88713
MODAL	Mode	258	0,018115	0,00015	0,00021	0,00003227	0,89649	0,89272	0,80003	0,00001598	0,00024	0,00071	0,85308	0,8484	0,88784
MODAL	Mode	259	0,018039	0,000009522	7,828E-08	0,00018	0,8965	0,89272	0,80021	0,00007526	0,00009787	0,00016	0,85316	0,8485	0,88799
MODAL	Mode	260	0,018013	0,00001889	0,00026	0,00032	0,89652	0,89298	0,80052	0,00023	0,00159	0,0000555	0,85338	0,85009	0,88805
MODAL	Mode	261	0,017958	0,0000128	0,00001789	4,479E-07	0,89653	0,893	0,80052	0,00001049	0,00006679	0,0000143	0,85339	0,85015	0,88806
MODAL	Mode	262	0,017928	0,00045	0,00061	0,00007305	0,89698	0,89361	0,8006	0,000001473	0,00006792	0,00138	0,8534	0,85022	0,88944
MODAL	Mode	263	0,017904	8,976E-10	0,00234	0,00034	0,89698	0,89595	0,80093	0,00106	0,00052	0,00081	0,85445	0,85074	0,89025
MODAL	Mode	264	0,017887	0,00035	0,0001	0,00004477	0,89734	0,89606	0,80098	0,000001798	0,00002044	0,00067	0,85445	0,85076	0,89093
MODAL	Mode	265	0,017836	0,000001816	0,000001277	0,00092	0,89734	0,89606	0,8019	0,00068	0,00045	0,0000152	0,85514	0,85121	0,89094
MODAL	Mode	266	0,01776	0,000052	0,00001745	0,00001216	0,89739	0,89607	0,80191	0,00004553	0,00068	0,000002284	0,85518	0,8519	0,89094
MODAL	Mode	267	0,017734	0,00001262	0,00016	0,00121	0,8974	0,89624	0,80312	0,00071	0,00108	0,0001	0,85589	0,85298	0,89105
MODAL	Mode	268	0,01769	0,00005057	0,00005616	0,000003241	0,89745	0,89629	0,80313	0,00002226	0,00011	0,00006026	0,85592	0,85309	0,89111
MODAL	Mode	269	0,017575	0,000004114	0,00063	0,00015	0,89746	0,89693	0,80327	0,00035	0,00004838	0,00112	0,85627	0,85313	0,89223
MODAL	Mode	270	0,01756	0,00041	0,00024	0,00005493	0,89787	0,89716	0,80333	0,00003583	0,000001252	0,00048	0,8563	0,85314	0,8927
MODAL	Mode	271	0,017484	0,00014	0,00113	0,00005474	0,89801	0,89829	0,80338	1,481E-07	0,00011	0,0024	0,8563	0,85324	0,89511
MODAL	Mode	272	0,017429	0,00021	0,00012	0,00049	0,89822	0,89841	0,80388	0,00014	0,00002117	0,000006405	0,85644	0,85327	0,89511
MODAL	Mode	273	0,01741	0,00049	0,000001168	0,00004161	0,89871	0,89841	0,80392	0,00001644	0,0000523	0,00008938	0,85646	0,85332	0,8952
MODAL	Mode	274	0,017375	0,000004037	0,00011	0,00058	0,89871	0,89852	0,80449	0,00023	0,00015	0,00001992	0,85669	0,85347	0,89522
MODAL	Mode	275	0,01736	0,00081	0,00025	4,864E-07	0,89953	0,89876	0,80449	0,000000324	0,00009171	0,00013	0,85669	0,85356	0,89535
MODAL	Mode	276	0,017293	0,00017	0,00047	0,00005432	0,89969	0,89924	0,80455	0,00004823	0,00004217	0,00043	0,85674	0,8536	0,89578
MODAL	Mode	277	0,017238	0,000003373	0,00036	9,216E-07	0,8997	0,8996	0,80455	0,00003585	0,0004	0,00005295	0,85678	0,85401	0,89583
MODAL	Mode	278	0,017212	0,00002801	0,00006793	0,00036	0,89972	0,89966	0,80491	0,00047	0,00014	0,00025	0,85724	0,85414	0,89608
MODAL	Mode	279	0,017195	0,00001778	0,00019	0,00021	0,89974	0,89985	0,80512	0,00029	0,00014	0,00009768	0,85753	0,85428	0,89618
MODAL	Mode	280	0,017128	0,00018	0,00001023	0,000002381	0,89993	0,89986	0,80512	0,00002459	0,00005408	0,00012	0,85756	0,85433	0,8963
MODAL	Mode	281	0,0171	0,00005864	0,00027	0,00001774	0,89999	0,90013	0,80514	8,636E-10	0,0001	0,00025	0,85756	0,85444	0,89656
MODAL	Mode	282	0,017063	0,00079	0,00016	0,00007523	0,90078	0,90029	0,80521	0,00011	0,00002522	0,00021	0,85767	0,85446	0,89677

MODAL	Mode	283	0,017032	0,00036	0,00054	0,00014	0,90114	0,90083	0,80535	0,00018	0,00019	0,00008785	0,85785	0,85465	0,89686
MODAL	Mode	284	0,016951	0,00052	0,00058	0,00048	0,90165	0,90141	0,80584	0,00041	0,0006	0,00028	0,85826	0,85525	0,89713
MODAL	Mode	285	0,016946	0,00037	0,00003043	0,00073	0,90203	0,90144	0,80657	0,00033	0,00015	0,00007351	0,85859	0,85541	0,89721
MODAL	Mode	286	0,01688	0,000008942	0,000003854	0,00001222	0,90203	0,90144	0,80658	0,00006395	0,000002463	0,00001033	0,85865	0,85541	0,89722
MODAL	Mode	287	0,01684	0,00007885	0,0000008	0,00046	0,90211	0,90144	0,80704	0,00012	0,0006	0,00009599	0,85877	0,856	0,89731
MODAL	Mode	288	0,016808	0,00002517	0,00001094	6,692E-09	0,90214	0,90146	0,80704	0,00004629	0,00027	0,00000134	0,85882	0,85628	0,89732
MODAL	Mode	289	0,016774	8,388E-07	0,00077	0,00037	0,90214	0,90222	0,80741	0,00015	0,00005925	0,00014	0,85896	0,85634	0,89746
MODAL	Mode	290	0,016735	0,000002622	2,487E-07	0,00027	0,90214	0,90222	0,80768	0,00006763	0,00018	2,899E-07	0,85903	0,85651	0,89746
MODAL	Mode	291	0,016706	0,00049	0,00005695	0,00021	0,90264	0,90228	0,80789	0,00044	0,00019	0,00001239	0,85948	0,8567	0,89747
MODAL	Mode	292	0,016669	0,00068	0,0001	0,0000429	0,90332	0,90238	0,80793	0,000008932	0,0000767	0,00106	0,85948	0,85678	0,89853
MODAL	Mode	293	0,016621	0,00014	0,00006174	4,859E-07	0,90346	0,90244	0,80793	0,0000281	0,000009312	0,00036	0,85951	0,85679	0,89889
MODAL	Mode	294	0,01658	0,00001266	0,00054	0,00003938	0,90347	0,90298	0,80797	0,00003686	0,000001694	0,00036	0,85955	0,85679	0,89925
MODAL	Mode	295	0,016532	0,000002985	0,00001215	0,00022	0,90347	0,90299	0,8082	0,00003341	0,00001266	0,00001497	0,85958	0,8568	0,89927
MODAL	Mode	296	0,016521	0,000002722	9,771E-07	0,00012	0,90347	0,90299	0,80832	0,00000542	0,000007171	0,000004737	0,85959	0,85681	0,89927
MODAL	Mode	297	0,016461	0,00011	0,000008759	0,000001742	0,90359	0,903	0,80832	0,00003922	0,00003026	0,00016	0,85963	0,85684	0,89943
MODAL	Mode	298	0,016378	0,00006122	0,000001904	4,484E-07	0,90365	0,903	0,80832	0,000007103	0,0004	0,000000171	0,85963	0,85724	0,89943
MODAL	Mode	299	0,016355	0,000003561	0,00012	0,00002063	0,90365	0,90313	0,80834	0,000001291	0,00007687	0,00015	0,85964	0,85731	0,89959
MODAL	Mode	300	0,016325	0,000006899	0,00008172	0,0002	0,90366	0,90321	0,80854	0,00017	0,00014	0,00018	0,8598	0,85745	0,89976

APENDIX 2

ARCHITECTURAL PLANS OF THE BUILDING

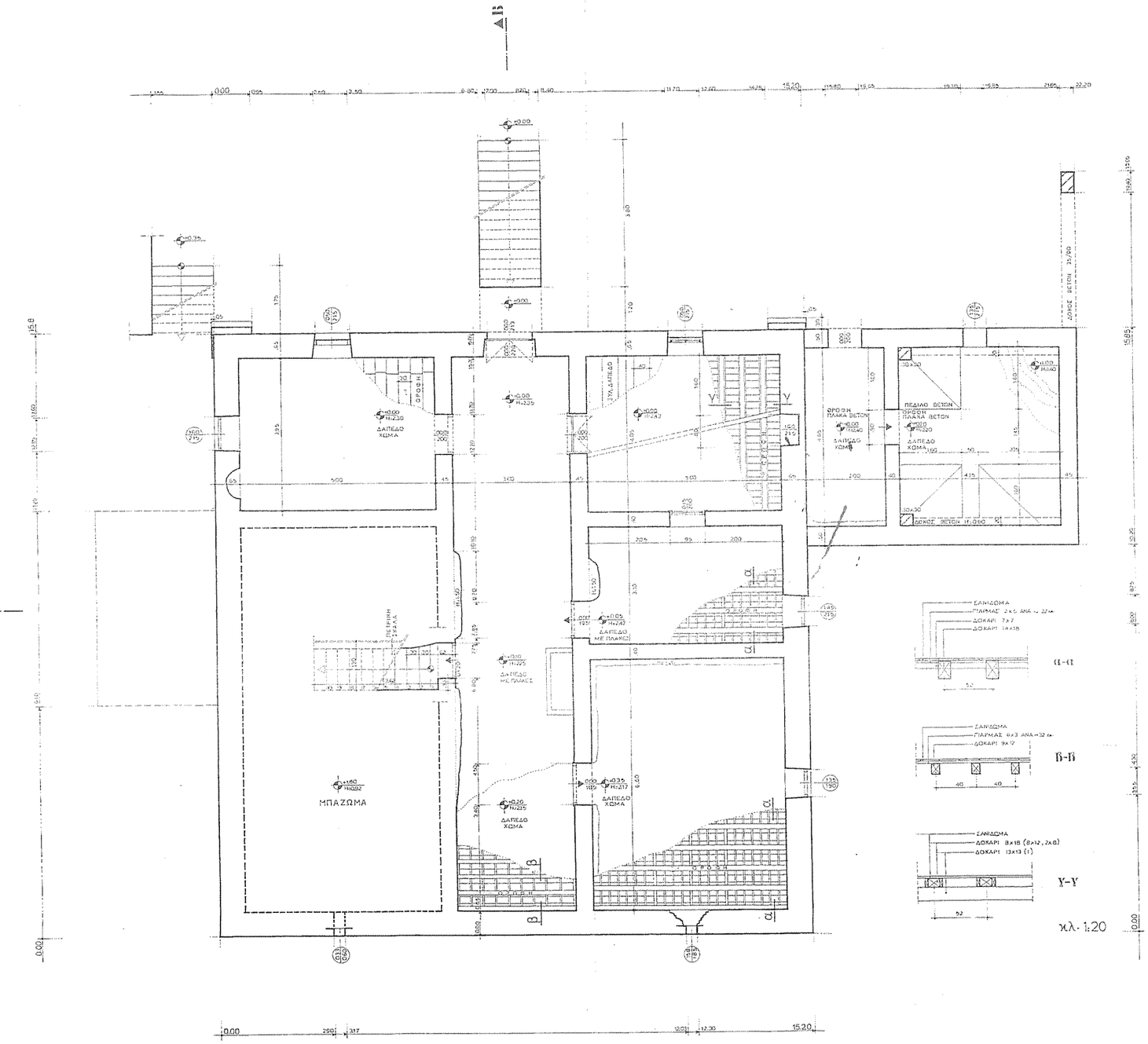

ΥΠΟΜΝΗΜΑ

α/β α : στάθμη εδάφους από 0.00
β : ύψος χώρου από σημειωμένη στάθμη (α)

α/β α : ύψος πλάκας κουφώματος από πατωμα
β : ύψος πρεκιού κουφώματος από πατωμα

ΓΡΑΜΜΑΤΕΙΑ Μ.Ο.Π. ΚΡΗΤΗΣ

ΕΡΕΥΝΗΤΙΚΟ – ΕΚΠΑΙΔΕΥΤΙΚΟ ΠΡΟΓΡΑΜΜΑ
ΠΑ ΤΗΝ ΑΠΟΚΑΤΑΣΤΑΣΗ – ΑΝΑΣΤΗΛΩΣΗ
ΝΕΟΚΛΑΣΣΙΚΟΥ ΚΤΙΡΙΟΥ ΣΤΑ ΧΑΝΙΑ

ΦΟΡΕΑΣ ΕΚΤΕΛΕΣΗΣ : Ε.Μ. ΠΟΛΥΤΕΧΝΕΙΟ

ΚΤΙΡΙΟ : Κατοικία Πρίγκηπα Γεωργίου
Ελευθερίου Βενιζέλου 131 – Χανιά

ΕΡΕΥΝΗΤΙΚΗ ΟΜΑΔΑ :
Επιστ. Υπευθ. : Κ. Α. Συρμακέζης Δρ. Πολ. Μηχ. Αν. Καθ. ΕΜΠ
Μ. Π. Χρονόπουλος Δρ. Πολ. Μηχ.
Α. Ε. Βιολάκη Αρχιτέκτων Μηχ.
Χ. Ν. Σπανός Πολιτικός Μηχ.

ΘΕΜΑ ΣΧΕΔΙΟΥ:	κάτοψη υπογείου	
ΑΡΙΘ. ΣΧΕΔΙΟΥ	ΚΛΙΜΑΚΑ	ΣΤΑΔΙΟ ΜΕΛΕΤΗΣ
A2	1:50	ΑΠΟΤΥΠΩΣΗ
τροποποιήσεις	2.	
	1.	
χρόνος μελέτης : 1993		

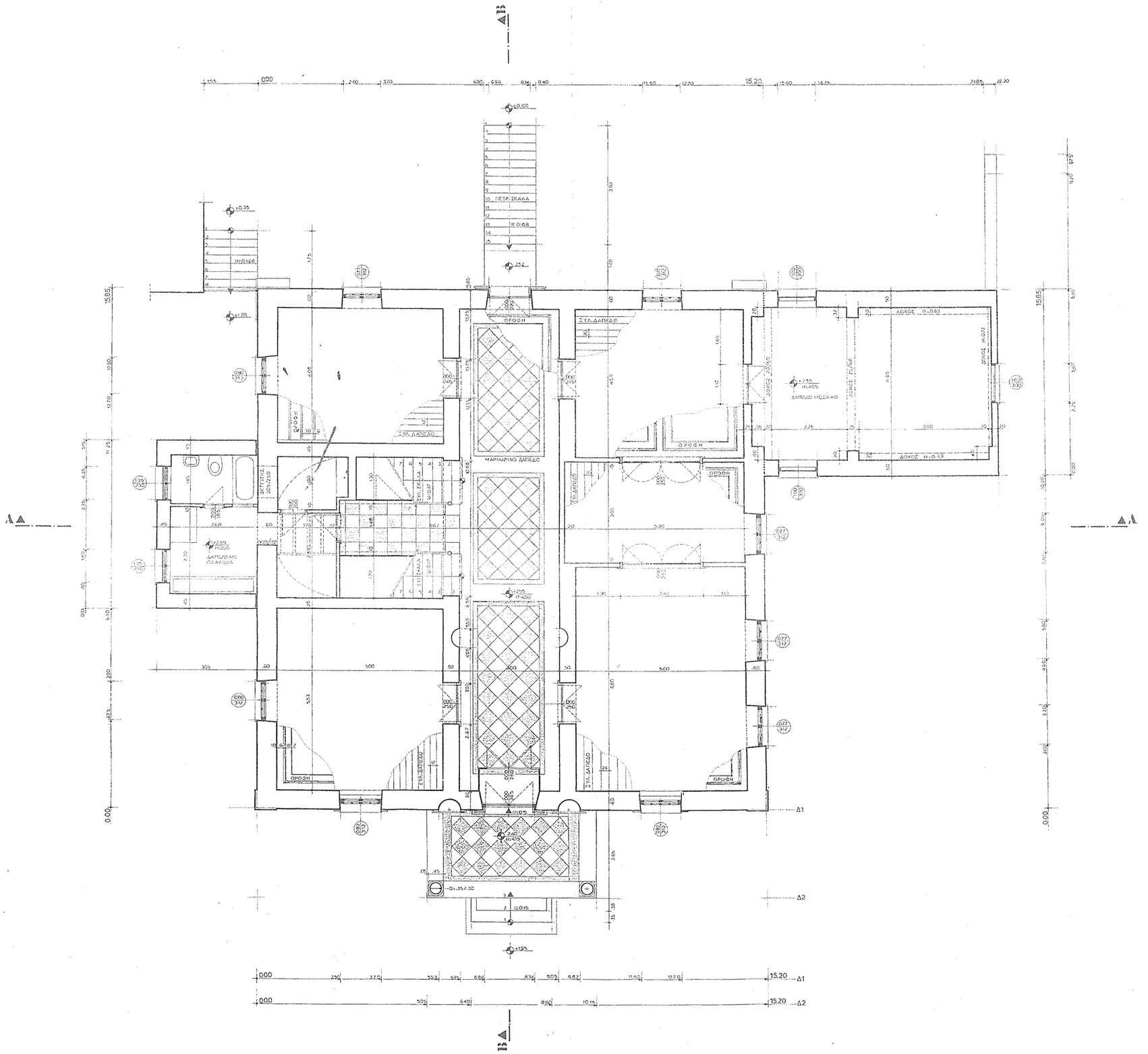

ΥΠΟΜΝΗΜΑ

α/β : α : στάθμη εδάφους από 0.00
β : ύψος χώρου από σημειωμένη στάθμη (α)

(α/β) : α : ύψος ποδιάς κουφώματος από πάτωμα
β : ύψος πρεκιού κουφώματος από πάτωμα

ΓΡΑΜΜΑΤΕΙΑ Μ.Ο.Π. ΚΡΗΤΗΣ

ΕΡΕΥΝΗΤΙΚΟ – ΕΚΠΑΙΔΕΥΤΙΚΟ ΠΡΟΓΡΑΜΜΑ ΓΙΑ ΤΗΝ ΑΠΟΚΑΤΑΣΤΑΣΗ – ΑΝΑΣΤΗΛΩΣΗ ΝΕΟΚΛΑΣΣΙΚΟΥ ΚΤΙΡΙΟΥ ΣΤΑ ΧΑΝΙΑ

ΦΟΡΕΑΣ ΕΚΤΕΛΕΣΗΣ : Ε.Μ. ΠΟΛΥΤΕΧΝΕΙΟ

ΚΤΙΡΙΟ : Κατοικία Πρίγκηπα Γεωργίου
Ελευθερίου Βενιζέλου 131 – Χανιά

ΕΡΕΥΝΗΤΙΚΗ ΟΜΑΔΑ :
Επιστ. Υπεύθ. : Κ. Α. Συρμακέζης Δρ. Πολ. Μηχ. Αν. Καθ. Ε.Μ.Π
Μ. Π. Χρονόπουλος Πολ. Μηχ.
Α. Ε. Βιολάκη Αρχιτέκτων Μηχ.
Χ. Ν. Σπανός Πολιτικός Μηχ.

ΘΕΜΑ ΣΧΕΔΙΟΥ:	κάτοψη ισογείου	
ΑΡΙΘ. ΣΧΕΔΙΟΥ	ΚΛΙΜΑΚΑ	ΣΤΑΔΙΟ ΜΕΛΕΤΗΣ
Α3	1:50	ΑΠΟΤΥΠΩΣΗ
τροποποιήσεις	2.	
	1.	

χρόνος μελέτης : 1993

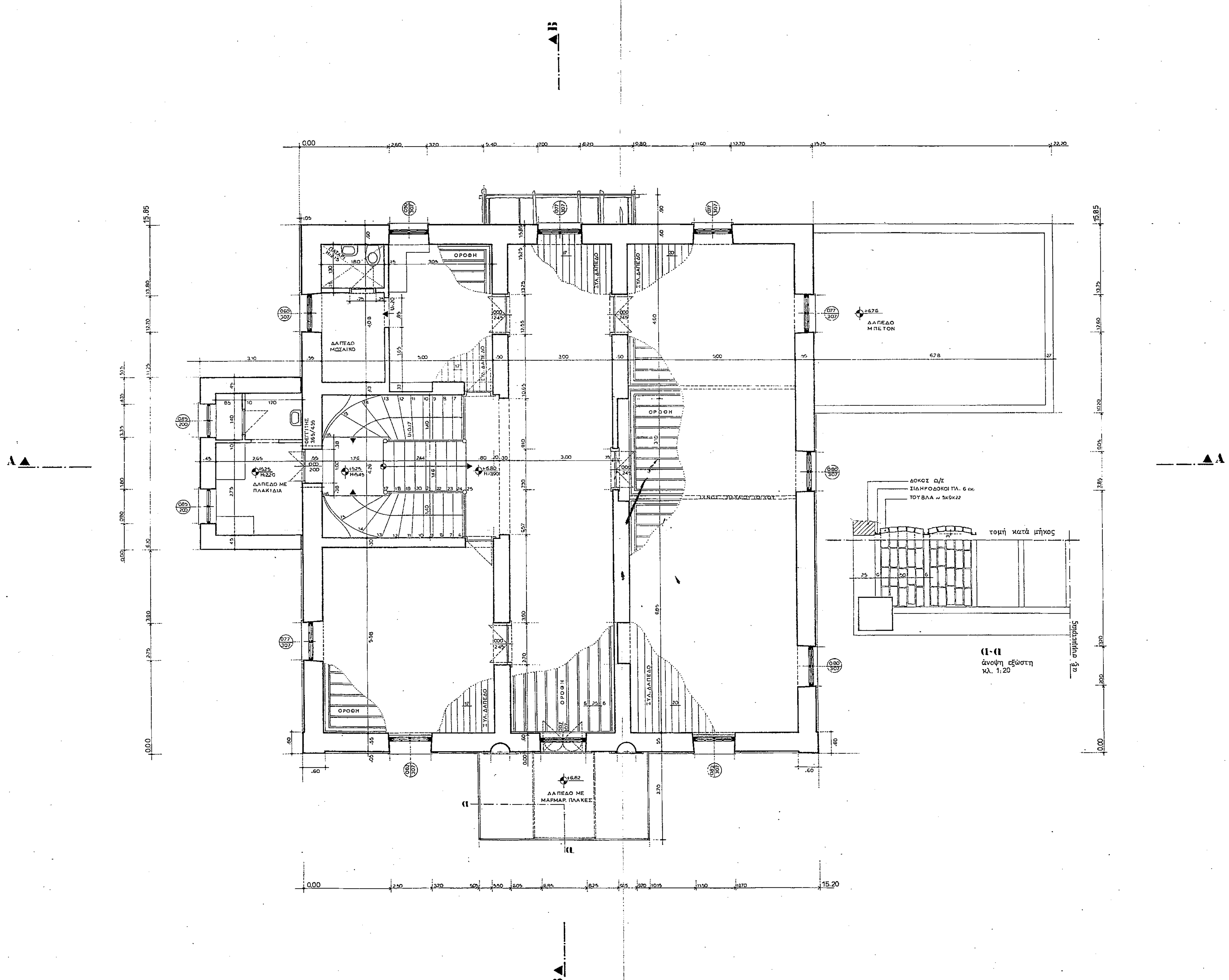

ΥΠΟΜΝΗΜΑ

α : στάθμη εδάφους από 0.00
β : ύψος χώρου από σημειωμένη στάθμη (α)

α : ύψος ποδιάς κουφώματος από πάτωμα
β : ύψος πρεκιού κουφώματος από πάτωμα

ΓΡΑΜΜΑΤΕΙΑ Μ.Ο.Π. ΚΡΗΤΗΣ

ΕΡΕΥΝΗΤΙΚΟ – ΕΚΠΑΙΔΕΥΤΙΚΟ ΠΡΟΓΡΑΜΜΑ ΓΙΑ ΤΗΝ ΑΠΟΚΑΤΑΣΤΑΣΗ – ΑΝΑΣΤΗΛΩΣΗ ΝΕΟΚΛΑΣΣΙΚΟΥ ΚΤΙΡΙΟΥ ΣΤΑ ΧΑΝΙΑ

ΦΟΡΕΑΣ ΕΚΤΕΛΕΣΗΣ : Ε.Μ. ΠΟΛΥΤΕΧΝΕΙΟ

ΚΤΙΡΙΟ : Κατοικία Πρίγκηπα Γεωργίου
Ελευθερίου Βενιζέλου 131 – Χανιά

ΕΡΕΥΝΗΤΙΚΗ ΟΜΑΔΑ :
Επιστ. Υπεύθ. : Κ. Α. Συρμακέζης Δρ. Πολ. Μηχ. Αν. Καθ. ΕΜΠ
Μ. Π. Χρονόπουλος Πολ. Μηχ.
Α. Ε. Βιολάκη Αρχιτέκτων Μηχ.
Χ. Ν. Σπανός Πολιτικός Μηχ.

ΘΕΜΑ ΣΧΕΔΙΟΥ:	κάτοψη ορόφου	
ΑΡΙΘ. ΣΧΕΔΙΟΥ	ΚΛΙΜΑΚΑ	ΣΤΑΔΙΟ ΜΕΛΕΤΗΣ
Α4	1:50	ΑΠΟΤΥΠΩΣΗ
τροποποιήσεις	2.	
	1.	

χρόνος μελέτης : 1993

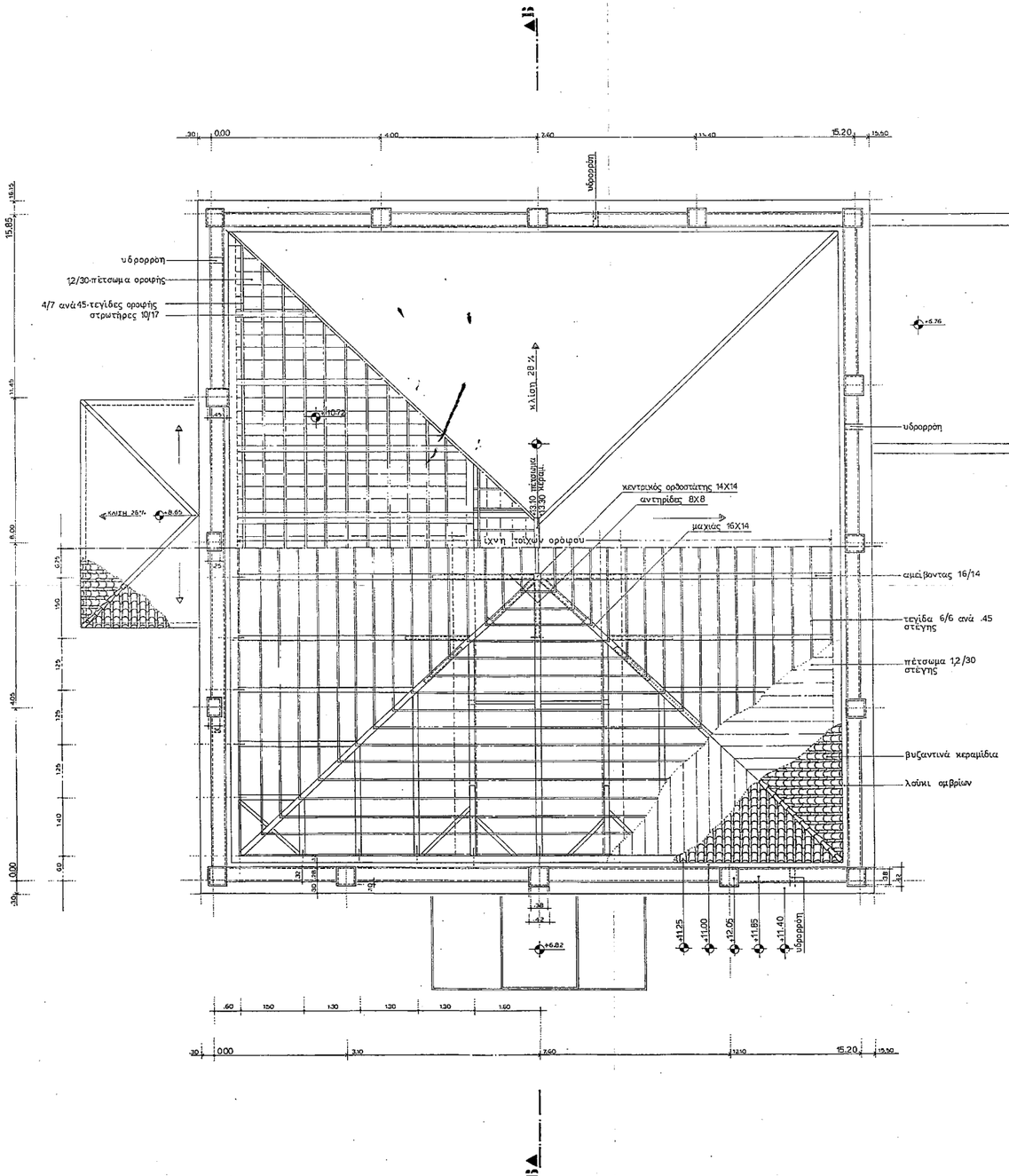

ΥΠΟΜΝΗΜΑ

α : στάθμη εδάφους από 0.00
β : ύψος χώρου από σημειωμένη στάθμη (α)

α : ύψος ποδιάς κουφώματος από πάτωμα
β : ύψος πρεκιού κουφώματος από πάτωμα

ΓΡΑΜΜΑΤΕΙΑ Μ.Ο.Π. ΚΡΗΤΗΣ

ΕΡΕΥΝΗΤΙΚΟ – ΕΚΠΑΙΔΕΥΤΙΚΟ ΠΡΟΓΡΑΜΜΑ ΓΙΑ ΤΗΝ ΑΠΟΚΑΤΑΣΤΑΣΗ – ΑΝΑΣΤΗΛΩΣΗ ΝΕΟΚΛΑΣΣΙΚΟΥ ΚΤΙΡΙΟΥ ΣΤΑ ΧΑΝΙΑ

ΦΟΡΕΑΣ ΕΚΤΕΛΕΣΗΣ : Ε.Μ. ΠΟΛΥΤΕΧΝΕΙΟ

ΚΤΙΡΙΟ : Κατοικία Πρίγκηπα Γεωργίου
Ελευθερίου Βενιζέλου 131 – Χανιά

ΕΡΕΥΝΗΤΙΚΗ ΟΜΑΔΑ :
Επιστ. Υπεύθ. : Κ. Α. Συρμακέζης Δρ. Πολ. Μηχ. Αν. Καθ. Ε.Μ.Π
Μ. Π. Χρονόπουλος Πολ. Μηχ.
Α. Ε. Βιολάκη Αρχιτέκτων Μηχ.
Χ. Ν. Σπανός Πολιτικός Μηχ.

ΘΕΜΑ ΣΧΕΔΙΟΥ:	κάτοψη δώματος-στέγης	
ΑΡΙΘ. ΣΧΕΔΙΟΥ	ΚΛΙΜΑΚΑ	ΣΤΑΔΙΟ ΜΕΛΕΤΗΣ
Α5	1:50	**ΑΠΟΤΥΠΩΣΗ**
τροποποιήσεις	2.	
	1.	
χρόνος μελέτης : 1993		

ΓΡΑΜΜΑΤΕΙΑ Μ.Ο.Π. ΚΡΗΤΗΣ

ΕΡΕΥΝΗΤΙΚΟ – ΕΚΠΑΙΔΕΥΤΙΚΟ ΠΡΟΓΡΑΜΜΑ
ΓΙΑ ΤΗΝ ΑΠΟΚΑΤΑΣΤΑΣΗ – ΑΝΑΣΤΗΛΩΣΗ
ΝΕΟΚΛΑΣΣΙΚΟΥ ΚΤΙΡΙΟΥ ΣΤΑ ΧΑΝΙΑ

ΦΟΡΕΑΣ ΕΚΤΕΛΕΣΗΣ : Ε.Μ. ΠΟΛΥΤΕΧΝΕΙΟ

ΚΤΙΡΙΟ : Κατοικία Πρίγκηπα Γεωργίου
Ελευθερίου Βενιζέλου 131 – Χανιά

ΕΡΕΥΝΗΤΙΚΗ ΟΜΑΔΑ :
Επιστ. Υπεύθ. : Κ. Α. Συρμακέζης Δρ. Πολ. Μηχ. Αν. Καθ. Ε.Μ.Π
Μ. Π. Χρονόπουλος Πολ. Μηχ.
Α. Ε. Βιολάκη Αρχιτέκτων Μηχ.
Χ. Ν. Σπανός Πολιτικός Μηχ.

ΘΕΜΑ ΣΧΕΔΙΟΥ:	τομή Α – Α	
ΑΡΙΘ. ΣΧΕΔΙΟΥ	ΚΛΙΜΑΚΑ	ΣΤΑΔΙΟ ΜΕΛΕΤΗΣ
A7	1 : 50	ΑΠΟΤΥΠΩΣΗ
τροποποιήσεις	2.	
	1.	
χρόνος μελέτης : 1993		

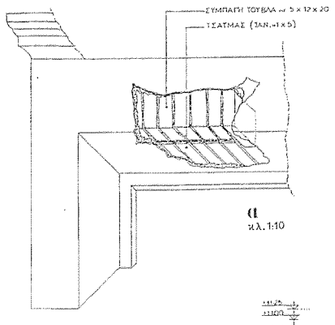

α
κλ. 1:10

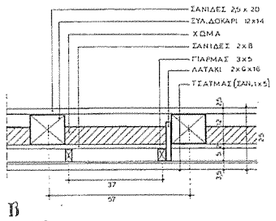

β
κλ. 1:10

ΓΡΑΜΜΑΤΕΙΑ Μ.Ο.Π. ΚΡΗΤΗΣ

ΕΡΕΥΝΗΤΙΚΟ – ΕΚΠΑΙΔΕΥΤΙΚΟ ΠΡΟΓΡΑΜΜΑ
ΠΑ ΤΗΝ ΑΠΟΚΑΤΑΣΤΑΣΗ – ΑΝΑΣΤΗΛΩΣΗ
ΝΕΟΚΛΑΣΣΙΚΟΥ ΚΤΙΡΙΟΥ ΣΤΑ ΧΑΝΙΑ

ΦΟΡΕΑΣ ΕΚΤΕΛΕΣΗΣ : Ε.Μ. ΠΟΛΥΤΕΧΝΕΙΟ

ΚΤΙΡΙΟ : Κατοικία Πρίγκηπα Γεωργίου
Ελευθερίου Βενιζέλου 131 – Χανιά

ΕΡΕΥΝΗΤΙΚΗ ΟΜΑΔΑ :
Επιστ. Υπεύθ. : Κ. Α. Συρμακέζης Δρ. Πολ. Μηχ. Αν. Καθ. Ε.Μ.Π
Μ. Π. Χρονόπουλος Πολ. Μηχ.
Α. Ε. Βιολάκη Αρχιτέκτων Μηχ.
Χ. Ν. Σπανός Πολίτικός Μηχ.

ΘΕΜΑ ΣΧΕΔΙΟΥ:	τομή Β - Β	
ΑΡΙΘ. ΣΧΕΔΙΟΥ	ΚΛΙΜΑΚΑ	ΣΤΑΔΙΟ ΜΕΛΕΤΗΣ
Α8	1 : 50	ΑΠΟΤΥΠΩΣΗ
τροποποιήσεις	2.	
	1.	
χρόνος μελέτης : 1993		

ΥΠΟΜΝΗΜΑ

1 Σοβάς
2 Λαξευτή λιθοδομή
3 Λαξευτή λιθοδομή επιχρισμένη
4 Αντηρίδα από λαξευτή λιθοδομή
5 Αργολιθοδομή
6 Δοκός Ω/Σ
7 Μάρμαρο
8 Σιδερένιο κιγκλίδωμα
9 Σιδερένιος ελκυστήρας
10 Σιδερένιο φουρούσι
11 Διακοσμητικά κιμάτια από λαξευτή πέτρα
12 Διακοσμητικά πέτρινα στοιχεία
13 Περιμετρική ταινία από λαξευτή πέτρα
14 Περιμετρική ταινία από τραβηκτό επίχρισμα
15 Περιθώριο κουφώματος από τραβηκτό επίχρισμα
16 Διακοσμητικά κιμάτια από γύψο
17 Βυζαντινά κεραμίδια
18 Ξύλινο κούφωμα με γαλλικά εξώφυλλα
19 Ξύλινο κούφωμα με προστατευτική σιδεριά
20 Ξύλινη τσιμπλαδωτή πόρτα με σιδεριά στον φεγγίτη
21 Σιδερένιο παράθυρο

ΓΡΑΜΜΑΤΕΙΑ Μ.Ο.Π. ΚΡΗΤΗΣ

ΕΡΕΥΝΗΤΙΚΟ – ΕΚΠΑΙΔΕΥΤΙΚΟ ΠΡΟΓΡΑΜΜΑ
ΓΙΑ ΤΗΝ ΑΠΟΚΑΤΑΣΤΑΣΗ – ΑΝΑΣΤΗΛΩΣΗ
ΝΕΟΚΛΑΣΣΙΚΟΥ ΚΤΙΡΙΟΥ ΣΤΑ ΧΑΝΙΑ

ΦΟΡΕΑΣ ΕΚΤΕΛΕΣΗΣ : Ε.Μ. ΠΟΛΥΤΕΧΝΕΙΟ

ΚΤΙΡΙΟ : Κατοικία Πρίγκηπα Γεωργίου
Ελευθερίου Βενιζέλου 131 – Χανιά

ΕΡΕΥΝΗΤΙΚΗ ΟΜΑΔΑ :
Επιστ. Υπεύθ. : Κ. Α. Συρμακέζης Δρ. Πολ. Μηχ. Αν. Καθ. ΕΜΠ
Μ. Π. Χρονόπουλος Πολ. Μηχ.
Α. Ε. Βιολάκη Αρχιτέκτων Μηχ.
Χ. Ν. Σπανός Πολιτικός Μηχ.

ΘΕΜΑ ΣΧΕΔΙΟΥ:	νότια όψη	
ΑΡΙΘ. ΣΧΕΔΙΟΥ	ΚΛΙΜΑΚΑ	ΣΤΑΔΙΟ ΜΕΛΕΤΗΣ
A9	1:50	ΑΠΟΤΥΠΩΣΗ
τροποποιήσεις	2.	
	1.	

χρόνος μελέτης : 1993

ΥΠΟΜΝΗΜΑ

1 Σοβάς
2 Λαξευτή λιθοδομή
3 Λαξευτή λιθοδομή επιχρισμένη
4 Αντηρίδα από λαξευτή λιθοδομή
5 Αργολιθοδομή
6 Δοκός Ω/Σ
7 Μάρμαρο
8 Σιδερένιο κιγκλίδωμα
9 Σιδερένιος ελκυστήρας
10 Σιδερένιο φουρούσι
11 Διακοσμητικά κυμάτια από λαξευτή πέτρα
12 Διακοσμητικά πέτρινα στοιχεία
13 Περιμετρική ταινία από λαξευτή πέτρα
14 Περιμετρική ταινία από τραβηκτό επίχρισμα
15 Περίβάριο κουφώματος από τραβηκτό επίχρισμα
16 Διακοσμητικά κυμάτια από γύψο
17 Βυζαντινά κεραμίδια
18 Ξύλινο κούφωμα με γαλλικά εξώφυλλα
19 Ξύλινο κούφωμα με προστατευτική σιδεριά
20 Ξύλινη ταμπλαδωτή πόρτα με σιδεριά στον φεγγίτη
21 Σιδερένιο παράθυρο

ΓΡΑΜΜΑΤΕΙΑ Μ.Ο.Π. ΚΡΗΤΗΣ

ΕΡΕΥΝΗΤΙΚΟ - ΕΚΠΑΙΔΕΥΤΙΚΟ ΠΡΟΓΡΑΜΜΑ
ΠΑ ΤΗΝ ΑΠΟΚΑΤΑΣΤΑΣΗ - ΑΝΑΣΤΗΛΩΣΗ
ΝΕΟΚΛΑΣΣΙΚΟΥ ΚΤΙΡΙΟΥ ΣΤΑ ΧΑΝΙΑ

ΦΟΡΕΑΣ ΕΚΤΕΛΕΣΗΣ : Ε.Μ. ΠΟΛΥΤΕΧΝΕΙΟ

ΚΤΙΡΙΟ : Κατοικία Πρίγκηπα Γεωργίου
Ελευθερίου Βενιζέλου 131 - Χανιά

ΕΡΕΥΝΗΤΙΚΗ ΟΜΑΔΑ :
Επιστ. Υπεύθ. : Κ. Α. Συρμακέζης Δρ. Πολ. Μηχ. Αν. Καθ. ΕΜΠ
Μ. Π. Χρονόπουλος Πολ. Μηχ.
Α. Ε. Βιολάκη Αρχιτέκτων Μηχ.
Χ. Ν. Σπανός Πολιτικός Μηχ.

ΘΕΜΑ ΣΧΕΔΙΟΥ:	βόρεια όψη	
ΑΡΙΘ. ΣΧΕΔΙΟΥ	ΚΛΙΜΑΚΑ	ΣΤΑΔΙΟ ΜΕΛΕΤΗΣ
A10	1 : 50	ΑΠΟΤΥΠΩΣΗ
τροποποιήσεις	2.	
	1.	
χρόνος μελέτης : 1993		

ΥΠΟΜΝΗΜΑ

1 Σοβάς
2 Λαξευτή λιθοδομή
3 Λαξευτή λιθοδομή επιχρισμένη
4 Αντηρίδα από λαξευτή λιθοδομή
5 Αργολιθοδομή
6 Δοκός Ω/Σ
7 Μάρμαρο
8 Σιδερένιο κιγκλίδωμα
9 Σιδερένιος ελκυστήρας
10 Σιδερένιο φουρούσι
11 Διακοσμητικά κυμάτια από λαξευτή πέτρα
12 Διακοσμητικά πέτρινα στοιχεία
13 Περιμετρική ταινία από λαξευτή πέτρα
14 Περιμετρική ταινία από τραβηκτό επίχρισμα
15 Περιθώριο κουφώματος από τραβηκτό επίχρισμα
16 Διακοσμητικά κυμάτια από γύψο
17 Βυζαντινά κεραμίδια
18 Ξύλινο κούφωμα με γαλλικά εξώφυλλα
19 Ξύλινο κούφωμα με προστατευτική σιδεριά
20 Ξύλινη ταμπλαδωτή πόρτα με σιδεριά στον φεγγίτη
21 Σιδερένιο παράθυρο

ΓΡΑΜΜΑΤΕΙΑ Μ.Ο.Π. ΚΡΗΤΗΣ

ΕΡΕΥΝΗΤΙΚΟ – ΕΚΠΑΙΔΕΥΤΙΚΟ ΠΡΟΓΡΑΜΜΑ
ΓΙΑ ΤΗΝ ΑΠΟΚΑΤΑΣΤΑΣΗ – ΑΝΑΣΤΗΛΩΣΗ
ΝΕΟΚΛΑΣΣΙΚΟΥ ΚΤΙΡΙΟΥ ΣΤΑ ΧΑΝΙΑ

ΦΟΡΕΑΣ ΕΚΤΕΛΕΣΗΣ : Ε. Μ. ΠΟΛΥΤΕΧΝΕΙΟ

ΚΤΙΡΙΟ : Κατοικία Πρίγκηπα Γεωργίου
Ελευθερίου Βενιζέλου 131 – Χανιά

ΕΡΕΥΝΗΤΙΚΗ ΟΜΑΔΑ :
Επιστ. Υπεύθ. : Κ. Α. Συρμακέζης Δρ. Πολ. Μηχ. Αν. Καθ. Ε.Μ.Π
Μ. Π. Χρονόπουλος Δρ. Πολ. Μηχ.
Α. Ε. Βιολάκη Αρχιτέκτων Μηχ.
Χ. Ν. Σπανός Πολιτικός Μηχ.

ΘΕΜΑ ΣΧΕΔΙΟΥ:	ανατολική όψη	
ΑΡΙΘ. ΣΧΕΔΙΟΥ	ΚΛΙΜΑΚΑ	ΣΤΑΔΙΟ ΜΕΛΕΤΗΣ
A11	1 : 50	ΑΠΟΤΥΠΩΣΗ
τροποποιήσεις	2.	
	1.	
χρόνος μελέτης : 1993		

ΥΠΟΜΝΗΜΑ

1 Σοβάς
2 Λαξευτή λιθοδομή
3 Λαξευτή λιθοδομή επιχρισμένη
4 Αντηρίδα από λαξευτή λιθοδομή
5 Αργολιθοδομή
6 Δοκός Ω/Σ
7 Μάρμαρο
8 Σιδερένιο κιγκλίδωμα
9 Σιδερένιος ελκυστήρας
10 Σιδερένιο φουρούσι
11 Διακοσμητικά κιμώτια από λαξευτή πέτρα
12 Διακοσμητικά πέτρινα στοιχεία
13 Περιμετρική ταινία από λαξευτή πέτρα
14 Περιμετρική ταινία από τραβηκτό επίχρισμα
15 Περιθώριο κουφώματος από τραβηκτό επίχρισμα
16 Διακοσμητικά κιμώτια από γύψο
17 Βυζαντινά κεραμίδια
18 Ξύλινο κούφωμα με γαλλικά εξώφυλλα
19 Ξύλινο κούφωμα με προστατευτική σιδεριά
20 Ξύλινη τσιμπλαδωτή πόρτα με σιδεριά στον φεγγίτη
21 Σιδερένιο παράθυρο

ΓΡΑΜΜΑΤΕΙΑ Μ.Ο.Π. ΚΡΗΤΗΣ

ΕΡΕΥΝΗΤΙΚΟ – ΕΚΠΑΙΔΕΥΤΙΚΟ ΠΡΟΓΡΑΜΜΑ ΓΙΑ ΤΗΝ ΑΠΟΚΑΤΑΣΤΑΣΗ – ΑΝΑΣΤΗΛΩΣΗ ΝΕΟΚΛΑΣΣΙΚΟΥ ΚΤΙΡΙΟΥ ΣΤΑ ΧΑΝΙΑ

ΦΟΡΕΑΣ ΕΚΤΕΛΕΣΗΣ : Ε.Μ. ΠΟΛΥΤΕΧΝΕΙΟ

ΚΤΙΡΙΟ : Κατοικία Πρίγκηπα Γεωργίου
Ελευθερίου Βενιζέλου 131 – Χανιά

ΕΡΕΥΝΗΤΙΚΗ ΟΜΑΔΑ :
Επιστ. Υπεύθ. : Κ. Α. Συρμακέζης Δρ. Πολ. Μηχ. Αν. Καθ. ΕΜΠ
Μ. Π. Χρονόπουλος Πολ. Μηχ.
Α. Ε. Βιολάκη Αρχιτέκτων Μηχ.
Χ. Ν. Σπανός Πολιτικός Μηχ.

ΘΕΜΑ ΣΧΕΔΙΟΥ:	δυτική όψη	
ΑΡΙΘ. ΣΧΕΔΙΟΥ	ΚΛΙΜΑΚΑ	ΣΤΑΔΙΟ ΜΕΛΕΤΗΣ
A12	1 : 50	ΑΠΟΤΥΠΩΣΗ
τροποποιήσεις	2.	
	1.	
χρόνος μελέτης : 1993		

APENDIX3

FAILURE RESULTS FOR THE MASONRY WALLS (MW)

Ag	face	fwc (kpa)	fwt (kpa)	wall-comb	joints number	Total failed joints	Total failed joints (%)	BTT	BTT(%)	BTC	BTC(%)	BCT	BCT(%)	BCC	BCC(%)
0,16	TOPMAX	3050	50	W1_2	640	434	67,81	265	41,41	168	26,25	1	0,15625	0	0
0,16	TOPMAX	3050	100	W1_2	640	340	53,13	236	36,88	104	16,25	0	0	0	0
0,16	TOPMAX	3050	150	W1_2	640	245	38,28	200	31,25	45	7,03	0	0	0	0
0,16	TOPMAX	3050	200	W1_2	640	176	27,50	162	25,31	14	2,19	0	0	0	0
0,16	TOPMAX	3050	250	W1_2	640	123	19,22	121	18,91	2	0,31	0	0	0	0
0,16	TOPMAX	3050	300	W1_2	640	90	14,06	90	14,06	0	0,00	0	0	0	0
0,16	TOPMAX	3050	350	W1_2	640	58	9,06	58	9,06	0	0,00	0	0	0	0
0,16	TOPMAX	3050	400	W1_2	640	39	6,09	39	6,09	0	0,00	0	0	0	0
0,16	TOPMAX	3050	450	W1_2	640	25	3,91	25	3,91	0	0,00	0	0	0	0
0,16	TOPMAX	3050	50	W2_2	349	183	52,44	100	28,65	83	23,78	0	0	0	0
0,16	TOPMAX	3050	100	W2_2	349	150	42,98	91	26,07	59	16,91	0	0	0	0
0,16	TOPMAX	3050	150	W2_2	349	111	31,81	80	22,92	31	8,88	0	0	0	0
0,16	TOPMAX	3050	200	W2_2	349	81	23,21	73	20,92	8	2,29	0	0	0	0
0,16	TOPMAX	3050	250	W2_2	349	71	20,34	66	18,91	5	1,43	0	0	0	0
0,16	TOPMAX	3050	300	W2_2	349	57	16,33	55	15,76	2	0,57	0	0	0	0
0,16	TOPMAX	3050	350	W2_2	349	43	12,32	43	12,32	0	0,00	0	0	0	0
0,16	TOPMAX	3050	400	W2_2	349	30	8,60	30	8,60	0	0,00	0	0	0	0
0,16	TOPMAX	3050	450	W2_2	349	25	7,16	25	7,16	0	0,00	0	0	0	0
0,16	TOPMAX	3050	50	W3_2	165	107	64,85	68	41,21	39	23,64	0	0	0	0
0,16	TOPMAX	3050	100	W3_2	165	83	50,30	61	36,97	22	13,33	0	0	0	0
0,16	TOPMAX	3050	150	W3_2	165	68	41,21	56	33,94	12	7,27	0	0	0	0
0,16	TOPMAX	3050	200	W3_2	165	57	34,55	51	30,91	6	3,64	0	0	0	0
0,16	TOPMAX	3050	250	W3_2	165	49	29,70	46	27,88	3	1,82	0	0	0	0
0,16	TOPMAX	3050	300	W3_2	165	42	25,45	39	23,64	3	1,82	0	0	0	0
0,16	TOPMAX	3050	350	W3_2	165	29	17,58	29	17,58	0	0,00	0	0	0	0
0,16	TOPMAX	3050	400	W3_2	165	22	13,33	22	13,33	0	0,00	0	0	0	0
0,16	TOPMAX	3050	450	W3_2	165	16	9,70	16	9,70	0	0,00	0	0	0	0
0,16	TOPMAX	3050	50	W4_2	228	120	52,63	65	28,51	55	24,12	0	0	0	0
0,16	TOPMAX	3050	100	W4_2	228	99	43,42	60	26,32	39	17,11	0	0	0	0
0,16	TOPMAX	3050	150	W4_2	228	71	31,14	52	22,81	19	8,33	0	0	0	0
0,16	TOPMAX	3050	200	W4_2	228	55	24,12	46	20,18	9	3,95	0	0	0	0
0,16	TOPMAX	3050	250	W4_2	228	46	20,18	43	18,86	3	1,32	0	0	0	0
0,16	TOPMAX	3050	300	W4_2	228	38	16,67	35	15,35	3	1,32	0	0	0	0
0,16	TOPMAX	3050	350	W4_2	228	29	12,72	29	12,72	0	0,00	0	0	0	0
0,16	TOPMAX	3050	400	W4_2	228	20	8,77	20	8,77	0	0,00	0	0	0	0
0,16	TOPMAX	3050	450	W4_2	228	17	7,46	17	7,46	0	0,00	0	0	0	0
0,16	TOPMAX	3050	50	W5_2	165	106	64,24	68	41,21	38	23,03	0	0	0	0
0,16	TOPMAX	3050	100	W5_2	165	83	50,30	60	36,36	23	13,94	0	0	0	0
0,16	TOPMAX	3050	150	W5_2	165	67	40,61	56	33,94	11	6,67	0	0	0	0
0,16	TOPMAX	3050	200	W5_2	165	57	34,55	50	30,30	7	4,24	0	0	0	0
0,16	TOPMAX	3050	250	W5_2	165	49	29,70	46	27,88	3	1,82	0	0	0	0
0,16	TOPMAX	3050	300	W5_2	165	41	24,85	39	23,64	2	1,21	0	0	0	0
0,16	TOPMAX	3050	350	W5_2	165	28	16,97	28	16,97	0	0,00	0	0	0	0
0,16	TOPMAX	3050	400	W5_2	165	21	12,73	21	12,73	0	0,00	0	0	0	0

0,16	TOPMAX	3050	450	W5_2	165	17	10,30	17	10,30	0	#REF!	0	0	0	0
0,16	TOPMAX	3050	50	W6_2	349	189	54,15	97	27,79	92	26,36	0	0	0	0
0,16	TOPMAX	3050	100	W6_2	349	125	35,82	74	21,20	51	14,61	0	0	0	0
0,16	TOPMAX	3050	150	W6_2	349	86	24,64	51	14,61	35	10,03	0	0	0	0
0,16	TOPMAX	3050	200	W6_2	349	61	17,48	42	12,03	19	5,44	0	0	0	0
0,16	TOPMAX	3050	250	W6_2	349	35	10,03	30	8,60	5	1,43	0	0	0	0
0,16	TOPMAX	3050	300	W6_2	349	19	5,44	19	5,44	0	0,00	0	0	0	0
0,16	TOPMAX	3050	350	W6_2	349	11	3,15	11	3,15	0	0,00	0	0	0	0
0,16	TOPMAX	3050	400	W6_2	349	9	2,58	9	2,58	0	0,00	0	0	0	0
0,16	TOPMAX	3050	450	W6_2	349	2	0,57	2	0,57	0	0,00	0	0	0	0
0,16	TOPMAX	3050	50	W7_2	77	68	88,31	54	70,13	14	18,18	0	0	0	0
0,16	TOPMAX	3050	100	W7_2	77	56	72,73	49	63,64	7	9,09	0	0	0	0
0,16	TOPMAX	3050	150	W7_2	77	47	61,04	36	46,75	11	14,29	0	0	0	0
0,16	TOPMAX	3050	200	W7_2	77	35	45,45	29	37,66	6	7,79	0	0	0	0
0,16	TOPMAX	3050	250	W7_2	77	23	29,87	23	29,87	0	0,00	0	0	0	0
0,16	TOPMAX	3050	300	W7_2	77	16	20,78	16	20,78	0	0,00	0	0	0	0
0,16	TOPMAX	3050	350	W7_2	77	11	14,29	11	14,29	0	0,00	0	0	0	0
0,16	TOPMAX	3050	400	W7_2	77	7	9,09	7	9,09	0	0,00	0	0	0	0
0,16	TOPMAX	3050	450	W7_2	77	4	5,19	4	5,19	0	0,00	0	0	0	0
0,16	TOPMAX	3050	50	W8_2	990	452	45,66	214	21,62	238	24,04	0	0	0	0
0,16	TOPMAX	3050	100	W8_2	990	250	25,25	190	19,19	60	6,06	0	0	0	0
0,16	TOPMAX	3050	150	W8_2	990	189	19,09	120	12,12	69	6,97	0	0	0	0
0,16	TOPMAX	3050	200	W8_2	990	95	9,60	61	6,16	34	3,43	0	0	0	0
0,16	TOPMAX	3050	250	W8_2	990	37	3,74	37	3,74	0	0,00	0	0	0	0
0,16	TOPMAX	3050	300	W8_2	990	28	2,83	28	2,83	0	0,00	0	0	0	0
0,16	TOPMAX	3050	350	W8_2	990	15	1,52	15	1,52	0	0,00	0	0	0	0
0,16	TOPMAX	3050	400	W8_2	990	7	0,71	7	0,71	0	0,00	0	0	0	0
0,16	TOPMAX	3050	450	W8_2	990	1	0,10	1	0,10	0	0,00	0	0	0	0
0,16	TOPMAX	3050	50	WA_2	192	32	16,67	23	11,98	9	4,69	0	0	0	0
0,16	TOPMAX	3050	100	WA_2	192	11	5,73	11	5,73	0	0,00	0	0	0	0
0,16	TOPMAX	3050	150	WA_2	192	2	1,04	2	1,04	0	0,00	0	0	0	0
0,16	TOPMAX	3050	200	WA_2	192	0	0,00	0	0,00	0	0,00	0	0	0	0
0,16	TOPMAX	3050	250	WA_2	192	0	0,00	0	0,00	0	0,00	0	0	0	0
0,16	TOPMAX	3050	300	WA_2	192	0	0,00	0	0,00	0	0,00	0	0	0	0
0,16	TOPMAX	3050	350	WA_2	192	0	0,00	0	0,00	0	0,00	0	0	0	0
0,16	TOPMAX	3050	400	WA_2	192	0	0,00	0	0,00	0	0,00	0	0	0	0
0,16	TOPMAX	3050	450	WA_2	192	0	0,00	0	0,00	0	0,00	0	0	0	0
0,16	TOPMAX	3050	50	WB_2	719	389	54,10	168	23,37	221	30,74	0	0	0	0
0,16	TOPMAX	3050	100	WB_2	719	198	27,54	150	20,86	48	6,68	0	0	0	0
0,16	TOPMAX	3050	150	WB_2	719	141	19,61	105	14,60	36	5,01	0	0	0	0
0,16	TOPMAX	3050	200	WB_2	719	77	10,71	58	8,07	19	2,64	0	0	0	0
0,16	TOPMAX	3050	250	WB_2	719	36	5,01	35	4,87	1	0,14	0	0	0	0
0,16	TOPMAX	3050	300	WB_2	719	21	2,92	21	2,92	0	0,00	0	0	0	0
0,16	TOPMAX	3050	350	WB_2	719	9	1,25	9	1,25	0	0,00	0	0	0	0

0,16	TOPMAX	3050	400	WB_2	719	6	0,83	6	0,83	0	0,00	0	0	0	0
0,16	TOPMAX	3050	450	WB_2	719	0	0,00	0	0,00	0	0,00	0	0	0	0
0,16	TOPMAX	3050	50	WC_2	113	112	99,12	98	86,73	14	12,39	0	0	0	0
0,16	TOPMAX	3050	100	WC_2	113	87	76,99	76	67,26	11	9,73	0	0	0	0
0,16	TOPMAX	3050	150	WC_2	113	74	65,49	67	59,29	7	6,19	0	0	0	0
0,16	TOPMAX	3050	200	WC_2	113	56	49,56	53	46,90	3	2,65	0	0	0	0
0,16	TOPMAX	3050	250	WC_2	113	47	41,59	43	38,05	4	3,54	0	0	0	0
0,16	TOPMAX	3050	300	WC_2	113	39	34,51	39	34,51	0	0,00	0	0	0	0
0,16	TOPMAX	3050	350	WC_2	113	32	28,32	32	28,32	0	0,00	0	0	0	0
0,16	TOPMAX	3050	400	WC_2	113	26	23,01	26	23,01	0	0,00	0	0	0	0
0,16	TOPMAX	3050	450	WC_2	113	19	16,81	19	16,81	0	0,00	0	0	0	0
0,16	TOPMAX	3050	50	WD_2	555	377	67,93	196	35,32	181	32,61	0	0	0	0
0,16	TOPMAX	3050	100	WD_2	555	278	50,09	156	28,11	122	21,98	0	0	0	0
0,16	TOPMAX	3050	150	WD_2	555	223	40,18	119	21,44	104	18,74	0	0	0	0
0,16	TOPMAX	3050	200	WD_2	555	125	22,52	89	16,04	36	6,49	0	0	0	0
0,16	TOPMAX	3050	250	WD_2	555	73	13,15	68	12,25	5	0,90	0	0	0	0
0,16	TOPMAX	3050	300	WD_2	555	59	10,63	51	9,19	8	1,44	0	0	0	0
0,16	TOPMAX	3050	350	WD_2	555	42	7,57	40	7,21	2	0,36	0	0	0	0
0,16	TOPMAX	3050	400	WD_2	555	25	4,50	25	4,50	0	0,00	0	0	0	0
0,16	TOPMAX	3050	450	WD_2	555	17	3,06	17	3,06	0	0,00	0	0	0	0
0,16	TOPMAX	3050	50	WE_2	558	405	72,58	325	58,24	80	14,34	0	0	0	0
0,16	TOPMAX	3050	100	WE_2	558	381	68,28	301	53,94	80	14,34	0	0	0	0
0,16	TOPMAX	3050	150	WE_2	558	356	63,80	281	50,36	75	13,44	0	0	0	0
0,16	TOPMAX	3050	200	WE_2	558	289	51,79	266	47,67	23	4,12	0	0	0	0
0,16	TOPMAX	3050	250	WE_2	558	243	43,55	238	42,65	5	0,90	0	0	0	0
0,16	TOPMAX	3050	300	WE_2	558	228	40,86	221	39,61	7	1,25	0	0	0	0
0,16	TOPMAX	3050	350	WE_2	558	212	37,99	199	35,66	13	2,33	0	0	0	0
0,16	TOPMAX	3050	400	WE_2	558	189	33,87	186	33,33	3	0,54	0	0	0	0
0,16	TOPMAX	3050	450	WE_2	558	140	25,09	140	25,09	0	0,00	0	0	0	0
0,16	TOPMAX	3050	50	WF_2	772	386	50,00	301	38,99	85	11,01	0	0	0	0
0,16	TOPMAX	3050	100	WF_2	772	198	25,65	156	20,21	42	5,44	0	0	0	0
0,16	TOPMAX	3050	150	WF_2	772	141	18,26	101	13,08	40	5,18	0	0	0	0
0,16	TOPMAX	3050	200	WF_2	772	77	9,97	58	7,51	19	2,46	0	0	0	0
0,16	TOPMAX	3050	250	WF_2	772	38	4,92	35	4,53	3	0,39	0	0	0	0
0,16	TOPMAX	3050	300	WF_2	772	21	2,72	21	2,72	0	0,00	0	0	0	0
0,16	TOPMAX	3050	350	WF_2	772	11	1,42	11	1,42	0	0,00	0	0	0	0
0,16	TOPMAX	3050	400	WF_2	772	5	0,65	5	0,65	0	0,00	0	0	0	0
0,16	TOPMAX	3050	450	WF_2	772	0	0,00	0	0,00	0	0,00	0	0	0	0
										0					
0,16	TOPMAX	3050	50	WG_2	218	201	92,20	159	72,94	42	19,27	0	0	0	0
0,16	TOPMAX	3050	100	WG_2	218	168	77,06	143	65,60	25	11,47	0	0	0	0
0,16	TOPMAX	3050	150	WG_2	218	149	68,35	107	49,08	42	19,27	0	0	0	0
0,16	TOPMAX	3050	200	WG_2	218	104	47,71	87	39,91	17	7,80	0	0	0	0
0,16	TOPMAX	3050	250	WG_2	218	67	30,73	62	28,44	5	2,29	0	0	0	0
0,16	TOPMAX	3050	300	WG_2	218	48	22,02	48	22,02	0	0,00	0	0	0	0

0,16	TOPMAX	3050	350	WG_2	218	35	16,06	35	16,06	0	0,00	0	0	0	0
0,16	TOPMAX	3050	400	WG_2	218	24	11,01	24	11,01	0	0,00	0	0	0	0
0,16	TOPMAX	3050	450	WG_2	218	14	6,42	14	6,42	0	0,00	0	0	0	0

Ag	face	fwc (kpa)	fwt (kpa)	wall-comb	joints number	Total failed joints	Total failed joints (%)	BTT	BTT(%)	BTC	BTC(%)	BCT	BCT(%)	BCC	BCC(%)
0,24	TOPMAX	3050	50	W1_2	640	536	83,75	413	64,53	123	19,22	0	0	0	0
0,24	TOPMAX	3050	100	W1_2	640	462	72,19	368	57,50	94	14,69	0	0	0	0
0,24	TOPMAX	3050	150	W1_2	640	373	58,28	320	50,00	53	8,28	0	0	0	0
0,24	TOPMAX	3050	200	W1_2	640	298	46,56	278	43,44	20	3,13	0	0	0	0
0,24	TOPMAX	3050	250	W1_2	640	239	37,34	233	36,41	6	0,94	0	0	0	0
0,24	TOPMAX	3050	300	W1_2	640	194	30,31	192	30,00	2	0,31	0	0	0	0
0,24	TOPMAX	3050	350	W1_2	640	155	24,22	154	24,06	1	0,16	0	0	0	0
0,24	TOPMAX	3050	400	W1_2	640	121	18,91	121	18,91	0	0,00	0	0	0	0
0,24	TOPMAX	3050	450	W1_2	640	96	15,00	96	15,00	0	0,00	0	0	0	0
0,24	TOPMAX	3050	50	W2_2	349	225	64,47	146	41,83	79	22,64	0	0	0	0
0,24	TOPMAX	3050	100	W2_2	349	182	52,15	120	34,38	62	17,77	0	0	0	0
0,24	TOPMAX	3050	150	W2_2	349	154	44,13	109	31,23	45	12,89	0	0	0	0
0,24	TOPMAX	3050	200	W2_2	349	131	37,54	103	29,51	28	8,02	0	0	0	0
0,24	TOPMAX	3050	250	W2_2	349	107	30,66	94	26,93	13	3,72	0	0	0	0
0,24	TOPMAX	3050	300	W2_2	349	86	24,64	81	23,21	5	1,43	0	0	0	0
0,24	TOPMAX	3050	350	W2_2	349	78	22,35	75	21,49	3	0,86	0	0	0	0
0,24	TOPMAX	3050	400	W2_2	349	69	19,77	67	19,20	2	0,57	0	0	0	0
0,24	TOPMAX	3050	450	W2_2	349	69	19,77	59	16,91	10	2,87	0	0	0	0
0,24	TOPMAX	3050	50	W3_2	165	130	78,79	102	61,82	28	16,97	0	0	0	0
0,24	TOPMAX	3050	100	W3_2	165	106	64,24	89	53,94	17	10,30	0	0	0	0
0,24	TOPMAX	3050	150	W3_2	165	89	53,94	77	46,67	12	7,27	0	0	0	0
0,24	TOPMAX	3050	200	W3_2	165	80	48,48	74	44,85	6	3,64	0	0	0	0
0,24	TOPMAX	3050	250	W3_2	165	67	40,61	63	38,18	4	2,42	0	0	0	0
0,24	TOPMAX	3050	300	W3_2	165	59	35,76	58	35,15	1	0,61	0	0	0	0
0,24	TOPMAX	3050	350	W3_2	165	50	30,30	50	30,30	0	0,00	0	0	0	0
0,24	TOPMAX	3050	400	W3_2	165	46	27,88	46	27,88	0	0,00	0	0	0	0
0,24	TOPMAX	3050	450	W3_2	165	42	25,45	42	25,45	0	0,00	0	0	0	0
0,24	TOPMAX	3050	50	W4_2	228	147	64,47	95	41,67	52	22,81	0	0	0	0
0,24	TOPMAX	3050	100	W4_2	228	119	52,19	78	34,21	41	17,98	0	0	0	0
0,24	TOPMAX	3050	150	W4_2	228	103	45,18	71	31,14	32	14,04	0	0	0	0
0,24	TOPMAX	3050	200	W4_2	228	86	37,72	67	29,39	19	8,33	0	0	0	0
0,24	TOPMAX	3050	250	W4_2	228	71	31,14	61	26,75	10	4,39	0	0	0	0
0,24	TOPMAX	3050	300	W4_2	228	55	24,12	52	22,81	3	1,32	0	0	0	0
0,24	TOPMAX	3050	350	W4_2	228	50	21,93	49	21,49	1	0,44	0	0	0	0
0,24	TOPMAX	3050	400	W4_2	228	45	19,74	43	18,86	2	0,88	0	0	0	0
0,24	TOPMAX	3050	450	W4_2	228	44	19,30	38	16,67	6	2,63	0	0	0	0
0,24	TOPMAX	3050	50	W5_2	165	129	78,18	102	61,82	27	16,36	0	0	0	0
0,24	TOPMAX	3050	100	W5_2	165	106	64,24	89	53,94	17	10,30	0	0	0	0
0,24	TOPMAX	3050	150	W5_2	165	89	53,94	78	47,27	11	6,67	0	0	0	0
0,24	TOPMAX	3050	200	W5_2	165	80	48,48	74	44,85	6	3,64	0	0	0	0
0,24	TOPMAX	3050	250	W5_2	165	66	40,00	63	38,18	3	1,82	0	0	0	0
0,24	TOPMAX	3050	300	W5_2	165	59	35,76	58	35,15	1	0,61	0	0	0	0
0,24	TOPMAX	3050	350	W5_2	165	52	31,52	52	31,52	0	0,00	0	0	0	0
0,24	TOPMAX	3050	400	W5_2	165	48	29,09	48	29,09	0	0,00	0	0	0	0

0,24	TOPMAX	3050	450	W5_2	165	42	25,45	42	25,45	0	0,00	0	0	0	0
0,24	TOPMAX	3050	50	W6_2	349	226	64,76	165	47,28	61	17,48	0	0	0	0
0,24	TOPMAX	3050	100	W6_2	349	186	53,30	143	40,97	43	12,32	0	0	0	0
0,24	TOPMAX	3050	150	W6_2	349	141	40,40	112	32,09	29	8,31	0	0	0	0
0,24	TOPMAX	3050	200	W6_2	349	105	30,09	92	26,36	13	3,72	0	0	0	0
0,24	TOPMAX	3050	250	W6_2	349	67	19,20	65	18,62	2	0,57	0	0	0	0
0,24	TOPMAX	3050	300	W6_2	349	55	15,76	55	15,76	0	0,00	0	0	0	0
0,24	TOPMAX	3050	350	W6_2	349	40	11,46	40	11,46	0	0,00	0	0	0	0
0,24	TOPMAX	3050	400	W6_2	349	32	9,17	32	9,17	0	0,00	0	0	0	0
0,24	TOPMAX	3050	450	W6_2	349	23	6,59	23	6,59	0	0,00	0	0	0	0
0,24	TOPMAX	3050	50	W7_2	77	71	92,21	65	84,42	6	7,79	0	0	0	0
0,24	TOPMAX	3050	100	W7_2	77	66	85,71	60	77,92	6	7,79	0	0	0	0
0,24	TOPMAX	3050	150	W7_2	77	52	67,53	48	62,34	4	5,19	0	0	0	0
0,24	TOPMAX	3050	200	W7_2	77	43	55,84	41	53,25	2	2,60	0	0	0	0
0,24	TOPMAX	3050	250	W7_2	77	33	42,86	31	40,26	2	2,60	0	0	0	0
0,24	TOPMAX	3050	300	W7_2	77	29	37,66	28	36,36	1	1,30	0	0	0	0
0,24	TOPMAX	3050	350	W7_2	77	24	31,17	24	31,17	0	0,00	0	0	0	0
0,24	TOPMAX	3050	400	W7_2	77	18	23,38	18	23,38	0	0,00	0	0	0	0
0,24	TOPMAX	3050	450	W7_2	77	13	16,88	13	16,88	0	0,00	0	0	0	0
0,24	TOPMAX	3050	50	W8_2	990	630	63,64	356	35,96	274	27,68	0	0	0	0
0,24	TOPMAX	3050	100	W8_2	990	399	40,30	272	27,47	127	12,83	0	0	0	0
0,24	TOPMAX	3050	150	W8_2	990	267	26,97	218	22,02	49	4,95	0	0	0	0
0,24	TOPMAX	3050	200	W8_2	990	179	18,08	162	16,36	17	1,72	0	0	0	0
0,24	TOPMAX	3050	250	W8_2	990	124	12,53	120	12,12	4	0,40	0	0	0	0
0,24	TOPMAX	3050	300	W8_2	990	87	8,79	86	8,69	1	0,10	0	0	0	0
0,24	TOPMAX	3050	350	W8_2	990	60	6,06	60	6,06	0	0,00	0	0	0	0
0,24	TOPMAX	3050	400	W8_2	990	34	3,43	34	3,43	0	0,00	0	0	0	0
0,24	TOPMAX	3050	450	W8_2	990	20	2,02	20	2,02	0	0,00	0	0	0	0
0,24	TOPMAX	3050	50	WA_2	192	68	35,42	56	29,17	12	6,25	0	0	0	0
0,24	TOPMAX	3050	100	WA_2	192	25	13,02	22	11,46	3	1,56	0	0	0	0
0,24	TOPMAX	3050	150	WA_2	192	5	2,60	3	1,56	2	1,04	0	0	0	0
0,24	TOPMAX	3050	200	WA_2	192	2	1,04	2	1,04	0	0,00	0	0	0	0
0,24	TOPMAX	3050	250	WA_2	192	0	0,00	0	0,00	0	0,00	0	0	0	0
0,24	TOPMAX	3050	300	WA_2	192	0	0,00	0	0,00	0	0,00	0	0	0	0
0,24	TOPMAX	3050	350	WA_2	192	0	0,00	0	0,00	0	0,00	0	0	0	0
0,24	TOPMAX	3050	400	WA_2	192	0	0,00	0	0,00	0	0,00	0	0	0	0
0,24	TOPMAX	3050	450	WA_2	192	0	0,00	0	0,00	0	0,00	0	0	0	0
0,24	TOPMAX	3050	50	WB_2	719	446	62,03	230	31,99	216	30,04	0	0	0	0
0,24	TOPMAX	3050	100	WB_2	719	340	47,29	199	27,68	141	19,61	0	0	0	0
0,24	TOPMAX	3050	150	WB_2	719	205	28,51	171	23,78	34	4,73	0	0	0	0
0,24	TOPMAX	3050	200	WB_2	719	156	21,70	130	18,08	26	3,62	0	0	0	0
0,24	TOPMAX	3050	250	WB_2	719	103	14,33	87	12,10	16	2,23	0	0	0	0
0,24	TOPMAX	3050	300	WB_2	719	68	9,46	58	8,07	10	1,39	0	0	0	0
0,24	TOPMAX	3050	350	WB_2	719	51	7,09	46	6,40	5	0,70	0	0	0	0

0,24	TOPMAX	3050	400	WB_2	719	28	3,89	26	3,62	2	0,28	0	0	0	0
0,24	TOPMAX	3050	450	WB_2	719	16	2,23	16	2,23	0	0,00	0	0	0	0
0,24	TOPMAX	3050	50	WC_2	113	112	99,12	104	92,04	8	7,08	0	0	0	0
0,24	TOPMAX	3050	100	WC_2	113	110	97,35	103	91,15	7	6,19	0	0	0	0
0,24	TOPMAX	3050	150	WC_2	113	99	87,61	92	81,42	7	6,19	0	0	0	0
0,24	TOPMAX	3050	200	WC_2	113	78	69,03	73	64,60	5	4,42	0	0	0	0
0,24	TOPMAX	3050	250	WC_2	113	71	62,83	67	59,29	4	3,54	0	0	0	0
0,24	TOPMAX	3050	300	WC_2	113	61	53,98	58	51,33	3	2,65	0	0	0	0
0,24	TOPMAX	3050	350	WC_2	113	52	46,02	51	45,13	1	0,88	0	0	0	0
0,24	TOPMAX	3050	400	WC_2	113	43	38,05	43	38,05	0	0,00	0	0	0	0
0,24	TOPMAX	3050	450	WC_2	113	39	34,51	39	34,51	0	0,00	0	0	0	0
0,24	TOPMAX	3050	50	WD_2	555	473	85,23	335	60,36	138	24,86	0	0	0	0
0,24	TOPMAX	3050	100	WD_2	555	379	68,29	286	51,53	93	16,76	0	0	0	0
0,24	TOPMAX	3050	150	WD_2	555	289	52,07	235	42,34	54	9,73	0	0	0	0
0,24	TOPMAX	3050	200	WD_2	555	215	38,74	190	34,23	25	4,50	0	0	0	0
0,24	TOPMAX	3050	250	WD_2	555	165	29,73	150	27,03	15	2,70	0	0	0	0
0,24	TOPMAX	3050	300	WD_2	555	127	22,88	120	21,62	7	1,26	0	0	0	0
0,24	TOPMAX	3050	350	WD_2	555	99	17,84	97	17,48	2	0,36	0	0	0	0
0,24	TOPMAX	3050	400	WD_2	555	71	12,79	71	12,79	0	0,00	0	0	0	0
0,24	TOPMAX	3050	450	WD_2	555	55	9,91	55	9,91	0	0,00	0	0	0	0
0,24	TOPMAX	3050	50	WE_2	558	461	82,62	384	68,82	77	13,80	0	0	0	0
0,24	TOPMAX	3050	100	WE_2	558	412	73,84	365	65,41	47	8,42	0	0	0	0
0,24	TOPMAX	3050	150	WE_2	558	377	67,56	349	62,54	28	5,02	0	0	0	0
0,24	TOPMAX	3050	200	WE_2	558	353	63,26	337	60,39	16	2,87	0	0	0	0
0,24	TOPMAX	3050	250	WE_2	558	332	59,50	322	57,71	10	1,79	0	0	0	0
0,24	TOPMAX	3050	300	WE_2	558	306	54,84	301	53,94	5	0,90	0	0	0	0
0,24	TOPMAX	3050	350	WE_2	558	267	47,85	265	47,49	2	0,36	0	0	0	0
0,24	TOPMAX	3050	400	WE_2	558	243	43,55	241	43,19	2	0,36	0	0	0	0
0,24	TOPMAX	3050	450	WE_2	558	227	40,68	227	40,68	0	0,00	0	0	0	0
0,24	TOPMAX	3050	50	WF_2	772	476	61,66	206	26,68	270	34,97	0	0	0	0
0,24	TOPMAX	3050	100	WF_2	772	354	45,85	182	23,58	172	22,28	0	0	0	0
0,24	TOPMAX	3050	150	WF_2	772	214	27,72	167	21,63	47	6,09	0	0	0	0
0,24	TOPMAX	3050	200	WF_2	772	161	20,85	120	15,54	41	5,31	0	0	0	0
0,24	TOPMAX	3050	250	WF_2	772	98	12,69	96	12,44	2	0,26	0	0	0	0
0,24	TOPMAX	3050	300	WF_2	772	67	8,68	67	8,68	0	0,00	0	0	0	0
0,24	TOPMAX	3050	350	WF_2	772	54	6,99	54	6,99	0	0,00	0	0	0	0
0,24	TOPMAX	3050	400	WF_2	772	19	2,46	19	2,46	0	0,00	0	0	0	0
0,24	TOPMAX	3050	450	WF_2	772	14	1,81	14	1,81	0	0,00	0	0	0	0
0,24	TOPMAX	3050	50	WG_2	218	208	95,41	182	83,49	26	11,93	0	0	0	0
0,24	TOPMAX	3050	100	WG_2	218	186	85,32	170	77,98	16	7,34	0	0	0	0
0,24	TOPMAX	3050	150	WG_2	218	165	75,69	142	65,14	23	10,55	0	0	0	0
0,24	TOPMAX	3050	200	WG_2	218	131	60,09	122	55,96	9	4,13	0	0	0	0
0,24	TOPMAX	3050	250	WG_2	218	96	44,04	94	43,12	2	0,92	0	0	0	0
0,24	TOPMAX	3050	300	WG_2	218	79	36,24	79	36,24	0	0,00	0	0	0	0

0,24	TOPMAX	3050	350	WG_2	218	65	29,82	65	29,82	0	0,00	0	0	0	0
0,24	TOPMAX	3050	400	WG_2	218	53	24,31	53	24,31	0	0,00	0	0	0	0
0,24	TOPMAX	3050	450	WG_2	218	43	19,72	43	19,72	0	0,00	0	0	0	0

Ag	face	fwc (kpa)	fwt (kpa)	wall-comb	joints number	Total failed joints	Total failed joints (%)	BTT	BTT(%)	BTC	BTC(%)	BCT	BCT(%)	BCC	BCC(%)
0,32	TOPMAX	3050	50	W1_2	640	600	93,75	514	80,31	86	13,44	0	0	0	0
0,32	TOPMAX	3050	100	W1_2	640	547	85,47	479	74,84	68	10,63	0	0	0	0
0,32	TOPMAX	3050	150	W1_2	640	486	75,94	436	68,13	50	7,81	0	0	0	0
0,32	TOPMAX	3050	200	W1_2	640	418	65,31	387	60,47	31	4,84	0	0	0	0
0,32	TOPMAX	3050	250	W1_2	640	345	53,91	328	51,25	17	2,66	0	0	0	0
0,32	TOPMAX	3050	300	W1_2	640	292	45,63	286	44,69	6	0,94	0	0	0	0
0,32	TOPMAX	3050	350	W1_2	640	250	39,06	248	38,75	2	0,31	0	0	0	0
0,32	TOPMAX	3050	400	W1_2	640	216	33,75	214	33,44	2	0,31	0	0	0	0
0,32	TOPMAX	3050	450	W1_2	640	177	27,66	176	27,50	1	0,16	0	0	0	0
0,32	TOPMAX	3050	50	W2_2	349	262	75,07	211	60,46	51	14,61	0	0	0	0
0,32	TOPMAX	3050	100	W2_2	349	211	60,46	180	51,58	31	8,88	0	0	0	0
0,32	TOPMAX	3050	150	W2_2	349	186	53,30	158	45,27	28	8,02	0	0	0	0
0,32	TOPMAX	3050	200	W2_2	349	159	45,56	140	40,11	19	5,44	0	0	0	0
0,32	TOPMAX	3050	250	W2_2	349	142	40,69	130	37,25	12	3,44	0	0	0	0
0,32	TOPMAX	3050	300	W2_2	349	124	35,53	117	33,52	7	2,01	0	0	0	0
0,32	TOPMAX	3050	350	W2_2	349	107	30,66	104	29,80	3	0,86	0	0	0	0
0,32	TOPMAX	3050	400	W2_2	349	91	26,07	90	25,79	1	0,29	0	0	0	0
0,32	TOPMAX	3050	450	W2_2	349	85	24,36	84	24,07	1	0,29	0	0	0	0
0,32	TOPMAX	3050	50	W3_2	165	149	90,30	128	77,58	21	12,73	0	0	0	0
0,32	TOPMAX	3050	100	W3_2	165	129	78,18	116	70,30	13	7,88	0	0	0	0
0,32	TOPMAX	3050	150	W3_2	165	112	67,88	105	63,64	7	4,24	0	0	0	0
0,32	TOPMAX	3050	200	W3_2	165	96	58,18	93	56,36	3	1,82	0	0	0	0
0,32	TOPMAX	3050	250	W3_2	165	88	53,33	87	52,73	1	0,61	0	0	0	0
0,32	TOPMAX	3050	300	W3_2	165	76	46,06	75	45,45	1	0,61	0	0	0	0
0,32	TOPMAX	3050	350	W3_2	165	68	41,21	68	41,21	0	0,00	0	0	0	0
0,32	TOPMAX	3050	400	W3_2	165	59	35,76	59	35,76	0	0,00	0	0	0	0
0,32	TOPMAX	3050	450	W3_2	165	56	33,94	56	33,94	0	0,00	0	0	0	0
0,32	TOPMAX	3050	50	W4_2	228	222	97,37	192	84,21	30	13,16	0	0	0	0
0,32	TOPMAX	3050	100	W4_2	228	196	85,96	177	77,63	19	8,33	0	0	0	0
0,32	TOPMAX	3050	150	W4_2	228	150	65,79	144	63,16	6	2,63	0	0	0	0
0,32	TOPMAX	3050	200	W4_2	228	115	50,44	114	50,00	1	0,44	0	0	0	0
0,32	TOPMAX	3050	250	W4_2	228	103	45,18	103	45,18	0	0,00	0	0	0	0
0,32	TOPMAX	3050	300	W4_2	228	90	39,47	90	39,47	0	0,00	0	0	0	0
0,32	TOPMAX	3050	350	W4_2	228	79	34,65	79	34,65	0	0,00	0	0	0	0
0,32	TOPMAX	3050	400	W4_2	228	68	29,82	68	29,82	0	0,00	0	0	0	0
0,32	TOPMAX	3050	450	W4_2	228	56	24,56	56	24,56	0	0,00	0	0	0	0
0,32	TOPMAX	3050	50	W5_2	165	148	89,70	128	77,58	20	12,12	0	0	0	0
0,32	TOPMAX	3050	100	W5_2	165	129	78,18	117	70,91	12	7,27	0	0	0	0
0,32	TOPMAX	3050	150	W5_2	165	112	67,88	105	63,64	7	4,24	0	0	0	0
0,32	TOPMAX	3050	200	W5_2	165	96	58,18	93	56,36	3	1,82	0	0	0	0
0,32	TOPMAX	3050	250	W5_2	165	88	53,33	87	52,73	1	0,61	0	0	0	0
0,32	TOPMAX	3050	300	W5_2	165	75	45,45	74	44,85	1	0,61	0	0	0	0
0,32	TOPMAX	3050	350	W5_2	165	66	40,00	66	40,00	0	0,00	0	0	0	0

0,32	TOPMAX	3050	400	W5_2	165	59	35,76	59	35,76	0	0,00	0	0	0	0
0,32	TOPMAX	3050	450	W5_2	165	57	34,55	57	34,55	0	0,00	0	0	0	0
0,32	TOPMAX	3050	50	W6_2	349	256	73,35	214	61,32	42	12,03	0	0	0	0
0,32	TOPMAX	3050	100	W6_2	349	219	62,75	194	55,59	25	7,16	0	0	0	0
0,32	TOPMAX	3050	150	W6_2	349	195	55,87	177	50,72	18	5,16	0	0	0	0
0,32	TOPMAX	3050	200	W6_2	349	160	45,85	151	43,27	9	2,58	0	0	0	0
0,32	TOPMAX	3050	250	W6_2	349	117	33,52	113	32,38	4	1,15	0	0	0	0
0,32	TOPMAX	3050	300	W6_2	349	92	26,36	92	26,36	0	0,00	0	0	0	0
0,32	TOPMAX	3050	350	W6_2	349	72	20,63	72	20,63	0	0,00	0	0	0	0
0,32	TOPMAX	3050	400	W6_2	349	59	16,91	59	16,91	0	0,00	0	0	0	0
0,32	TOPMAX	3050	450	W6_2	349	46	13,18	46	13,18	0	0,00	0	0	0	0
0,32	TOPMAX	3050	50	W7_2	77	73	94,81	69	89,61	4	5,19	0	0	0	0
0,32	TOPMAX	3050	100	W7_2	77	69	89,61	65	84,42	4	5,19	0	0	0	0
0,32	TOPMAX	3050	150	W7_2	77	66	85,71	62	80,52	4	5,19	0	0	0	0
0,32	TOPMAX	3050	200	W7_2	77	52	67,53	50	64,94	2	2,60	0	0	0	0
0,32	TOPMAX	3050	250	W7_2	77	45	58,44	44	57,14	1	1,30	0	0	0	0
0,32	TOPMAX	3050	300	W7_2	77	37	48,05	37	48,05	0	0,00	0	0	0	0
0,32	TOPMAX	3050	350	W7_2	77	33	42,86	33	42,86	0	0,00	0	0	0	0
0,32	TOPMAX	3050	400	W7_2	77	30	38,96	30	38,96	0	0,00	0	0	0	0
0,32	TOPMAX	3050	450	W7_2	77	24	31,17	24	31,17	0	0,00	0	0	0	0
0,32	TOPMAX	3050	50	W8_2	990	776	78,38	546	55,15	230	23,23	0	0	0	0
0,32	TOPMAX	3050	100	W8_2	990	613	61,92	475	47,98	138	13,94	0	0	0	0
0,32	TOPMAX	3050	150	W8_2	990	487	49,19	404	40,81	83	8,38	0	0	0	0
0,32	TOPMAX	3050	200	W8_2	990	382	38,59	334	33,74	48	4,85	0	0	0	0
0,32	TOPMAX	3050	250	W8_2	990	315	31,82	284	28,69	31	3,13	0	0	0	0
0,32	TOPMAX	3050	300	W8_2	990	258	26,06	235	23,74	23	2,32	0	0	0	0
0,32	TOPMAX	3050	350	W8_2	990	210	21,21	197	19,90	13	1,31	0	0	0	0
0,32	TOPMAX	3050	400	W8_2	990	173	17,47	167	16,87	6	0,61	0	0	0	0
0,32	TOPMAX	3050	450	W8_2	990	145	14,65	141	14,24	4	0,40	0	0	0	0
0,32	TOPMAX	3050	50	WA_2	192	119	61,98	109	56,77	10	5,21	0	0	0	0
0,32	TOPMAX	3050	100	WA_2	192	54	28,13	51	26,56	3	1,56	0	0	0	0
0,32	TOPMAX	3050	150	WA_2	192	20	10,42	18	9,38	2	1,04	0	0	0	0
0,32	TOPMAX	3050	200	WA_2	192	6	3,13	5	2,60	1	0,52	0	0	0	0
0,32	TOPMAX	3050	250	WA_2	192	2	1,04	2	1,04	0	0,00	0	0	0	0
0,32	TOPMAX	3050	300	WA_2	192	0	0,00	0	0,00	0	0,00	0	0	0	0
0,32	TOPMAX	3050	350	WA_2	192	0	0,00	0	0,00	0	0,00	0	0	0	0
0,32	TOPMAX	3050	400	WA_2	192	0	0,00	0	0,00	0	0,00	0	0	0	0
0,32	TOPMAX	3050	450	WA_2	192	0	0,00	0	0,00	0	0,00	0	0	0	0
0,32	TOPMAX	3050	50	WB_2	719	510	70,93	328	45,62	182	25,31	0	0	0	0
0,32	TOPMAX	3050	100	WB_2	719	414	57,58	296	41,17	118	16,41	0	0	0	0
0,32	TOPMAX	3050	150	WB_2	719	304	42,28	265	36,86	39	5,42	0	0	0	0
0,32	TOPMAX	3050	200	WB_2	719	249	34,63	219	30,46	30	4,17	0	0	0	0
0,32	TOPMAX	3050	250	WB_2	719	192	26,70	178	24,76	14	1,95	0	0	0	0

0,32	TOPMAX	3050	300	WB_2	719	156	21,70	146	20,31	10	1,39	0	0	0	0
0,32	TOPMAX	3050	350	WB_2	719	116	16,13	116	16,13	0	0,00	0	0	0	0
0,32	TOPMAX	3050	400	WB_2	719	87	12,10	87	12,10	0	0,00	0	0	0	0
0,32	TOPMAX	3050	450	WB_2	719	61	8,48	61	8,48	0	0,00	0	0	0	0
0,32	TOPMAX	3050	50	WC_2	113	112	99,12	108	95,58	4	3,54	0	0	0	0
0,32	TOPMAX	3050	100	WC_2	113	112	99,12	108	95,58	4	3,54	0	0	0	0
0,32	TOPMAX	3050	150	WC_2	113	108	95,58	104	92,04	4	3,54	0	0	0	0
0,32	TOPMAX	3050	200	WC_2	113	101	89,38	97	85,84	4	3,54	0	0	0	0
0,32	TOPMAX	3050	250	WC_2	113	84	74,34	81	71,68	3	2,65	0	0	0	0
0,32	TOPMAX	3050	300	WC_2	113	77	68,14	74	65,49	3	2,65	0	0	0	0
0,32	TOPMAX	3050	350	WC_2	113	70	61,95	67	59,29	3	2,65	0	0	0	0
0,32	TOPMAX	3050	400	WC_2	113	62	54,87	60	53,10	2	1,77	0	0	0	0
0,32	TOPMAX	3050	450	WC_2	113	55	48,67	53	46,90	2	1,77	0	0	0	0
0,32	TOPMAX	3050	50	WD_2	555	524	94,41	427	76,94	97	17,48	0	0	0	0
0,32	TOPMAX	3050	100	WD_2	555	466	83,96	392	70,63	74	13,33	0	0	0	0
0,32	TOPMAX	3050	150	WD_2	555	402	72,43	355	63,96	47	8,47	0	0	0	0
0,32	TOPMAX	3050	200	WD_2	555	320	57,66	292	52,61	28	5,05	0	0	0	0
0,32	TOPMAX	3050	250	WD_2	555	268	48,29	251	45,23	17	3,06	0	0	0	0
0,32	TOPMAX	3050	300	WD_2	555	215	38,74	207	37,30	8	1,44	0	0	0	0
0,32	TOPMAX	3050	350	WD_2	555	175	31,53	170	30,63	5	0,90	0	0	0	0
0,32	TOPMAX	3050	400	WD_2	555	139	25,05	137	24,68	2	0,36	0	0	0	0
0,32	TOPMAX	3050	450	WD_2	555	114	20,54	113	20,36	1	0,18	0	0	0	0
0,32	TOPMAX	3050	50	WE_2	558	489	87,63	416	74,55	73	13,08	0	0	0	0
0,32	TOPMAX	3050	100	WE_2	558	447	80,11	401	71,86	46	8,24	0	0	0	0
0,32	TOPMAX	3050	150	WE_2	558	422	75,63	391	70,07	31	5,56	0	0	0	0
0,32	TOPMAX	3050	200	WE_2	558	390	69,89	373	66,85	17	3,05	0	0	0	0
0,32	TOPMAX	3050	250	WE_2	558	365	65,41	357	63,98	8	1,43	0	0	0	0
0,32	TOPMAX	3050	300	WE_2	558	351	62,90	346	62,01	5	0,90	0	0	0	0
0,32	TOPMAX	3050	350	WE_2	558	336	60,22	334	59,86	2	0,36	0	0	0	0
0,32	TOPMAX	3050	400	WE_2	558	316	56,63	315	56,45	1	0,18	0	0	0	0
0,32	TOPMAX	3050	450	WE_2	558	295	52,87	295	52,87	0	0,00	0	0	0	0
0,32	TOPMAX	3050	50	WF_2	772	528	68,39	310	40,16	218	28,24	0	0	0	0
0,32	TOPMAX	3050	100	WF_2	772	431	55,83	291	37,69	140	18,13	0	0	0	0
0,32	TOPMAX	3050	150	WF_2	772	314	40,67	267	34,59	47	6,09	0	0	0	0
0,32	TOPMAX	3050	200	WF_2	772	252	32,64	214	27,72	38	4,92	0	0	0	0
0,32	TOPMAX	3050	250	WF_2	772	183	23,70	174	22,54	9	1,17	0	0	0	0
0,32	TOPMAX	3050	300	WF_2	772	145	18,78	145	18,78	0	0,00	0	0	0	0
0,32	TOPMAX	3050	350	WF_2	772	110	14,25	119	15,41	-9	-1,17	0	0	0	0
0,32	TOPMAX	3050	400	WF_2	772	78	10,10	91	11,79	-13	-1,68	0	0	0	0
0,32	TOPMAX	3050	450	WF_2	772	46	5,96	52	6,74	-6	-0,78	0	0	0	0
0,32	TOPMAX	3050	50	WG_2	218	214	98,17	204	93,58	9	4,13	0	0	0	0
0,32	TOPMAX	3050	100	WG_2	218	204	93,58	197	90,37	6	2,75	0	0	0	0
0,32	TOPMAX	3050	150	WG_2	218	180	82,57	177	81,19	3	1,38	0	0	0	0

0,32 TOPMAX	3050	200 WG_2	218	157	72,02	156	71,56	1	0,46	0	0	0	0
0,32 TOPMAX	3050	250 WG_2	218	125	57,34	125	57,34	0	0,00	0	0	0	0
0,32 TOPMAX	3050	300 WG_2	218	109	50,00	109	50,00	0	0,00	0	0	0	0
0,32 TOPMAX	3050	350 WG_2	218	94	43,12	94	43,12	0	0,00	0	0	0	0
0,32 TOPMAX	3050	400 WG_2	218	82	37,61	82	37,61	0	0,00	0	0	0	0
0,32 TOPMAX	3050	450 WG_2	218	72	33,03	72	33,03	0	0,00	0	0	0	0

ground	Ag	face	fwc (kpa)	fwt (kpa)	wall-comb	joints number	Total failed joints	Total failed joints (%)	BTT	BTT(%)	BTC	BTC(%)	BCT	BCT(%)	BCC	BCC(%)
	0,4	BOTMAX	3050	50	W1_2	640	602	94,06	500	78,13	102	15,94	2	0,31	0	0
	0,4	BOTMAX	3050	100	W1_2	640	547	85,47	477	74,53	68	10,63	2	0,31	0	0
	0,4	BOTMAX	3050	150	W1_2	640	482	75,31	439	68,59	41	6,41	0	2,00	0	0
	0,4	BOTMAX	3050	200	W1_2	640	430	67,19	399	62,34	30	4,69	1	0,16	0	0
	0,4	BOTMAX	3050	250	W1_2	640	384	60,00	365	57,03	19	2,97	0	0,00	0	0
	0,4	BOTMAX	3050	300	W1_2	640	350	54,69	337	52,66	13	2,03	0	0,00	0	0
	0,4	BOTMAX	3050	350	W1_2	640	313	48,91	306	47,81	7	1,09	0	0,00	0	0
	0,4	BOTMAX	3050	400	W1_2	640	281	43,91	277	43,28	4	0,63	0	0,00	0	0
	0,4	BOTMAX	3050	450	W1_2	640	256	40,00	254	39,69	2	0,31	0	0,00	0	0
											0					
B	0,4	TOPMAX	3050	50	W1_2	640	629	98,28	574	89,69	55	8,59	0	0,00	0	0
B	0,4	TOPMAX	3050	100	W1_2	640	593	92,66	545	85,16	48	7,5	0	0,00	0	0
B	0,4	TOPMAX	3050	150	W1_2	640	556	86,88	515	80,47	41	6,41	0	0,00	0	0
B	0,4	TOPMAX	3050	200	W1_2	640	501	78,28	472	73,75	29	4,53	0	0,00	0	0
B	0,4	TOPMAX	3050	250	W1_2	640	444	69,38	427	66,72	17	2,66	0	0,00	0	0
	0,4	TOPMAX	3050	300	W1_2	640	396	61,88	386	60,31	10	1,56	0	0,00	0	0
	0,4	TOPMAX	3050	350	W1_2	640	337	52,66	335	52,34	2	3,12	0	0,00	0	0
	0,4	TOPMAX	3050	400	W1_2	640	300	46,88	298	46,56	2	3,13	0	0,00	0	0
	0,4	TOPMAX	3050	450	W1_2	640	260	40,63	259	40,47	1	1,56	0	0,00	0	0
B	0,4	TOPMAX	3050	50	W2_2	349	281	80,52	244	69,91	37	10,6	0	0,00	0	0
B	0,4	TOPMAX	3050	100	W2_2	349	243	69,63	220	63	23	6,59	0	0,00	0	0
B	0,4	TOPMAX	3050	150	W2_2	349	216	61,89	200	57,31	16	4,58	0	0,00	0	0
B	0,4	TOPMAX	3050	200	W2_2	349	189	54,15	176	50,43	13	3,72	0	0,00	0	0
B	0,4	TOPMAX	3050	250	W2_2	349	166	47,56	159	45,56	7	2	0	0,00	0	0
	0,4	TOPMAX	3050	300	W2_2	349	152	43,55	149	42,69	3	8,6	0	0,00	0	0
	0,4	TOPMAX	3050	350	W2_2	349	137	39,26	135	38,68	2	5,73	0	0,00	0	0
	0,4	TOPMAX	3050	400	W2_2	349	122	34,96	120	34,38	2	5,73	0	0,00	0	0
	0,4	TOPMAX	3050	450	W2_2	349	110	31,52	109	31,23	1	2,87	0	0,00	0	0
	0,4	TOPMAX	3050	50	W3_2	165	152	92,12	136	82,42	16	9,70	0	0	0	0
	0,4	TOPMAX	3050	100	W3_2	165	143	86,67	130	78,79	13	7,88	0	0	0	0
	0,4	TOPMAX	3050	150	W3_2	165	130	78,79	122	73,94	8	4,85	0	0	0	0
	0,4	TOPMAX	3050	200	W3_2	165	113	68,48	107	64,85	6	3,64	0	0	0	0
	0,4	TOPMAX	3050	250	W3_2	165	104	63,03	101	61,21	3	1,82	0	0	0	0
	0,4	TOPMAX	3050	300	W3_2	165	93	56,36	93	56,36	0	0,00	0	0	0	0
	0,4	TOPMAX	3050	350	W3_2	165	88	53,33	88	53,33	0	0,00	0	0	0	0
	0,4	TOPMAX	3050	400	W3_2	165	78	47,27	78	47,27	0	0,00	0	0	0	0
	0,4	TOPMAX	3050	450	W3_2	165	66	40,00	66	40,00	0	0,00	0	0	0	0
	0,4	TOPMAX	3050	50	W4_2	228	203	89,04	182	79,82	21	9,21	0	0	0	0
	0,4	TOPMAX	3050	100	W4_2	228	187	82,02	167	73,25	20	8,77	0	0	0	0
	0,4	TOPMAX	3050	150	W4_2	228	166	72,81	152	66,67	14	6,14	0	0	0	0
	0,4	TOPMAX	3050	200	W4_2	228	151	66,23	142	62,28	9	3,95	0	0	0	0
	0,4	TOPMAX	3050	250	W4_2	228	136	59,65	132	57,89	4	1,75	0	0	0	0
	0,4	TOPMAX	3050	300	W4_2	228	115	50,44	115	50,44	0	0,00	0	0	0	0
	0,4	TOPMAX	3050	350	W4_2	228	109	47,81	109	47,81	0	0,00	0	0	0	0
	0,4	TOPMAX	3050	400	W4_2	228	97	42,54	97	42,54	0	0,00	0	0	0	0
	0,4	TOPMAX	3050	450	W4_2	228	76	33,33	76	33,33	0	0,00	0	0	0	0

0,4	TOPMAX	3050	50	W5_2	165	153	92,73	136	82,42	17	10,30	0	0	0	0
0,4	TOPMAX	3050	100	W5_2	165	143	86,67	131	79,39	12	7,27	0	0	0	0
0,4	TOPMAX	3050	150	W5_2	165	130	78,79	121	73,33	9	5,45	0	0	0	0
0,4	TOPMAX	3050	200	W5_2	165	112	67,88	107	64,85	5	3,03	0	0	0	0
0,4	TOPMAX	3050	250	W5_2	165	103	62,42	101	61,21	2	1,21	0	0	0	0
0,4	TOPMAX	3050	300	W5_2	165	92	55,76	92	55,76	0	0,00	0	0	0	0
0,4	TOPMAX	3050	350	W5_2	165	88	53,33	88	53,33	0	0,00	0	0	0	0
0,4	TOPMAX	3050	400	W5_2	165	77	46,67	77	46,67	0	0,00	0	0	0	0
0,4	TOPMAX	3050	450	W5_2	165	66	40,00	66	40,00	0	0,00	0	0	0	0
0,4	TOPMAX	3050	50	W6_2	349	279	79,94	249	71,35	30	8,60	0	0	0	0
0,4	TOPMAX	3050	100	W6_2	349	244	69,91	223	63,90	21	6,02	0	0	0	0
0,4	TOPMAX	3050	150	W6_2	349	215	61,60	203	58,17	12	3,44	0	0	0	0
0,4	TOPMAX	3050	200	W6_2	349	198	56,73	190	54,44	8	2,29	0	0	0	0
0,4	TOPMAX	3050	250	W6_2	349	174	49,86	170	48,71	4	1,15	0	0	0	0
0,4	TOPMAX	3050	300	W6_2	349	139	39,83	138	39,54	1	0,29	0	0	0	0
0,4	TOPMAX	3050	350	W6_2	349	112	32,09	112	32,09	0	0,00	0	0	0	0
0,4	TOPMAX	3050	400	W6_2	349	89	25,50	89	25,50	0	0,00	0	0	0	0
0,4	TOPMAX	3050	450	W6_2	349	75	21,49	75	21,49	0	0,00	0	0	0	0
0,4	TOPMAX	3050	50	W7_2	77	75	97,40	73	94,81	2	2,60	0	0	0	0
0,4	TOPMAX	3050	100	W7_2	77	70	90,91	69	89,61	1	1,30	0	0	0	0
0,4	TOPMAX	3050	150	W7_2	77	69	89,61	68	88,31	1	1,30	0	0	0	0
0,4	TOPMAX	3050	200	W7_2	77	63	81,82	63	81,82	0	0,00	0	0	0	0
0,4	TOPMAX	3050	250	W7_2	77	53	68,83	53	68,83	0	0,00	0	0	0	0
0,4	TOPMAX	3050	300	W7_2	77	46	59,74	46	59,74	0	0,00	0	0	0	0
0,4	TOPMAX	3050	350	W7_2	77	41	53,25	41	53,25	0	0,00	0	0	0	0
0,4	TOPMAX	3050	400	W7_2	77	36	46,75	36	46,75	0	0,00	0	0	0	0
0,4	TOPMAX	3050	450	W7_2	77	34	44,16	34	44,16	0	0,00	0	0	0	0
0,4	TOPMAX	3050	50	W8_2	990	810	81,82	591	59,70	218	22,02	1	0,10	0	0
0,4	TOPMAX	3050	100	W8_2	990	656	66,26	522	52,73	134	13,54	0	0,00	0	0
0,4	TOPMAX	3050	150	W8_2	990	528	53,33	454	45,86	74	7,47	0	0,00	0	0
0,4	TOPMAX	3050	200	W8_2	990	412	41,62	366	36,97	46	4,65	0	0,00	0	0
0,4	TOPMAX	3050	250	W8_2	990	329	33,23	306	30,91	23	2,32	0	0,00	0	0
0,4	TOPMAX	3050	300	W8_2	990	256	25,86	243	24,55	13	1,31	0	0,00	0	0
0,4	TOPMAX	3050	350	W8_2	990	197	19,90	192	19,39	5	0,51	0	0,00	0	0
0,4	TOPMAX	3050	400	W8_2	990	152	15,35	151	15,25	1	0,10	0	0,00	0	0
0,4	TOPMAX	3050	450	W8_2	990	120	12,12	120	12,12	0	0,00	0	0,00	0	0
0,4	TOPMAX	3050	50	WA_2	192	143	74,48	132	68,75	11	5,73	0	0,00	0	0
0,4	TOPMAX	3050	100	WA_2	192	86	44,79	86	44,79	0	0,00	0	0,00	0	0
0,4	TOPMAX	3050	150	WA_2	192	48	25,00	48	25,00	0	0,00	0	0,00	0	0
0,4	TOPMAX	3050	200	WA_2	192	19	9,90	19	9,90	0	0,00	0	0,00	0	0
0,4	TOPMAX	3050	250	WA_2	192	8	4,17	8	4,17	0	0,00	0	0,00	0	0
0,4	TOPMAX	3050	300	WA_2	192	4	2,08	4	2,08	0	0,00	0	0,00	0	0
0,4	TOPMAX	3050	350	WA_2	192	0	0,00	0	0,00	0	0,00	0	0,00	0	0
0,4	TOPMAX	3050	400	WA_2	192	0	0,00	0	0,00	0	0,00	0	0,00	0	0
0,4	TOPMAX	3050	450	WA_2	192	0	0,00	0	0,00	0	0,00	0	0,00	0	0
0,4	TOPMAX	3050	50	WB_2	719	564	78,44	423	58,83	136	18,92	5	0,70	0	0

0,4	TOPMAX	3050	100	WB_2	719	478	66,48	387	53,82	89	12,38	2	0,28	0	0
0,4	TOPMAX	3050	150	WB_2	719	404	56,19	345	47,98	59	8,21	0	0,00	0	0
0,4	TOPMAX	3050	200	WB_2	719	333	46,31	293	40,75	40	5,56	0	0,00	0	0
0,4	TOPMAX	3050	250	WB_2	719	273	37,97	250	34,77	23	3,20	0	0	0	0
0,4	TOPMAX	3050	300	WB_2	719	228	31,71	215	29,90	13	1,81	0	0	0	0
0,4	TOPMAX	3050	350	WB_2	719	169	23,50	164	22,81	5	0,70	0	0	0	0
0,4	TOPMAX	3050	400	WB_2	719	135	18,78	133	18,50	2	0,28	0	0	0	0
0,4	TOPMAX	3050	450	WB_2	719	101	14,05	101	14,05	0	0,00	0	0	0	0
0,4	TOPMAX	3050	50	WC_2	113	112	99,12	111	98,23	1	0,88	0	0	0	0
0,4	TOPMAX	3050	100	WC_2	113	112	99,12	111	98,23	1	0,88	0	0	0	0
0,4	TOPMAX	3050	150	WC_2	113	112	99,12	111	98,23	1	0,88	0	0	0	0
0,4	TOPMAX	3050	200	WC_2	113	107	94,69	106	93,81	1	0,88	0	0	0	0
0,4	TOPMAX	3050	250	WC_2	113	101	89,38	100	88,50	1	0,88	0	0	0	0
0,4	TOPMAX	3050	300	WC_2	113	87	76,99	86	76,11	1	0,88	0	0	0	0
0,4	TOPMAX	3050	350	WC_2	113	77	68,14	76	67,26	1	0,88	0	0	0	0
0,4	TOPMAX	3050	400	WC_2	113	73	64,60	72	63,72	1	0,88	0	0	0	0
0,4	TOPMAX	3050	450	WC_2	113	69	61,06	68	60,18	1	0,88	0	0	0	0
0,4	TOPMAX	3050	50	WD_2	555	541	97,48	467	84,14	74	13,33	0	0	0	0
0,4	TOPMAX	3050	100	WD_2	555	497	89,55	432	77,84	65	11,71	0	0	0	0
0,4	TOPMAX	3050	150	WD_2	555	445	80,18	398	71,71	47	8,47	0	0	0	0
0,4	TOPMAX	3050	200	WD_2	555	370	66,67	356	64,14	14	2,52	0	0	0	0
0,4	TOPMAX	3050	250	WD_2	555	338	60,90	299	53,87	39	7,03	0	0	0	0
0,4	TOPMAX	3050	300	WD_2	555	301	54,23	225	40,54	76	13,69	0	0	0	0
0,4	TOPMAX	3050	350	WD_2	555	267	48,11	189	34,05	78	14,05	0	0	0	0
0,4	TOPMAX	3050	400	WD_2	555	198	35,68	171	30,81	27	4,86	0	0	0	0
0,4	TOPMAX	3050	450	WD_2	555	162	29,19	162	29,19	0	0,00	0	0	0	0
0,4	TOPMAX	3050	50	WE_2	558	512	91,76	450	80,65	62	11,11	0	0	0	0
0,4	TOPMAX	3050	100	WE_2	558	482	86,38	439	78,67	43	7,71	0	0	0	0
0,4	TOPMAX	3050	150	WE_2	558	448	80,29	425	76,16	23	4,12	0	0	0	0
0,4	TOPMAX	3050	200	WE_2	558	425	76,16	414	74,19	11	1,97	0	0	0	0
0,4	TOPMAX	3050	250	WE_2	558	410	73,48	400	71,68	10	1,79	0	0	0	0
0,4	TOPMAX	3050	300	WE_2	558	381	68,28	376	67,38	5	0,90	0	0	0	0
0,4	TOPMAX	3050	350	WE_2	558	367	65,77	366	65,59	1	0,18	0	0	0	0
0,4	TOPMAX	3050	400	WE_2	558	352	63,08	351	62,90	1	0,18	0	0	0	0
0,4	TOPMAX	3050	450	WE_2	558	338	60,57	338	60,57	0	0,00	0	0	0	0
0,4	TOPMAX	3050	50	WF_2	772	578	74,87	430	55,70	148	19,17	0	0	0	0
0,4	TOPMAX	3050	100	WF_2	772	492	63,73	397	51,42	95	12,31	0	0	0	0
0,4	TOPMAX	3050	150	WF_2	772	425	55,05	345	44,69	80	10,36	0	0	0	0
0,4	TOPMAX	3050	200	WF_2	772	347	44,95	302	39,12	45	5,83	0	0	0	0
0,4	TOPMAX	3050	250	WF_2	772	276	35,75	254	32,90	22	2,85	0	0	0	0
0,4	TOPMAX	3050	300	WF_2	772	237	30,70	214	27,72	23	2,98	0	0	0	0
0,4	TOPMAX	3050	350	WF_2	772	156	20,21	157	20,34	-1	-0,13	0	0	0	0
0,4	TOPMAX	3050	400	WF_2	772	134	17,36	124	16,06	10	1,30	0	0	0	0
0,4	TOPMAX	3050	450	WF_2	772	98	12,69	95	12,31	3	0,39	0	0	0	0
0,4	TOPMAX	3050	50	WG_2	218	216	99,08	207	94,95	9	4,13	0	0	0	0
0,4	TOPMAX	3050	100	WG_2	218	206	94,50	201	92,20	5	2,29	0	0	0	0

0,4	TOPMAX	3050	150	WG_2	218	187	85,78	181	83,03	6	2,75	0	0	0	0
0,4	TOPMAX	3050	200	WG_2	218	161	73,85	161	73,85	0	0,00	0	0	0	0
0,4	TOPMAX	3050	250	WG_2	218	133	61,01	133	61,01	0	0,00	0	0	0	0
0,4	TOPMAX	3050	300	WG_2	218	112	51,38	112	51,38	0	0,00	0	0	0	0
0,4	TOPMAX	3050	350	WG_2	218	97	44,50	97	44,50	0	0,00	0	0	0	0
0,4	TOPMAX	3050	400	WG_2	218	86	39,45	86	39,45	0	0,00	0	0	0	0
0,4	TOPMAX	3050	450	WG_2	218	75	34,40	75	34,40	0	0,00	0	0	0	0